



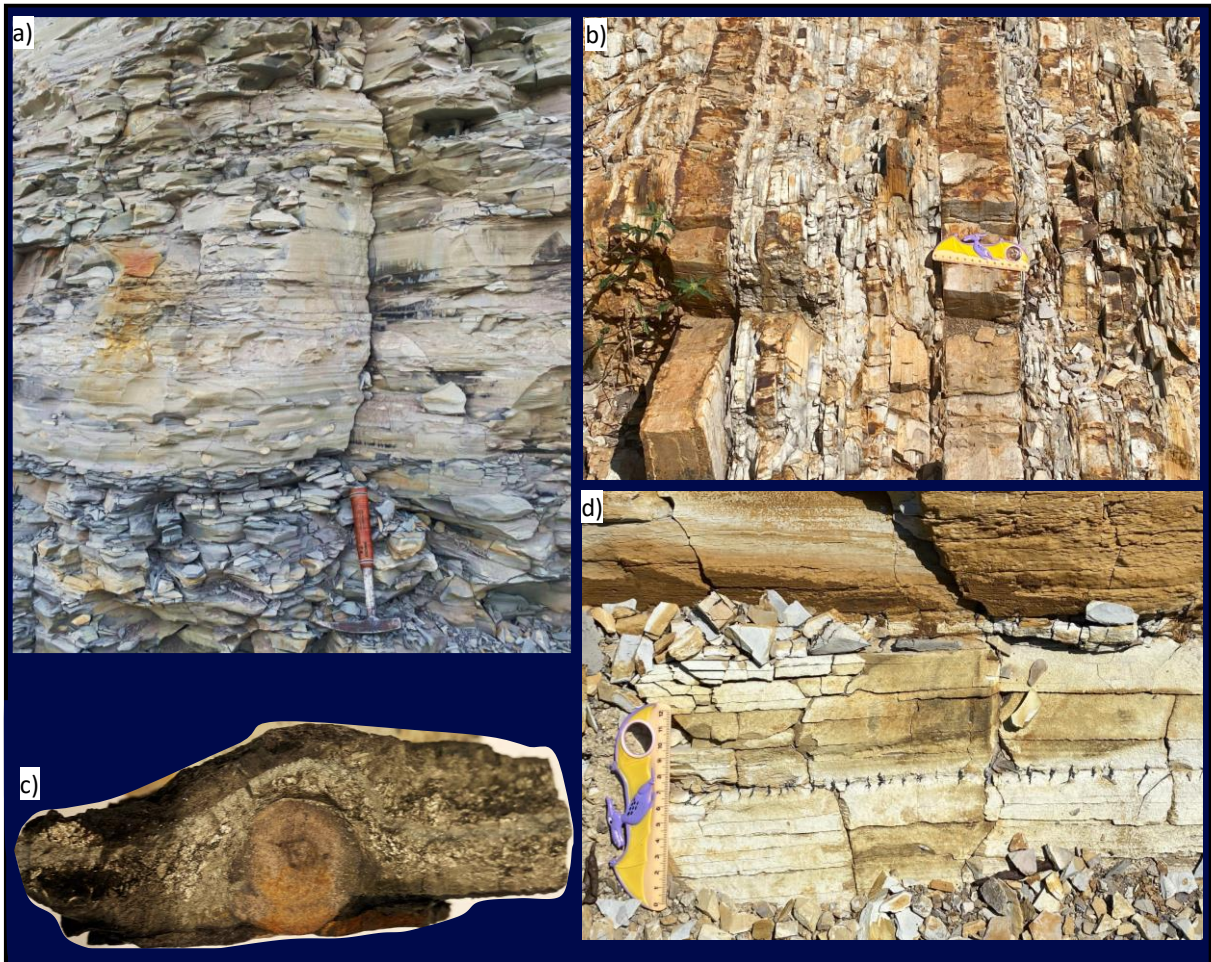
Oklahoma Geological Survey
Nicholas W. Hayman, *Director*

Guidebook 40

ISSN 2996-4652

An Atlas of Woodford Shale Outcrops in Southern Oklahoma

Andrew Cullen & David Hull
Big Hill Adventures Practical Geoscience
2023



The University of Oklahoma

Norman, Oklahoma

OKLAHOMA GEOLOGICAL SURVEY

Nick Hayman, Director

TABLE OF CONTENTS

SURVEY STAFF

Benjamin Allen	Granular Physicist	Cari Pryor	HR and Financial Manager
Scott Bryant	Warehouse Coordinator	Cesalea Ray	GIS Specialist
Mason Cullen	Machine Shop Technician	Netra Regmi	Hazards Geologist
Jeff Dillon	Core & Cuttings Customer Liason	Ryan Rosol	Warehouse Coordinator
Chrishelle Drew	Financial Specialist	Russell Standridge	GIS Specialist
Carla Eichler	Field Geologist	Tom Stanley	Field Geologist
Fernando Ferrer	Seismic Analyst	Joyce Stiehler	Assistant to the Director
Lindsey Hunt	Electron Probe Operator	Fnu "Ming" Suriamin	Petroleum Geologist & Petrophysicist
Carter Lewis	Research Associate	Richard Tarver	OPIC Manager
Binmadi Milad	Geostorage Specialist	Andrew Thiel	Seismic Specialist
Paul Ogwari	Geophysicist	Jacob Walter	State Seismologist
Junwen Peng	Geologist	Molly Yunker	Education & Outreach Coordinator

Title Page Illustration

Collage of photographs illustrating some of interesting features of the Woodford outcrops in this atlas. a) Phosphate nodules at Wyche quarry b) Brittle-ductile couplets at YMCA/Camp Classen, c) Pyrite bed compacting over phosphate nodule at Wyche quarry d) Early expelled oil on bedding plane and in fractures at McAlester Cemetery Quarry.

TABLE OF CONTENTS

Chapters	Sections	
	1.1.	Preface i
1	Introduction	1.2 Introduction 1
		1.3 Geological Overview 10
2	Lawrence Uplift	2.1 Wyche Quarry 34
		2.2 Hass G 58
		2.3 Woodford Log 66
		2.4 Other LU Locations 73
3	Arbuckle Mountains	3.0 Arbuckle Mountain Sections 76
		3.1 Hunton Quarry Anticline 77
		3.2 Heart of the Arbuckles 87
		3.3 I35 North 95
		3.4 Camp Classen 101
		3.5 I35 South 111
		3.6 Other Arbuckle Sections 126
4	Ardmore/Marietta Basin	4.1 McAlister Cemetery 128
		4.2 Jetta Core TX 149
5	Arkoma Basin Ouachitas	5.1 Wapanucka 153
		5.2 Scratch Hill 160
		5.3 Other Arkoma Outcrops 169
6	Discussion	6.1 Regional Fracturing 171
		6.2 REE Enrichment in Phosphate Nodules 172
		6.3 Mass Extinctions Hg anomalies 180
		6.4 Paleogeography / Ocean Circulation 187
7	Field Trip Routes	7.1 Different Field Trip Routes 196

1.1 PREFACE

This atlas of Woodford Shale outcrops in south central Oklahoma attempts to collate various studies, including unpublished theses, into a single document. Chapters 2, 3, 4, and 5 cover distinct geographic domains that represent a proximal to distal transect of the Latest Devonian to Earliest Mississippian depositional system in this region of southern Laurentia. Chapter 6 discusses some yet to be answered research questions in a global context. This atlas is not a field trip guidebook per se. It is a menu from which different configurations of field trips and seminars can be constructed. Examples of several different field trips are given in Chapter 7. This atlas has a modular format so that future additions, updates, and corrections can be made without wholesale revision of the entire document.

Our work on outcrops of this world-class petroleum source rock began in 2020 partly to escape the tedium of the Great Pandemic Lockdown. Better to see the rocks than just read about them. This time also coincided with a contraction of Woodford Shale research that followed the passing of Dr. Roger Slatt (OU Woodford Consortium) and the retirement of Brian Cardott (Oklahoma Geological Survey), which also coincided with a sharp drop in Oklahoma's rig count driven by low commodity prices. As our studies progressed, we realized there were some significant differences in the interpretation of the Woodford Shale. We also realized the decades of studies represent the building blocks that can be used to frame Laurentia-scale studies to improve our understanding of the paleogeographic and palaeoceanographic evolution during the end Devonian mass extinctions as the Rheic sea narrowed during the assembly of Pangea.

Most of the outcrops visited are on private land. We are most grateful to each of those landowners who granted access to their property: Jessie Wyche, Tommy and Linda Chaffin, Bill Lance, Sarah Jolly, and Terry Maris. We would like to acknowledge Carl Symcox, Austin McGlannan, and Galen Miller for their assistance in the field work. We are grateful to Nick Hayman, Director of the Oklahoma Geologic Survey editorial suggestions and for partially funding of our analytical program. Carter Lewis of the Oklahoma Geologic Survey provided additional proof-reading suggestions. Although there are undoubtedly a few typographic errors and passages that could be improved, we believe these should not detract from the utility of this atlas. Lastly, we acknowledge that this guidebook would never have been completed without the forbearance and support of our spouses.

Andrew Cullen
David Hull
November 2023

1.2 INTRODUCTION (REGIONAL SETTING & GLOBAL CONSIDERATIONS):

The Woodford Shale of southern Oklahoma is known from outcrops in the Arbuckle Mountains region and extensive subsurface data from the Anadarko, Arkoma, and Ardmore basins. These basins are contemporaneous with other basins of southern Laurentia that also have sections of similar age organic-rich mud rocks (Figure 1.2.1).

The Woodford Shale is principally known as a world-class siliceous marine petroleum source rock (Cardott and Comer, 2020.) with geomechanical properties suitable for exploitation as an “unconventional” reservoir (Slatt et al., 2018). For the sake of brevity, we shall simply use the name Woodford hereafter rather than its full stratigraphic name. The Woodford is correlative to the New Albany Shale in the Illinois basin and outcrops of the Chattanooga Shale in Arkansas, Tennessee, and Kentucky. The Arkansas Novaculite is also correlative with the Woodford (Figure 1.2.2). The Arkansas Novaculite and older Paleozoic units exposed in the Ouachita fold-thrust belt are interpreted as the deepwater facies of equivalent shallow marine rocks exposed the Arbuckle Mountains- respectively known as the Ouachita and Arbuckle facies (Gatewood and Faye, 1991). The depositional interval of the Woodford encompasses 1) The development of widespread anoxia in the epicontinental seas southern Laurentia with the resultant voluminous organic carbon sequestration and 2) The transition from greenhouse to icehouse conditions marked by rising and then falling eustatic sea level and the development of early Mississippian glaciation.

Conodont biostratigraphy establishes that the Woodford ranges in age from the late Frasnian through the Famennian and into the early Tournasian spanning Late Devonian and earliest Mississippian (Over, 1990, 1992). The rapid expansion of land plants in the Devonian-Mississippian interval is arguably one of the most important developments in Earth’s Phanerozoic evolution leading to a precipitous drop in atmospheric CO₂ (Algeo and Strickler, 1988.). The expansion of land plant was accompanied by increasingly deeper and complex roots systems that led increased chemical weathering and the development of deeper soil profiles (Figure 1.2.3) both of which affected the delivery of organic matter and weathered bedrock to the shallow marine shelves. The increase in the delivery of organic matter may have led to an increase in levels of eutrophication on the shallow marine shelves helping to produce oxygen starved bottom waters favoring sequestration of large volumes of organic carbon (Balter et al., 2017).

The Woodford spans the Famennian-Frasnian (F/F) and Devonian-Carboniferous (D/C) mass extinctions events. Both extinction events dramatically reduced biodiversity of shallow

marine life, but D/C extinctions stand out for the major reduction in terrestrial forests. These forests were particularly concentrated in the Appalachian region of Laurentia and experienced massive wildfires in the Famennian (Lu et al., 2021). The Woodford has large, silicified trunks of *Archaeopteris* preserved at several localities (Sections 2.1 and 2.4). An influx of plant-sourced phosphorus into the shallow marine environment may have triggered the widespread precipitation of phosphate nodules near the D/C boundary in the Woodford and New Albany/Chattanooga shales (Figure 1.2.2 and Section 6.3).

Proposed F/F and D/C extinction mechanisms include changes in global sea-level, global temperatures, and ocean circulation patterns episodes of marine anoxia, asteroid/comet impacts; large igneous province volcanism, and supernova cosmic ray bombardment (MacLeod, 2013; Bond and Grasby, 2018). These mechanisms are not mutually exclusive, and some may be regarded as secondary feed-back responses. Sedimentological and geochemical expression of these extinction events, which have been studied at numerous locations globally (e.g., Germany, Poland, Morocco, Uzbekistan, Vietnam), show an increase organic carbon preservation, negative deflection in $\delta^{13}\text{C}$ secular isotope trends, elevated Hg levels, and changes in pyrite framboid abundance & (Rackocinski et al., 2020; Carmichael et al., 2021). Thus, in addition to its importance from a petroleum systems perspective, the Woodford contains critical biogeochemical information on climate evolution and mass extinctions that need studied and integrated into global studies.

Section	Key Outcrops	Latitude	Longitude
2.1	Wyche Quarry	34°40'21"N	96°38"W
2.2	Haas G	34°40'48"N	96°39'53"W
2.3	Woodford Log	34°40'43"N	96°39'54"W
3.1	Hunton Quarry Anticline	34°25'36"N	97° 1'52"W
3.2	Heart of the Arbuckles	34°26'38"N	97° 7'41"W
3.3	I35-North	34°26'38"N	97° 41.91"W
3.4	YMCA / Camp Classen	34°27'40"N	97° 9'5.54"W
3.5	I-35 South (Last Ridge)	34°21'6"N	97° 8'56"W
4.1	McAlister Cemetery Quarry	34° 4'39"N	97° 9'19"W
5.1	Wapanucka	34°22'45"N	96°20'04"W
5.2	Scratch Hill	34°22'32"N	96°06'35"W

Table 1.1.1 Location of key Woodford outcrops covered in this atlas.

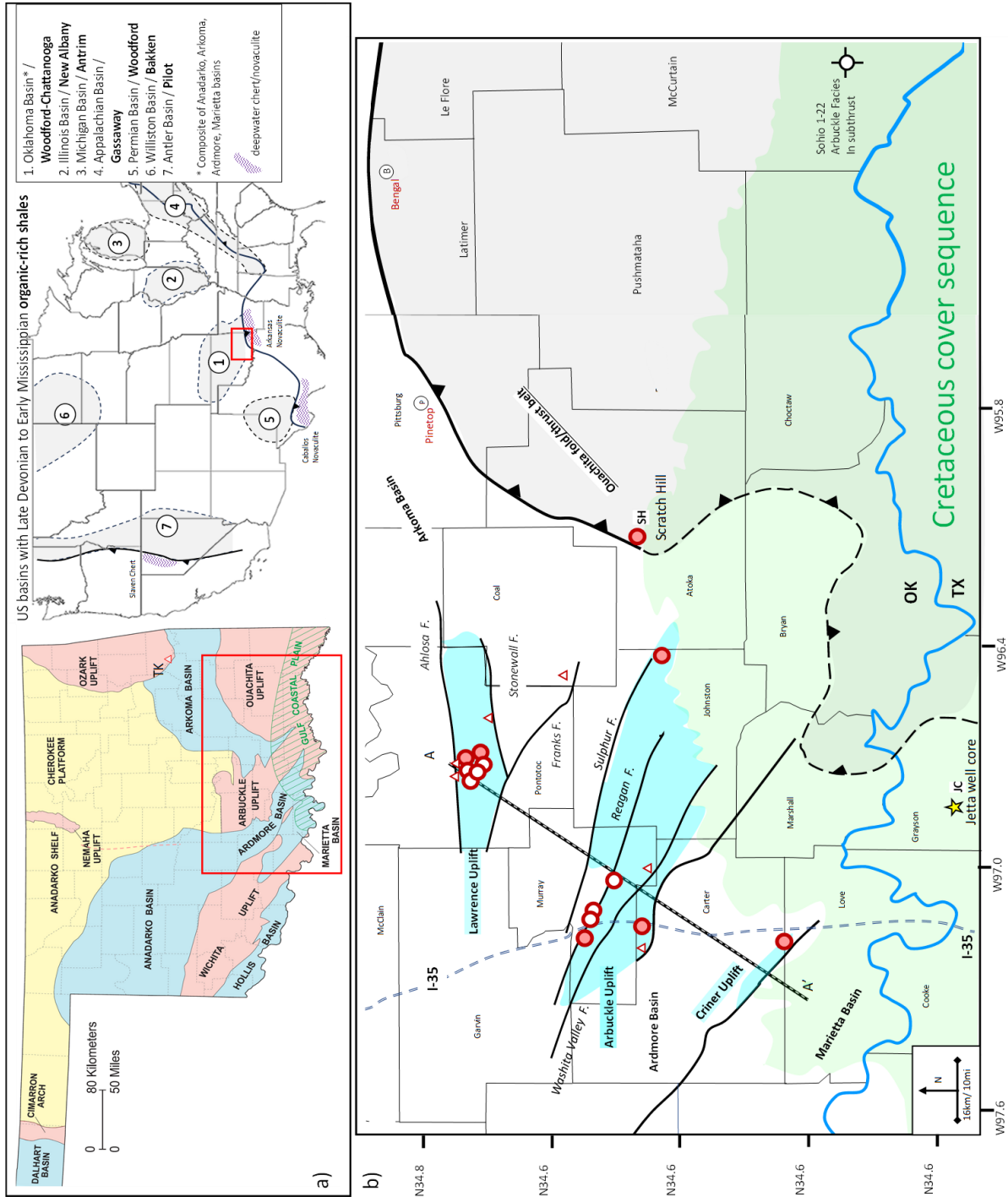


Figure 1.2.1 a) Oklahoma geological provinces (Northcutt and Campbell, 1995); and key North American basins (light gray b) Southern Oklahoma geological features. Outcrop locations: filled red circles-outcrops reviewed with biostratigraphic, open circles-outcrops reviewed lacking biostratigraphy, open triangles-other outcrops with biostratigraphy. Interstate-35 is in blue dashed double line. A-A' cross section (figure 1.2.5)

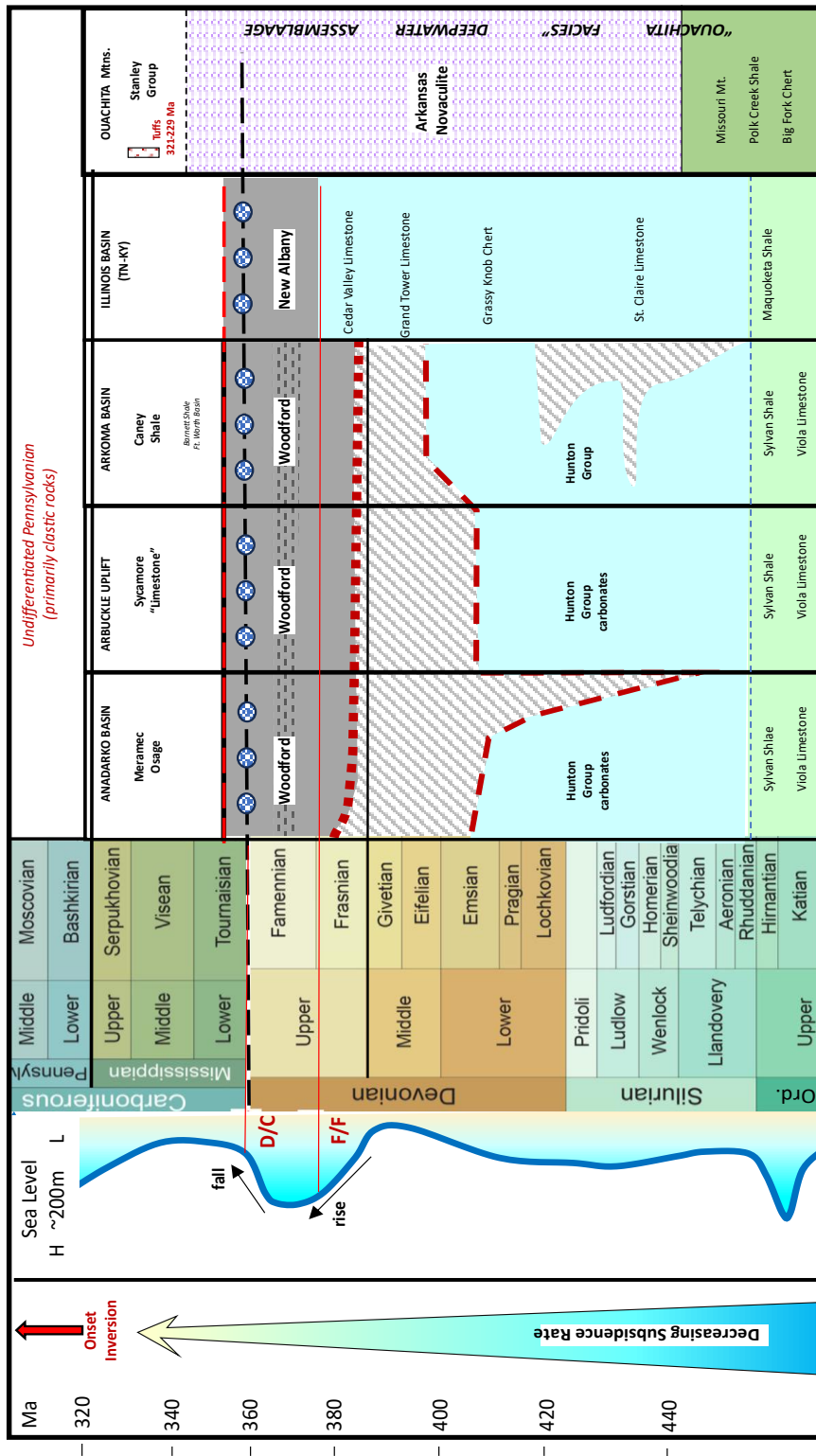


Figure 1.2.2 Intra-basin stratigraphic correlation chart with long-term eustatic curve (after McGlannan et al., 2022). Dashes in Woodford mark clay-rich middle member. Blue patterned circles in Upper Woodford denote phosphate nodules.

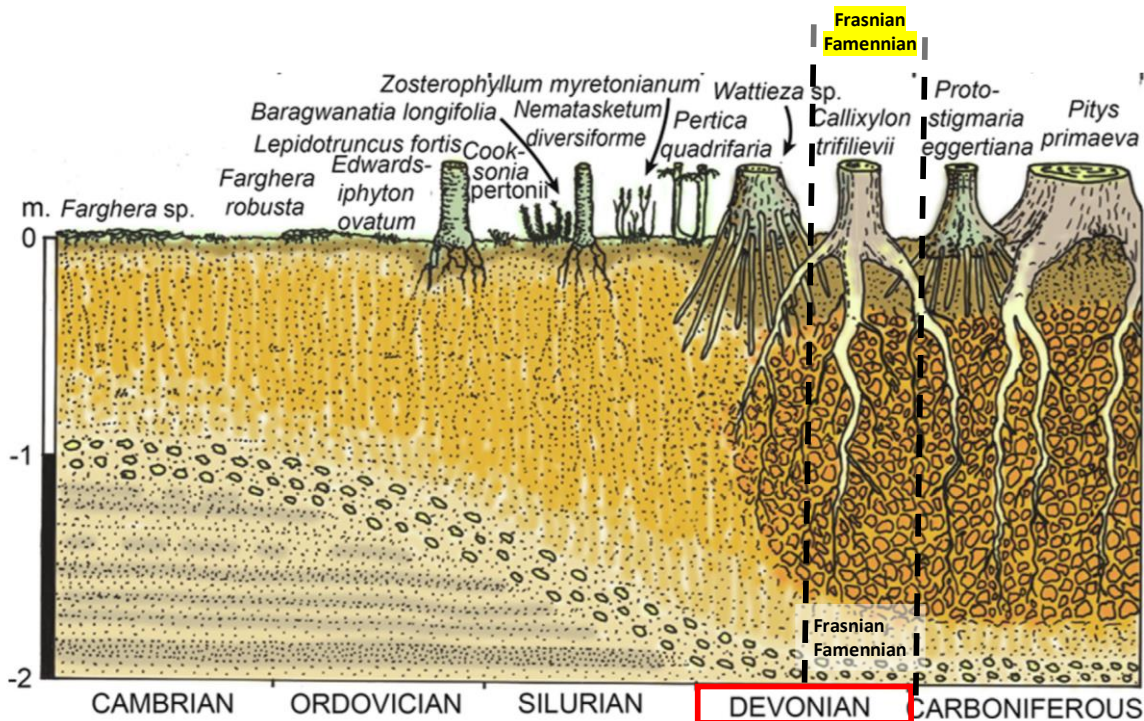


Figure 1.2.3 Evolutionary deepening of Paleozoic root systems (Retallick, 2022)

Woodford outcrops from the Lawrence Uplift through the Arbuckle Mountains to the Criner Hills uplift in the Ardmore Basin are a 100mi/162km long basin ward transect into progressively deeper water (Figure 1.2.4). The Arkansas Novaculite outcrop at Scratch Hill represents the deepwater Ouachita facies.

- Key Outcrops
1. Wyche Quarry, Hass-G, CR-1620, Woodford Log, Pyrite balls (C-1 is Current #1 core hole)
 2. I-35 North, Hunton Quarry anticline, Heart of the Arbuckles, Camp Classen / YMCA spillway
 3. I-35 South
 4. MCQ-McAlister Cemetery Quarry

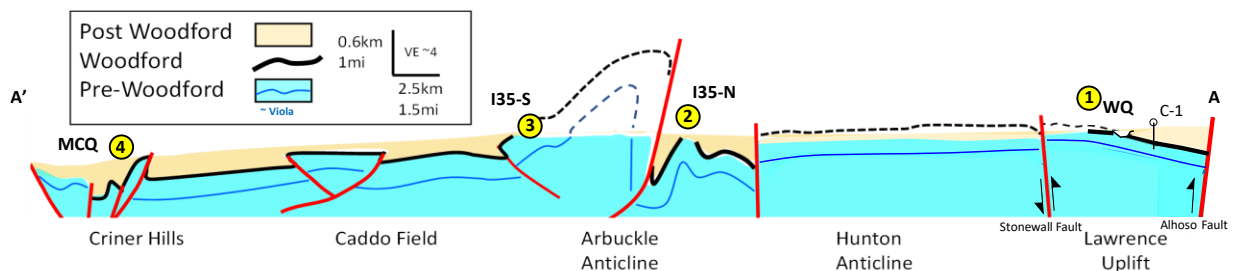


Figure 1.2.4 N-S regional schematic structural cross section on figure 1.2.1 showing principal Woodford outcrops from the Lawrence uplift to the Ardmore basin.

Lawrence Uplift: The Lawrence uplift is a relatively undeformed horst block bounded by the steeply-dipping to vertical Alhoso and Stonewall faults (Figure 1.2.5). Gently dipping (<5°) Woodford Shale is at or near the surface across a NW-SE striking outcrop pattern is exposed in numerous shallow shale pits that afford nice views of bed tops. Partial vertical sections are exposed along the banks of Jack Fork Creek and in the Wyche Quarry. Additionally extensive work has been done on two shallow cores, most notably the Wyche #1, that penetrated the entire Woodford section.

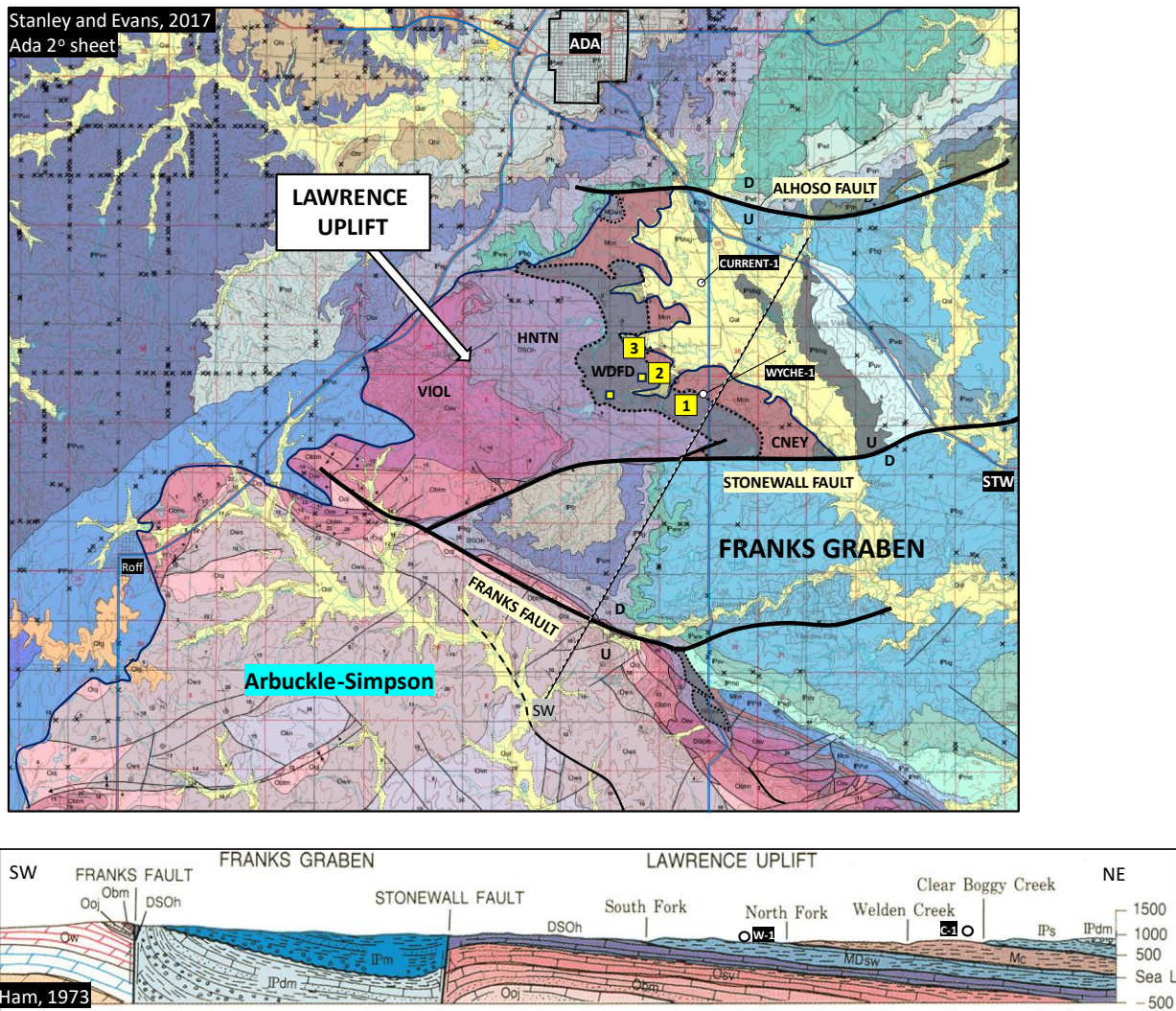


Figure 1.2.5 Geological map of the Lawrence uplift and cross section (Stanley and Evans, 2014; Ham, 1973). Key outcrops 1) Wyche Quarry 2) Hass-G 3) County Road 1620 (Woodford Log). Other locations in small yellow circles.

Arbuckle Mountains / Criner Hills: The Arbuckle Mountains and Criner Hills sections occur on the anticlinal limbs of fault propagation folds (Figure 1.2.6). These structures formed during Pennsylvanian-age basin inversion during the assembly of Pangea. Roadcuts expose excellent cross-sectional views of the Woodford, bed tops are poorly exposed. Owing to steep dips outcrops along road cuts are relatively limited. At the McAlister Cemetery Quarry a full section of Woodford on the NE limb of the Overbrook anticline in the Criner Hills has been bladed off and is well exposed.

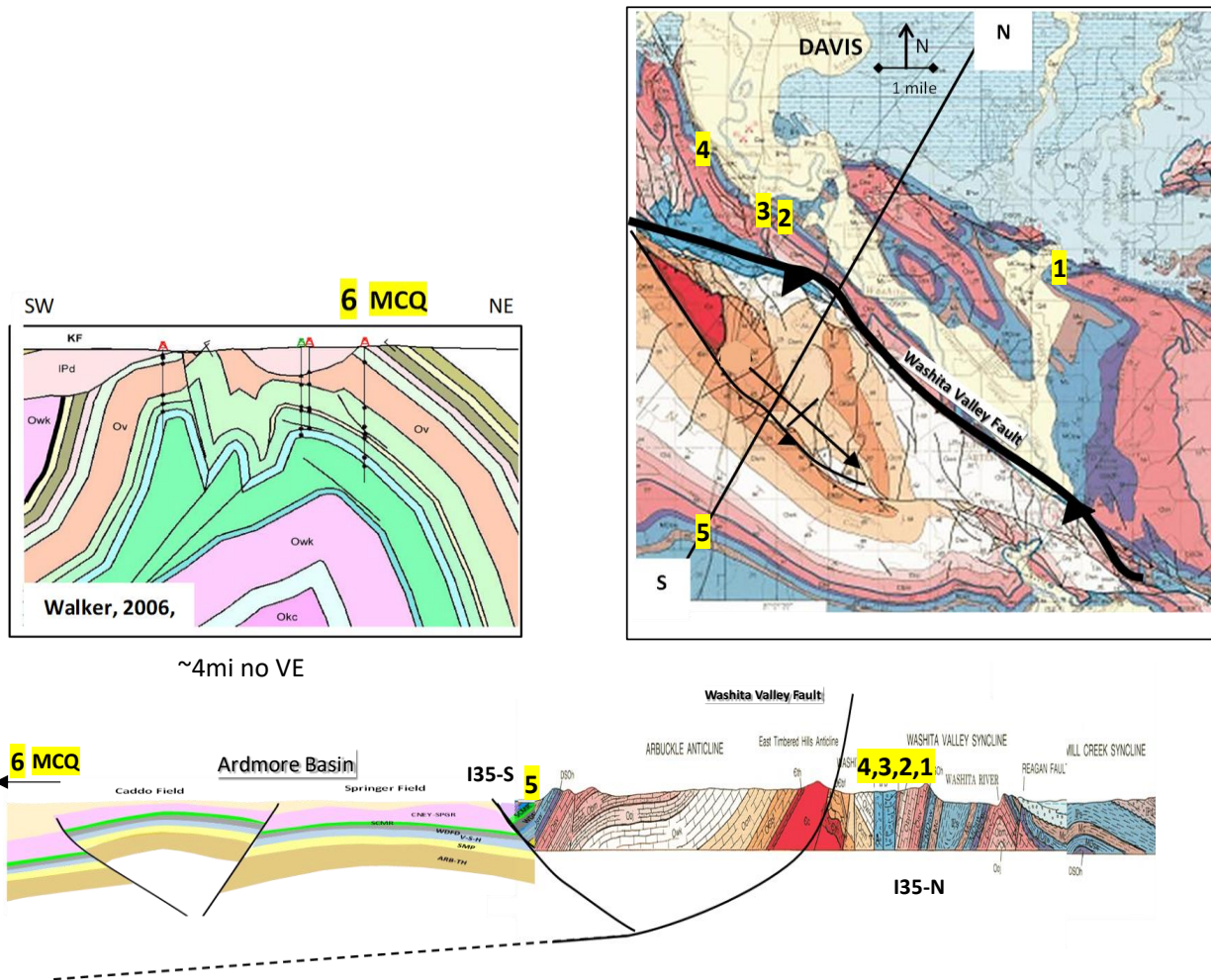


Figure 1.2.6 Geological map of part of the Arbuckle Mountains (Ham, 1958) with regional cross section (Miller and Cullen, 2019) and cross section through MCQ (McAlister Cemetery Quarry). 1) Hunton Quarry Anticline, 2) Heart of the Arbuckles, (SH-77D) 3) I-35S, 4) Camp Classen-YMCA Spillway, 5) McAlister Cemetery Quarry.

Ouachita Mountains: At Scratch Hill near Atoka OK, there is an excellent exposure of the Arkansas Novaculite (Section 5.2) which is considered as deepwater facies equivalent to the Woodford Shale. The Scratch Hill outcrop lies along Black Knob Ridge in the hanging wall of the Choctaw fault (Figure 1.2.7). The Choctaw fault is the frontal thrust of the Ouachita fold-thrust belt. The fault represents the structural contact between shallow and deepwater rocks of the Arbuckle and Ouachita facies, respectively. There is at least 100mi of lateral displacement along the Choctaw fault (Arbenz, 2008) that must be accounted for when reconstructing Late Devonian deposition environments and paleoceanography.

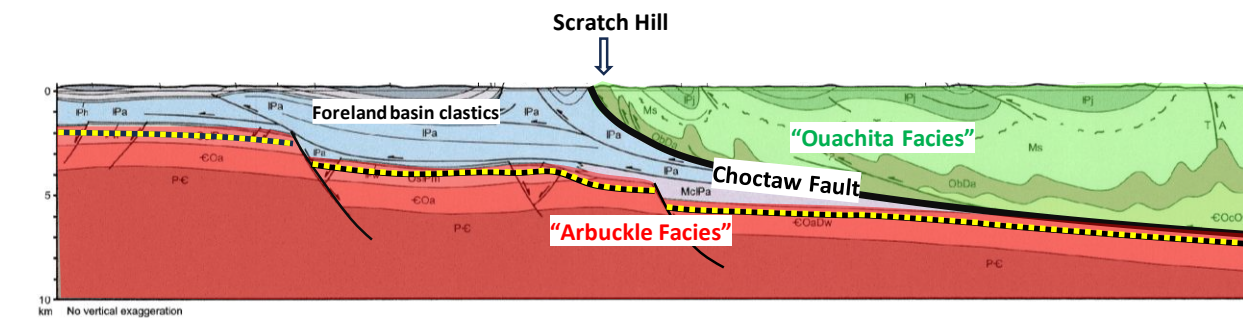


Figure 1.2.7 Regional structural cross section at Scratch Hill showing thrusting of the deepwater Ouachita facies units over the shallow water Arbuckle facies units along the frontal Choctaw fault. The heavy dashed yellow line represents the approximate top of the Woodford in the footwall. (modified from Arbenz, 2008)

References

- Algeo, T.J., Scheckler, S.E., 1998. Terrestrial-marine teleconnections in the Devonian: links between the evolution of land plants, weathering processes, and marine anoxic events. *Philosophical Transaction Royal Society London, Biological Science* 353, p. 113–130.
- Arbenz, J.K., 2008, Structural framework of the Ouachita Mountains, in N.H. Suneson, ed., *Stratigraphic and structural evolution of the Ouachita Mountains and Arkoma Basin, southeastern Oklahoma and west-central Arkansas: application to petroleum exploration: Oklahoma Geological Survey, Circular 112A*, p. 1-40.
- Balter, V. Renaud, S., Girard, C., Joachimski, M., 2008, Record of climate-driven morphological changes in 376 Ma Devonian fossils, *Geology*. 36-11, p.907-910.

- Bond, D.P. and Grasby, S.E., 2017, On the causes of mass extinctions, *Palaeogeography, Palaeoclimatology, Palaeoecology* 478, p. 3–29.
- Cardott, B.J., and Comer, J.B., 2020, Woodford Shale (Upper Devonian to Mississippian) from Hydrocarbon Source Rock to Reservoir, *Oklahoma Geological Survey Bulletin* 152, 100 p.
- Carmichael, S.K., Waters, J.A., Königshof, P., Suttner, T.J., Kido, E., 2019. Paleogeography and paleoenvironments of the Late Devonian Kellwasser event: A review of its sedimentological and geochemical expression. *Global Planetary Change*, 183, p. 1-17.
- Gatewood, L.E., and R.O. Fay, 1991, The Arbuckle/Ouachita facies boundary in Oklahoma, in K.S. Johnson, ed., *Late Cambrian-Ordovician geology of the southern Midcontinent, 1989 symposium*: Oklahoma Geological Survey, Circular 92, p. 171-180.
- Ham, W.E., and others, 1954 *Geological Map and Sections of the Arbuckle Mountains, Oklahoma*: edited by and reproduced as Oklahoma Geological Survey Circular 91.
- Lu, M., Ikejiri, T., and Han, Y., 2021, A synthesis of the Devonian wildfire record: Implications for paleogeography, fossil flora, and paleoclimate, *Palaeogeography, Palaeoclimatology, Palaeoecology* 571, p. 1-16.
- MacLeod, N., 2013, *The Great Extinctions: What Causes Them and How They Shape Life*, Firefly Books, United Kingdom.
- Northcutt R. A. and Campbell J. A., 1995, *Geologic Provinces of Oklahoma Map*. Oklahoma Geological Survey, OF5-95.
- Rakocinski, M., Marynowski, L., Agnieszka, P., & others, 2020, Volcanic related methylmercury poisoning as the possible driver of the end-Devonian Mass Extinction, *Nature Reports* 10-7344, 8p.
- Retallick, G. J., 2022, Ordovician-Devonian lichen canopies before evolution of woody trees, *Gondwana Research*, 106, p. 211-223.
- Slatt, R., and Woodford Consortium students, 2018, Conventional analysis of unconventional resource shales, *Oklahoma City Geological Society Shale Shaker*, 69-6, p. 269-329.
- Stanley, T. and Evans, S., 2000, *Geological Map of the Ada 2° Quadrangle, Oklahoma* Geological Survey, OGQ 97.
- Walker, W.M., 2006, *Structural analysis Criner Hill, South-Central Oklahoma*, MSc Thesis, Baylor University, 73p.

In the Late Devonian to Early Mississippian the present-day midcontinent was an epeiric sea with a wide shelf and long low gradient ramp that extended southward into the Rheic Ocean. Plate and paleogeographic reconstructions show the Rheic Ocean was relatively wide with strong seasonal wind variations potentially influencing the delivery of fines to the margin (Figure 1.3.2).

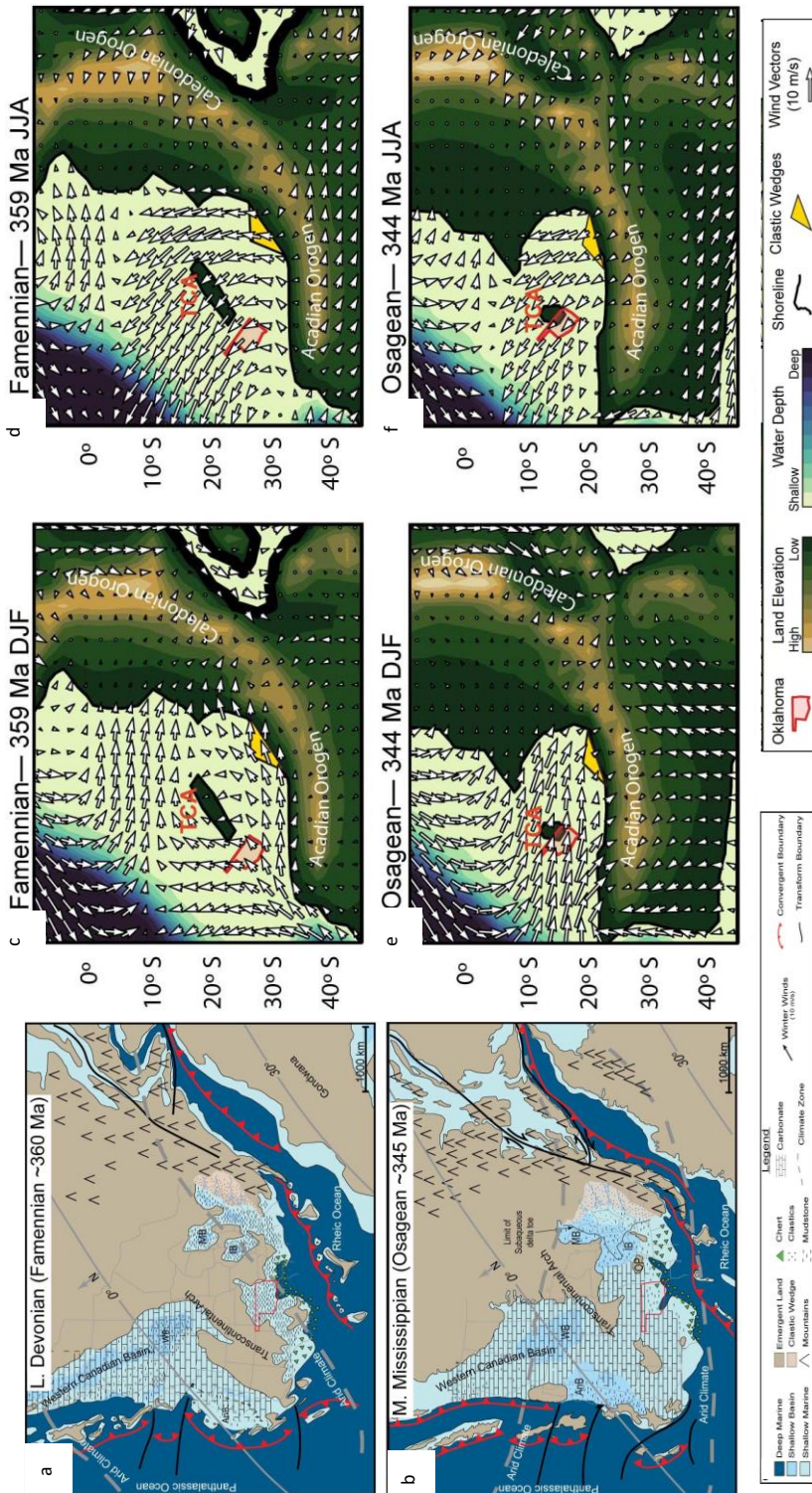


Figure 1.3.2
a,b) Paleogeographic/tectonic reconstructions at 360ma and 345ma.

c) d) Famennian paleo-wind models for Dec.-Feb and June-Aug.

e) f) Osagean paleo-wind models for Dec.-Feb and June-Aug. (McGlannan et al., 2022)

The Woodford is extensively studied. Since the earliest work of Taff (1902) more than 350 publications and student theses relating to the Woodford Shale have been completed; see the bibliography of Cardott and Comer (2020). These studies fall into 4 broad themes: lithostratigraphy, sequence stratigraphy, biostratigraphy, and petroleum systems/ organic geochemistry. The following geological framework is derived primarily from the summaries and reviews of Slatt et al., (2018) and Cardott and Comer (2020):

1. The Woodford has a thickness of 0ft -700ft and can be divided into 3 basic subdivisions (Upper, Middle, Lower) on the basis petrophysical measurements and different percentages of its dominant lithofacies: organic-rich silicic mudrock and silicic shale, silty shale and chert (Figure 1.3.2a and 1.3.3b).
2. Relative to the more silicic Upper and Lower members, the Middle Woodford is more clay-rich and ductile which consistent the long term eustatic curve that implies the maximum flooding surface in the Middle Woodford (see figure 1.2.2).
3. The Woodford is a world-class oil prone source rock with a broad range of thermal maturity related largely to maximum burial (Figure 1.3.3c). Organic petrographic shows an abundance of marine algae which is consistent with the modified van Krevlen diagrams from RockEval data.
4. The Frasnian-Famennian boundary is near the basal Lower Woodford. The Devonian-Carboniferous boundary is near the top of the Upper Woodford. Thus, most of the Woodford is Famennian in age (Figure 1.3.3a, see discussion of biostratigraphy below).
5. The Woodford was deposited as a transgressive systems tract (TST) over a major unconformity (sequence boundary) on the Hunton Group carbonates that were karsted and incised over a ~20myr interval prior to deposition of the Woodford (Figures 1.3.3a, and 1.2.2).

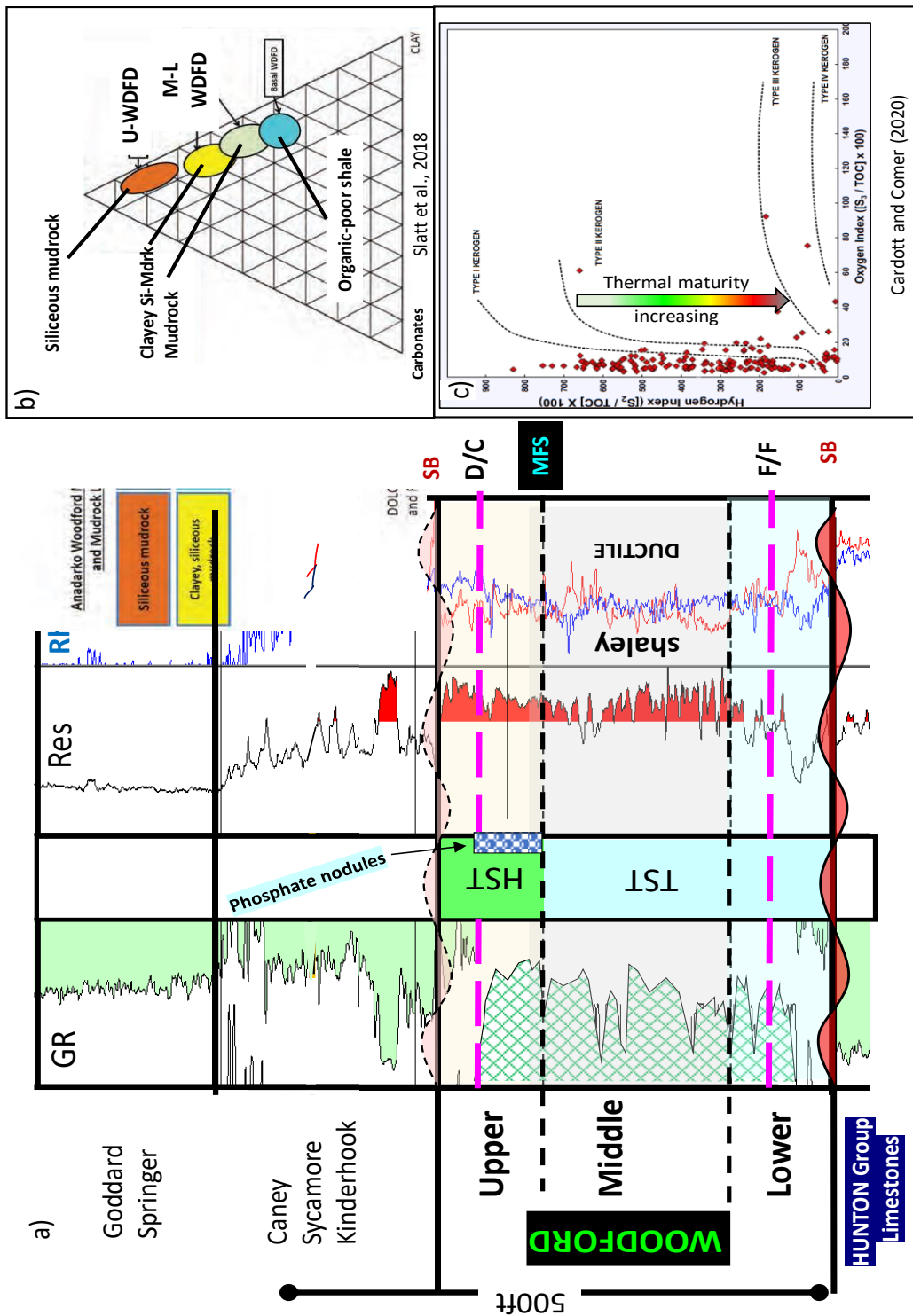


Figure 1.3.3: a) Woodford wireline type log with key surfaces: SB, sequence boundary; MFS, maximum flooding surface. HST, highstand system tract; TST, transgressive system tract; D/C Devonian-Carboniferous boundary; F/F Frasnian-Famennian boundary b) Quartz-carbonate-clay Ternary diagram from XRD data for different Woodford members, c) Modified van Krevlen diagram for Woodford source rocks- decreasing HI reflects increasing thermal maturity.

1.3.2 Woodford Biostratigraphy and Key Surfaces:

Cardott and Chaplin (1993) and Cardott and Comer (2020) provide a good overview of the biota and fauna recovered from the Woodford. The Woodford has a rich microfossils assemblage that include conodonts, radiolaria, sponge spicules, algae, acritarchs, and pollen. Macrofossils are rare but include brachiopods, arthropods, and cephalopods. Additionally, large silicified Callixylon trunks of the progymnosperm Archaeopteris tree occur have been documented at several outcrops (see sites 2.1, 2.3 and review of Suneson, 2010). Trace fossils and burrows are rare and commonly dwarfed/ stressed where present. The bioturbation tends to occur in the lighter colored mudrocks indicative of episodes of more oxygenated bottom waters. Conodont biostratigraphy (Table 1.3.1) provides the best chronostratigraphic framework to constrain the age of contacts, extinction boundaries and the maximum flooding surface in the Woodford (Hass and Huddle, 1965; Over, 1990; Over 1992).

Basal Contact: The Woodford was deposited over of the Hunton Group carbonates along a time transgressive unconformable contact that becomes younger up dip (Figure 1.3.4). With the exception of an early Frasnian age (lower rhenana conodont zone) on the Lawrence uplift (Over 1990), the age of the basal Woodford is poorly constrained. However, no Givetian conodonts have been identified in the Woodford literature. Thus, the Lower Woodford member is considered as early Frasnian in age. Studies and mapping of the Woodford-Hunton contact (Amsden, 1975; Amsden and Rowland, 1967) show that the Hunton Group carbonates were eroded and karsted during a ~20myr interval prior to deposition of the Woodford and the greater Taghenic onlap sequence. Local mapping of 12 Woodford intervals on the Cherokee Platform shows that the unconformity has 100ft of relief (McCollough, 2017). Although the low areas filling during the ensuing sea level rise are referred to as incised valleys, the karsted nature of the surface and a lack of well identified fluvial systems suggest that dissolution valleys may be a better genetic term.

Table 1.3.1 Late Devonian Earliest Mississippian conodont zones used by Over (1990). Inset shows approximate position of the major extinction boundaries relative to top of the Hunton and top of the Woodford.

	Late Devonian				Frasnian			Devonian			Early			Carboniferous				
	An trangularis	L. rhenana	M. rhenana	U. rhenana	linguliformis	L. trangularis	M. trangularis	U. trangularis	L. expansa	M. expansa	Famennian	U. expansa	Lower praesuclata	Upper praesuclata	suclata	Kinderhookian / Tournasian	Lower duplicata	Upper duplicata
<i>Si. obsoluta</i>																		
<i>Si. cooperi</i> m-2																		
<i>Si. duplicata</i> sensu Hass																		
<i>Si. duplicata</i> m-2																		
<i>Si. duplicata</i> m-1																		
<i>Si. sulcata</i>																		
<i>Ps. primus</i>																		
<i>Pr. kockeli</i>																		
<i>Pr. collinsoni</i>																		
<i>Pr. meishneri</i>																		
<i>Si. praesuclata</i>																		
<i>Ps. mfb</i> trigonicus																		
<i>Pa gr. gonioclymemie</i>																		
<i>Pelekysgnathus</i> guiz																		
<i>Bi. aculeatus</i>																		
<i>Pa. gracilis</i> expansa																		
<i>Pa. gracilis</i> gracillius																		
<i>Br. ornata</i>																		
<i>Bibispathodus</i>																		
<i>Po. communis</i> com																		
<i>Bi. stabilis</i> m-1																		
<i>Pa. minuta</i> minuta																		
<i>Pa. per. perilobata</i>																		
<i>Pa. regularis</i>																		
<i>Pa. tenuipunctata</i>																		
<i>Pa. del. clarki</i>																		
<i>Pa. del. delicatula</i>																		
<i>Pa. subperlobata</i>																		
<i>Pa. trangularis</i>																		
<i>Pa. praetringularis</i>																		
<i>Ag. ubiquitous</i>																		
<i>Pa. linguliformus</i>																		
<i>An. asymmetricus</i>																		
<i>Pa. rhenana</i>																		
<i>Pa. unicornus</i>																		
<i>An. trangularis</i>																		
<i>Ad. lobata</i>																		
<i>Ad. bigas</i>																		
<i>Pa. proversa</i>																		
<i>Pa. punctata</i>																		
<i>Pa. transstans</i>																		

Section	F/F boundary above HUNTON meters	DC Boundary below top WDFD	References
McAlister Cemetery Quarry	11.5	2	Over, 1990, Cullen Hg spike
I-35 South	covered	4.5	Over 1990, 1992; Kondas 2018
Wapanucka Shale Pit	covered	81	Over 1990, 1992
Goose Creek	covered	0.8	Over 1990, 1992
Ebby Dam	covered	0.5	Over 1990, 1992
Hass-G	covered	0.6	Over 1990, 1992
Weldon Type	covered	0.6	Over 1990, 1992
Guest Ranch	covered	0.6	Over 1990, 1992
Henryhouse Ck. HASS-A	3.3	covered	Over 1990
YMCA / HASS-B	16.15	covered	Over, 1990, Crick, 2002; Aujfil, 2007.
Wyche / Ryan	26	truncated (Over)	Molinares-Blanco, 2013, T-R sequences
Hass En	0.21	covered	Over 1990 (1 mi west of Wyche)
Burning Mtn	0.2	covered	Over 1990

Table 1.3.1 Late Devonian to Early Mississippian conodonts and zones after from Over (1990, 1992). Inset shows distances to D/C and top Woodford and F/F and Hunton.

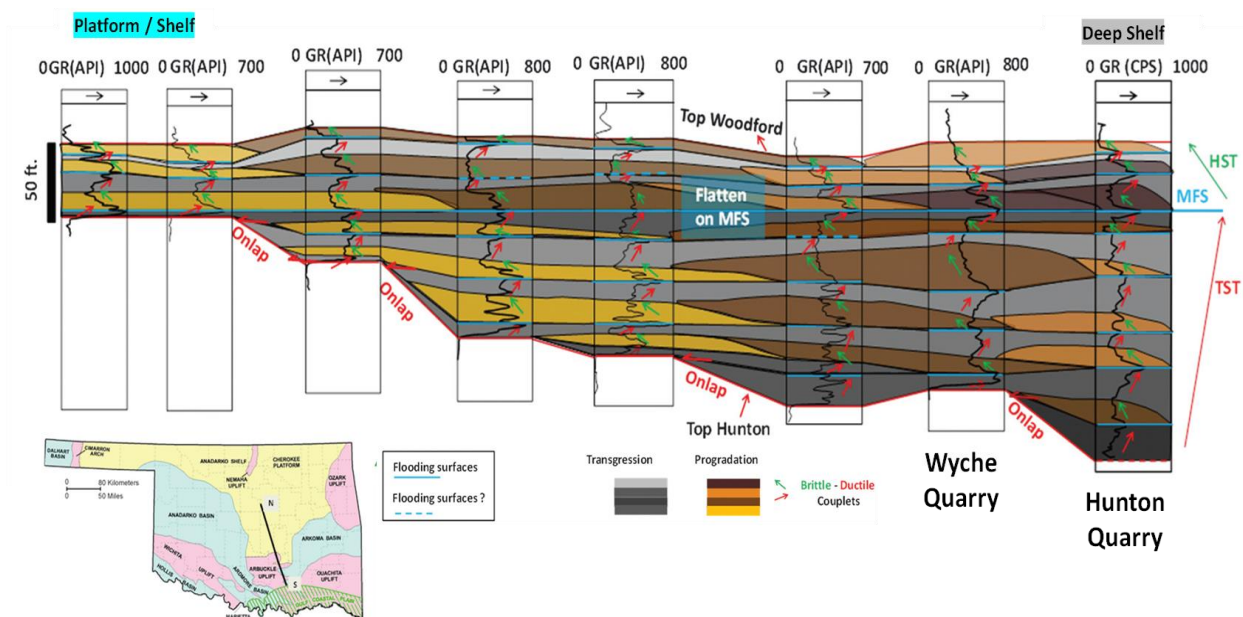


Figure 1.3.4 Regional gamma ray stratigraphic section, MFS as datum, showing progressive onlap of basal Woodford and stacking of Woodford parasequences in transgressive and high stand systems tracts (McCullough, 2012).

Frasnian-Famennian Boundary: The Frasnian-Famennian boundary is defined by the first appearance of *Pa triangularis* and of *Pa del delicatula* (Over, 1990; see Table 1.3.1). From these studies the F/F boundary is known from 5 widely spaced locations from the Lawrence uplift to McAlister Cemetery Quarry (Table 1.3.2). The thickness of the Frasnian section ranges from 53ft at the YMCA/Hass-B location to less than 1ft at Burning Mountain in the Arbuckle Mountains and Hass-En location on the Lawrence uplift. The range in thickness is consistent with documented onlap and relief on the Hunton Group below the basal Woodford sequence boundary. An alternative method for placement of the F/F boundary using chemostratigraphy was proposed by Turner et al., (2016), who was working at the Hunton Quarry Anticline (Section 3.1) where there is no biostratigraphic control. This method places the “Chemostratigraphic FF Boundary” above the maximum flooding surface which is 80-90ft higher in the section than at nearby outcrops where the F/F boundary is biostratigraphically determined (Figure 1.3.5 and Table 1.3.2). Therefore, unless calibrated by co-located conodont biostratigraphy, we strongly object using chemostratigraphic data to determine the F/F boundary.

Locations	Frasnian Thickness m	Carboniferous Thickness m	References
Hass-G	covered	0.6	Hass and Huddle, 1965; Over, 1992
Weldon Type	covered	0.6	Over, 1992
Dump Draw Ryan Shale Pit	covered	top truncated	Over, 1992
Hass En	0.21	covered	Hass and Huddle, 1965; Over, 1990
Wyche Pit & Wyche-1	26	no data	Turner et al., 2016; Molineres et al., 2019
Goose Creek	covered	0.8	Over, 1990
Ebby Dam	covered	0.5	Over, 1990
Burning Mtn	0.2	covered	Over 1990
Hunton Quarry Anticline	50	no data	Turner et al., 2016
Hass-B YMCA	15.7	covered	Over, 1990; Crick, et al., 2002
Hass-A Henry House Creek	3.3	covered	Hass and Huddle, 1965; Over, 1990
Speake Ranch	61	30	Molinales et al., 2019
I-35 South	covered	4.5	Over, 1992; Kondas 2018
McAlister Cemetery Quarry	16	0/2?	Over, 2002; , Cullen, 2018
McAlister Cemetery Quarry	65	no data	Molinales et al., 2019
Wapanucka Shale Pit	covered	55 / 30	Over, 1992; Puckette et al., 2013

Table 1.3.2 Key sections where F/F and D/C boundaries have been established. Green highlights are conodont constrained distances, yellow highlights are chemostratigraphically constrained distances.

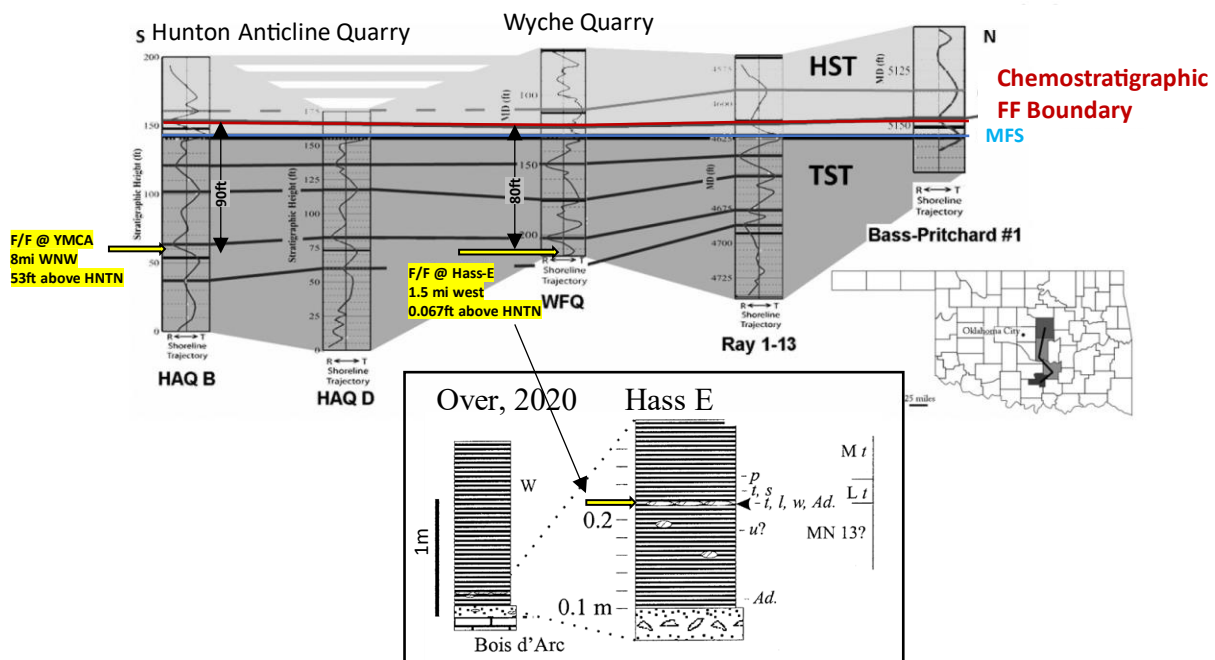


Figure 1.3.5 Chemosequence Stratigraphic correlations from Turner et al., (2016). Datum is the maximum flooding surface (MFS). Yellow text denotes nearest F/F boundary locations and distances to sections displayed (Over, 1990; Crick et al., 2002).

The Maximum Flooding Surface: The maximum flooding surface (mfs) lies within the Middle Woodford and is defined and mapped from wireline logs, particularly from the gamma ray and density logs. There may be small differences in the precise positioning of the mfs depending on different geologists' weighting and interpretation of the different log curves. Even considering this uncertainty the mfs is probably the most consistent and widely mapped intra-Woodford pick. In measured outcrop the handheld gamma ray is used to position the mfs. As noted above the mfs is closely associated with the Chemostratigraphic FF Boundary of Turner et al., (2016); low continental input (Zr, Ti) and higher redox sensitive metals (U, Mo). Considering the unconformities at the top and base of the Woodford, we consider the mfs as the most reliable stratigraphic datum for flattening regional cross sections.

The Devonian-Carboniferous Boundary: On the basis on conodont biostratigraphy the Devonian-Carboniferous (D/C) boundary has been determined at 7 locations within the study area. This boundary was primarily defined by the first appearance *Siphonodella sulcate* and the last appearance *Palmatolepis gracilis gracillis* (Over, 1992; Table 1.3.1). The precise position of the D/C boundary at these outcrops may eventually be shifted to account for proposed revisions in global Famennian conodont zonations which emphasize assemblages (zones) of first appearances (Spallata et al., 2017). The D/C boundary is well constrained at 5 locations on the Lawrence uplift (Table 1.3.2). With the exception of the Wapanucka section in the Arkoma basin (Section 5.1), the Mississippian/Tournasian section of the Upper Woodford is thin and may be truncated at the Wyche Quarry (Section 2.1) and the McAlister Cemetery Quarry (Section 4.1). The D/C boundary is well constrained at the I-35S roadcut and is supported by palynology data (Kondas et al., 2016).

Top Woodford Sequence Boundary: The relationship between the top of the Woodford and overlying Mississippian strata is complex. Although there is no evidence for subaerial exposure the combination of non-deposition and evidence for submarine erosion at different locations strongly suggests the presence of a sequence boundary associated with the early Tournasian lowstand. On the Lawrence uplift the pre-Welden shale and Welden Limestone represents an extremely condensed Kinderhookian to Osagean section. In the Arbuckle Mountains and Ardmore basin, given current biostratigraphic data, there is an ~11myr gap below the influx of siliciclastic-carbonate mass flow deposits on the Sycamore Limestone submarine fans (Figure 6.1.5). The

limestones and greenish shales of the earliest Mississippian interval appear to record period of oxic bottom waters before a return to more reduced conditions represented by the deposition of the bituminous Caney Shale during the subsequent transgression.

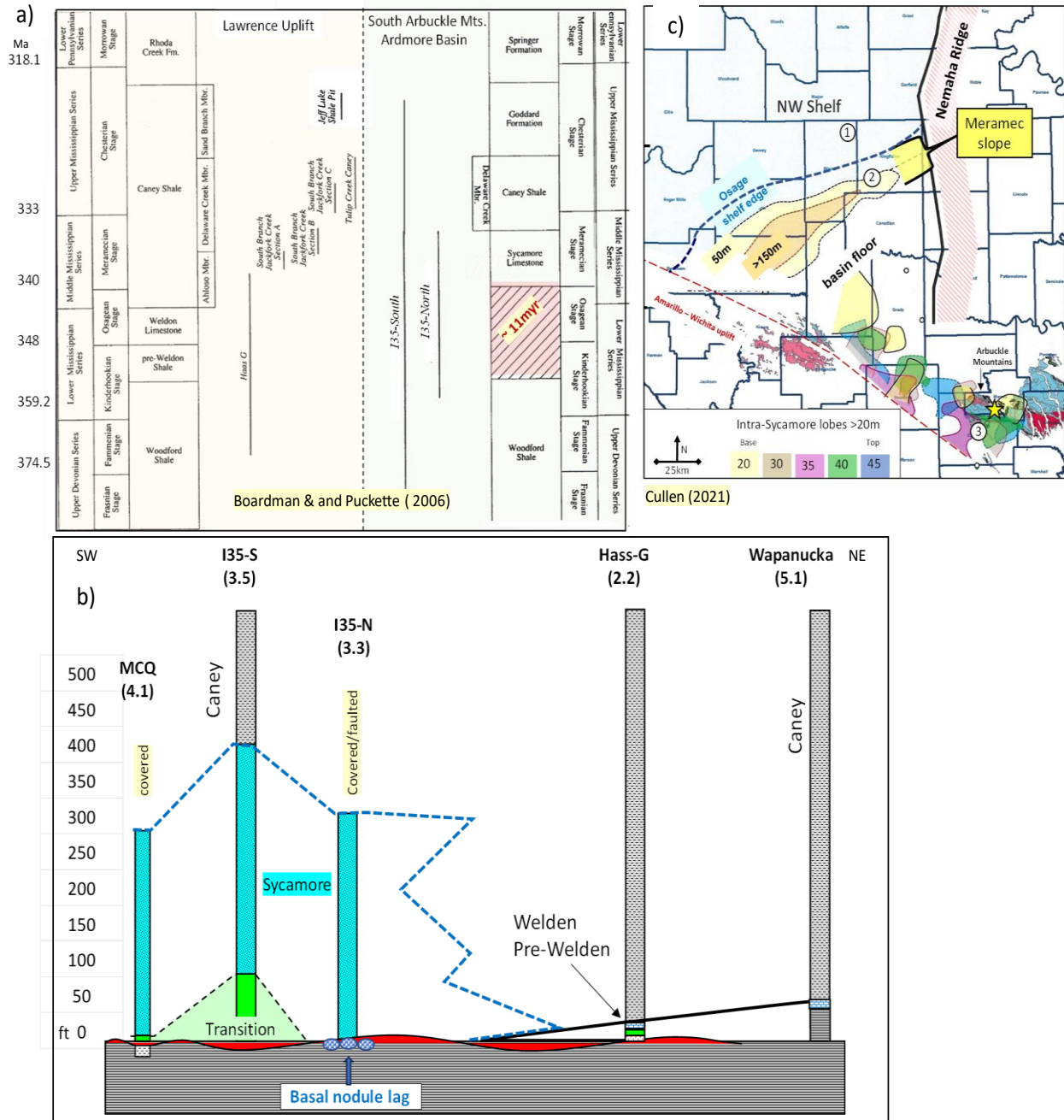


Figure 1.3.6 a) Time-stratigraphic correlation from the Lawrence uplift to the Ardmore basin (Boardman and Puckette, 2016) b) lithostratigraphic correlations c) Paleogeographic map showing confinement of Sycamore to the Ardmore basin and incipient uplift of the Nemaha Ridge (Cullen, 2021).

1.3.3 Woodford Lithofacies: Over the prior decades various workers studying outcrops and cores have defined up to 12 different lithofacies for the Woodford (Table 1.3.3). The diversity in these proposed lithofacies reflect differences in parameters such as texture, color, degree of lamination, weathering traits, diagenetic features, XRF elemental data, and whether thin petrography was used to augment hand sample descriptions. We have set aside some of these variables to layout a relatively simple field-based facies scheme. Whilst there may be inherit problems with this approach as certain diagenetic features - notably pyrite, phosphate, and glauconite- are treated as features within the facies - these can supplemental descriptors to aid a better understanding to the overall framework. We find that Ruppel’s (2016) shale depositional model (Figure 1.3.7) is of great utility when applied to the Woodford as done by (Ekwunife, 2017).

Author	Yr.	# facies	Descriptions / Definitions	Location (Section)	Lat Long
Aufill	2007	5	Defined lithologic intervals of laminated, fissile, to massive Si-mudrock and corresponding chert	YMCA / Camp Classen (3.4)	34°27'40.83"N 97° 9'5.54"W
Serna-Bernal	2014	4	Si-Shale, Si-siltstone, Laminated chert, Laminated fine-xln dolomite,	McAlister Cemetery Quarry (4.1)	34° 4'39.43"N 97° 9'19.30"W
McCollough	2014	9	Black laminated mudrock, Black massive mudrock, Laminate mudrock, Massive mudrock, Siliceous siltstone, Calcareous siltstone,	Rya-1 Pottawottamie. Co.	34°58'43.67"N 97° 4'0.39"W
Turner et al	2015	8	Siliceous mudrock, Siliceous shale, Calcareous mudrock, Siliceous shale w/ PO, Siliceous-argillic mudrock, argillic mudrk w/ detrital qtz.	Wyche Core (2.1)	34°40'43.17"N 96°39'53.96"W
Galvis	2017	7	Arillaceous shale, Siliceous shale, Brown siliceous mudstone, Siliceous mudstone, chert, Siliceous dolomitic shale, Dolomitic mudstone	Speake Ranch (3.6)	34°22'39.55"N 97°20'10.03"W
Becerra-Rondon	2017	4	Siliceous shale, Chert, Dolo-mudstone, Siliceous domolitic mudstone	I35-S WDFD (3.5)	34°21'6.83"N 97° 8'56.39"W
Ekwunife	2018	8	Clay shale, mud shale, clay-mud shale, Siliceous mudshale, Siliceous mudstone, chert, Dolomitic -mudstone, bleached rock	McAlister Cemetery Quarry (4.1)	34° 4'39.43"N 97° 9'19.30"W
Brito	2019	6	Siliceous mudstone, Siliceous shale, Black chert, Arillaceous shale, Green clayst, Dolomitic mudstone	Maritetta Basin, TX (4.2)	33°43'33.79"N 96°45'33.68"W

Table 1.3.3 Comparison of different Woodford lithofacies defined by different authors

Ruppel defined 4 interfingering facies: 1) land derived siliciclastics, 2) argillaceous mudrock, 3) highly siliceous mudrock, and 4) siliceous ooze/chert. Spatially these facies, one through four, represent a basinward decrease in terrestrially derived clay and silt and a concomitant increase in the percentage of intrabasinal siliceous radiolarian tests that are prone to early diagenesis. The extremely low depositional gradient means that even small changes in sea level can drive large lateral shifts in facies. From Walther’s Law it follows that the lateral interfingering of adjacent facies is expressed vertically as interbedded brittle-ductile couplets intermixing petroleum source rocks with petroleum reservoir rocks that are both critical in making the Woodford Shale a prolific unconventional reservoir (Slatt and Abousleiman, 2011).

Our model, like other variants, interprets facies changes largely as a function of fluctuations in sea level across the broad flat shelf of the Oklahoma Basin's epeiric sea while omitting significant nuances.

These facies models do a good job at the regional scale but are less effective when dealing with more localized or temporal factors (Figure 1.3.9) including paleotopography (Kvale, 2014; Cardott and Comer, 2022), restriction, sediment supply, antecedent structure, differential compaction and temporally changing atmospheric-oceanographic variables (wind direction, wind speed, ocean bottom currents in relation the Eckman effect and seasonality of surface winds upwelling (Wignall, 1994). Further work on these temporal and local parameters is likely to yield insights on the processes controlling: 1) the distribution of phosphate & controls on nodule morphology, 2) the varied concentration pyrite, 3) development of euxenic episodes and 4) drivers of mass extinction events.

Facies Descriptions: (see Figures 1.3.7 and 1.3.8)

Land Derived Siliciclastics: This facies is found exclusively near the basal Woodford contact. Brito (2019) notes it is 66% clay and 27% tectosilicates. The facies is commonly bioturbated/unlaminated and very low in TOC (Brito offers no value but <1% where described). It is very ductile due to the high clay. This basal succession is present McAlister Cemetery Quarry (Section 4.1) and Speake Ranch (Section 3.6). This facies is commonly described at the base of the Woodford, regardless of which part is overlapping the underlying rock. In places it is siltier and related to incised valley-fill e.g., the Misner sandstone, but this is localized and likely represents a pre-transgression erosional stratigraphic remnant at the base of the Woodford. Argillaceous shales of this facies can weather green and papery on the outcrop and these are not necessarily the land derived claystones described here, however, with a bit of digging fresh rock often proves to be dark, laminated, and relatively organic-rich (figure 1.3.8c).

Argillaceous Mudrock: Brito describes argillaceous mudrocks as 40% clay and 40% quartz+feldspar with TOC between 7-10% but this can be less outside of Brito's study area. The TOC is algal-dominated and tasmanities cysts are abundant. Pyrite can be abundant in these rocks, both nodular and framboidal. These facies are commonly laminated but have been identified to be slightly bioturbated with nerities traces or dwarfed ill-formed trace fossils. This facies is often the "ductile" component in the brittle ductile couplets. The quartz is mostly detrital grains and does

not contribute much to lithifying cement. As such compaction can destroy porosity preventing these rocks from contributing unconventional reservoir rock but they can be excellent source rocks.

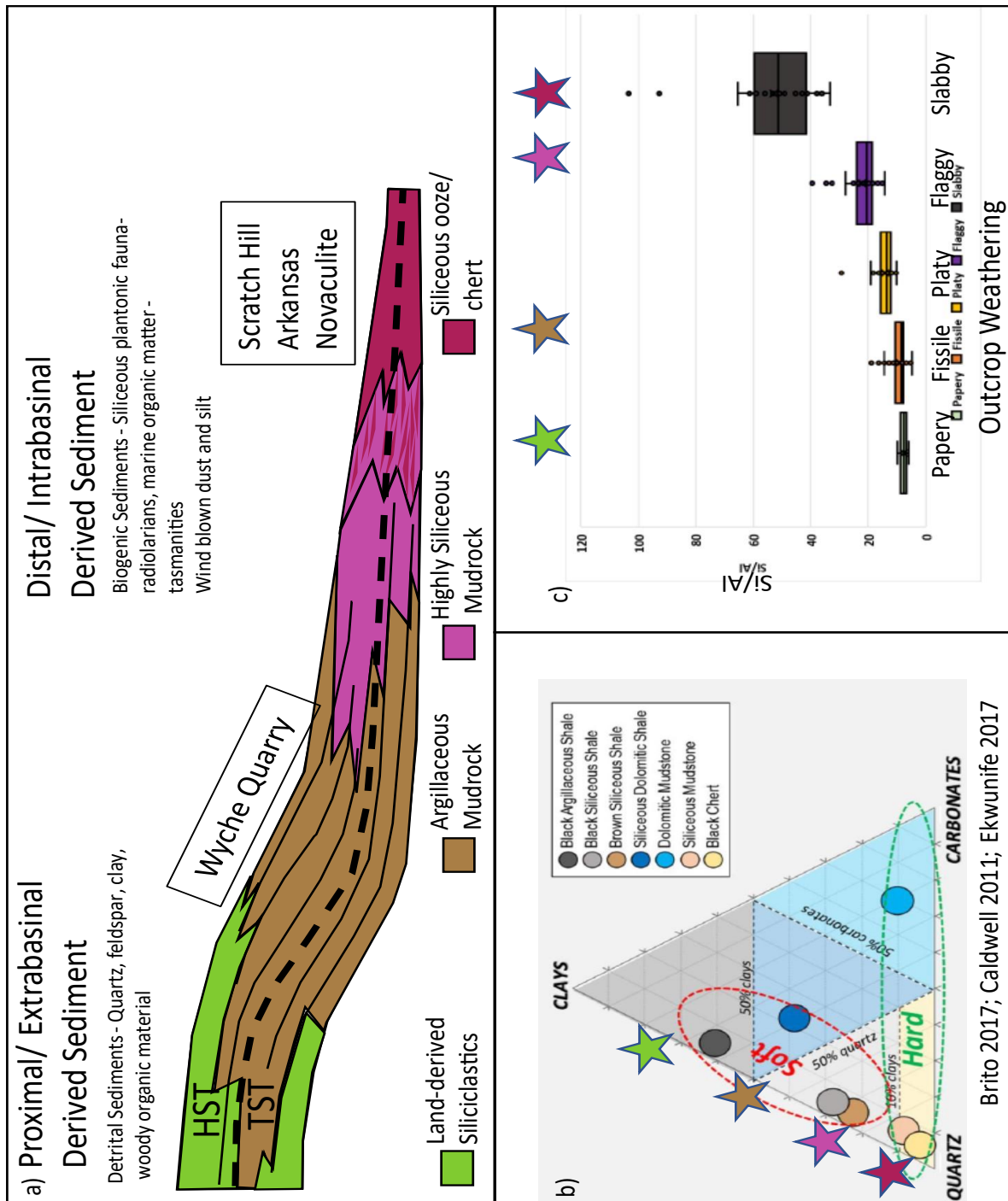


Figure 1.3.7: a) Adaption of Ruppel's (2016) clastic shale system, showing positions of endpoint locations. b) Brito's (2019) facies on ternary coupled with our simplified facies scheme. c) Weathering style (Ekwunfe, 2017) with Ruppel's facies in colored stars.

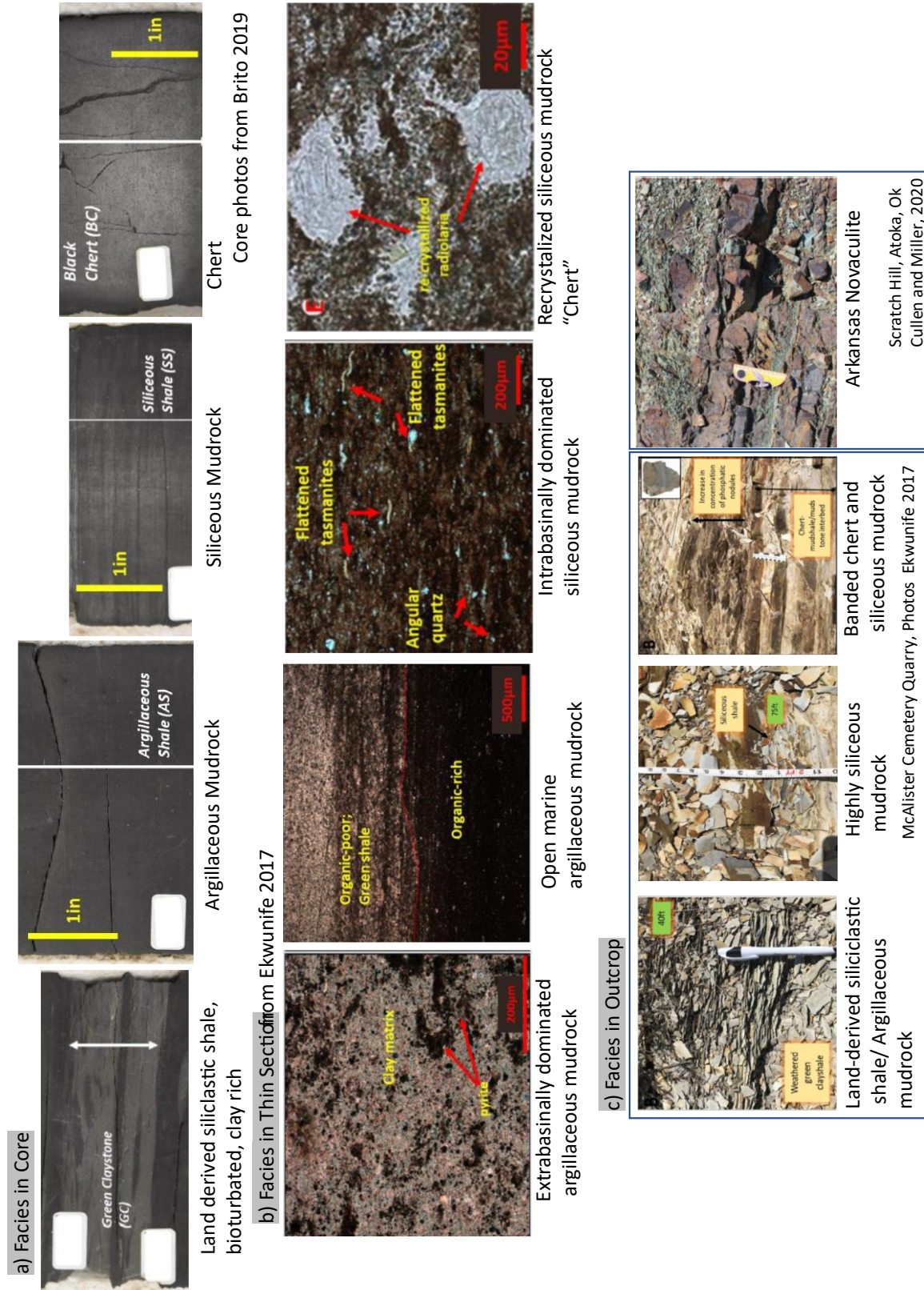


Figure 1.3.8 Photographs of most common lithofacies in a) core, b) thin section and c) outcrop.

Argillaceous mudrocks dominate the Lower and Middle Woodford and its qualities can vary significantly due to its broad depositional range. It often weathers poorly and can be papery or fissile (Figure 1.3.8c).

Siliceous Mudrock: Distal to the area dominated by argillaceous mudrock deposition siliceous mudrock is found. This facies tends to have substantially more intrabasinal particles than previously discussed facies. The facies is commonly 60-70% quartz+feldspar with 20-30% clay and 4-8% TOC (Figure 1.3.8b). This facies is almost always laminated and bioturbation is exceptionally rare. If the facies is massive it is more than likely homogeneously laminated. Pyrite can be common in these rocks. The quartz can be either detrital grains or authogenic/biogenic in the form of radiolarians. As such there can be enough cement to prevent compaction without occluding porosity. This facies is very common in the Middle and Upper Woodford. This rock resists weathering and produces low relief outcrops littered with platy debris (Figure 1.3.8c).

Siliceous Ooze/Chert: The most distal facies, siliceous ooze/ chert is usually interbedded with the siliceous mudstone but it can form much thicker beds more distally. The facies is typically close to 90% tectosilicates (with little to no feldspar) and less than 10% clay. Within the petroleum system it is typically 2-4% TOC but it can be less distally. Due to the high quartz cement content, mostly from radiolarians, this facies strongly resists compaction, but porosity is commonly occluded by cement. This also can prevent it from acquiring a laminated appearance. This facies resists weathering and is always the brittle component of brittle-ductile couplets common in the Woodford.

Dolomitic Mudrocks: Dolomitic mudrocks are also present in the Woodford as very hard beds. They are relatively rare or under recognized due to confusion with chert beds. These are the only significant carbonate beds observed in the Woodford. Brito (2019) reports these to be 50% dolomite, 35% quartz and 10% clay and have 2-4% TOC (Ekuwenfie, 2017). These rocks are usually highly uncompacted and very well cemented. Some workers have suggested the more massive dolomite beds at the Hunton Quarry Anticline (Section 3.1) are recrystallized calciturbidites. An alternative interpretation, which we favor, is that the massive ferroan dolomite beds are organogenic dolomites formed by sulfate reduction and methanogenesis as has been interpreted for similar beds elsewhere (Mazzulo, 2020). Both geochemical processes are known to occur or likely to occur in the Woodford.

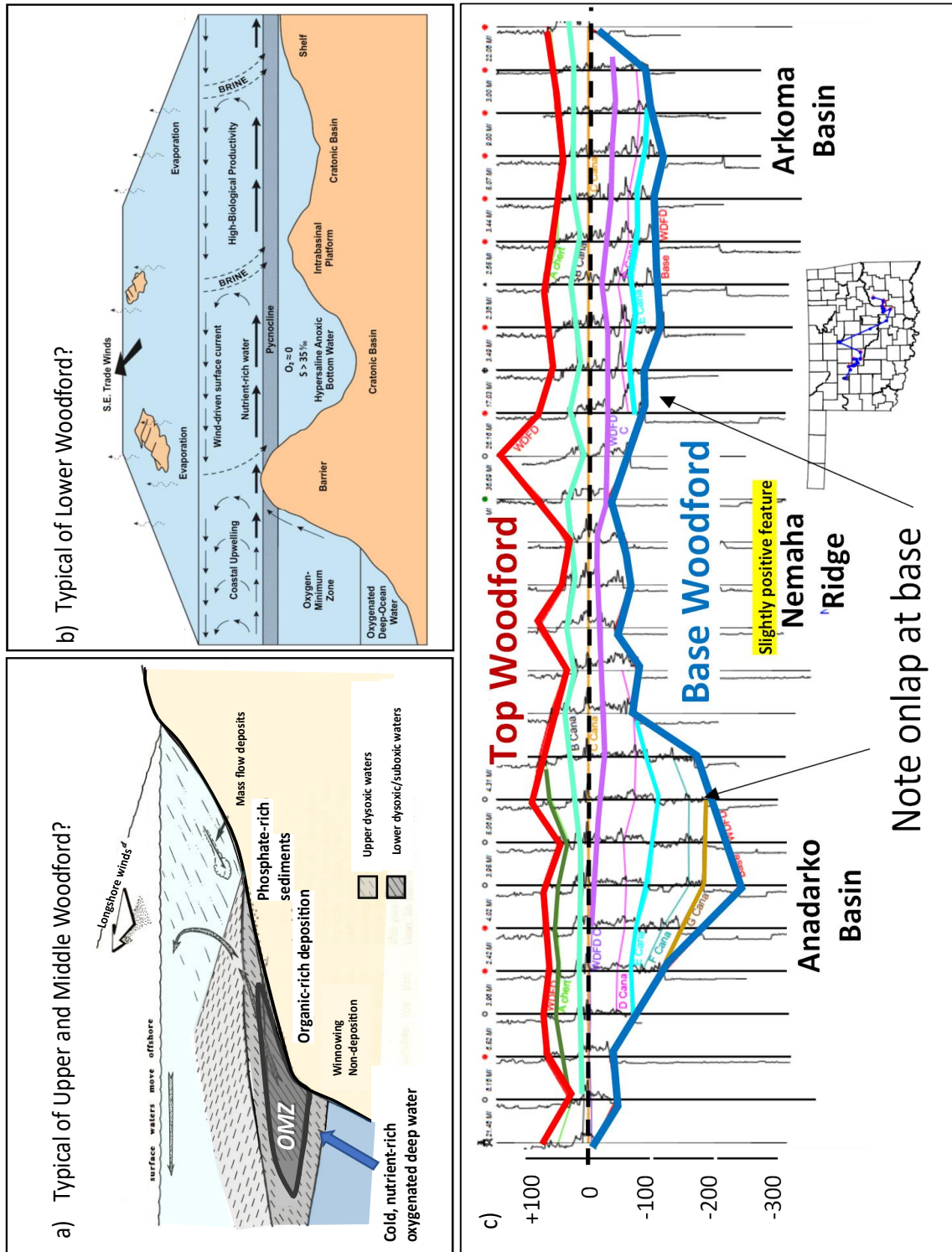
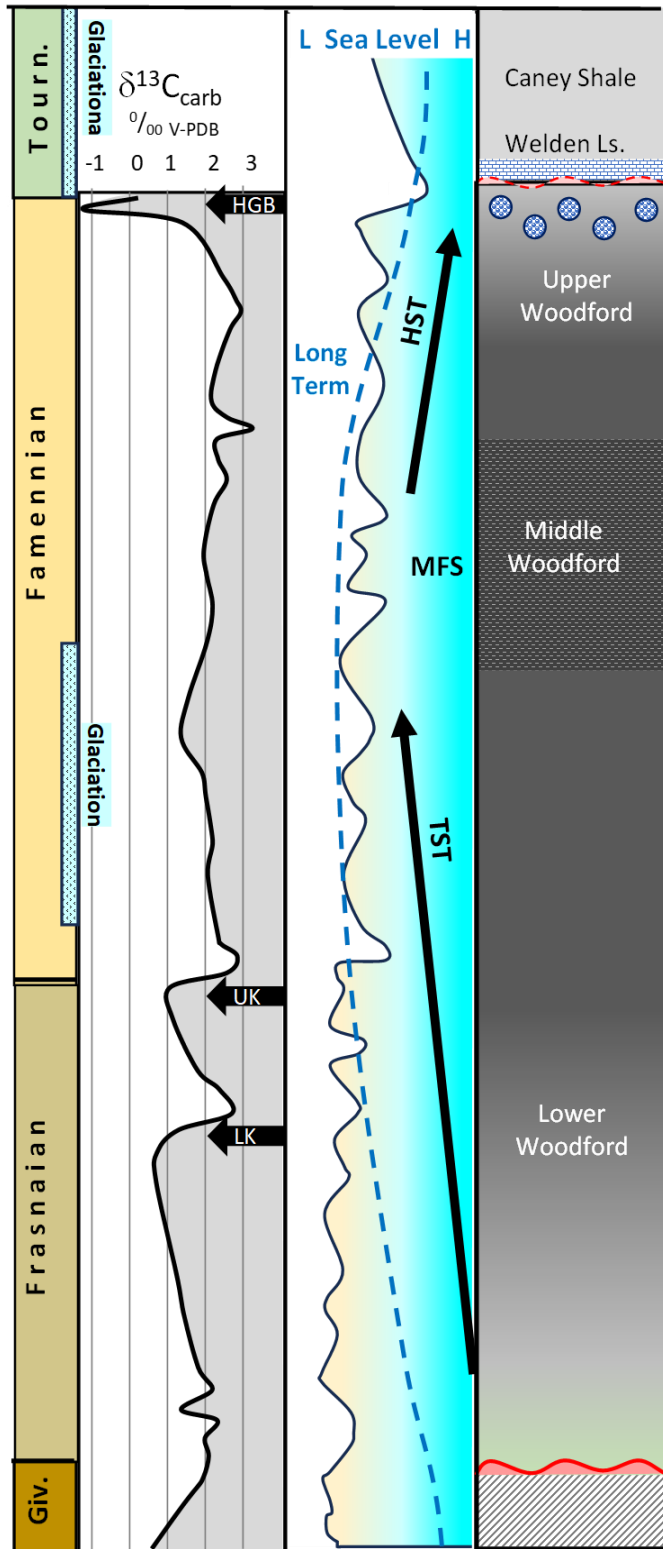


Figure 1.3.9 Environmentally and bathymetric driven facies controls a) Simplification of an upwelling zone showing areas of phosphate deposition, turbidite input, and deep oxygen-rich water (Wignall 1994). b) Local restriction/ paleotopography which may be more significant (Cardott and Comer 2021). c) Strike section showing that lower and middle units onlap and cover bathymetric highs features (Kvale and Bynum, 2014).



1.3.4 Woodford Sequence Stratigraphy:

The Lower and Upper Woodford were deposited during a major rise & fall in long-term eustatic sea level, respectively, and correspond to transgressive (TST) and high stand (HST) systems tracts (Figure 1.3.10). The maximum flooding surface (mfs) occurs in the Middle Woodford which has relatively higher clay and organic carbon percentages. Shorter term sea level fluctuations superimposed on the long-term trends produce a subset of up to 7 transgressive and regressive parasequences (Slatt et al., 2018). The turn-around in sea level from highstand to falling stage likely occurred within the upper Woodford.

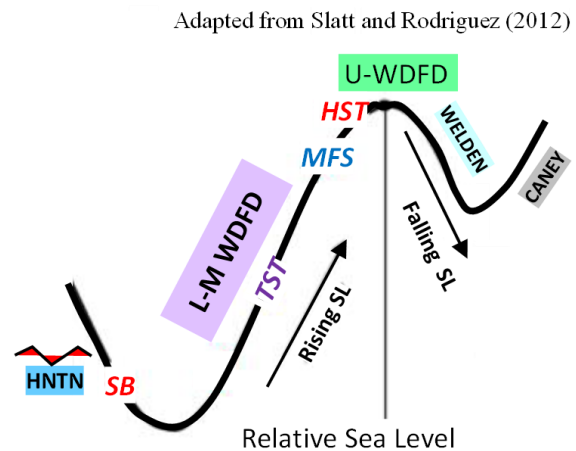


Figure 1.3.10 Idealized Woodford sequence stratigraphic framework in relation to $\delta^{13}\text{C}$ organic, sea level fluctuations, and glacial episodes. Inset shows systems tracts in relation to Devonian-Mississippian first order cycle.

1.3.5 Woodford Petroleum Geology: From a petroleum systems perspective the Woodford Shale is unarguably the most important stratigraphic unit in the Midcontinent. As a source rock it has generated and expelled the majority of oil and gas produced in Oklahoma and Kansas and is the dominant critical factor that makes the Anadarko basin a “Super Basin” (Fritz and Mitchell, 2021). Woodford mudrocks and shales also serve as the top and lateral seal for structural and stratigraphic traps in the underlying Hunton Group carbonates. Additionally, naturally fractured Woodford is known to produce from several anticlinal traps in the Ardmore and Marietta basins, e.g., the Caddo field about 6mi south of the I35-S outcrops (Section 3.5).

Over the last twenty years hydraulic fracture stimulation of horizontal wells in the Woodford Shale has exponentially increased its importance as a self-sourced reservoir. Since 2010 more than 6,000 horizontal Woodford wells have been completed in Oklahoma (Figure 1.3.12b). Critical subsurface success factors underpinning the Woodford horizontal play are its widespread distribution of more than 150ft of thickness, high original organic content, a broad range of thermal maturity, and a high percentage of brittle siliceous-brittle beds, and (Figure 1.3.11a).

The ratio of siliceous-brittle beds to argillaceous-ductile beds (brittle-ductile couplets) is an important success factor; siliceous beds are more easily fractured but have lower TOC, hydrocarbons-in-place, and slower penetration rates (Slatt et al., 2018). Most operators strive to land their laterals in target zones that optimize both geomechanical properties and hydrocarbon storage.

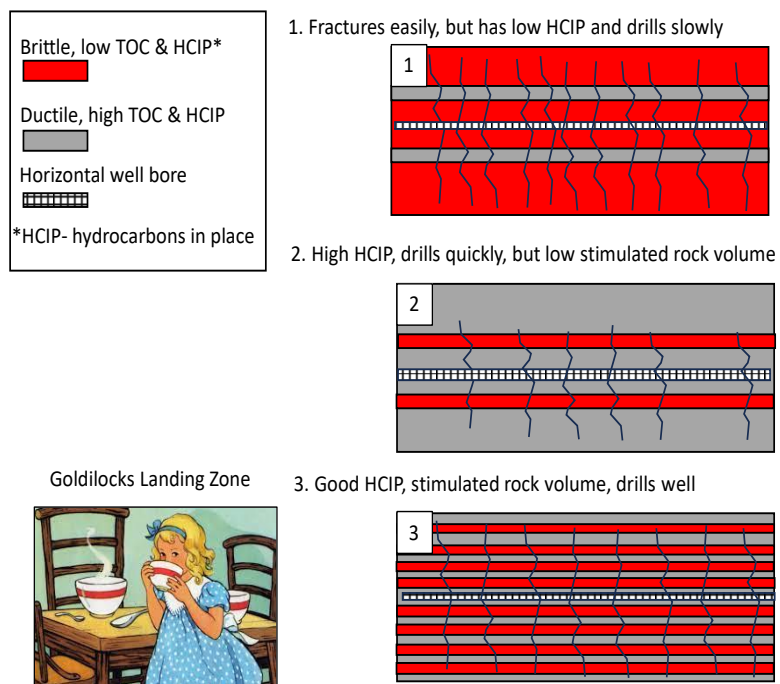


Figure 1.3.11 Idealized Woodford geomechanical end members.

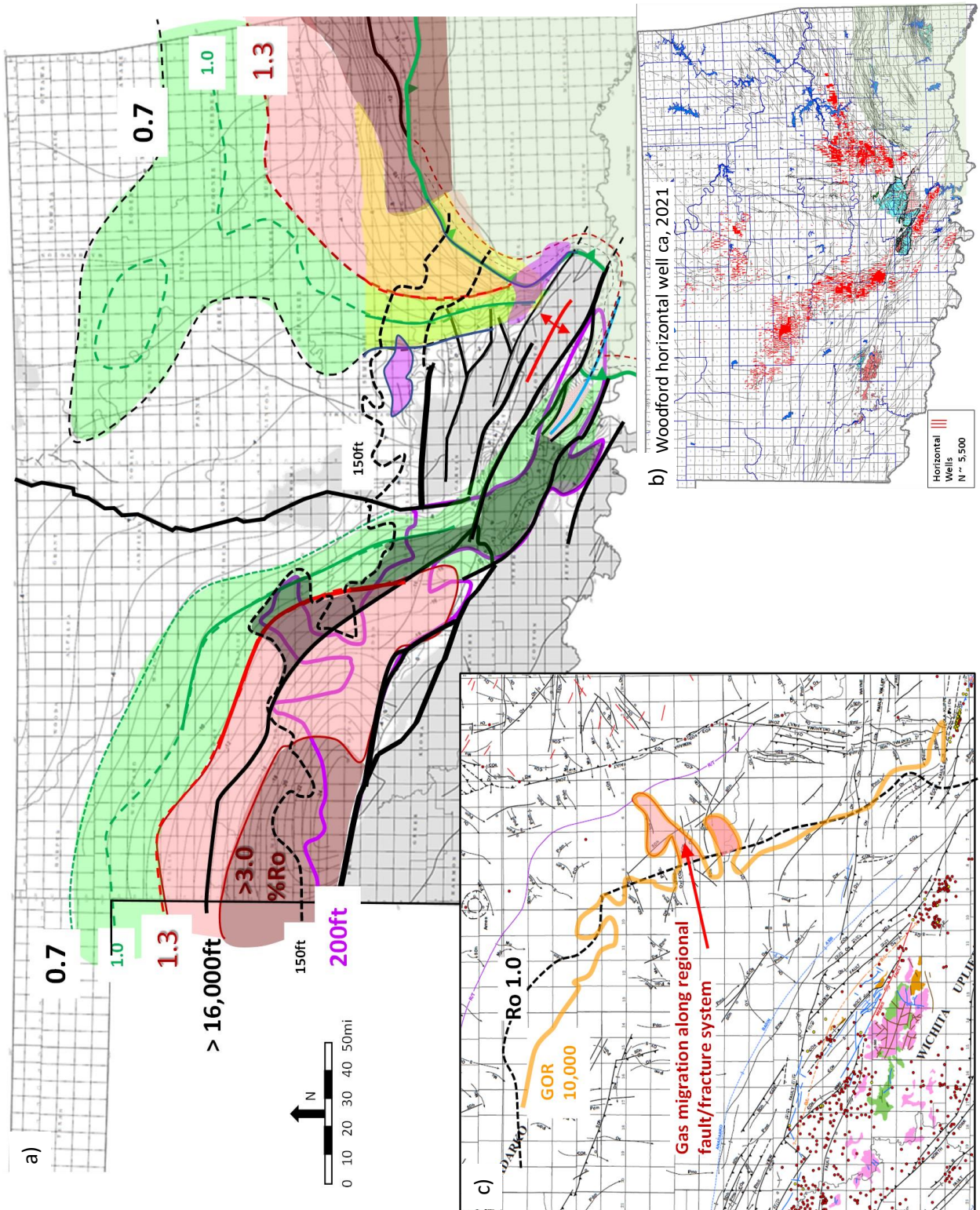


Figure 1.3.12 adapted from Cullen 2021 a) Structure, isopach, and %Ro map (structure map from Evans, et al., 2018; vitrinite reflectance data, Cardott, 2013) b) Horizontal completions c) GOR map showing migration of gas (higher GOR) along regional fault-fracture systems.

Initially operators targeted the gas window of the Woodford horizontal play. As the intensity of the fracture stimulations increased the play was successfully extended into the oil window. Maturity data such as vitrinite reflectance, Gas-Oil Ratio, and API oil gravity were used to refine leasing and appraisal strategies. These variables generally have positive correlations with each other. However, in places gas migration along regional fault-fracture systems gives a false impression of higher maturity than other indicators (Figure 1.3.11c). In addition to geomechanical information, the geometry and intensity of natural fracture systems in the Woodford are important component of outcrop observations (Figure 1.3.12), particularly in light of the notable concomitant increase in the magnitude of completions-induced seismicity as the intensity of Woodford completions, fracture stimulation in pounds per foot, nearly doubled (Cullen, 2020).



Figure 1.3.13 Photographs of outcrop fracture sets in the Woodford, a) Wyche Quarry (2.1) b) S. Jack Fork Creek (2.3) c) Hunton Quarry Anticline (3.1), d) I77-D Heart of the Arbuckles (3.2).

1.3.6 References:

Brito, R., 2019, The Woodford Shale in the Marietta Basin, University of Oklahoma PhD (unpublished), 208 p.

Cardott, B.J., and J.R. Chaplin, 1993, Guidebook for selected stops in the western Arbuckle Mountains, southern Oklahoma: Oklahoma Geological Survey, Special Publication 93-3, 55 p.

Cardott, B.J., 2012, Thermal maturity of Woodford Shale gas and oil plays, Oklahoma, USA, *International Journal of Coal Geology* 103, p. 109–119

Cardott, B.J., and Comer, J.B., 2020, Woodford Shale (Upper Devonian to Mississippian) from Hydrocarbon Source Rock to Reservoir, *Oklahoma Geological Survey Bulletin* 152, 100 p.

Crick, R.E., Ellwood, B.B., Feist, R., El Hassani, A., Schindler, E., Dreesen, R., Over, D.J., and Girard, C., 2002, Magnetostratigraphy susceptibility of the Frasnian/Famennian boundary: *Palaeogeography, Palaeoclimatology, Palaeoecology*, v. 181, p. 67–90.

Cullen, A.B., 2020, Completions-Induced Seismicity in the STACK-SCCOP area of central Oklahoma: Alpha SE, Oklahoma. *Oklahoma City Geological Society Shale Shaker*, 71, p.36-45.

Donovan R.N., 1986, The Geology of the Slick Hills, in Donovan, R. N., ed., *The Slick Hills of southwestern Oklahoma—Fragments of an aulacogen?*: Donovan, R. N., ed., *Oklahoma Geological Survey Guidebook* 24, p. 1-12

Ekwunife, I. C., 2017, Assessing mudrock Characteristics, high-resolution chemostratigraphy, and sequence stratigraphy of the Woodford Shale in the McAlister Cemetery Quarry, Ardmore Basin, Oklahoma, University of Oklahoma MSc thesis, 168 p.

Evans, S.C., Allen, J.P., Brown., D.P., 2018, Preliminary Structure Map of the Woodford Shale, Oklahoma, Oklahoma Geological Survey, Open File Report OF17-2018

Fritz, R.D. and Mitchell, J.R., 2021, The Anadarko “Super” Basin: 10 key characteristics to understand its productivity, *AAPG Bulletin* 105-6, p. 1199–1231.

Gay, P. S., 2003, The Nemaha Trend- A system of compressional thrust-fold, strike-slip structural features in Kansas and Oklahoma, *Oklahoma City Geological Society Shale Shaker*, 54, p. 9-17.

Golonka, J., 2020, Late Devonian paleogeography in the framework of global plate tectonics, *Global and Planetary Change*, 186, p.1-19.

Hass, W.H., and J.W. Huddle, 1965, Late Devonian and early Mississippian age of the Woodford Shale in Oklahoma as determined from conodonts, in Geological Survey Research 1965: U.S. Geological Survey Professional Paper 525-D, p. 125-132.

Hoffman, P., Dewey, J.F., Burke, K., 1974, Aulacogens and their genetic relation to geosynclines, with a Proterozoic example from Great Slave Lake, Canada. In: Dott Jr., R.H., Shaver, R.H. (Eds.), Modern and Ancient Geosynclinal Sedimentation: SEPM Special Publication, 19, pp. 38–55.

Infante-Paez, L., L.-F. Cardona, B. McCullough, and R. Slatt, 2017, Seismic analysis of paleotopography and stratigraphic controls on total organic carbon: Rich sweet spot distribution in the Woodford Shale, Oklahoma, USA: Interpretation, v. 5-1, p. 33-47.

Johnson, K.S., and B.J. Cardott, 1992, Geologic framework and hydrocarbon source rocks of Oklahoma, in K.S. Johnson and B.J. Cardott, eds., Source rocks in the southern Midcontinent, 1990 symposium: OGS Circular 93, p. 21-37.

Kvale, E.P., and J. Bynum, 2014, Regional upwelling during Late Devonian Woodford deposition in Oklahoma and its influence on hydrocarbon production and well completion, AAPG Search and Discovery Article #80410, 34 p

Keller, R.G. and Baldrige, W.S., 2008, The Southern Oklahoma Aulacogen, Developments in Geotectonics Chapter 25, p.426-436.

Mazzullo, S.J., 2000. Organogenic Dolomitization In Peridial to Deep Sea Sediments: Journal of Sedimentary Research. V84, 1185-1199.

McGlannan, A., Bonar, A., Pfeifer, L., Steinig, S., Valdes, Adams, S., Duarte, D., Milad, B. Cullen, A., Soreghan, G.S., 2022, An Eolian Dust Origin for Clastic Fines of Devonian-Mississippian Mudrocks of the Greater North American Midcontinent, Journal of Sedimentary Research, v.92, p.1198-1206.

Over, D. J., 1990, Conodont biostratigraphy of the Woodford Shale (Late Devonian- Early Carboniferous) in the Arbuckle Upper Mountains, South-Central Oklahoma, Texas Tech University PhD Dissertation, 186 p.

Over, D. J., 1992, Conodonts and the Devonian-Carboniferous Boundary in the Upper Woodford Shale, Arbuckle Mountains, South-Central Oklahoma, Journal of paleontology, Vol. 66, No. 2, p. 293-311.

Perry, W.J. 1989, Tectonic evolution of the Anadarko Basin region: United States Geological Survey Professional Paper 1866-A, 28 p.

Ruppel, S.C., 2016, Can sequence stratigraphic concepts be applied in mudrock systems? AAPG Search and Discovery Article #51380, Adapted from oral presentation given at AAPG Annual Convention & Exhibition, Houston, Texas.

Shatski, N.S., 1946, The great Donets basin and the Wichita system; comparative tectonics of ancient platforms. *Akademiya Nauk SSSR Izvestiya, Seriya Geologicheskaya* 6, p. 57–90.

Slatt, R.M. and Y. N. Abousleiman, 2011, Merging sequence stratigraphy and geomechanics for unconventional gas shales, *The Leading Edge*, March, p.274-282.

Slatt, R.M., and students of Stack-Merge-SCOOP industry consortium, 2018, Conventional analysis of unconventional resource shales: *Oklahoma City Geological Society, Shale Shaker*, v. 69, p. 292-328

Spalletta, C., Perri, M.C., Over, J., Corradin, C., 2017, Famennian (Upper Devonian) conodont zonation: revised global standard, *Bulletin of Geosciences* 92, p.31-57.

Suneson, N., 2010, Petrified Wood in Oklahoma, *Oklahoma City Geological Society Shale Shaker*, v.60-6, 21p.

Taff, J.A., 1902, Description of the Atoka quadrangle [Indian Territory]: U.S. Geological Survey Geologic Atlas Folio79, scale 1:125,000, 8 p. (named Woodford Chert)

van der Meer, D., Scotese, C.R., Mills, B, and others, 2022, Long-term Phanerozoic global mean sea level: Insights from strontium isotope variations and estimates of continental glaciation, *Gondwana Research* 11, p. 103–121

Wickham, J.S., 1978, The southern Oklahoma Aulacogen, in *Structural Style of the Arbuckle region: Geological Society of America, South-Central Section Guidebook for Field Trip #3*.

Wignall, P.B., 1994, *Black Shales*, Clarendon Press – Oxford Monograph, 127p.

2.1 Wyche Quarry Area 2N-6E SW/NE Sec 2: The Wyche Quarry is an active shale pit about 0.5mi south of the Hass G section and about 1mi to 0.5mi east of the composite sections of DDRSP, Dump Draw Ryan Shale Pit, site of Over (1992; Figure 2.1.1). This is a currently active quarry that can only be visited on weekends, with permission of the operator. Smaller groups in SUVs can descend to the quarry floor. Larger tour bus groups can park at the top and walk down to east side of the quarry where key features can be seen on the quarry floor and wall.

The vertical walls of the Wyche quarry expose about 70ft of upper Woodford and the quarry floor covers approximately 12 acres (Figure 2.1.2). These fresh exposes offer an excellent 3D view of the Woodford. About 600ft east of the quarry the Wyche-1 is a research well that cored and logged the entire 270ft Woodford section. The core from this well was studied for lithostratigraphy, chemostratigraphy, organic geochemistry, and palynology. When combined with the wireline log data and integrated with observations in the quarry, this represents one of most complete analytical data sets that can be used to calibrate subsurface studies (Buckner et al., 2009; Turner et al., 2015; Connock et al., 2018). Because of the relatively simple flat-lying structure of the Lawrence, the Wyche-1 can be confidently projected 600ft into the eastern wall of the Wyche quarry (Figure 2.1.3).

As discussed below, however, there is uncertainty whether the uppermost section should be considered as Woodford (Buckner, 2009) or pre-Welden shale (Molinares, 2013; Turner et al., 2015; Slatt et al., 2018). Nearby outcrops along south Jack Fork Creek provided a critical dataset for our understanding of the Devono-Mississippian section of the Lawrence uplift Woodford (Over, 1990, 1992; Boardman and Puckette, 2006). There are 7 features of the Wyche area that deserve specific attention:

1: Only siliceous and argillaceous shales in the Upper Woodford are exposed. The Middle and Lower Woodford lie below the present quarry floor. The absence of chert is consistent with spatial arrangement of lithofacies (see Section 1.3; figure 1.3.7). As discussed further below there is significant disagreement as to whether the upper 60-70ft of core should be treated as pre-Weldon Shale (Turner et al., 2015). This is doubtful. Consider the simple structure of the Lawrence uplift, the Wyche-1 can confidently be projected into the quarry wall (Figure 2.1.3) which imply the entire 70ft wall is pre-Welden shale when the pre-Welden shale never exceeds 1ft in thickness at nearby outcrops (Figure 2.1.4d).

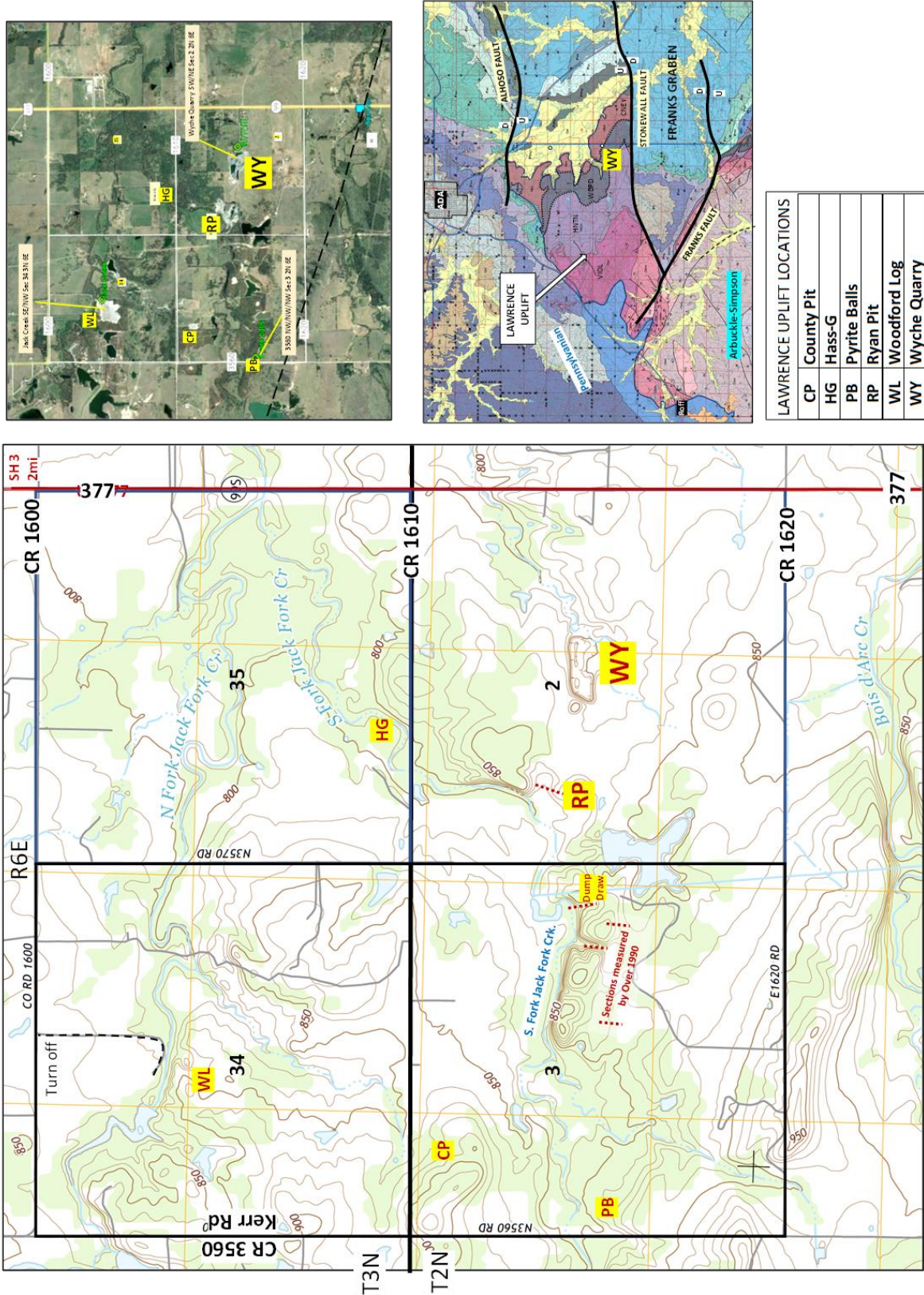


Figure 2.1.1 Location map of Lawrence uplift Woodford outcrops; Google Earth image and regional geological map. Locations DDRSP sections courtesy of Over, personal communication.

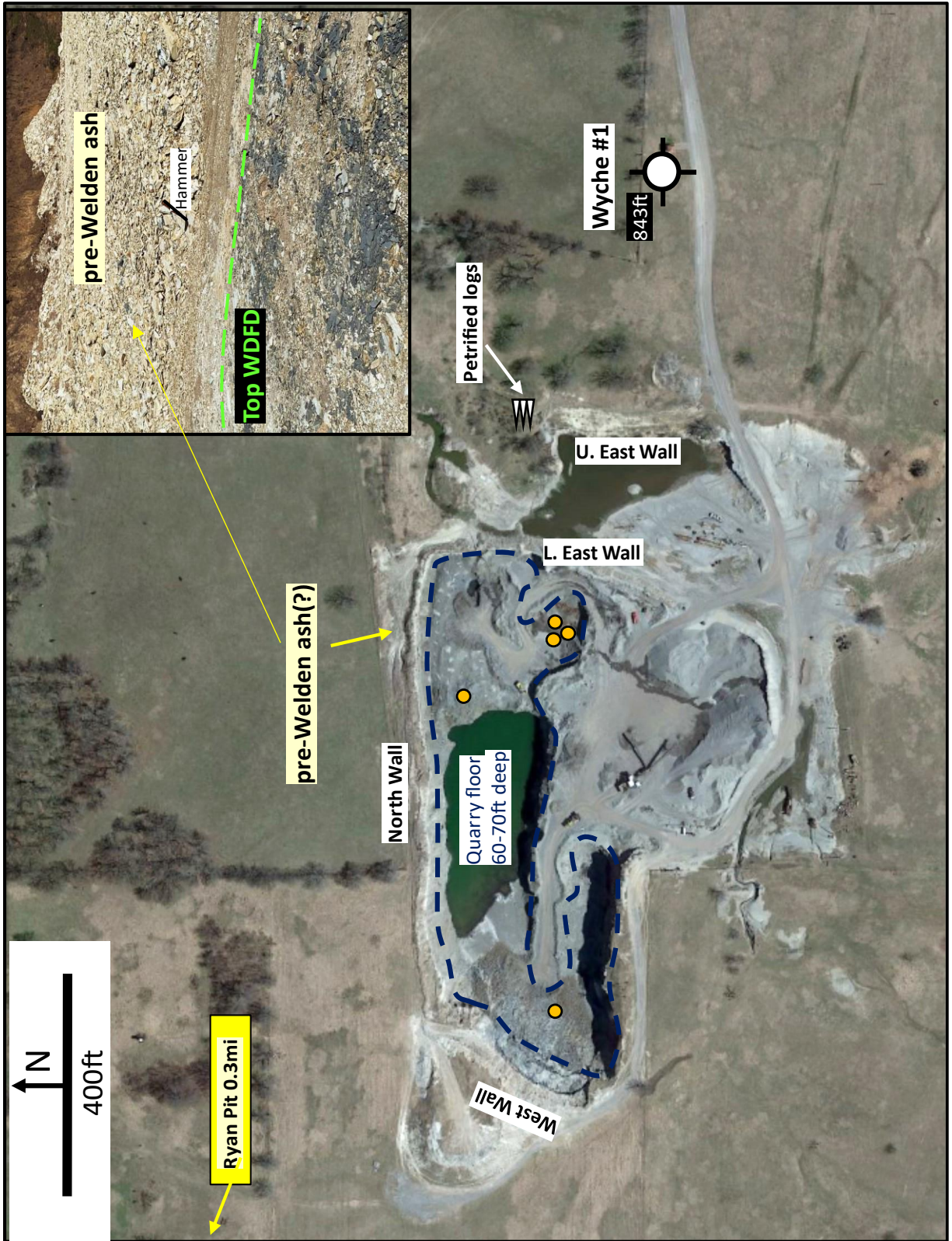


Figure 2.1.2 Aerial view of Wyche quarry and Wyche-1 about 600ft east of quarry floor. Key features shown are: orange filled circles- large pyrite saucers, white triangles- petrified logs. The inset photo is the recently excavated Woodford-pre-Welden ash contact.

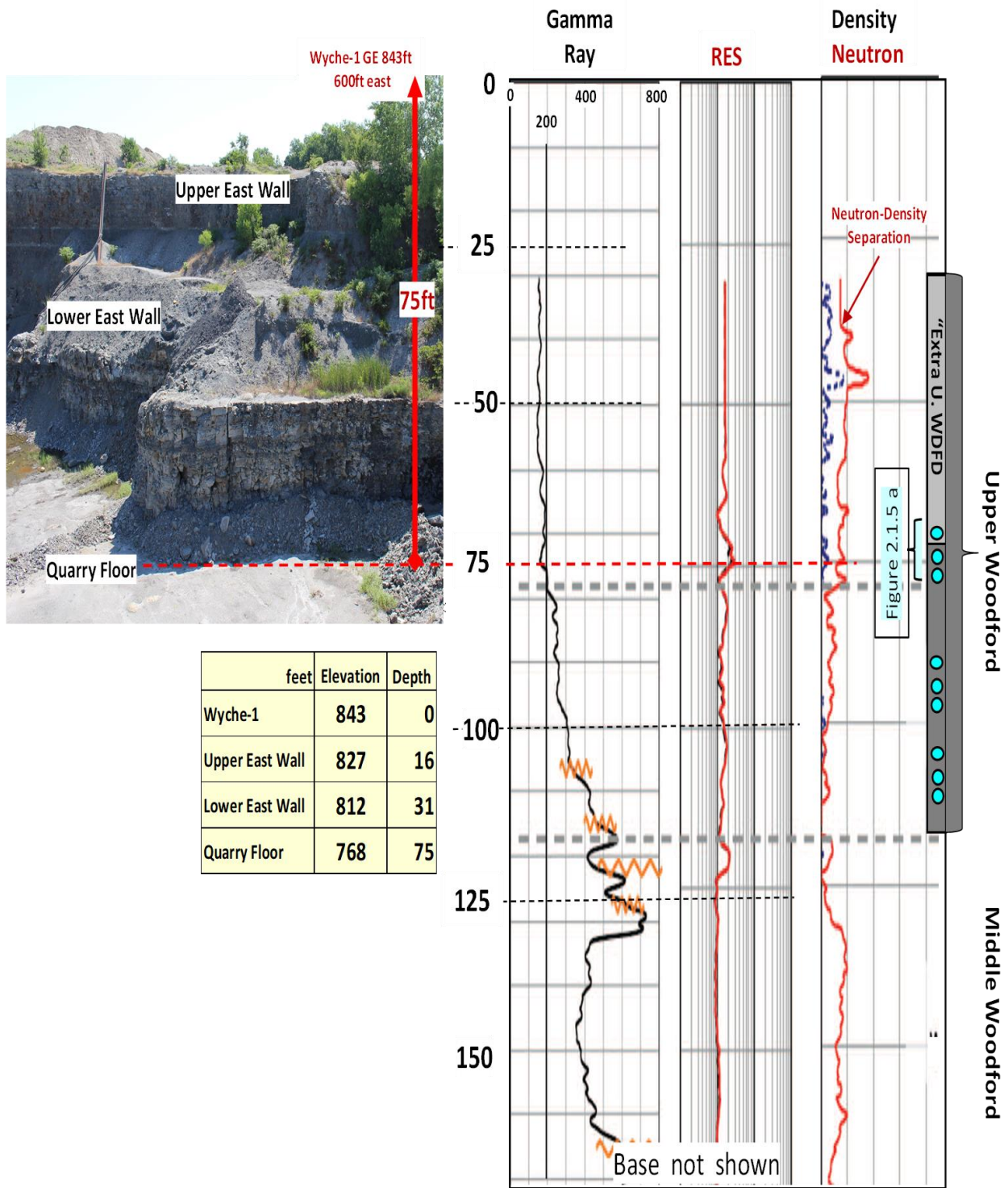


Figure 2.1.3 Wireline logs from Wyche-1 projected 600ft into the eastern quarry wall. Phosphate nodules- blue circles. Top Middle Woodford pick from Turner et al., 2015. “Extra” upper Woodford section on log is the same as the pre-Welden shale section of Turner et al., 2015.

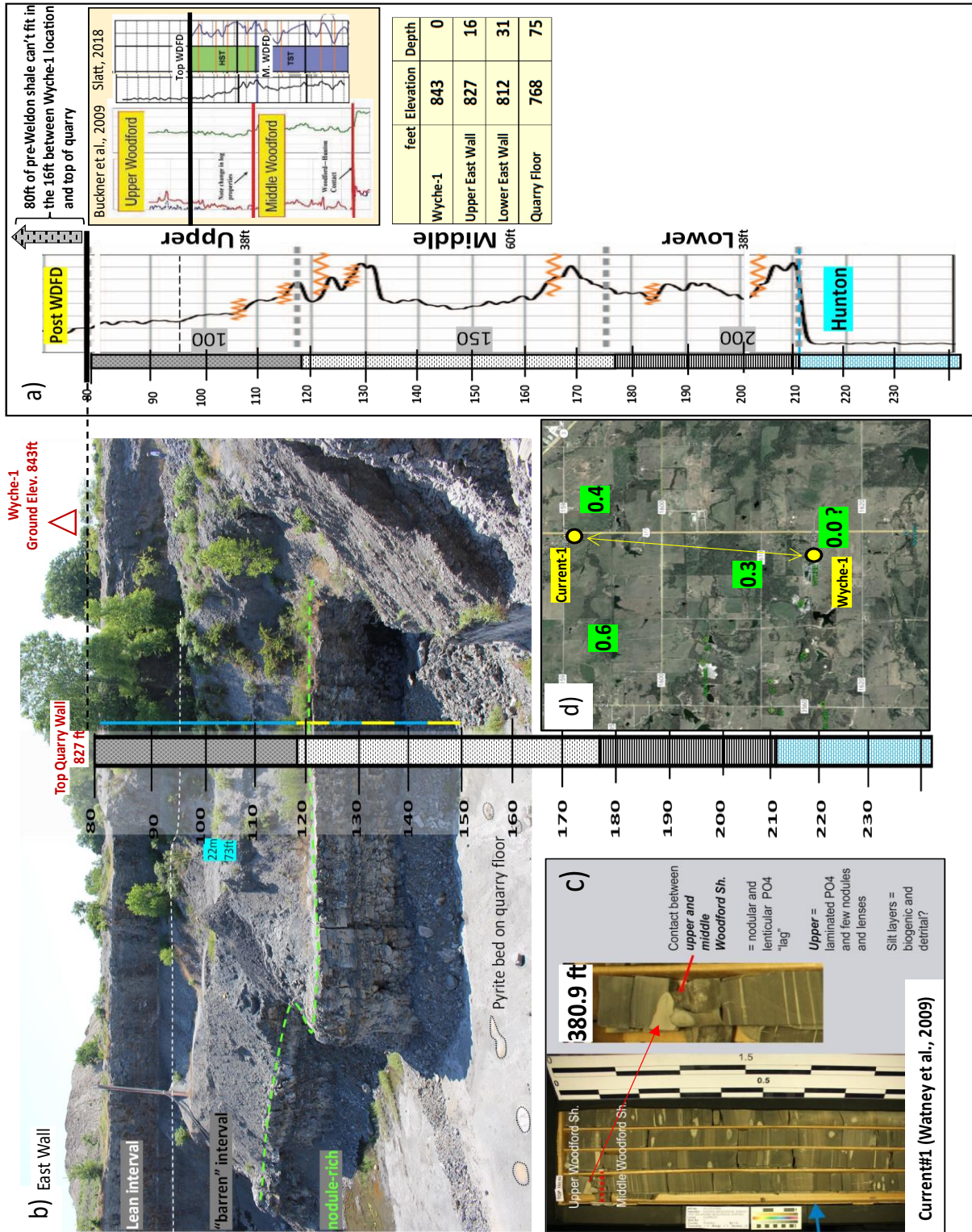


Figure 2.1.4 a) Wyche-1 gamma ray log with tops from Turner et al., (2015) and different interpretations of upper Woodford (Buckner 2009; Slatt et al., 2018). b) View of quarry wall with Wyche-1 superimposed. Green dashed line is the top of an interval rich in phosphate nodules also is seen in the c) Current-1 core 2.5mi north. d) Feet of pre-Welden shale in green boxes.

2. The Upper Woodford has a 30ft /10m interval with abundant phosphate that persists along the entire quarry walls. The phosphates nodules exhibit a vertical change in morphology from spherical to elliptical nodules to lenticular thin beds (Figures 2.1.5 and 2.1.6). On the western quarry floor loose, spherical nodules are abundant than elliptical nodules (Figure 2.1.7a and b). As observed at other Woodford outcrops, the phosphate nodules typically have well developed compactional drape (2.1.7c) indicating they precipitated at or very near the sea floor - predating deposition of the overlying mudrocks.

Overlying this phosphatic interval, the uppermost Woodford is very lean in phosphate nodules, has thin, lenticular phosphorite beds that are expressed as spikes in P on the XRF chemostratigraphic log (Figure 2.1.9). The XRF data indicates that the nodule-rich interval continues about 50ft below the present floor of the quarry, which makes for a relatively thick interval (80ft/25m) of phosphate enrichment. A relatively thick interval of Upper Woodford phosphate nodules is present in the Current-1 core about 2.5mi due north of the Wyche quarry (Figure 2.1.4c, d).

3: On the current quarry floor there are widespread, large pyrite concretions. These are particularly well exposed on the southeastern side where more than a dozen pyrite concretions up to 3ft/1m in diameter are confined to a single bed (Figure 2.1.9). We were unable to determine their full thickness, but these “saucers” of pyrite can be up to 2ft thick according to the quarry operator. Such massive nodules represent a significant horizontal drilling hazard. Such pyritic beds appear to be rare as we have not seen nor read about such extensive pyritic beds elsewhere.

The paragenesis and timing of pyrite crystallization is not fully determined. Like the phosphate nodules they appear to be relatively early in the diagenetic history as inferred by divots of pyrite nodules that make an undulous top reflecting soft sediment deformation below and differential compaction above (Figure 2.1.9). Such massive amounts of pyrite is consistent with biomarker data (Figure 2.1.10) and chemostratigraphy that indicate episodes of anoxic (no oxygen) and euxenic (sulfidic) conditions, particularly in the Middle Woodford (Connock et al., 2018; Turner et al., 2015). Of particular significance, in the Middle Woodford, is the presence of biomarkers related to anoxygenic phototrophic green sulfur bacteria (family *Chlorobiaceae*) that indicate the development of photic zone euxenia. This family of bacteria grows only under strictly anoxic and sulfidic conditions using H₂S rather than H₂O as the electron donor for photosynthesis.

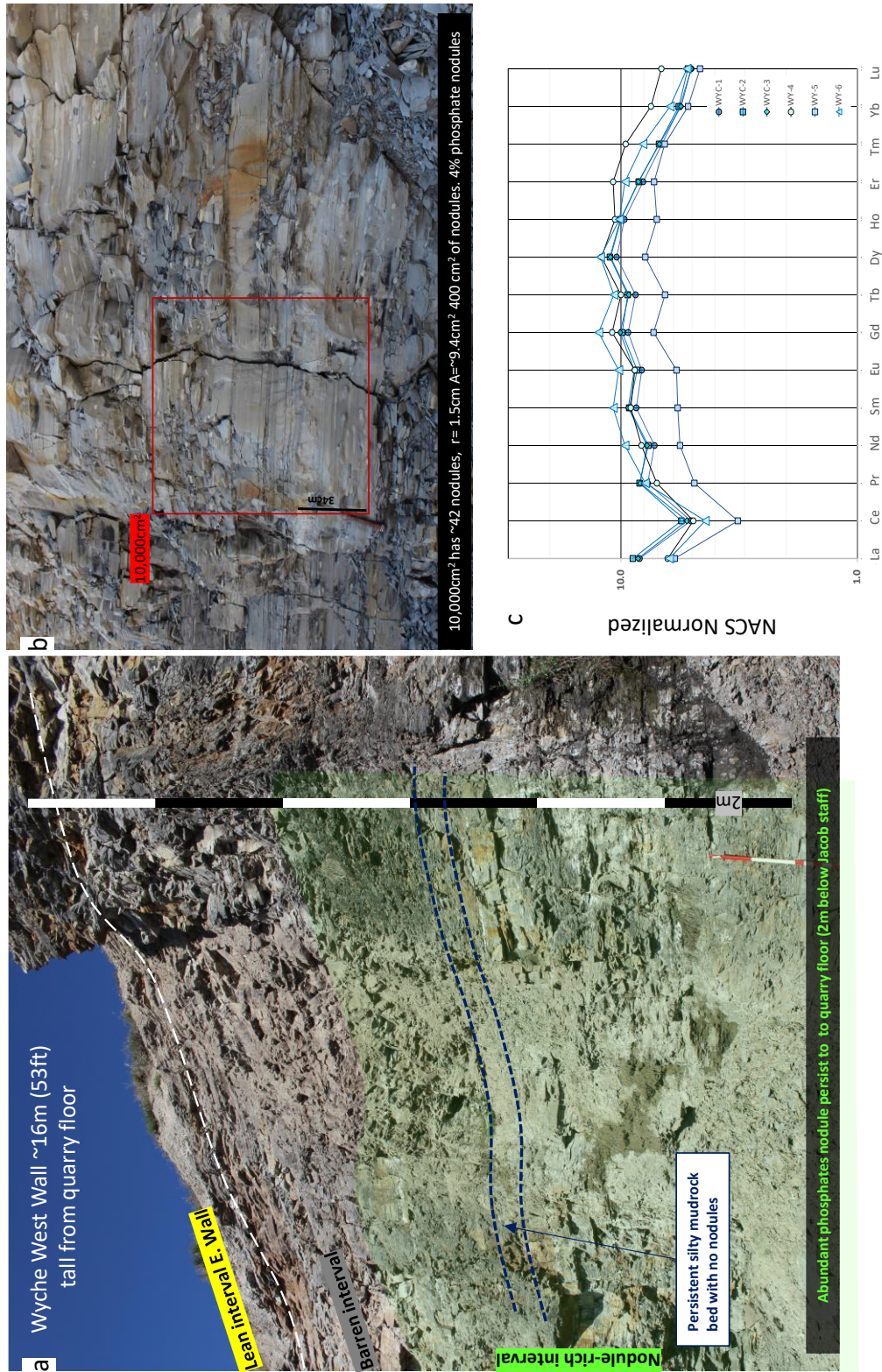


Figure 2.1.5 a) Two intervals of phosphate nodules in west wall of quarry capped by barren/lean interval in Upper Woodford b) Estimate of nodule percentage c) ICP-MS data from 3 phosphate nodules showing rare earth element enrichment relative to North American Composite Shale.



Figure 2.1.6 Close up of beds with nodule stratigraphy of decreasing sphericity upward into phosphorite beds.



Figure 2.1.7 a) Southwest quarry floor, spherical phosphate nodules and pyrite concretion (yellow dashed line). b) South quarry floor, spherical phosphate nodules. c) Pyrite compacting around spherical nodule with dark core.

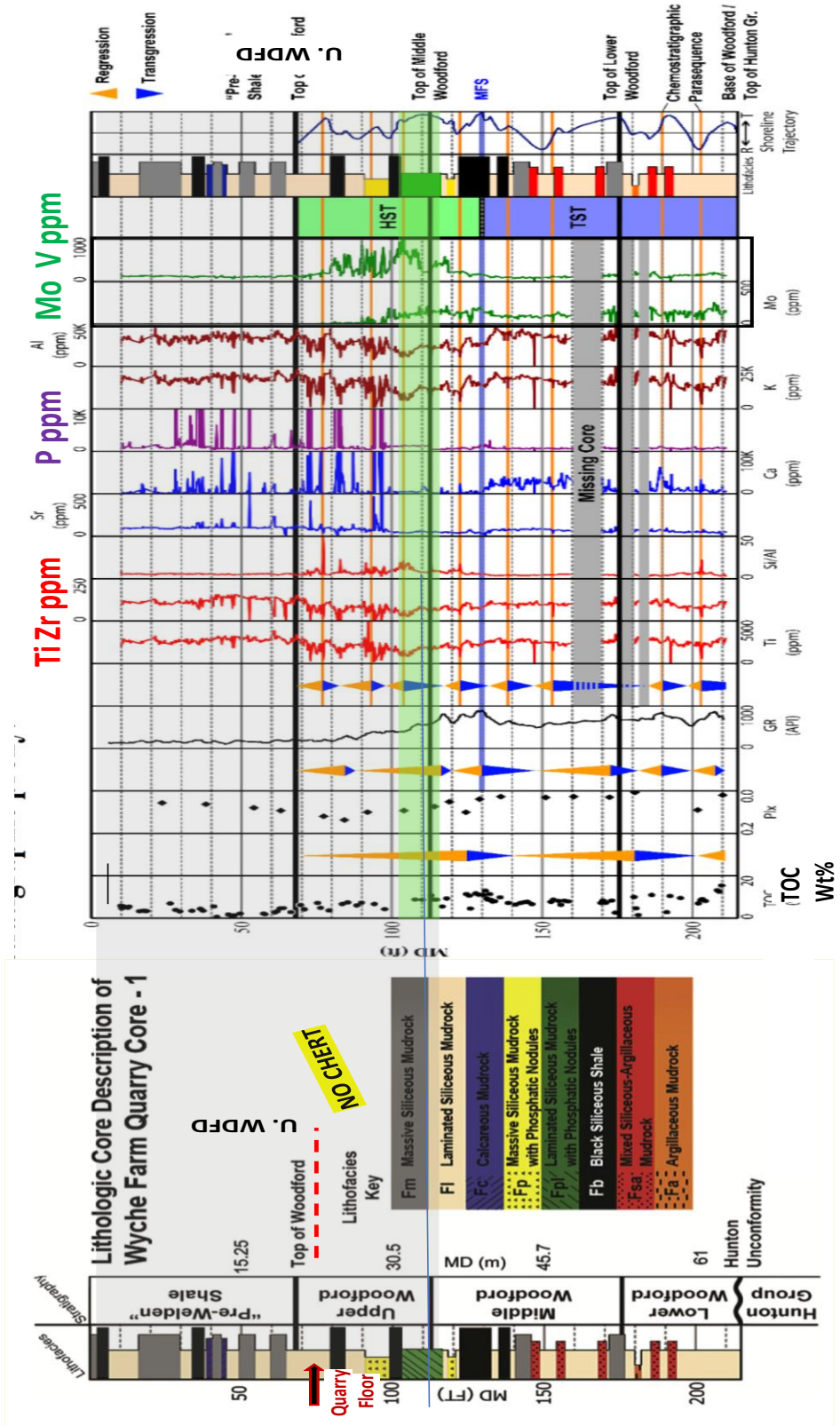


Figure 2.1.8 Wyche core lithofacies & chemostratigraphy. Middle Woodford shows evidence for water column stratification and photic zone euxinia (Connock et al., 2018). P-spikes indicate vertical extent of phosphate nodule and beds. Redox sensitive elements Mo and V are highlighted.

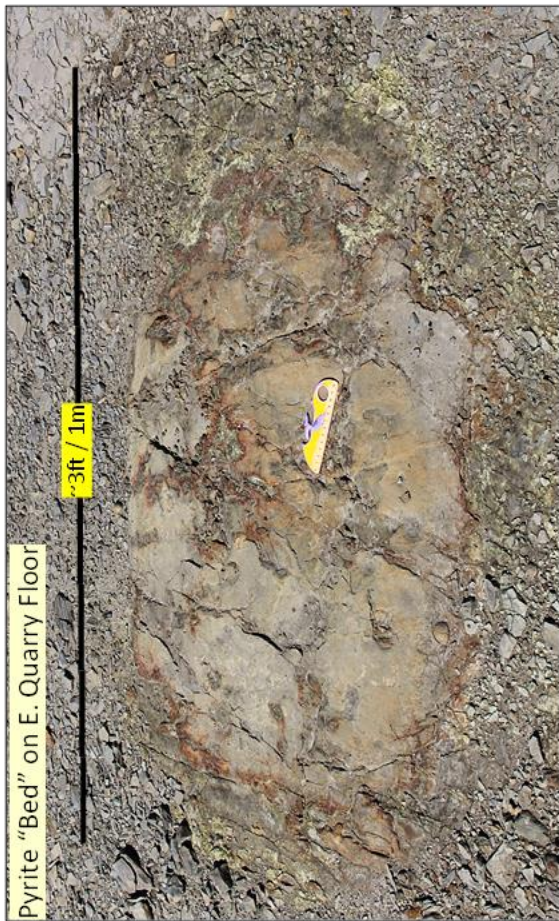


Figure 2.1.9 Bed with massive pyrite concretions on southern floor of quarry (yellow polygons). Some concretions have embedded phosphate nodules.

4. One of the most intriguing features at the Wyche quarry is the presence of 3 petrified logs above the upper east rim (Figure 2.1.2.). The full length of each log is not exposed, but each is at least 10ft long. All 3 logs have similar diameters greater than 2ft. Preservation of internal features of these logs is not of the same quality as the extremely large, charred log at Site CR 1610 (see Section 2.3). Although fragments of petrified tree trunks (*Callixylon*; Archeopteris tree) in the Woodford are not uncommon most specimens are single, isolated, modest-sized (2-3ft) specimens (Suneson, 2010). To find three relatively large logs together is previously unknown, at least in Oklahoma. What is particularly intriguing is the that fact all 3 logs lie with a similar E-W lineation. According to the quarry operator, the logs have not been dug up and moved; they are in place. The distance to the shoreline and Devonian forests is not known, but a reasonable estimate from regional paleogeography is at least 100mi (Figure 1.3.2). Given that distance, and the lack of any evidence of subaerial exposure, it is difficult to believe these logs simply fell in place. However improbable, the most logical remaining explanation for the Wyche quarry logs is that they were washed out to sea, perhaps in a major flooding event, and then go caught in the same ocean currents & processes before they became waterlogged and sank together to be preserved in the dysoxic muddy water bottom.

5: There are 2 dominant fracture sets that can be seen on the quarry walls and a third set observed on floor of the quarry. Both sets are nearly vertical. From the work of Ataman (2008) and Ghosh and Slatt (2019) the main fracture sets have the following characteristics (Figure S1-14): Group 1 fractures (N85E average strike) are regular, have a systematic spacing (4ft), and tend to be mineral filled; Group 2 fractures have aspects of being a conjugate system (NE-SW and NW-SE average strike) are less systematic, tend to be open, and terminate against (post-date) Group 1. Borehole imaging in the Wyche borehole shows the Upper Woodford is more highly fractured than the Middle or Lower Woodford. The Upper Woodford typically has greater silica cement than the underlying Woodford (Slatt et al 2017) and therefore a greater propensity to fracture.

6: Another interesting feature of the Wyche quarry is a tannish white unit recently uncovered during operations at the top of the quarry (Figure 2.1.13). The unit is about 10ft thick and has very limited extent. It is extremely siliceous, yet relatively porous. It adheres to the tongue and has a low density. At the base there are beds with molds of phosphate nodule molds as well as a few loose reworked? phosphate nodules. Some beds have subtle current ripples and a few fragments

of petrified wood have been found. Almost out of a process of elimination, we interpret this bed as recrystallized water laid ash. An attempt to age date this unit failed owing to insufficient recovery of zircons.

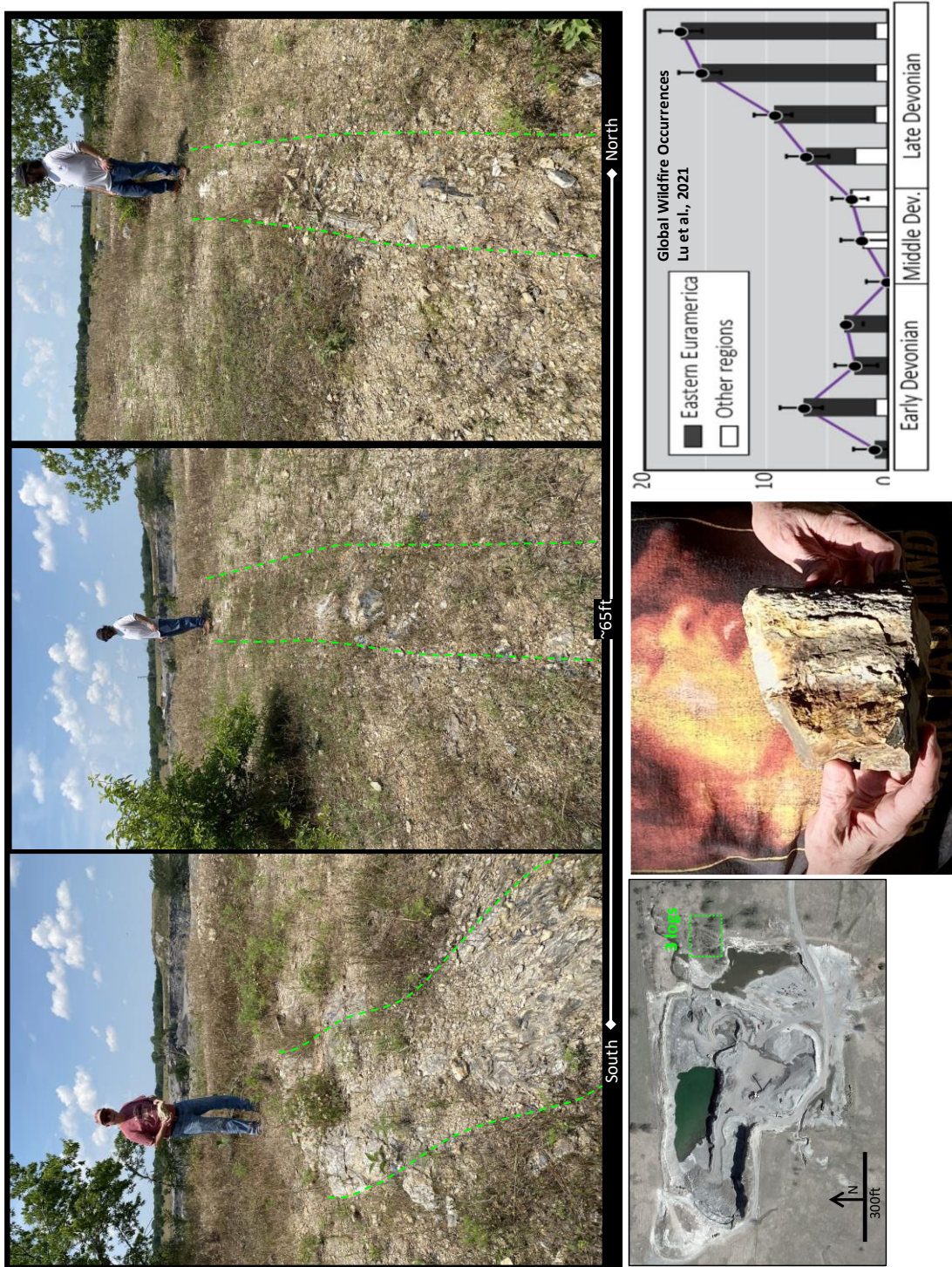
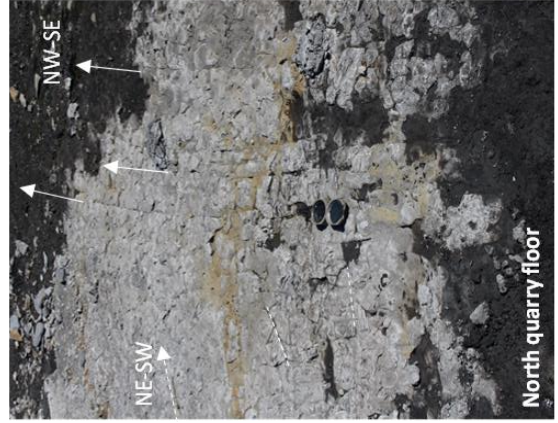
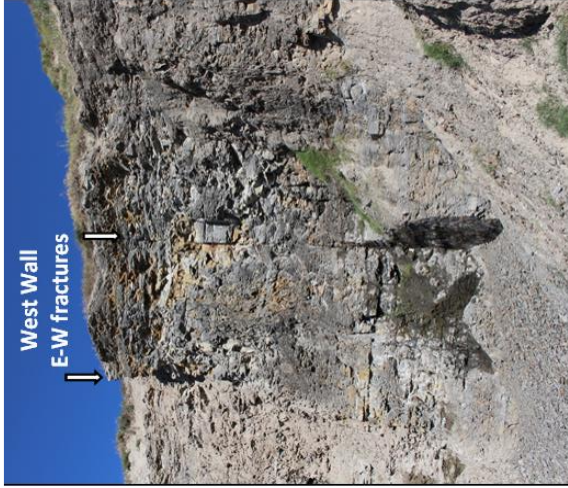
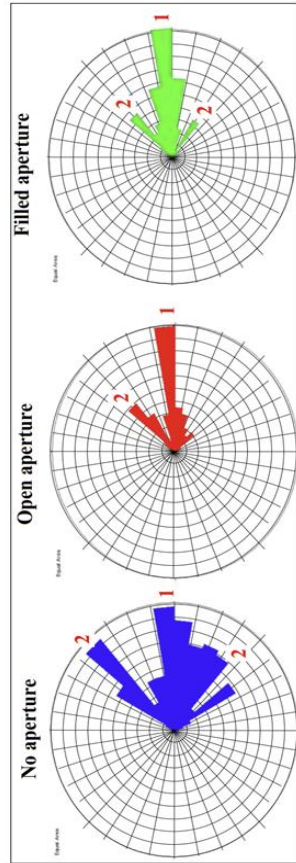


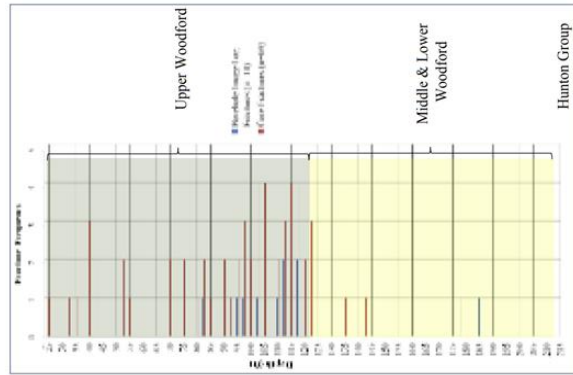
Figure 2.1.11 Top photos 3 large silicified logs oriented E-W about 65ft apart. Lower figure shows location map, a hand sample, a plot of Devonian global wildfire percentages (Lu et al., 2021).

FRACTURE MEASUREMENTS ON QUARRY FLOOR

- ▶ Group 1: 75-105° (W-E) ▶ Measure size of fracture apertures and filling material.
- ▶ Group 2: 30-45° (NE-SW) ▶ Most of the fractures with filled aperture are in Group 1 105-120° (NW-SE)



Fracture Histogram



BEHIND-OUTCROP CORING AND LOGGING

- ▶ 14 fractures interpreted on the borehole image log. Mean strike orientation of 50°
- ▶ 69 fractures identified in core
- ▶ Most fractures are in the Upper Woodford Shale Member, higher quartz and lower clay content.

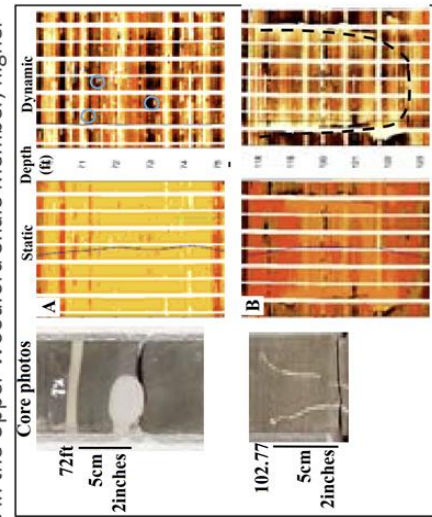


Figure 2.1.12 Fracture analysis from Ghosh (2017) and Ataman (2008)

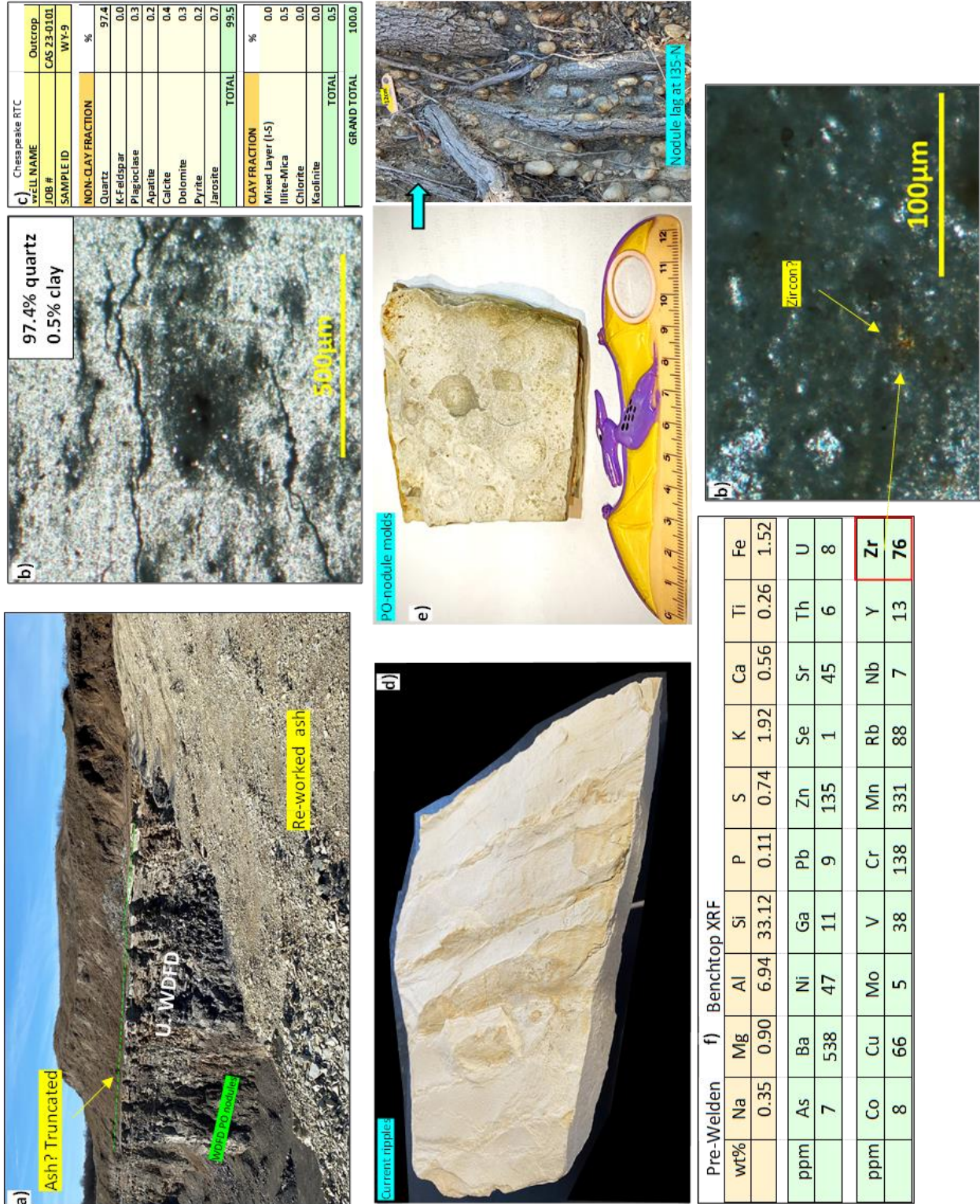


Figure 2.1.13 a) Ash bed on Woodford N. Quarry wall b) 2 photomicrographs; upper right w/ possible zircon c) XRD analysis d) Hand sample with ripples e) Hand sample with molds of phosphate nodules and I35-N nodule conglomerate f) Bench top XRF data.

7: If time permits a visit to the Ryan shale pit ~0.3mi west of the Wyche quarry is recommended (Figure 1.2.14). One can drive across an open field most of the way. The upper 30ft of Woodford is gray fissile mudrock, barren of phosphate. Irregular and ovoid phosphate nodules occur lower in the pit. The pre-Welden shale, if present, is covered. In the float on the hill above the pit there are pieces of Weldon Limestone including silicified oolitic cross bedded grainstones and Favosites corals. These shallow marine, high energy carbonates suggest a short-lived drop in sea level associated with top Woodford disconformity prior to deposition of the Caney Shale.

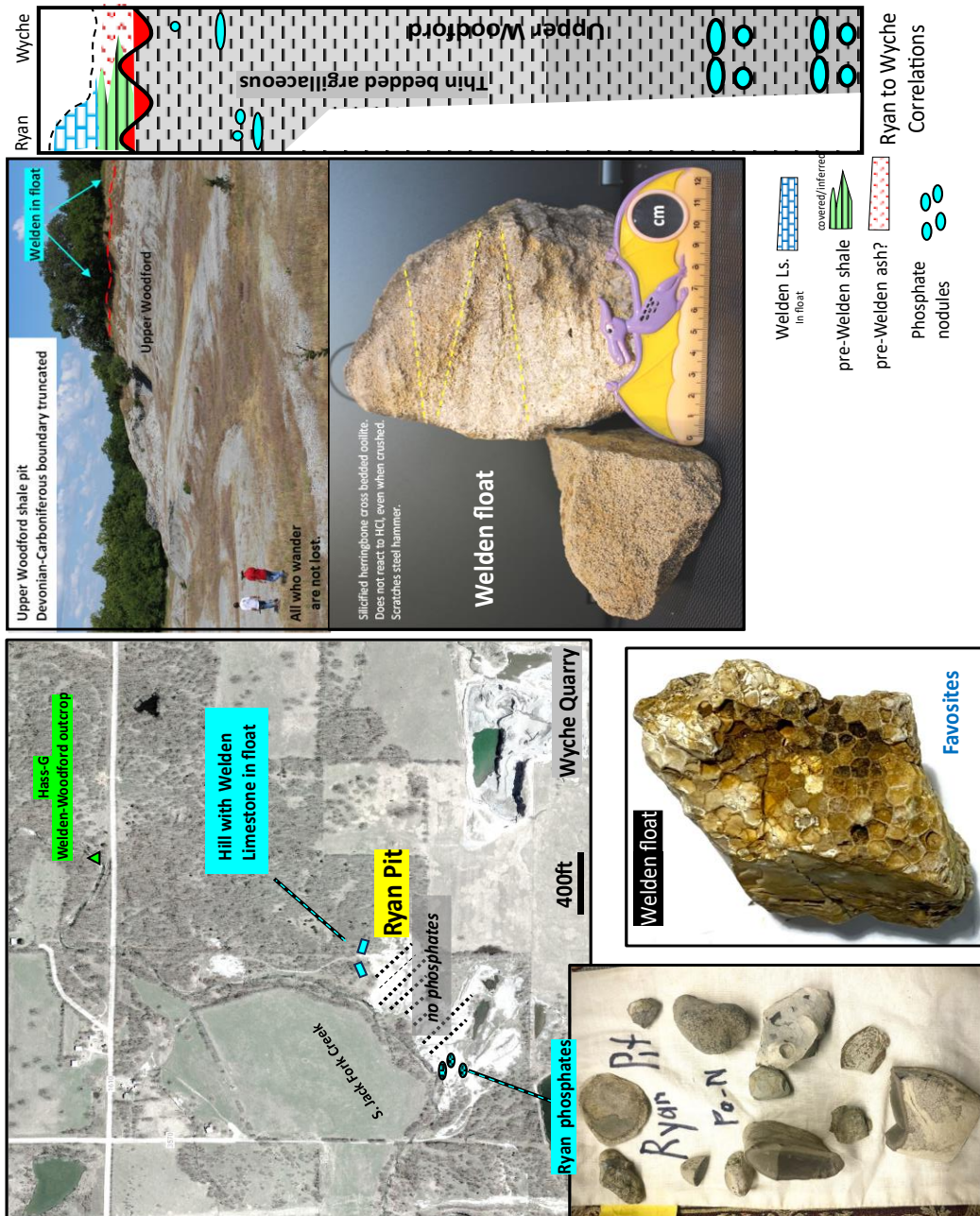


Figure 2.1.14 A collage of features at the Ryan shale pit west of the Wyche quarry.

Despite numerous studies of the Wyche area there are several unresolved issues. First, it must be noted that Over (1990, 1992) did not visit the Wyche Quarry. His Dump Draw Ryan Shale Pit (DDRSP) site is a composite of several sections from gullies into the major cut bank of South Jack Fork Creek and the Ryan Shale Pit (Figure 2.1.1a). Over's DDRSP Woodford stratigraphic section shows a 165ft/50m section of Woodford. However, the maximum topographic relief in the area is 42ft/12.7m (Figure 2.1.1). Thus, there is insufficient room for a 165ft outcropping section. Given the nearly flat dips, it is likely that there was overlap and repeat of parts of the middle section measured (Jeffery Over, personal communication). Without giving a specific location Over (1992) shows the Woodford is unconformably overlain by the Caney Shale. The Late Famennian (Upper praesuclata), Kinderhookian, and Osagean are missing. At the Ryan pit and Wyche quarry, there is no Caney present. Therefore, it is not clear to what extent the Caney is present in the Wyche area.

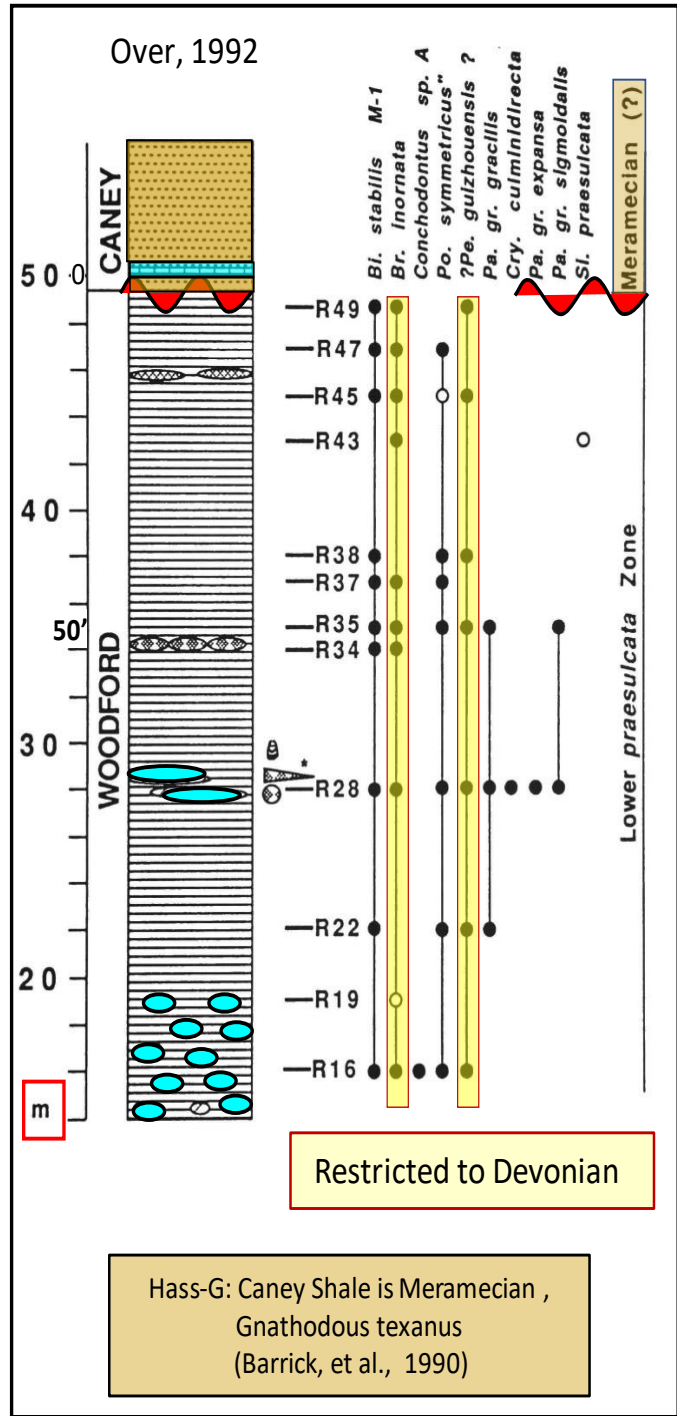


Figure 2.1.15 Stratigraphic column from Over, 1992

The second problem is disagreement in position of the top of the Woodford in the Wyche-1 and Wyche quarry (Figures 2.1.3; 2.14a). Molinares (2013), Turner et al., (2015) and Slatt (2018) interpret the upper 80ft in the Wyche core as pre-Welden shale, which correlates to the entire quarry wall. Over (1990) and Buckner et al., (2009) assigned this 80ft section to the Upper Woodford. The section in question is clearly Devonian not Mississippian (Over 1990). We note that at multiple locations on the Lawrence uplift the pre-Welden shale never exceeds 1ft in thickness (Figure 2.1.4d). Outcrops of the pre-Welden shale are light greenish mudrock- bear little resemblance to the grey to black Woodford mudrocks (Figure 2.1.16). Thus, the biostratigraphy, isopach, and lithology data support treating the entire Wyche-1 core and quarry wall as Upper Woodford. Compared to Upper Woodford in the Arbuckle Mountains and Ardmore basin the Wyche-1 wireline logs have some interesting features that likely underpinned the interpretation of thick pre-Welden shale (2.1.3d): 1) The extra section has a lower gamma ray (<200) than the rest of the Woodford). 2) There is a distinct separation on the neutron-density logs, indicative of being shalier than the interval below, however, the gamma ray reads low. 3) The resistivity is slightly elevated, nearly constant. We interpret features 2, and 3 to reflect the presence of bound fresh water above the water table.

Lastly, as discussed in Section 1.3.2 there are significant differences in the position of the Frasnian-Famennian boundary between conodont biostratigraphic and chemostratigraphic methods.

Section (<i>Lawrence uplift locations</i>)	F/F boundary m. above HUNTON	DC Boundary m. below top WDFD	References
<i>Hass-G</i>	covered	0.6	Hass and Huddle, 1965; Over, 1990
<i>Weldon Type</i>	covered	0.6	Over 1990, 1992
<i>Hass En</i>	0.21	covered	Hass and Huddle, 1965; Over, 1990
<i>Wyche / Ryan</i>	26	truncated (Over)	Turner et al., 2016
<i>Goose Creek</i>	covered	0.8	Over 1990, 1992
<i>Ebby Dam</i>	covered	0.5	Over 1990, 1992
<i>Guest Ranch</i>	covered	0.6	Over 1990, 1992
Burning Mtn	0.2	covered	Over 1990
Hunton Quarry Anticline	50	covered	Turner et al., 2016
Hass-B YMCA	15.7	covered	Over, 1990; Crick, et al., 2002
Hass-A Henry House Creek	3.3	covered	Hass and Huddle, 1965; Over, 1990
I-35 South	covered	4.5	Over 1990, 1992; Kondas 2018
McAlister Cemetery Quarry	12-15	2?	Over, 1990, 2002; , Cullen Hg spike
McAlister Cemetery Quarry	69	no data	Molinares et al., 2019
Wapanucka Shale Pit	covered	81	Over 1990, 1992

Table 1.3.2 Key sections where F/F and D/C boundaries have been established with comparison to chemostratigraphic F/F boundary of Turner et al., 2016.



Figure 2.1.16 a) Wyche-1 core across purported pre-Welden / Woodford contact. No change in lithology, and the continuation of phosphate nodules (blue P's) b) Photo of Hass-G outcrop: WLS- Welden Limestone, P-WSh- pre-Welden Shale, WDFD- Woodford Shale. c) Photo of greenish pre-Welden Shale.

Molinares (2013) placed the F/F relatively high in the Wyche core attempting to match the global Devonian T-R (Transgressive-Regressive) cycles of Johnson et al., (2008). Molinares et al., (2019) compared $\delta^{13}\text{C}_{\text{organic}}$ isotope trends to the global secular $\delta^{13}\text{C}$ curve to place the F/F high in the section. To confidently use stable carbon isotope data requires biostratigraphic constraints; numerous additional T-R cycles can be defined by consistently honoring small GR deflections (figure 2.1.17a) and accommodating periods of slow and fast sedimentation at different localities requires stretching and shrinking the global secular $\delta^{13}\text{C}$ to match local observations. Organic-rich shales of the middle Famennian Dasberg Event also have a slight positive deflection in $\delta^{13}\text{C}_{\text{organic}}$ (Stock and Sandberg, 2019) in the Wyche core.

For the Wyche data set Molinares (2013) put the top of the Devonian below a thick section of pre-Welden Shale, which we interpret as upper Woodford (see discussion regarding Figure 2.1.3). Therefore, the global curve needs to be stretched to the top of the core (Figure 2.1.17b). At the En site, 2mi west of the Wyche-1 high quality conodont at places the F/F just 0.77ft above the Hunton (Over; 1990) which strongly suggests that most of the Frasnian section is missing, not deposited(?). Thus, these data can equally suggest that the entire section in in the Wyche-1 core and the Wyche quarry is Famennian in age (Figure 2.1.7c).

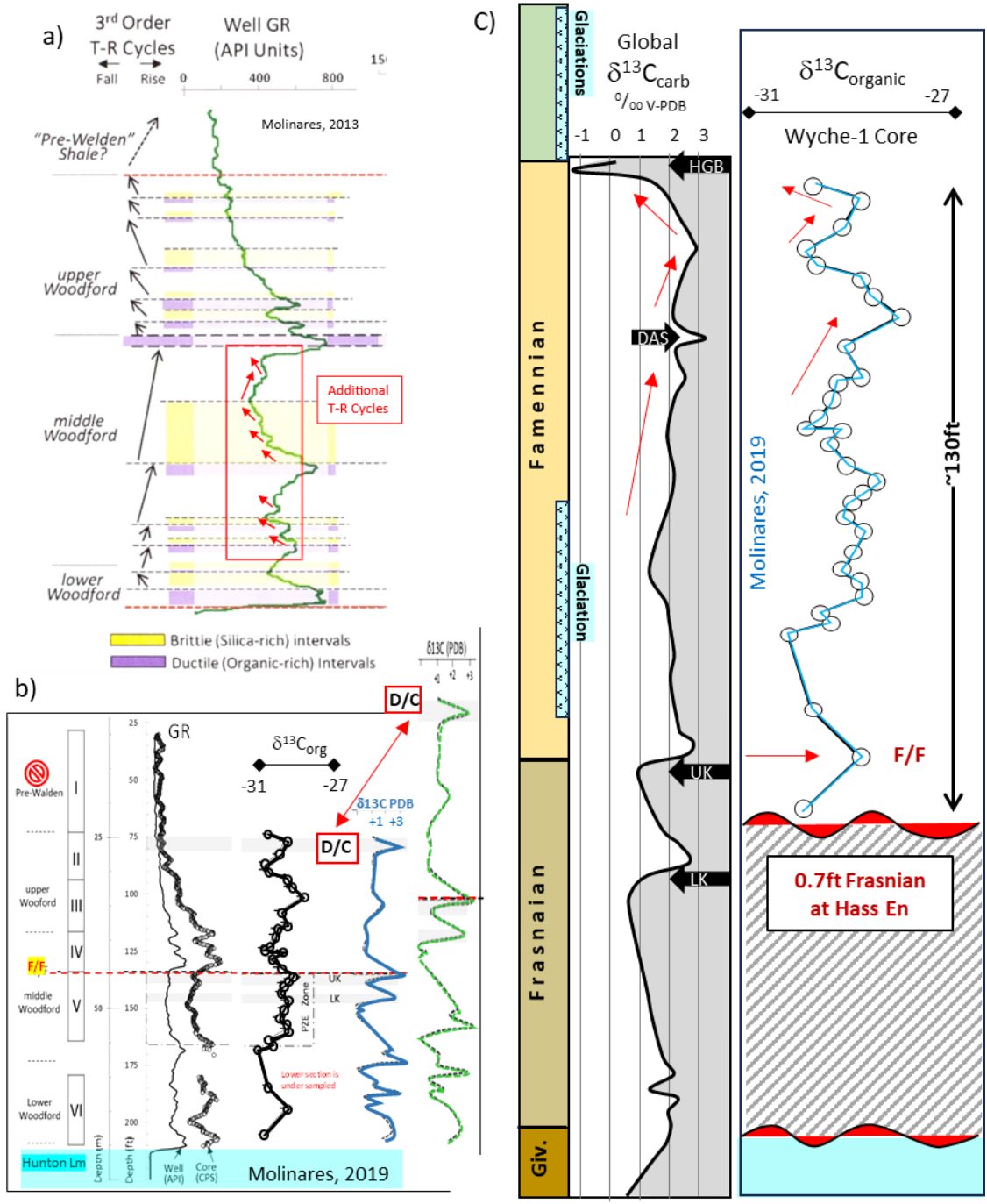


Figure 2.1.17 a) Molinares (2013) transgressive-regressive cycles in Wyche core with additional small cycles in red arrows. b) Molinares et al., (2019) using $\delta^{13}C_{organic}$ to position of F/F boundary relative to global $\delta^{13}C$ curve in blue; green curve is the $\delta^{13}C_{organic}$ data stretched to honor upper section at Wyche as Famennian in age. c) Fitting the $\delta^{13}C_{organic}$ data to the global curve to honor the very thin Frasnian section at the En site 2mi west of Wyche (Over, 1990). UK and LK denote upper and lower Kellwasser events; DAS= Dasberg Event, HGB= Hangenburg Event.

REFERENCES

Ataman, O., 2008, Natural fracture systems in the Woodford Shale, Arbuckle Mountains, Oklahoma: Stillwater, Oklahoma State University, unpublished M.S. thesis, 139 p.

Barrick, J.E., J.N. Haywa-Branch, and D.J. Over, 1990, Stop 6: Woodford Shale (Late Devonian-Early Mississippian), pre-Weldon Shale, Weldon Limestone, and basal Caney Shale (Mississippian); Hass G section, in S.M. Ritter, ed., Early and middle Paleozoic conodont biostratigraphy of the Arbuckle Mountains, southern Oklahoma: OGS Guidebook 27, p. 23-25.

Boardman, D.R., and Puckette, J., 2006, Stratigraphy and paleontology of Upper Mississippian Barnett Shale of Texas and the Caney Shale of Southern Oklahoma, Oklahoma Geologic Survey Open file Report 6-2006, 89p.

Buckner T., Slatt R. M., Coffey B. and Davis R. J., 2009, Stratigraphy of the Woodford Shale from behind-outcrop drilling , logging, and coring . In AAPG Annual Convention, San Antonio, TX. AAPG Search and Discovery, article #50147

Connock, G., Nguyen, T.X., Philp, R.P., 2018, The development and extent of photic-zone euxinia concomitant with Woodford Shale deposition, AAPG Bulletin 102-6, p. 959–986

Ghosh, S.G., 2017, Integrated studies on Woodford Shale natural fracture attributes, origin, and their relation to hydraulic fracturing: Norman, University of Oklahoma, unpublished PhD dissertation, 264 p.

Johnson, J.G., G. Klapper , and C.A. Sandberg , 1985, Devonian eustatic fluctuations in Euramerica: Geological Society of America Bulletin, v. 96, p. 567-587.

Lu, M., Ikejiri, T., and Lu, Y., 2012, A synthesis of the Devonian wildfire record: Implications for paleogeography, fossil flora, and paleoclimate, Palaeogeography, Palaeoclimatology, Palaeoecology 571, p.1-16.

Molinares Blanco, C.E., 2013, Stratigraphy and palynomorphs composition of the Woodford Shale in the Wyche Farm Shale Pit, Pontotoc County, Oklahoma: Norman, University of Oklahoma, unpublished M.S. thesis, 90 p.

Molinares Blanco, C.E., 2019, Paleoenvironments and sediments around the Frasnian/Famennian (F/F) transition in the Woodford Shale, south central Oklahoma—A multiproxy approach: Norman, University of Oklahoma, unpublished PhD dissertation, 88 p.

Over, D. J., 1990, Conodont biostratigraphy of the Woodford Shale (Late Devonian- Early Carboniferous) in the Arbuckle Upper Mountains, South-Central Oklahoma, Texas Tech University PhD Dissertation, 186 p.

Over, D. J., 1992, Conodonts and the Devonian-Carboniferous Boundary in the Upper Woodford Shale, Arbuckle Mountains, South-Central Oklahoma, *Journal of Paleontology*, Vol. 66, No. 2, p. 293-311.

Over, D.J., 2002, The Frasnian/Famennian boundary in central and eastern United States, *Palaeogeography, Palaeoclimatology, Palaeoecology* 181, p.153-169.

Slatt, R., and Woodford Consortium students, 2018, Conventional analysis of unconventional resource shales, *Oklahoma City Geological Society Shale Shaker*, 69-6, p. 269-329.

Suneson, N.H., 2010, Petrified wood in Oklahoma, *Oklahoma City Geological Society Shale Shaker*, 60-6, p.1-21.

Stock, CA., Sandberg, CW., 2019, Latest Devonian (Famennian, expansa Zone) conodonts and sponge-microbe symbionts in Pinyon Peak Limestone, Star Range, southwestern Utah, lead to reevaluation of global Dasberg Event, *Palaeogeography, Palaeoclimatology, Palaeoecology*, 534, p.1-14.

Turner, B., C. Molinares-Blanco, and R. Slatt, 2015, Chemostratigraphic, palynostratigraphic, and sequence stratigraphic analysis of the Woodford Shale, Wyche Farm Quarry, Pontotoc County, Oklahoma: Interpretation, v. 3, p.1-9

Watney L., Boardman, D.R., Suneson, N.H., Puckette, J., and others, 2009, Preliminary High-Resolution Stratigraphic Analysis of the Caney and Woodford Shales in a Continuous Shallow Corehole (KGS-OGS Current #1) from the Lawrence Uplift in Pontotoc County, Oklahoma, *Kansas Geological Survey OFR 2009-5*, 4p.

2.2 Hass G: The Hass-G outcrop (SE/SE Sec. 35 T3N R6E) is on a cut bank on the south side of South Jack Fork Creek 100ft north of CR1610 about 3/4mi west of US 377 (Figure 2.2.1). When water levels are very low one can simply walk down the creek bed; otherwise, one must make their way through patches of thorny brush and down an embankment to the base of the outcrop (Figure 2.2.2). CR1610 is a narrow unpaved road. This location is not suitable for tour buses.

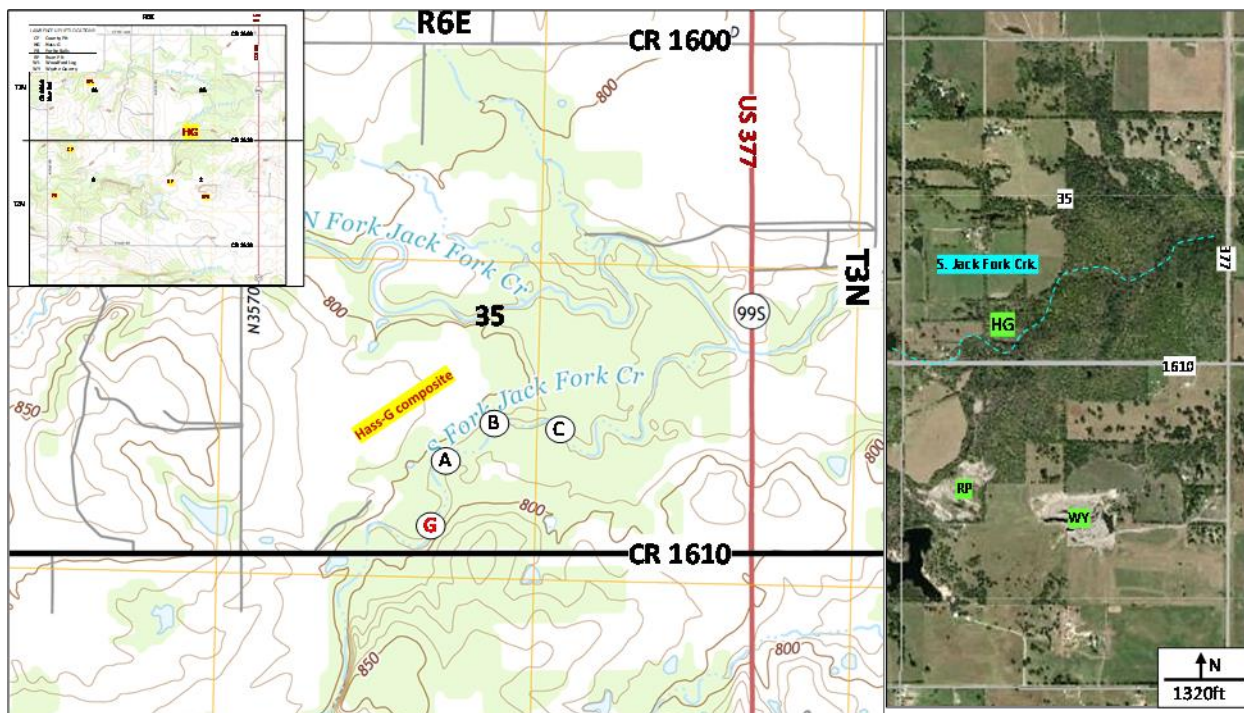


Figure 2.2.1 Location map for Hass-G with Google Earth image. A, B, C refer to locations of the composite stratigraphic section of Puckette and Boardman (2016).

Hass G is an import, albeit compact, outcrop on the Lawrence uplift. Several key features should be noted.

1. It is the best exposed and easily accessible outcrop where the Devonian-Carboniferous (Kinderhookian) boundary (DCB) has been determined by conodont biostratigraphic studies; Hass and Huddle (1965) and Over (1992) place the DCB about 2ft/60cm below a sharp contact with the distinctive greenish pre-Welden shale which is in turn overlain by the argillaceous ostracod/trilobite wackestones of the Welden Limestone Figure 2.2.2). In the context of interpreting the Wyche-1 core (Section 2.1), it should be noted that similar to other outcrops on the Lawrence uplift the pre-Welden shale at Hass-G is very thin (~1ft).

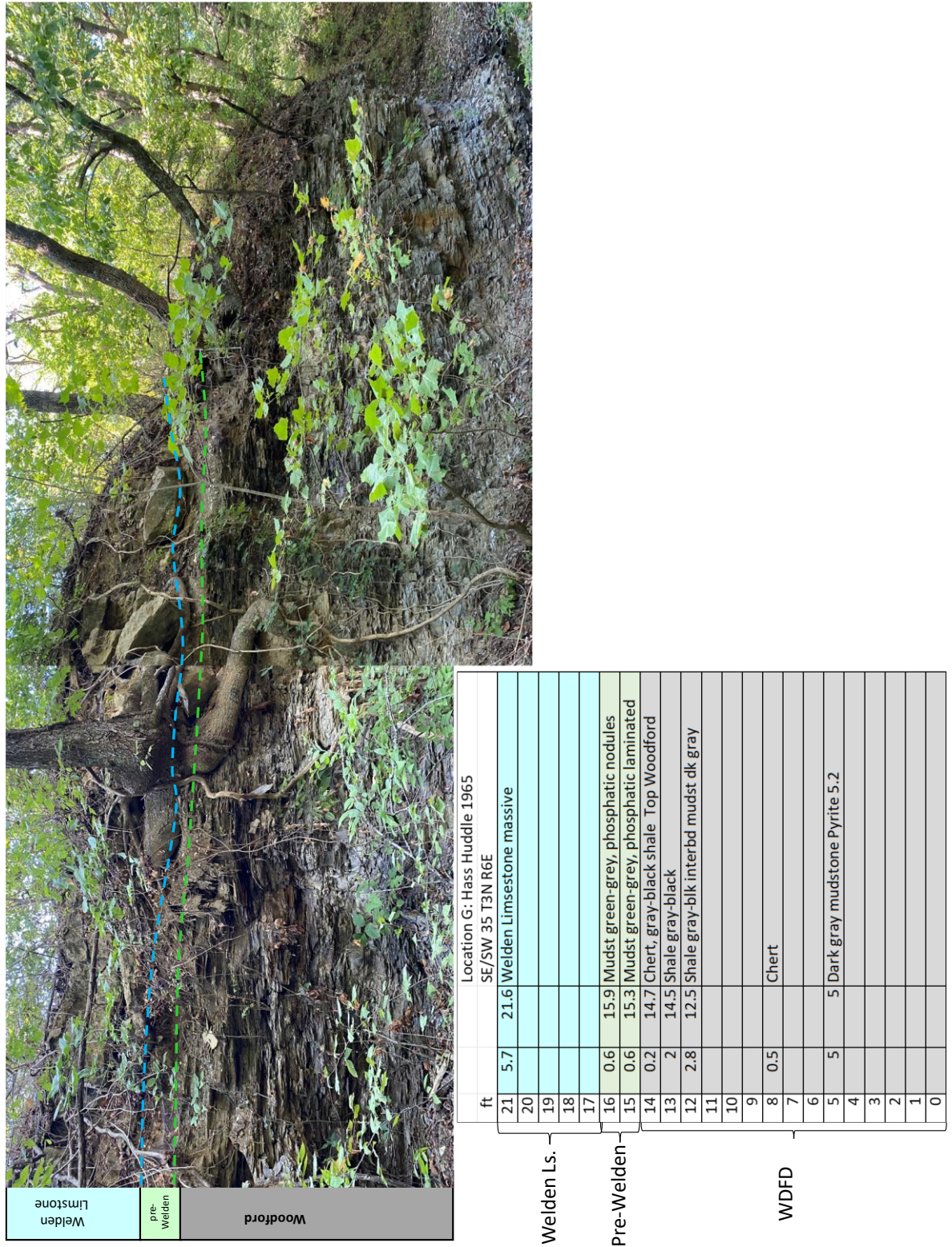


Figure 2.2.2 Simplified stratigraphic section and photo of Hass-G outcrop along S. Jack Fork Creek

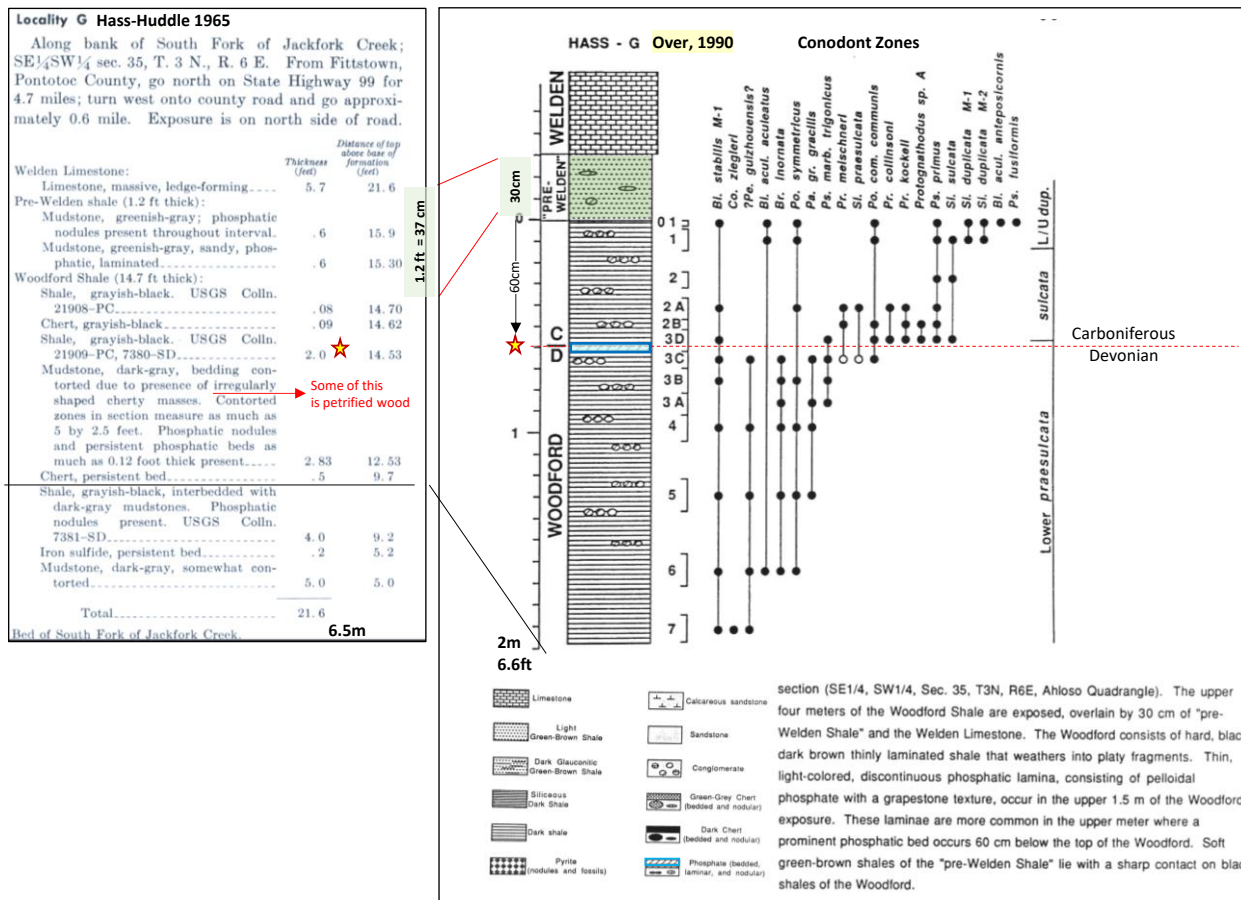


Figure 2.2.3 Hass-G stratigraphic sections of Hass and Huddle (1965) and Over (1990, 1992) with conodont zones.

2. At Hass-G the Woodford is predominately a thin-bedded, platy, dark gray siliceous mudrock. A limited amount of source rock characterization (Table 2.2.1) shows the Woodford to be an immature, organic-rich, marine source rock (Vro ~0.33%, TOC ~6.6-12.9%, HI ~603). These data are consistent with the viewpoint that the Lawrence uplift was never deeply buried.

SAMPLE	S1 (mg/g)	S2 (mg/g)	S3 (mg/g)	Tmax (°C)	S1+S2	Calc. Vro%	TOC (% wt)	HI
HG-0							12.7	
HG-60							6.6	
HG-100	1.16	77.73	1.16	416.0	78.89	0.33	12.9	603
cm below pre-Welden	Calculated%VRO = 0.0180 x Tmax - 7.16 (Jarvie et al., 2001)							

Table. 2.2.1 Woodford %TOC and Rock-Eval data at Hass-G.

- Thin lenticular beds and nodules of phosphate nodules occur in the uppermost part of the Woodford (Figures 2.2.4a and 2.2.4b). The upper part of this section also has several pieces of petrified wood (Figures 2.2.5a and 5b) which have the appearance of small branches measuring several inches wide and lacking bark, unlike the large logs describe at other locations including the Woodford Log location (Section 2.3).



Figure 2.2.4 a) Photograph of phosphate nodules b) Photograph of lenticular phosphate beds.



Figure 2.2.5 a) and b) Photographs of silicified branches (W).

When Jack Fork Creek is low one can see two well-developed nearly vertical fracture sets (NNE and EW) in the top of a more massive Woodford bed (Figure 2.2.6a). These fractures do not extend up into and through the overlying thinly bedded clay-rich Woodford exposed in the wall of the cut bank (Figure 2.2.6b), nicely illustrating the concept of brittle-ductile mechanical stratigraphy.



Figure 2.2.6 a) Fracture sets bed top b) Cliff face fractures that die out in shaly unit above.

The inorganic geochemistry of the Hass-G location is as interesting as it is perplexing. Three samples were analyzed by ICP-MS. The numbering on HG-0, 60, and 100 refers to the distance in centimeters below the Pre-Welden shale; HG-60 is near the DCB. Relative to the other samples HG-0 is strongly enriched in numerous elements such as Ag, As, Cu, Hg, Mo, Ni, Se, and V (Figure 2.2.7a). Orth et al., (1988) also noted anomalous metal concentrations at Hass-G in the Woodford, Pre-Welden shale, and Welden Limestone including Pt and Ir anomalies. The lack of microspherules and Pt:Ir ratios led those workers to suggest the anomalous geochemistry reflect poorly understood bacterial activity. Alternatively, the elevated Hg and Hg/TOC values in HD-0 (Table 2.2.2) could reflect volcanic input as documented elsewhere globally at the DCB (Rakocinski et al, 2020). The behavior of the REE's is quite interesting. HG-0 is notably depleted in REEs relative to HG-60 and HG-100 Figure 2.2.7b). HG-0 is from an interval that has phosphate lenses and nodules. Pending further analytical work we suspect that the lenses and nodules are preferentially concentrating the REEs in the phosphate-apatite crystal structure's trivalent cation sites.

a)

SAMPLE	Ag	Al	As	Ba	Be	Bi	Ca	Cd	Co	Cr	Cs	Cu	Fe	Ga	Ge
	ppm	%	ppm	ppm	ppm	ppm	%	ppm	ppm	ppm	ppm	ppm	%	ppm	ppm
HG-0	10.45	4.11	85	640	2.11	1.00	3.3	9.03	15.3	135	5.9	424	4.26	19.8	0.28
HG-60	0.89	5.49	27.6	330	2.32	0.24	5.9	2.89	5.7	132	7.3	135.5	1.82	13.3	0.24
HG-100	1.32	5.31	21.6	300	2.4	0.4	4.8	3.81	9	182	6.4	94.1	2.04	12.8	0.27

	Hf	Hg	In	K	Li	Mg	Mn	Mo	Na	Nb	Ni	Pb	Rb	Re	S
	ppm	ppm	ppm	%	ppm	%	ppm	ppm	%	ppm	ppm	ppm	ppm	ppm	%
HG-0	1.9	1.85	0.07	1.89	22.1	0.61	62	285	0.24	7.3	1050	149.5	95.2	0.631	1.37
HG-60	2.5	0.183	0.05	2.41	27.9	0.70	82	27	0.33	9.2	143	20.9	122.5	0.066	0.31
HG-100	2.2	0.255	0.05	2.26	27.2	0.69	80	58	0.30	8.0	377	26.5	108.5	0.336	0.57

	Sb	Sc	Se	Sn	Sr	Ta	Te	Th	Ti	Tl	U	V	W	Zn	Zr
	ppm	ppm	ppm	ppm	ppm	ppm	ppm	ppm	%	ppm	ppm	ppm	ppm	ppm	ppm
HG-0	56.6	10.1	82	2.2	370	0.48	2.95	6.69	0.223	39.1	27.7	1735	1.7	790	80.1
HG-60	5.3	11.6	7	2.2	158	0.64	0.8	9.55	0.274	5.42	37.3	387	2.2	272	88.6
HG-100	6.01	10.3	19	2.1	127.5	0.57	0.29	7.71	0.264	5.25	59.4	590	1.8	500	78.6

	La	Ce	Dy	Er	Eu	Gd	Ho	Lu	Nd	Pr	Sm	Tb	Tm	Yb	Y
	ppm	ppm	ppm												
HG-0	30.4	36.1	3.49	1.96	0.87	4.09	0.65	0.29	27.2	6.66	5.04	0.56	0.27	1.9	24.1
HG-60	87.1	82.8	12.35	6.33	2.72	13.85	2.3	0.7	80.5	20.1	15.05	1.92	0.8	4.8	89.5
HG-100	76.8	82.9	11.3	6.03	2.3	12.2	2.16	0.64	68.7	16.3	13.05	1.73	0.76	4.54	81.2

RED Bold = Highly enriched

Yellow = depleted

All samples are organic-rich mudrocks

All samples have >10,000ppm P

b)

Sample	Fm.	Hg ppm	Hg ppb	TOC wt%	Hg ppb / TOC
HG-0-Hg	WDFD Shale	1.85	1850	12.70	146
HG-60-Hg	WDFD Shale	0.183	183	6.57	28
HG-100-Hg	WDFD Shale	0.255	255	12.90	20

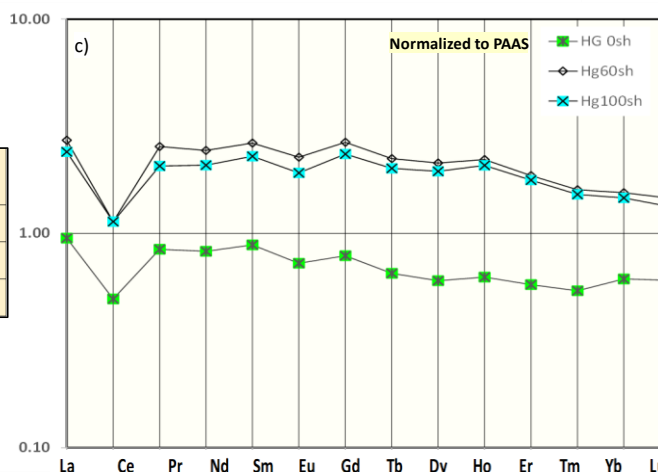


Figure 2.2.7 a) ICP-MS data for 3 shale samples collected at 0, 60, and 100cm from top WDFD. Bold red numbers highlight anomalously high metal concentrations at D/C boundary. b) Mercury data normalized to %TOC. HG-0-Hg is anomalously enriched. c) Rare Earth Element concentrations in 3 shales normalized the Post Archean Average Shale (McClennan, 1989).

6. In addition to a well-defined Devonian-Carboniferous boundary at Hass-G, there additional outcrops downstream along South Jack Creek that expose the pre-Welden shale, Welden Limestone, and basal Caney Shale. crop out (A, B, C on Figure 2.2.1). Studies of these outcrops (Haywa-Branch and Barrick, 1990; Over and Barrick, 1990; Boardman and Puckette, 2006) integrated with Hass-G enable the construction composite stratigraphic column that encompasses the entire Late Devonian to Early Mississippian section on the Lawrence uplift (Figure 2.2.8).

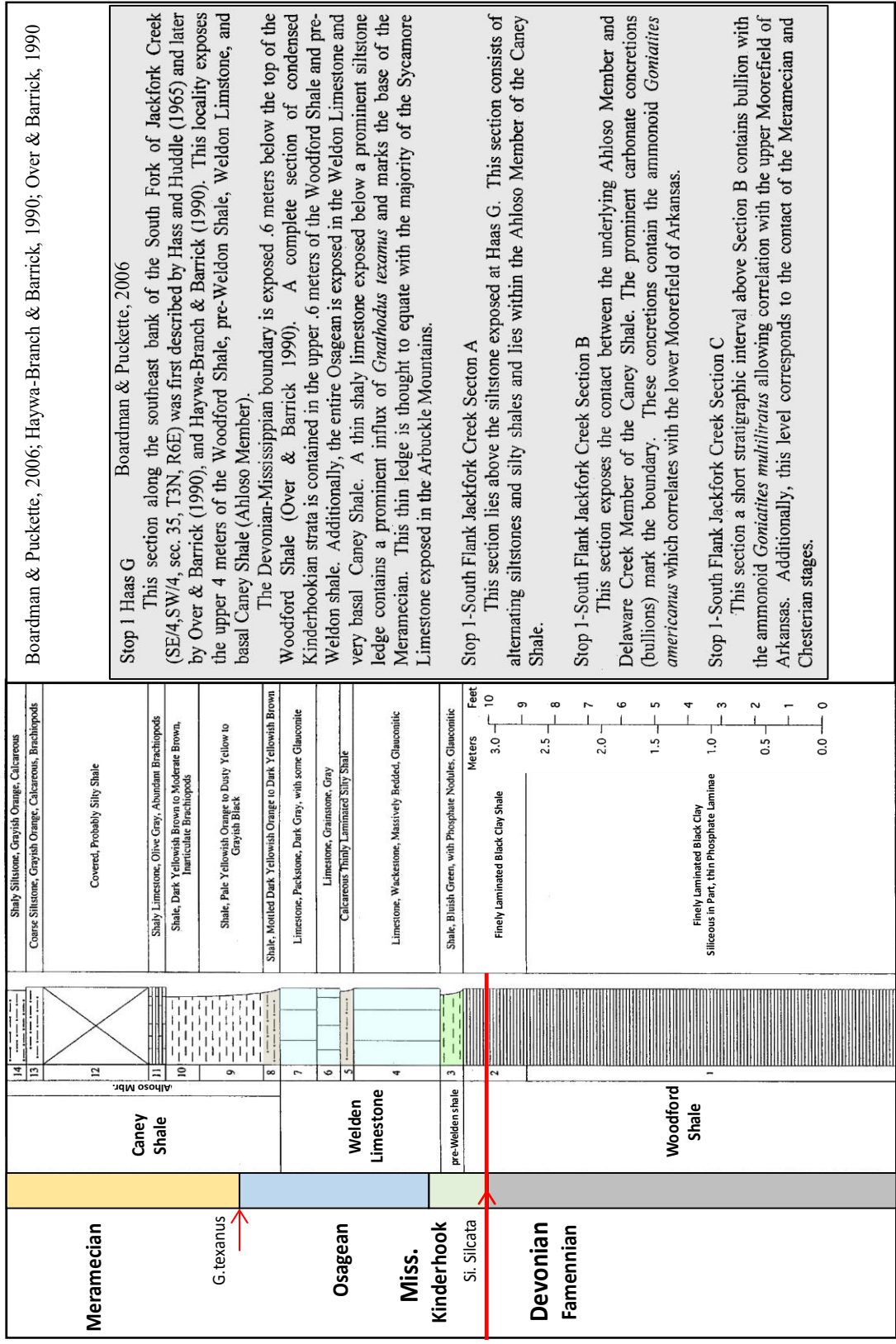


Figure 2.2.8 Composite stratigraphic section along South Jack Fork Creek, Hass-G location.

REFERENCES

- Boardman, D.R., and Puckette, J., 2006, Stratigraphy and paleontology of Upper Mississippian Barnett Shale of Texas and the Caney Shale of Southern Oklahoma, Oklahoma Geologic Survey Open file Report 6-2006, 89p.
- Hass, W.H., and J.W. Huddle, 1965, Late Devonian and early Mississippian age of the Woodford Shale in Oklahoma as determined from conodonts, in Geological Survey Research 1965: U.S. Geological Survey Professional Paper 525-D, p. 125-132.
- Haywa-Branch, J.N., and Barrick, J.E., 1990, Conodont stratigraphy of the Welden Limestone (Osagean/Mississippian) Lawrence Uplift South-Central Oklahoma, in S.M. Ritter, ed., Early to middle Paleozoic conodont biostratigraphy of the Arbuckle Mountains, southern Oklahoma: Oklahoma Geological Survey, Guidebook 27, p. 75-85.
- McLennan, S.M. (1989) REE in sedimentary rocks: Influence of provenance and sedimentary processes. *Reviews Mineralogy* 21, 170-199.
- Orth, C.J., L.R. Quintana, J.S. Gilmore, J.E. Barrick, J.N. Haywa, and S.A. Spesshardt, 1988, Pt-group metal anomalies in the Lower Mississippian of southern Oklahoma: *Geology*, v. 16, p. 627-630.
- Over, D.J., and J.E. Barrick, 1990, The Devonian/Carboniferous boundary in the Woodford Shale, Lawrence uplift, south-central Oklahoma, in S.M. Ritter, ed., Early to middle Paleozoic conodont biostratigraphy of the Arbuckle Mountains, southern Oklahoma: Oklahoma Geological Survey, Guidebook 27, p. 63-73
- Over, D. J., 1990, Conodont biostratigraphy of the Woodford Shale (Late Devonian- Early Carboniferous) in the Arbuckle Upper Mountains, South-Central Oklahoma, Texas Tech University PhD Dissertation, 186 p.
- Over, D. J., 1992, Conodonts and the Devonian-Carboniferous Boundary in the Upper Woodford Shale, Arbuckle Mountains, South-Central Oklahoma, *Journal of paleontology*, Vol. 66, No. 2, p. 293-311.
- Rakociński, M., Marynowski, L., Agnieszka, P., & others, 2020, Volcanic related methylmercury poisoning as the possible driver of the end-Devonian Mass Extinction, *Nature Reports* 10-7344, 8p.

2.3 Woodford Log: North Jack Fork Creek T3N R6E C Sec 34: This stop is an expansive inactive shallow shale pit on the south side of North Jack Fork Creek about ½ mile County Road 1600 (Figure 2.3.1). The original culvert over the creek has washed out and access is by a small track through the woods. The location is not accessible by tour bus. Permission from the quarry owner is recommended.

The stellar feature of this location is a giant (34ft long) silicified tree trunk (Figure 2.3.2 a, b). Here the Woodford is almost exclusively a light to dark gray, fissile siliceous mudrock (Figure 2.3.2a and c) that makes a characteristic crunching sound when walked upon. The vertical extent of section exposed is limited. From local stratigraphic considerations (Hass-G, Section 2.2), its lighter color, and lack of phosphate nodules, we place this section in the Upper Woodford. In a small excavation on the west side of entrance to the quarry thin layers of current laminated argillaceous siltstone are present (Figure 2.3.2d).

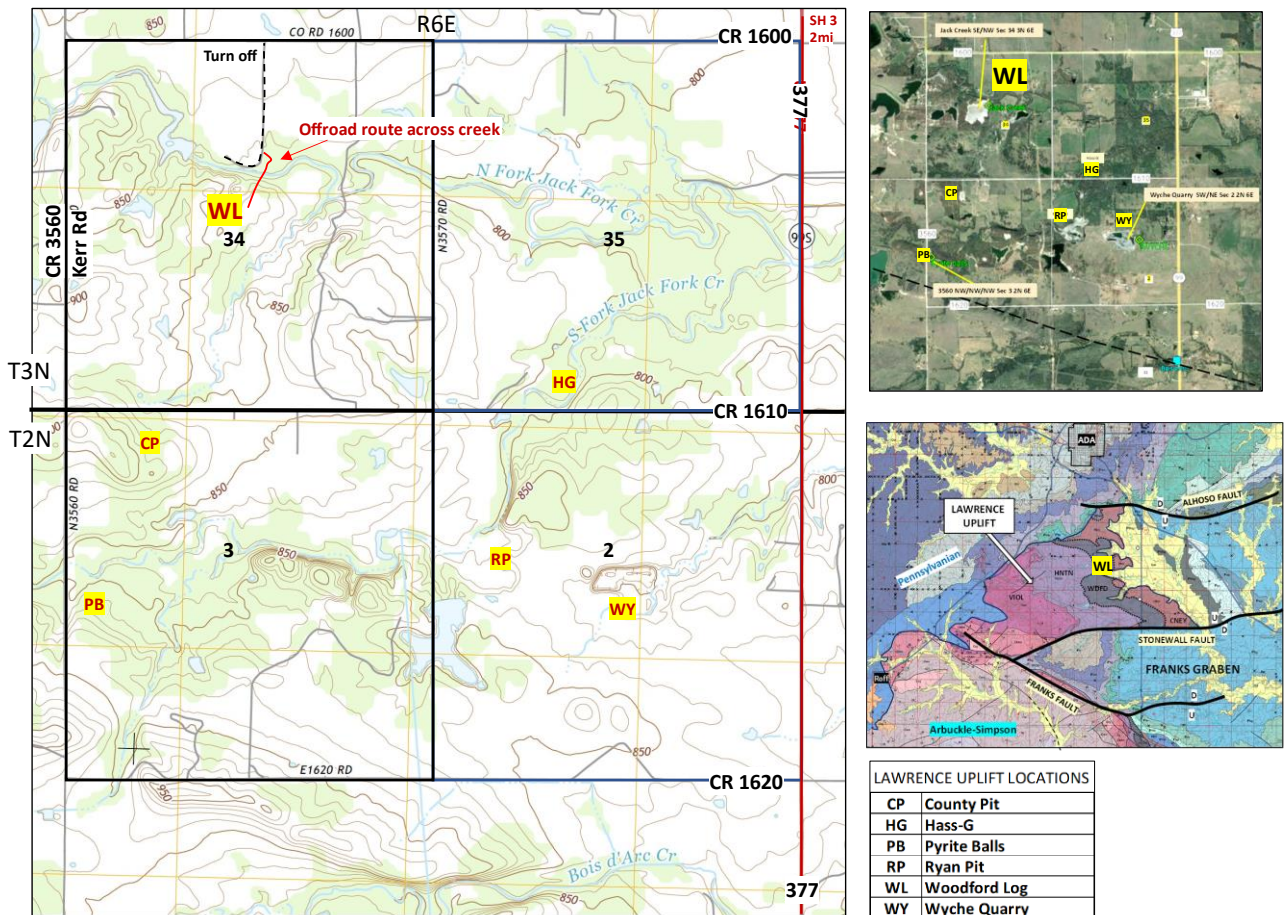


Figure 2.3.1 Location map and Google Earth image of Woodford Log (WL) location of CR 1600.



Figure 2.3.2 a) Photo of giant silicified tree trunk b) Aerial view of Woodford tree trunk with 2 geologists for scale. c) Platy brittle Woodford shale with small crenulation, yellow arrow. d) Thin siltstone beds in quarry pit wall.

In addition to the Woodford log this location several interesting structural features. Two prominent fracture sets can be seen on the bed tops (Figure 2.3.3). The E-W striking fractures (also prominent at the Wyche quarry) are more widely spaced but have a much greater length than a NW-striking set of fractures. On the small west wall of the quarry one can see some vertical fracturing are preferentially confined to the more siliceous unit, nicely illustrating the concept of brittle (siliceous) / ductile (shaley) mechanical stratigraphy (Figure 2.3.4). These features are a good stimulus for a discussion of a preferred direction of a horizontal well to optimize stimulated rock volume upon hydraulic fracture stimulation.



Figure 2.3.3 Well developed fracture set of bed tops.

The giant Woodford tree trunk (34ft x 3.5ft) is a silicified *Callixylon* log and is likely the largest specimen recorded in the Woodford (Cullen et al., 2021). Petrified wood is widespread but not abundant in the Woodford (Suneson, 2010). The Lower Woodford has a meter-sized block of petrified wood along Henry House Creek, Hass-A (Auffill, 2007). Smaller branches of petrified wood is relatively abundant in the Upper Woodford at Hass-G (Section 2.2). In addition to its remarkable length, the petrified log at this site exquisitely preserves bark that appears to be burned (Figure 2.3.5a, b) and details of vascular tissue (Figure 2.3.6c). Compactional drape around the log is very well expressed (Figure 2.3.6d). How such a large log came to be deposited in the Woodford is a matter of conjecture. We propose that the original tree was burned in a massive forest fire, floated out to sea, eventually became water saturated, sank into the dysoxic muddy ocean floor below storm weather wave base, and was subsequently buried.



Figure 2.3.4 Quarry wall with minor discontinuous fractures (yellow arrows) in more brittle B-2 unit that do not cut through the more argillaceous bounding beds, B1 and B3.

The term *Callixylon* was originally reserved for the trunks and limbs of a species of tree, *Archeopteris*. Its leaves and branches are rarely found together. It wasn't until 1960 that they were assigned to a single biological taxon by Beck (1960) who established that *Archeopteris* is a progymnosperms that resembles a large top heavy Christmas tree with relatively small leaves (Figure 2.3.7a,b). *Archeopteris* had a short evolutionary run from the middle Frasnian to extinction at the end of the Devonian. It is curious that despite large fragments of wood, virtually no smaller leafy, humic organic matter occurs in the Woodford, a world class marine algal source rock. We hypothesize that the Famennian Wildfire Explosion in Euramerica (Lu et al., 2022; Figure 2.3.7.c, d) preferentially burned leaves and small branches leaving behind mostly larger tree trunks.

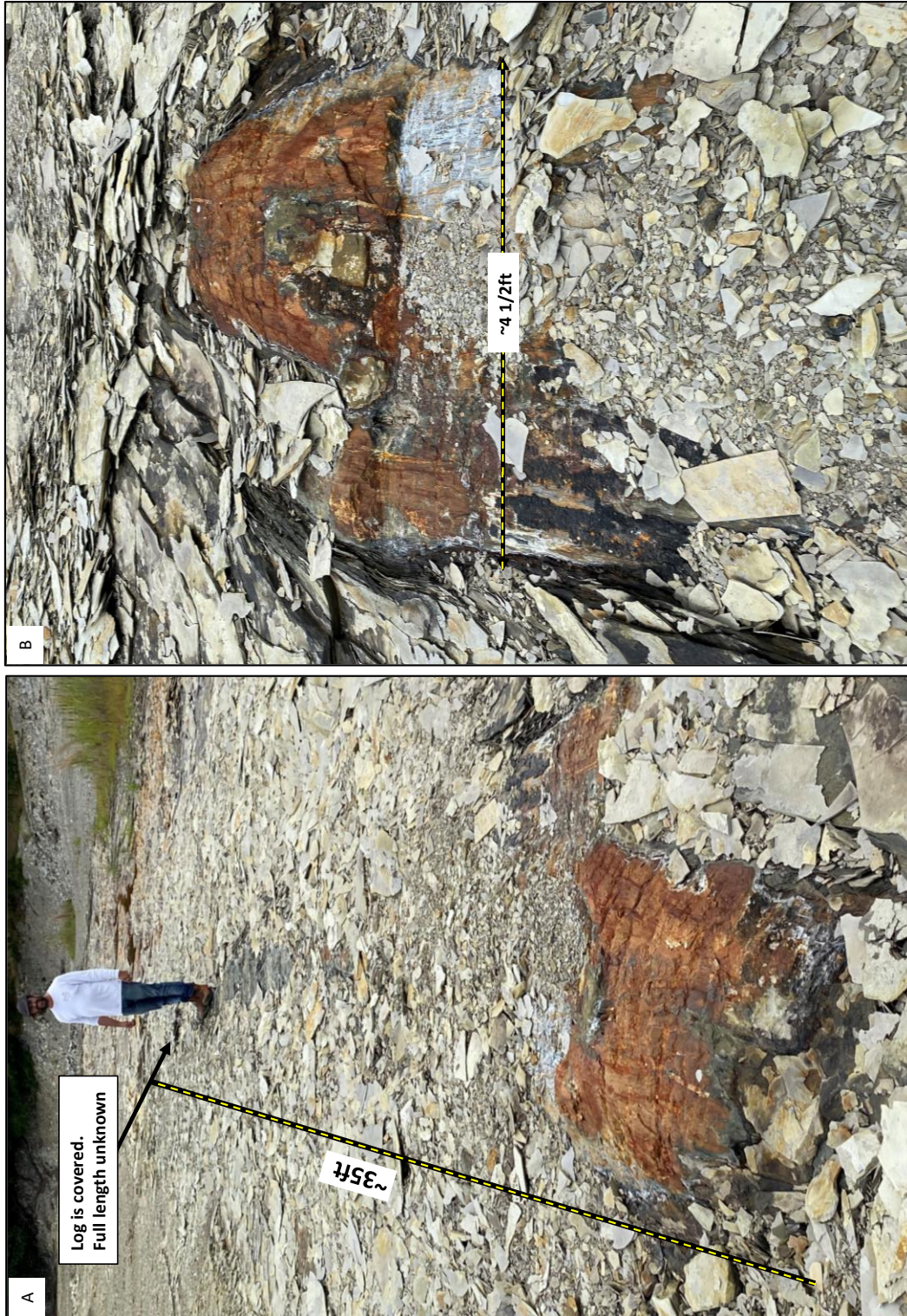


Figure 2.3.5 A) Photo showing length and girth of silicified log B) Close up photo of the base of the log.

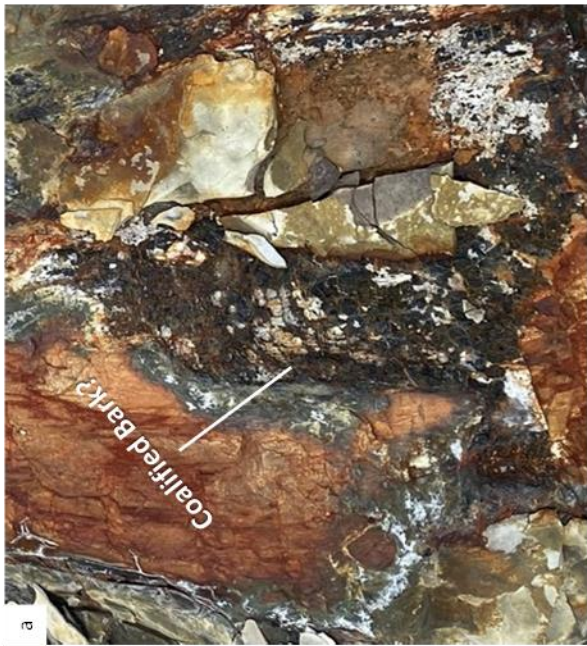
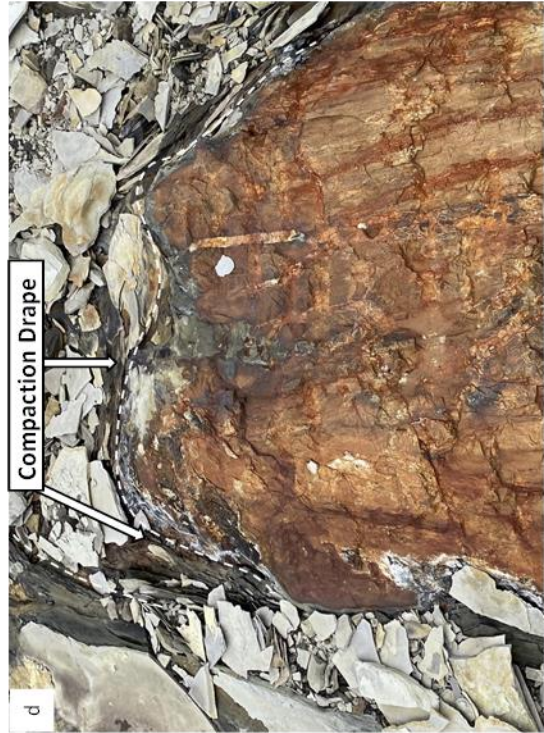
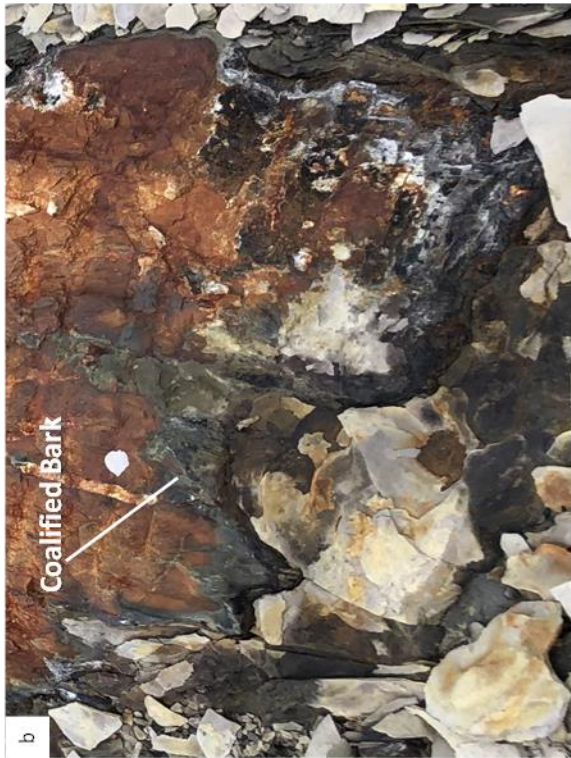


Figure 2.3.6 Detailed preservation of bark, vascular tissue, compactional drape associated with Woodford log.

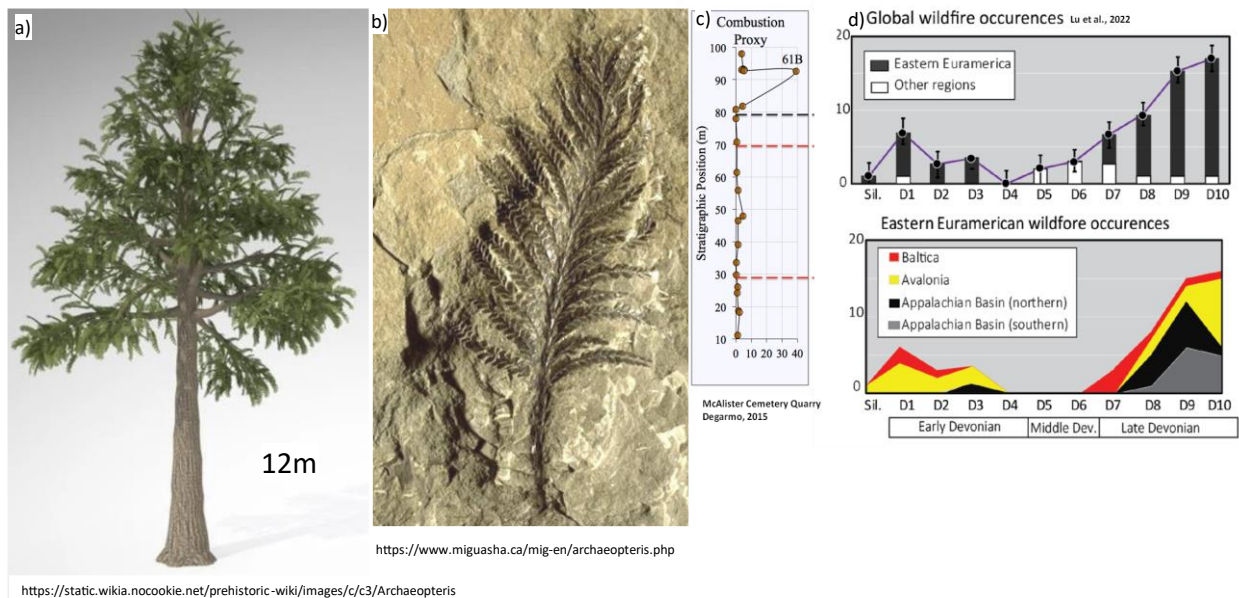


Figure 2.3.7 a) Idealized representation of the full Archeopteris tree, b) Photo of fossilized leaves, c) Plot of combustion proxy biomarker vs. stratigraphic position at McAlister Cemetery Quarry (DeGarmo, 2015), d) Global and regional Euramerican Devonian wildfire occurrences (Lu et al., 2022)

REFERENCES

Aufill, M., 2007, High resolution magnetic susceptibility of the Oklahoma Woodford Shale and relationship to variations in outcrop spectral-gamma response: Oklahoma State University, unpublished M.S. thesis, 210 p.

Beck, C.B., 1960, Connection between Archeopteris and Callixylon. *Science* 131:1524-1525

Cullen, AB., Hull, D. Turko, M., 2021, An Intact Thirty-four foot long petrified log in the Woodford Shale, Oklahoma: A question of preserving geological heritage, *Oklahoma City Geological Society Shale Shaker*, v.72-4, 12p.

Lu, M., Ikejiri, T., and Lu, Y., 2012, A synthesis of the Devonian wildfire record: Implications for paleogeography, fossil flora, and paleoclimate, *Palaeogeography, Palaeoclimatology, Palaeoecology* 571, p.1-16.

Suneson, N., 2010, Petrified Wood in Oklahoma, *Oklahoma City Geological Society Shale Shaker*, v.60-6, 21p.

2.4 Additional Lawrence Uplift Locations:

We have included two exposures Woodford on the Lawrence uplift not been previously described. The exposures are shallow shale pits are directly adjacent to county roads between outcrops previously discussed. Although easily accessible, both locations are small with limited vertical exposure. Consider these as short optional stops rather than must-see localities.

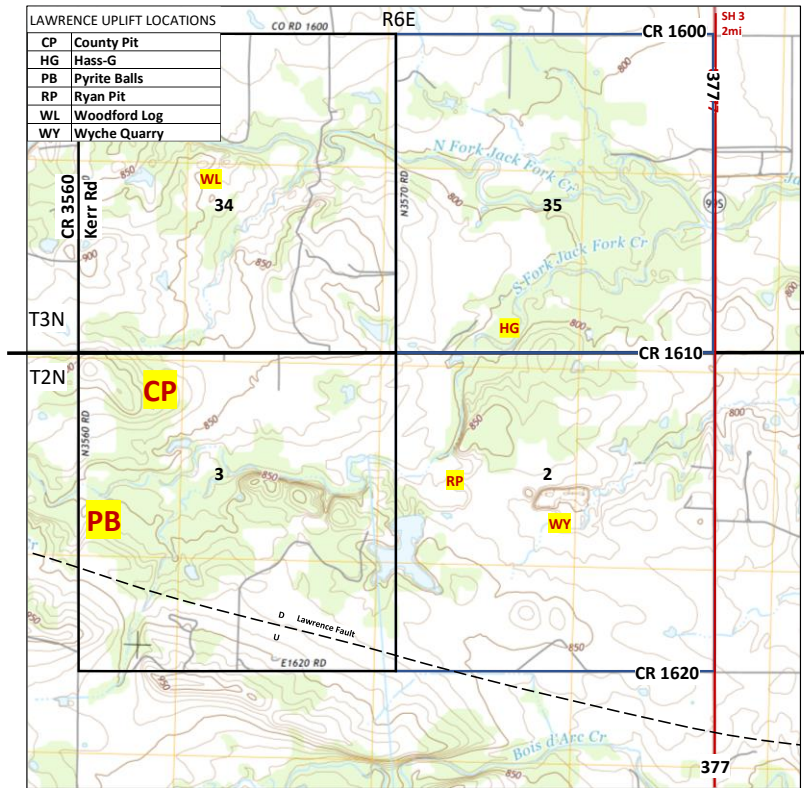


Figure 2.4.1 Location map for Pyrite Balls and County Pit sites

Pyrite Balls: About 30ft of Woodford is exposed on the east side of CR3560, which becomes Kerr Lab Road heading north to Ada. The outcrop is dominated by thin-bedded to papery dark gray mudstone which transitions to flaggy/ slatey mudstone at the top of the outcrop. Phosphate nodules appear to be absent and there is minor chert in the float towards the top of the hill. Of interest at this location is a 2-3ft pyrite bearing bed. The pyrite occurs as small lenses and as spectacular balls up to 2in/6cm in diameter that are encrusted with aggregates of euhedral pyrite crystals 3-4mm across (Figure 2.4.2).

There are only a few of these large pyrite balls at this outcrop and we have not seen such well-developed aggregates of this morphology elsewhere in the Woodford. *Therefore, unless you are specifically studying pyrite geochemistry in the Woodford before collecting one, please ask yourself if a photo would suffice.*



Figure 2.4.2 Aerial and road view of Pyrite Palls location off CR3560. Photo of ball composed of massive pyrite coated with aggregated euhedral pyrite crystals.

County Pit 3510: This location is 500ft south of CR1610 about 1mi from Hass-G and 0.8mi from the Pyrite Ball locations (Figure 2.4.1). About 1.4 acres has been stripped away by the county to expose the tops of several beds of Woodford. Vertical exposure is minimal. The CP location has two noteworthy features. The first is a very well exposed fractures in the bed tops. These can be grouped into 3 sets: NW-SE, E-W and NE-SW. The NE-SW fractures are more closely spaced and abundant. This location is suitable for a more rigorous statistical fracture study. Second, the exposed beds have abundant rounded phosphate nodules, with REE enrichment similar to those at the Wyche Quarry (Figure 2.4.3c).

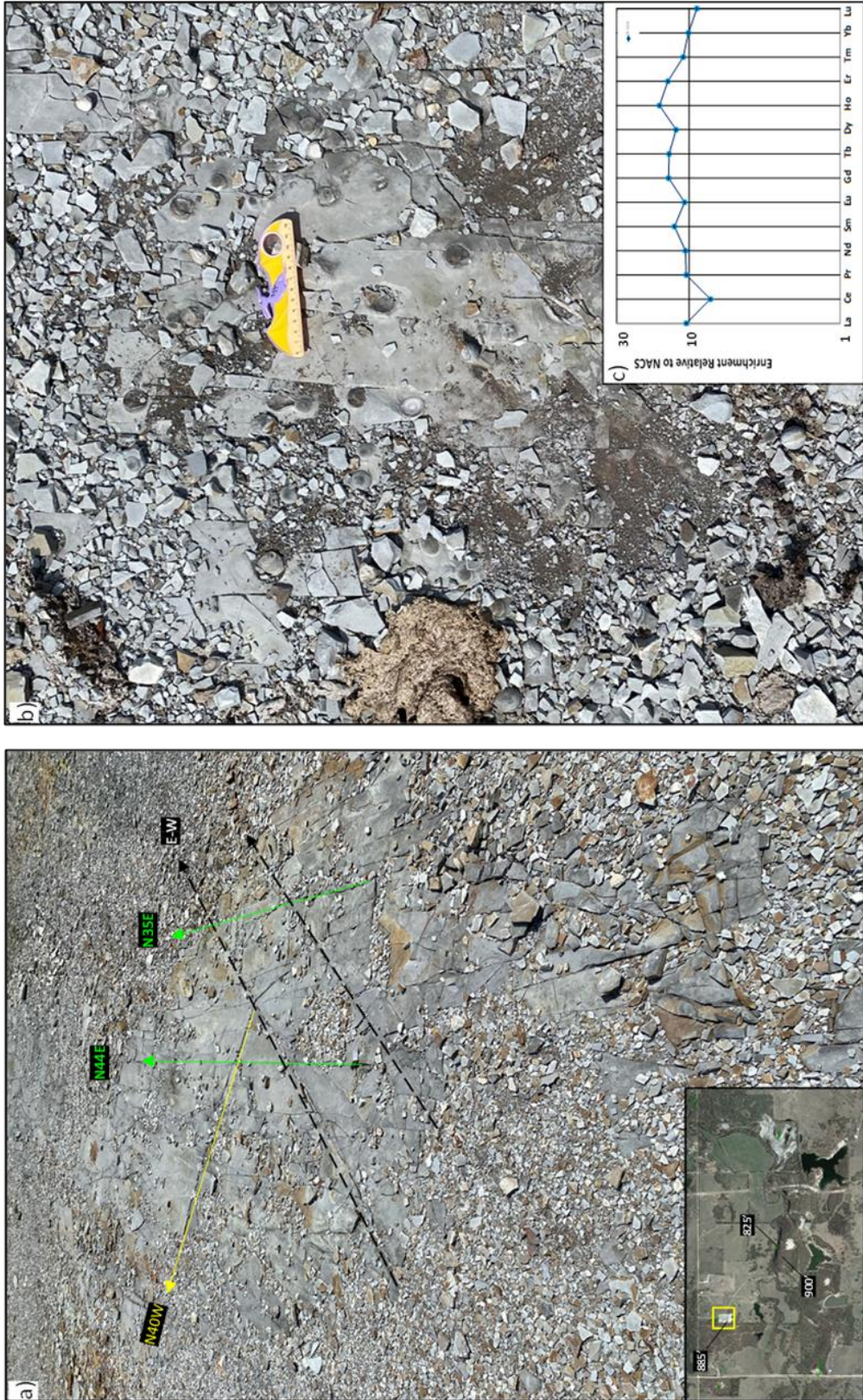


Figure 2.4.3 a) Fracture sets at CP b) Concentrically banded spherical phosphate nodules c) REE plot normalized to North American Composite Shale showing up to 10X enrichment.

3.1: Hunton Quarry Anticline 1S-3E C-31: Stop 3.1 is on the nose of a NW plunging anticline that is related to the Tishomingo-Belton anticline along the Reagan Fault (Figures 3.0). If coming from Ada & Sulphur one travels west of the Goddard Youth Camp Road (Figure 3.1.1). There is sufficient room to park a motor on the north side of the road. At this location there is a quarry in the Hunton Group and several Woodford shale pit. This location is a frequently visited stop owing to the textbook example of a gently folded anticline with a small thrust fault in the Cravett Member of the Bois d'Arc Formation, Hunton Group (Stanley, 2013; Figure 3.1.3). Given the excellent Hunton exposure we recommend visiting the quarry and then walking east to the base of the Woodford in shale pit B (Figure 3.1.2).



Figure 3.1.1 Location and road map for Hunton Quarry Anticline

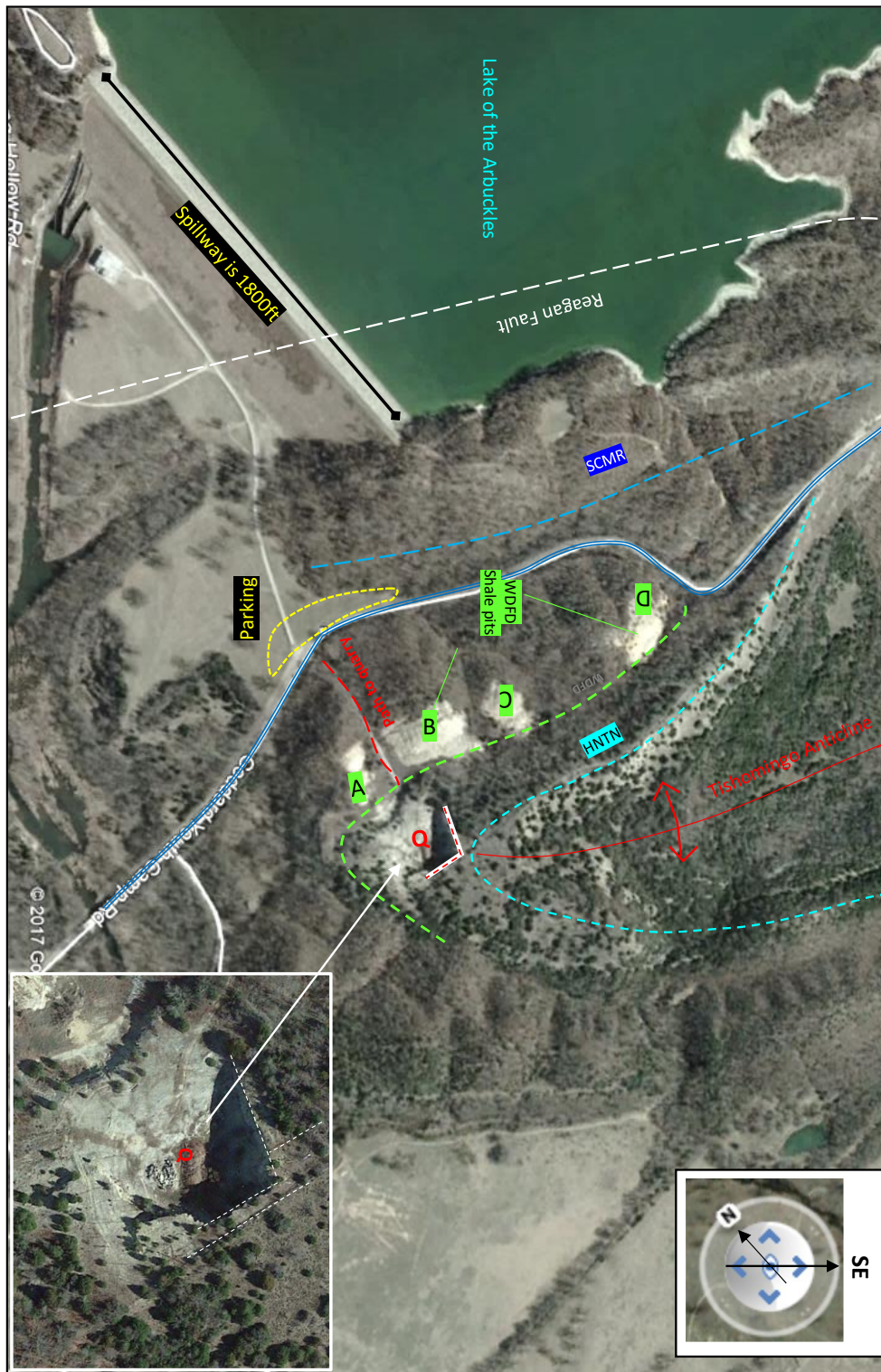


Figure 3.1.2 Aerial view of Hunton quarry (Q), Woodford shale pits (A,B, C,D) and a sketch of geological contacts on NW-plunging anticline along the Reagan Fault.

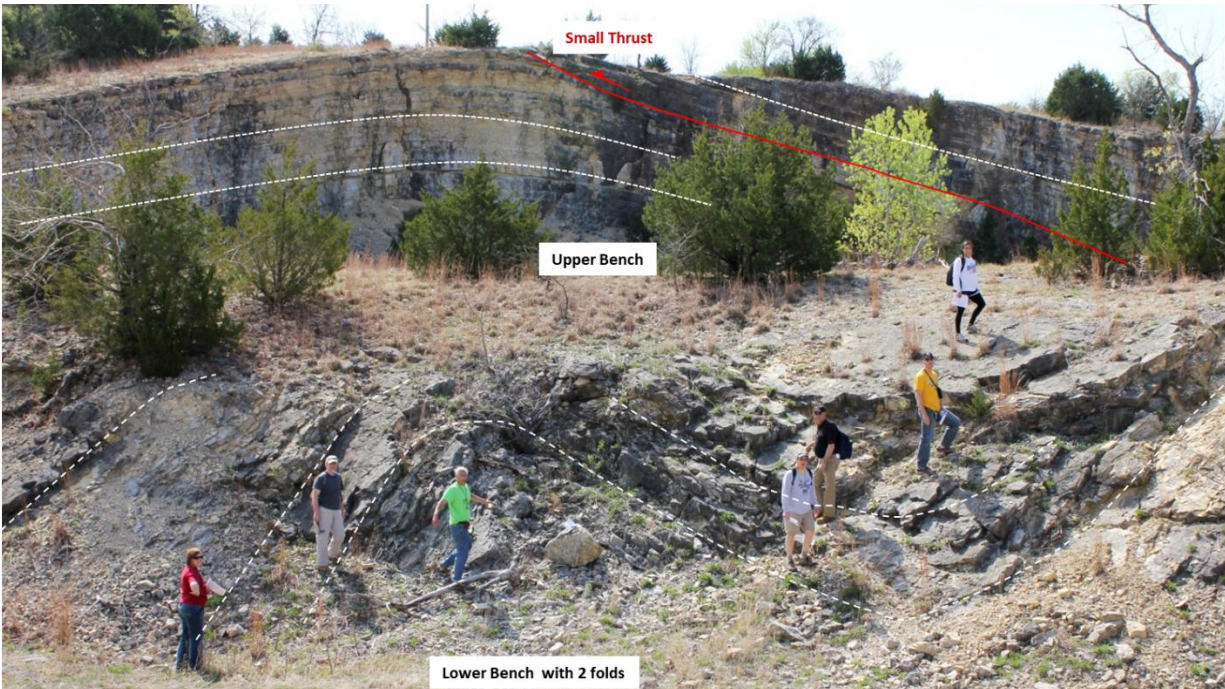


Figure 3.1.3 Hunton quarry anticline with small thrust fault. Note the double fold in the thinner bedded lower bench.

The quarrymen exploited two nearly orthogonal vertical fracture sets (N20°E and N70°W; Figures 3.1.2, 3.1.4). On the west side of the quarry, Cullen (2017) documented the WNW fractures tend to be calcite-cemented and closed; whereas the NNE be open with minor calcite fill and have occasional horizontal slickenlines with down-stepping asperities that suggest right lateral movement (Figure 3.1.5). These two vertical orthogonal fracture sets do not fit Mohr-Coulombic shear fracture relationships suggesting two episodes of fracturing. The slicklines suggest the N20°E may record an additional phase of deformation. Regardless of the interpretation of these observations, interesting questions are posed regarding preferred azimuth of horizontal wells and/or placement of injector-producer pairs in a secondary recovery project.

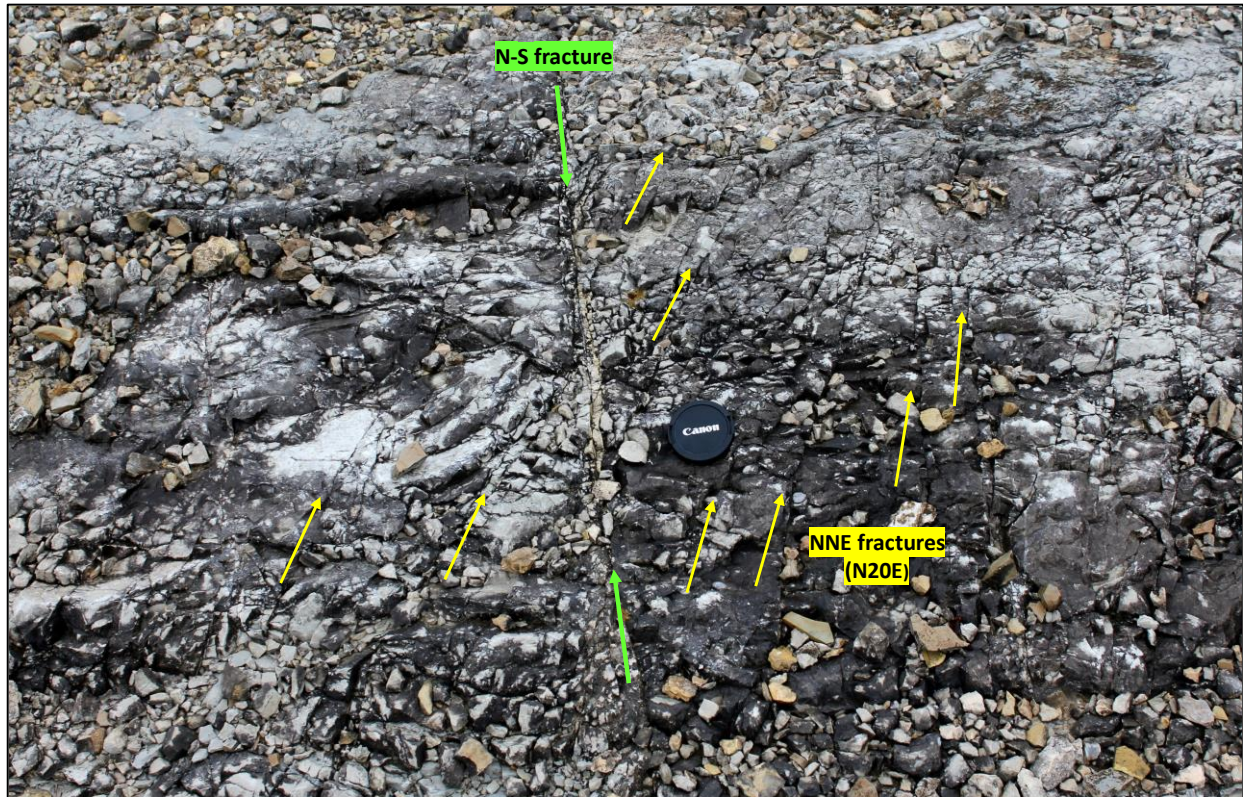


Figure 3.1.4 Well-developed fracture sets in Hunton Group limestones.



Figure 3.1.5 Vertical fracture sets in Hunton limestones with the NNE set (1) tending to be open with some having horizontal slickenlines with probable right-lateral motion. The NW set (2) are cemented and closed.

The main purpose of this stop is to examine the Woodford Shale where a nearly complete section has been studied by Turner et al., (2016) and Tréanton (2014). At this location the Woodford shale is primarily composed of fissile dark gray to black siliceous shale interbedded with light gray silty mudrock. Bedded chert is rare and there is one prominent ferroan-dolomitic bed in the Lower Woodford (Figure 3.1.7). The lower Woodford also exhibits excellent brittle ductile couplets (Figure 3.1.8). Also of note are several porous white beds near the top of the Middle Woodford that are composed of recrystallized radiolarians and sponge spicules. Similar porous white quartzose beds are present in the Upper Woodford at McAllister Cemetery Quarry, stop 4.1.

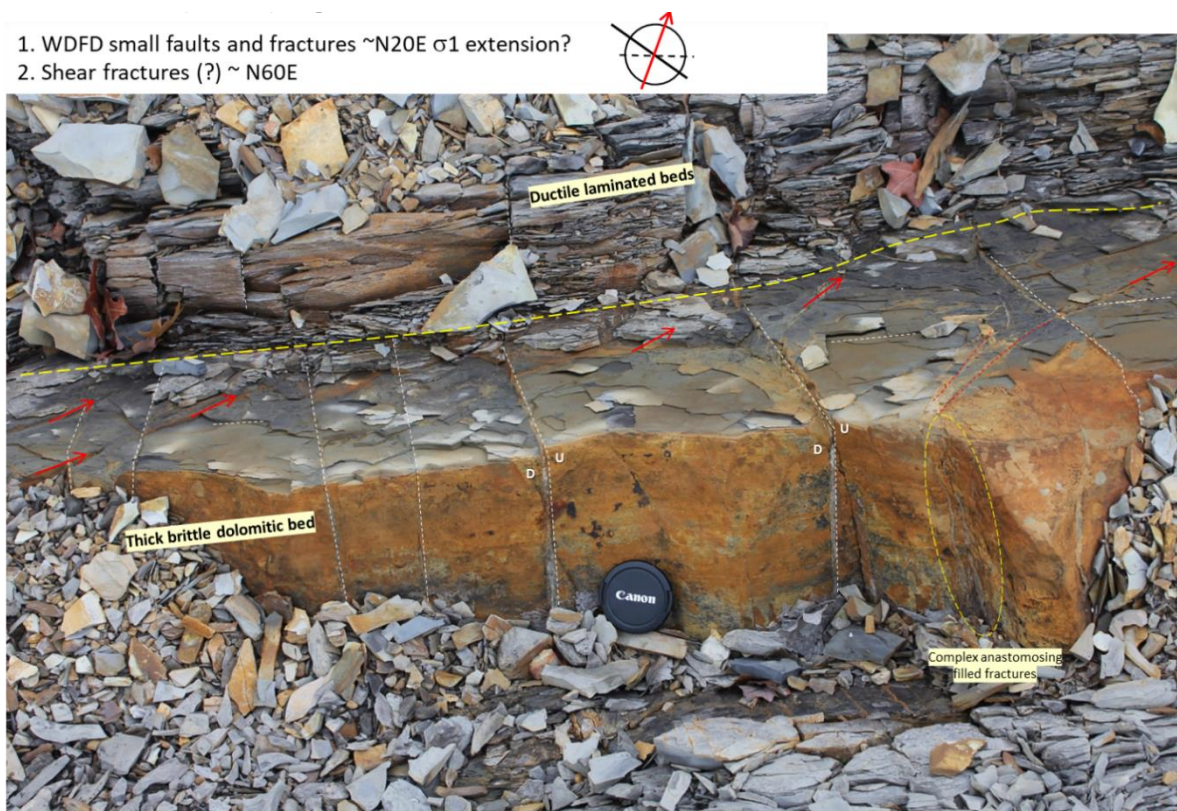


Figure 3.1.6 Ferroan dolomite bed with well-developed fracture sets of similar orientation as limestones in the Hunton quarry. Note 1) the NNE set has some minor (cm-scale) displacement-down to the west 2) The fractures do not extend through the overlying ductile laminated beds.



Figure 3.1.7 Excellent example of brittle-ductile couplets in the Lower Woodford.

There are only a few phosphate nodules in the Upper Woodford and these are smaller than phosphate nodules at most other locations (Figure 3.1.8). They are associated with the finely laminated siliceous shale facies at Pit B. At Pit D only a single phosphate nodule was logged by Tréanton (2014). Although the uppermost section of the Upper Woodford is covered on a dip slope at that location, loose nodules in the colluvium are quite rare.

Whilst pits B and D are only separated by along strike by 1,200ft (363m) correlating these transects is not straight forward. Three correlations considered, by Tréanton. The one preferred (red star) is good for the Middle Woodford, but which requires (red star) is very good for the middle section but requires adding missing (covered) section at both the base and top of Pit D (inset lower left of Figure 3.1.9).



Figure 3.1.7 Small, loose, phosphate nodules from Upper Woodford.

Another problematic issue highlighting short distance lateral variability can be seen in the poor match in the XRD-based chemostratigraphic facies (Figure 3.1.10). Both profiles show the increase in terrestrial input (Zr, Ti, Al). The strong redox facies and Mo-clay facies in the Lower and Middle Woodford at Pit B, respectively, are substantially suppressed at Pit D. Moreover, recall that at the Wyche location the strong redox elements were associated with the stratigraphically shallower interval at the flooding surface at the Middle-Upper Woodford transition.

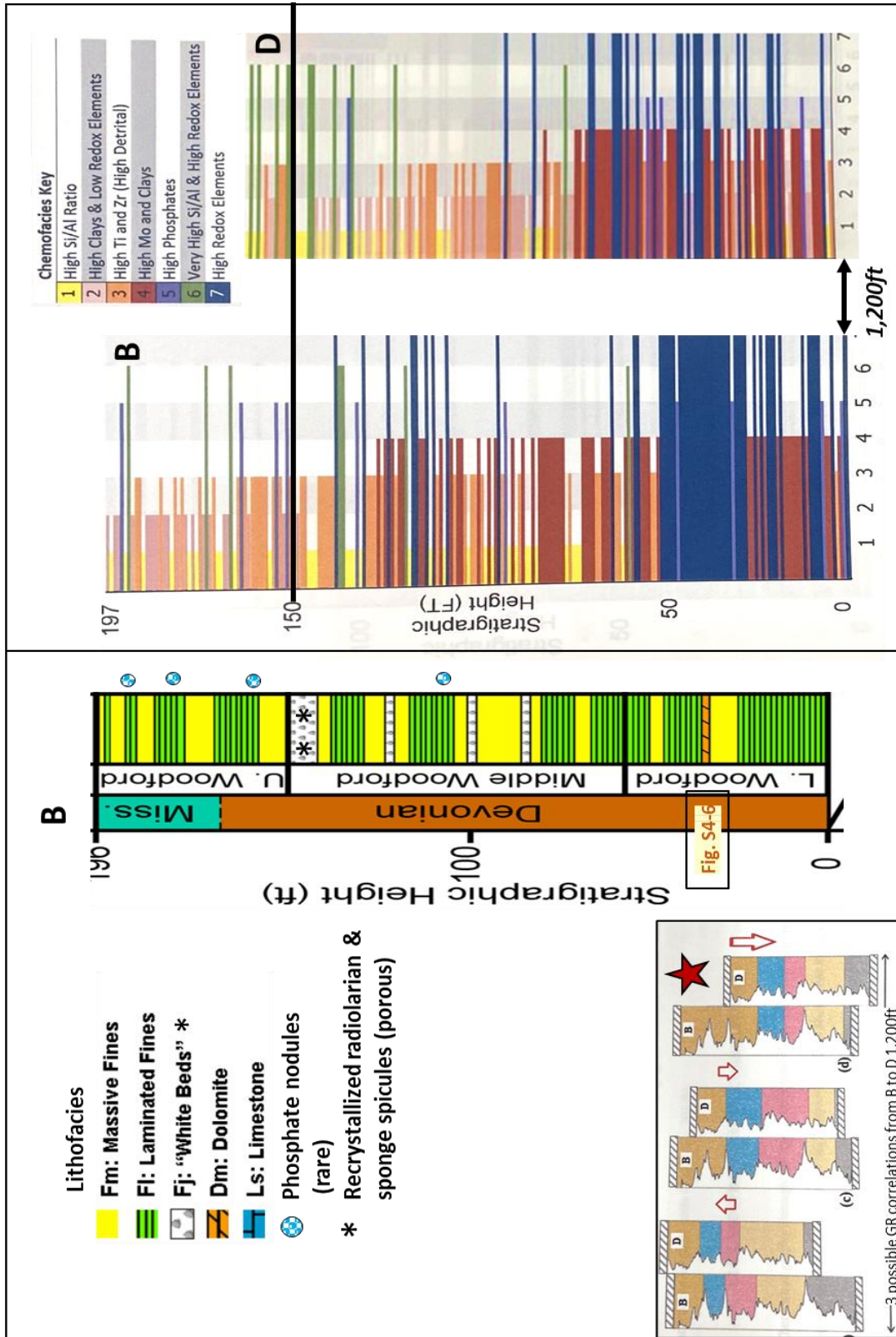


Figure 3.1.9 Lithofacies and chemofacies profile correlation between HAQ-B and HAQ-D (from Treanton 2014 and Turner et al., 2020)

REFERENCES

Cullen, A., 2017, Devonian-Mississippian petroleum systems of southern Laurasia: What makes the STACK-Merge-SCOOP play in Oklahoma so special: American Association of Petroleum Geologists, Search and Discovery Article No. 10998, 28 p.

Ham, W.E., M.E. McKinley, and others, 1954; revised by K.S. Johnson, 1990, Geologic map and sections of the Arbuckle Mountains, Oklahoma: Oklahoma Geological Survey, Map GM-31.

Stanley, T.M., 2013, The Hunton Anticline Quarry: Oklahoma City Geological Society, Shale Shaker, v. 64, p. 228- 237.

Tréanton, J., 2014, Outcrop-derived chemostratigraphy of the Woodford Shale, Murray County, Oklahoma: Norman, Oklahoma, University of Oklahoma, unpublished M.S. thesis, 83 p.

Turner, B.W., J.A. Tréanton, and R.M. Slatt, 2016, The use of chemostratigraphy to refine ambiguous sequence stratigraphic correlations in marine mudrocks. An example from the Woodford Shale, Oklahoma, USA: London, Journal of the Geological Society, v. 173, p. 854-868.

3.2: SH-77-D, The Heart of the Arbuckles. This outcrop is one of several good exposures on the north side of the Arbuckle Mountains (Figure 3.2.1). There is sufficient room off SH-77D for a motor coach; access is excellent. This stop is primarily to look at the multiple fracture sets in the Lower Woodford on the overturned limb of the Washita Valley syncline (Figure 3.2.2). The Woodford-Hunton contact is exposed at the SE end of this outcrop (Figure 3.3.3), but dense vegetation and a steep loose hillside make it difficult to visit with a large group.

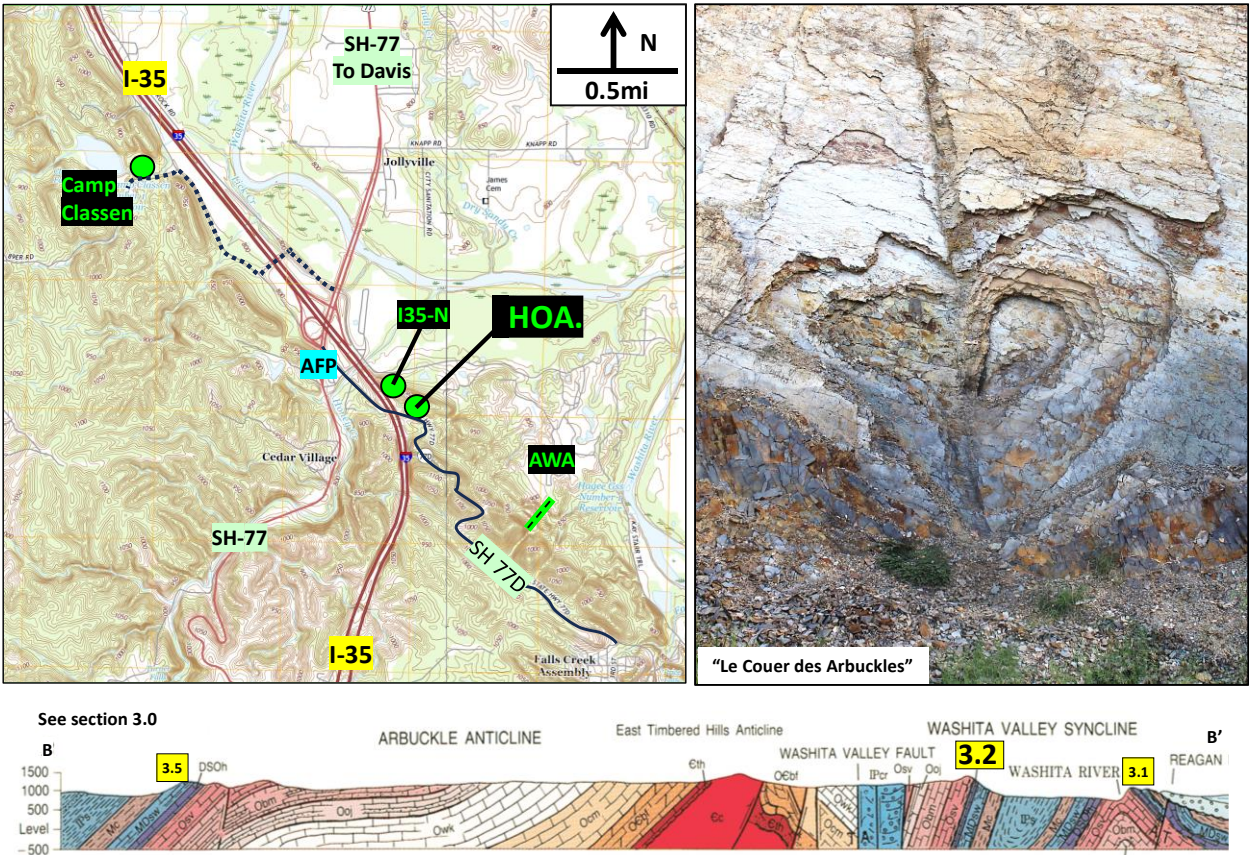
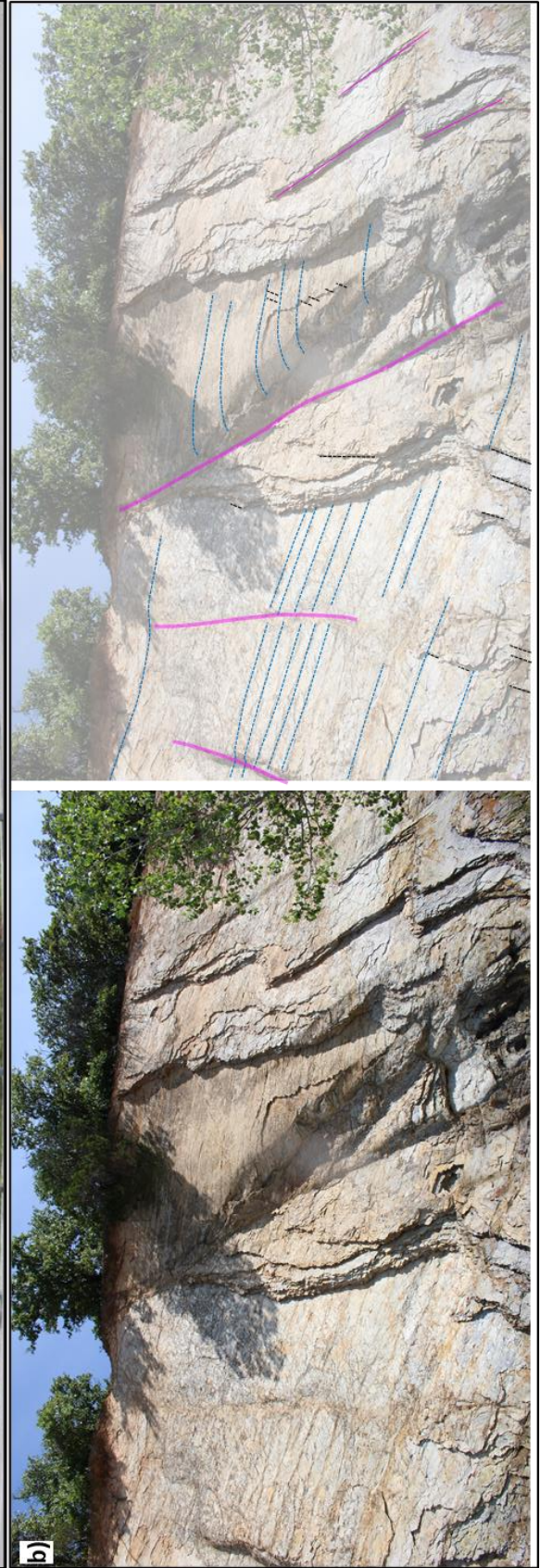


Figure 3.2.1 Location map and photo for Heart of the Arbuckles (HOA). Other Woodford outcrops in green text in black boxes, AWA- Arbuckle Wilderness Area. AFP is Arbuckle Fried Pies, a very convenient stop for restrooms. Location of section 3.2 is shown on the underlying cross section.

Three principal fracture sets cut through the Woodford here (Figure 3.2.2, 3.2.4, and 3.2.5). One interesting feature of this outcrop is the distinct fractures that are confined to thin argillaceous (ductile beds). These fractures may be related to flexural slip in the development of local structure rather than region stresses. This outcrop offers good examples of brittle-ductile couplets controlled by bed brittleness (Figure 3.2.5). In a detailed study of this outcrop Ghosh et al., (2017, 2018) identified 5 fracture sets and related their development and timing to regional structural history (Figure 3.2.8).

Figure 3.2.2 a) Panoramic view of overturned "wall" of lower Woodford looking NE along SH77D. B) Example of fractures in Woodford



Thickness
(feet)

Basal Woodford Shale

27. Interbedded shale and chert, very light gray (N8) to very pale blue (5B8/2) weathered and fresh. Shale intervals are slightly silty and exhibit well-developed fissility; laminae 0.5–1.0 in. thick. Shale intervals separated by 0.5–1.0-in.-thick chert beds; chert bedding contacts planar to slightly wavy owing to abundant phosphate nodules. Upper part of unit was not measured 5.0+
26. Fissile shale, dark gray (N3) to light olive gray (5Y5/2) weathered and fresh; shale silty, exhibiting well-developed fissility. Interval contains abundant woody material; a poorly preserved orthid brachiopod was collected at base. Upper contact is sharp and planar 0.80
25. Cherty sandstone, light brownish gray (5YR6/1) weathered and fresh; sandstone is fine grained, quartz rich, and indurated, with minor amounts of clay and silt in matrix; thin chert stringers as discontinuous lenses or pods. Upper contact is sharp and planar 0.33
24. Silty sandstone, moderate blue green (5BG4/6) weathered and fresh. Similar to unit 25, above, but contains a higher silt and clay content in matrix and is much more friable; bedding appears laminated. Chert lenses in basal 2.0–3.0 in. of unit. Upper contact is erosional, as unit 25 may be channeled down by as much as 3.0 in. into unit 24. Maximum thickness 0.46
23. Calcareous siltstone, yellowish gray (5Y7/2) to grayish yellow (5Y8/4) weathered and fresh; siltstone well laminated, with bedding laminae 0.10–0.25 in. thick; calcareous throughout but increasingly calcareous toward base as unit grades down into an argillaceous carbonate mudstone. Upper contact gradational 2.5
22. Calcareous chert (Fig. 47), labeled as "Woodford brown? carbonate" by Amsden (1960, p. 240); dark yellowish orange (10YR6/6) weathered and fresh, with grayish brown (5YR3/2) staining on fractures and bedding planes; massive, well-indurated bed, consisting of zones of chert mixed with carbonate and clastic(?) material. Laminated argillaceous mudstone interbedded with chert common in upper one-third of unit; massive chert in middle one-third of unit, with fracturing and shearing of chert common; basal one-third consists of a very fine grained siltaceous sandstone (or siltstone) interbedded with chert laminae. Horizontal and vertical burrows common along base of unit. Upper contact gradational over 6.0 in.; lower contact with Hunton Group appears sharp but slightly wavy 3.2

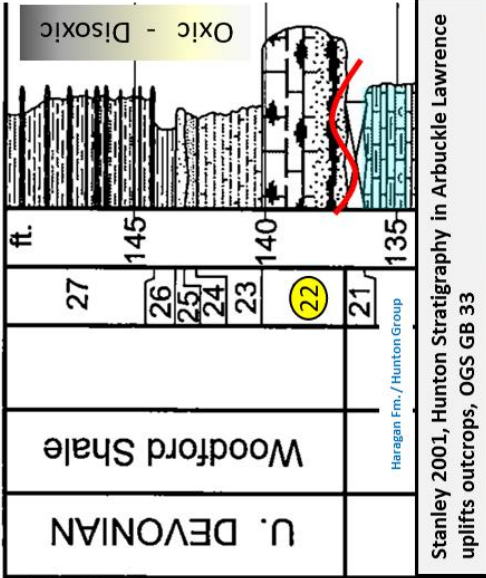
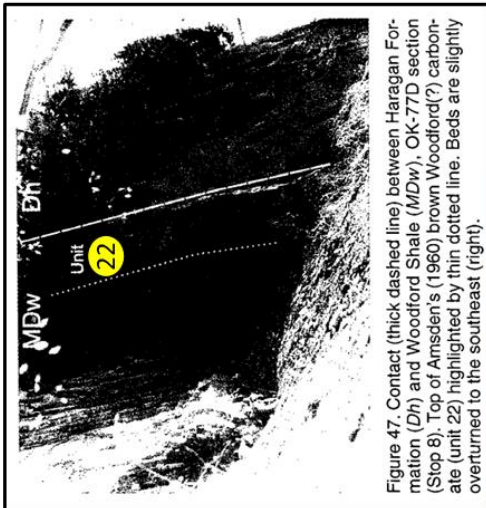


Photo approximately of Figure 47 (Stanley, 2001)

Figure 3.2.3 Description and photo of Hunton-Woodford contact along SH-77D (Stanley, 2013)

Haragan Fm. / Hunton Group

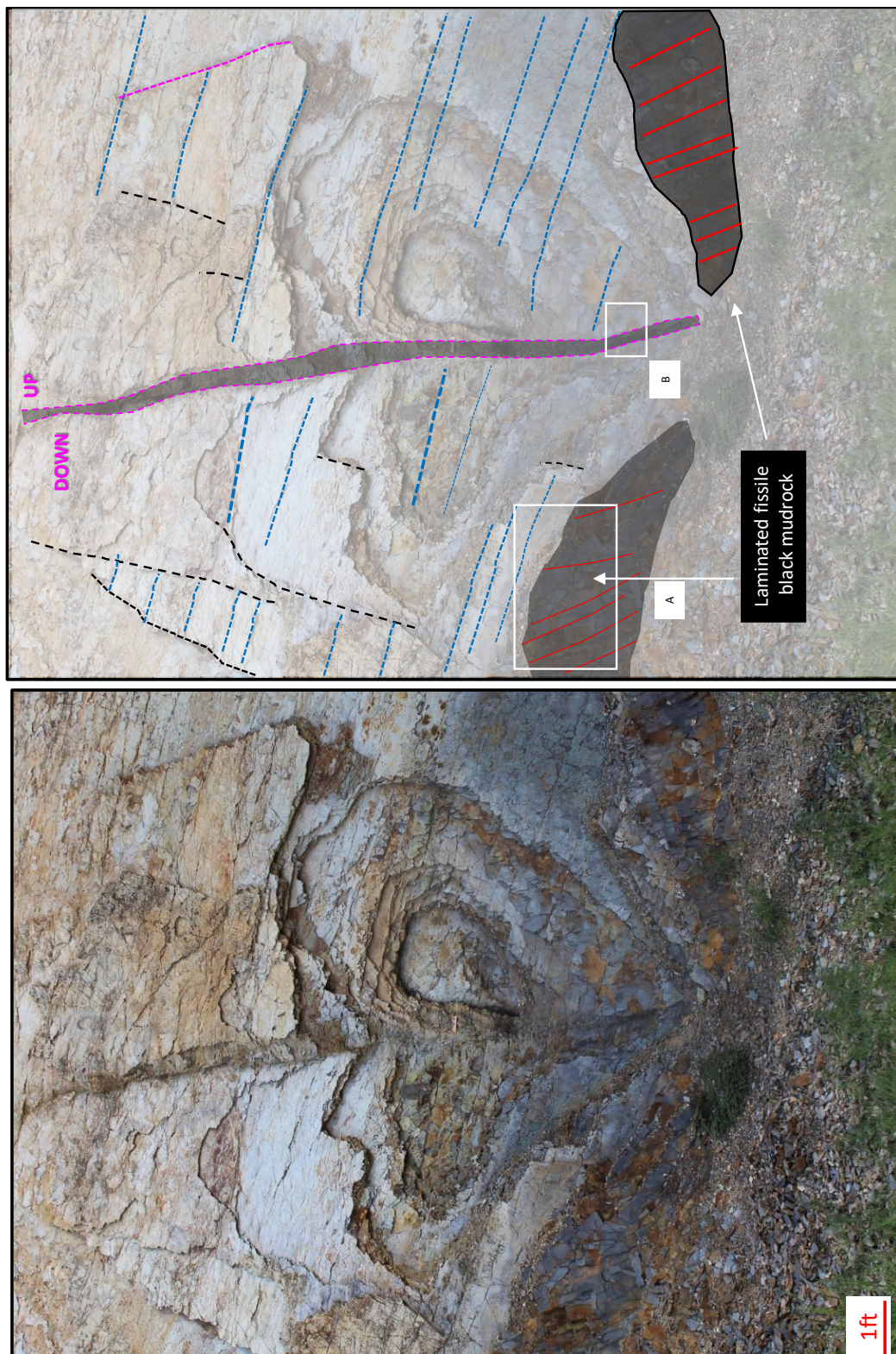


Figure 3.4 Photo and interpretation of 3 different fractures in the heart, in blue, red, and black dashed lines. The heart is cut vertically by a small fault. A and B mark photos in figure 3.2.5

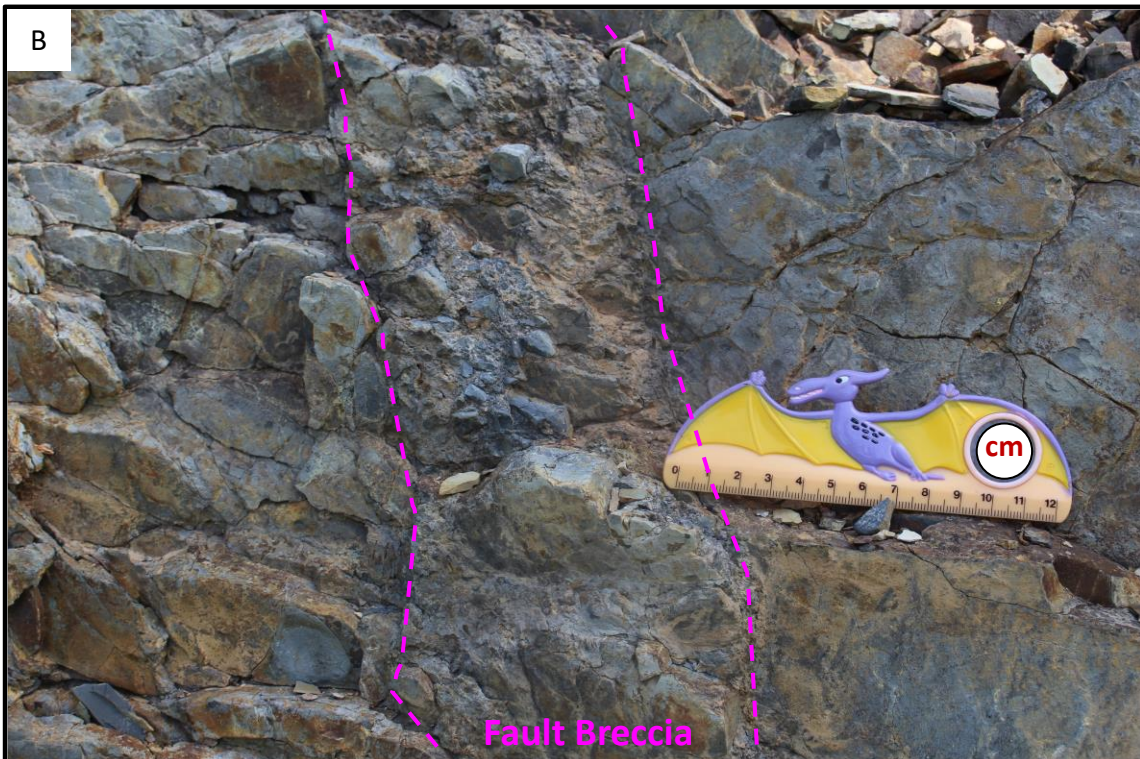


Figure 3.2.5 A) Contrast in fracture geometry and density between thin of black shale and more competent siliceous mudrock, B) Fault breccia running through the center of the heart.



Figure 3.2.6 Photo & interpretation (below) of brittle-ductile couplets. Fractures (brown lines) do not extend into more argillaceous beds highlighted in thin black lines. This outcrop is on the south side of SH- 77D.

Ghosh et al, 2017, JPT, The US-77D road cut exposes 5 fracture sets on large bed faces

- (a) US-77D wall in the lower Woodford Shale.
- (b) Traces showing set 1, 3, and 5 fractures. Set 4 fractures are not clear on (a and b) due to their small sizes. Notice that a majority of set 3 (yellow) and set 5 (black) fractures terminate on set 1 (white) fractures.
- (c) A closeup view of carbonaceous, argillaceous mudstones (more ductile) beds along with chert beds.
- (d) Trace of set 2 fractures (orange) that are absent in the brittle beds. Set 4 fractures (red) are nonsystematic and shorter compared with the other sets and terminate on set 2 fractures in the carbonaceous, argillaceous mudstones. Set 4 and 5 fractures abut or cross cut each other in the chert beds..

Out of the several fracture sets identified in the Woodford Shale, two sets (E-W and NE-SW) were interpreted as the oldest sets based on crosscutting and fill. These sets date back to before the Mid-Virgilian Arbuckle Orogeny and likely have different generation timings. The relatively silica- and carbonate-rich beds primarily contain the E-W fractures and the highly clay- and organic-rich beds mainly contain the NE-SW fractures. The E-W and NE-SW sets origins (both not related to local structural bending) are likely more numerous in the flat subsurface compared to fractures sets whose origins are related to structural bending. These two fracture sets probably also control the fluid flow in the subsurface. Younger fracture sets show more influence of local folding and are overrepresented in the outcrops with tilted beds. Therefore, they do not likely control relatively flat subsurface fluid flow. Although some fractures (fold or non-fold related) only have one type of cement or bitumen fill, others have two types of fills, bitumen along with another cement, or two types of cement (non-bitumen) indicating that these fractures underwent more than one stage of opening. A negative correlation between fracture intensity and bed thickness, and a positive relationship between fracture intensity and quartz/ carbonate content exist in the studied location.

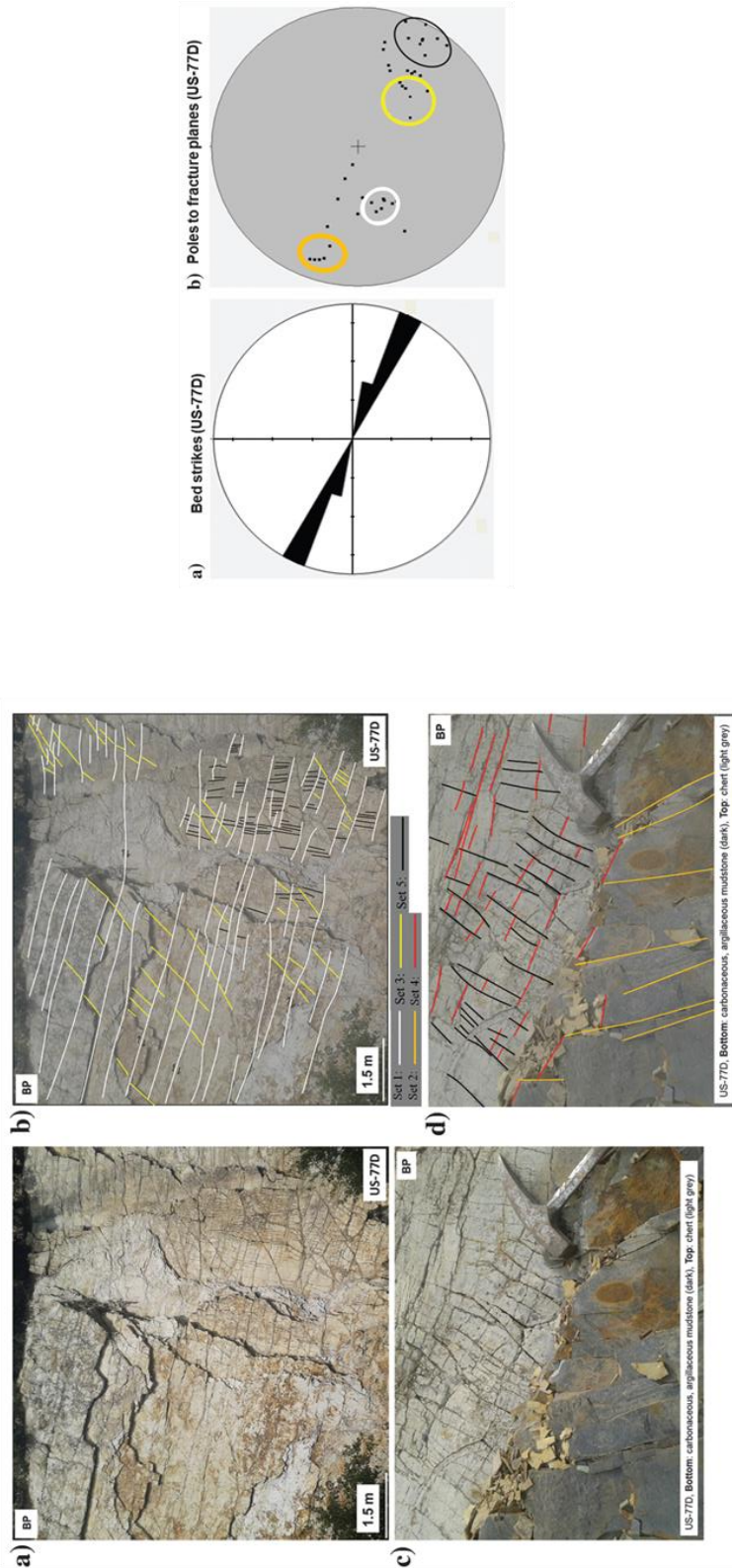


Figure 3.2.8 Summary of work published by Ghosh et al., (2017, 2018) documenting the timing of multiple fracture set in relation of regional deformation history.

REFERENCES

Cullen, A., 2018, My favorite outcrop(s): The Woodford Shale SH-77D: Le Couer de Arbuckle Mountains, OK: Oklahoma City Geological Society, Shale Shaker, v. 69, no. 5, p. 258-268.

Ghosh, S.G., 2017, Integrated studies on Woodford Shale natural fracture attributes, origin, and their relation to hydraulic fracturing: Norman, University of Oklahoma, unpublished PhD dissertation, 264 p.

Ghosh, S., J.N. Hooker, C.P. Bontempi, and R.M. Slatt, 2018, High-resolution stratigraphic characterization of natural fracture attributes in the Woodford Shale, Arbuckle Wilderness and US-77D outcrops, Murray County, Oklahoma: Interpretation, v. 6, no. 1, p. SC29 - SC41.

Ghosh, S., D. Becerra, and R. Slatt, 2019, Discussion of: My favorite outcrop(s): The Woodford Shale SH-77D: Le Couer de Arbuckle Mountains, O.K.: Oklahoma City Geological Society, Shale Shaker, v. 70, p. 138-143.

Stanley, T.M., 2001, Stratigraphy and facies relationships of the Hunton Group, northern Arbuckle Mountains and Lawrence uplift, Oklahoma: OGS Guidebook 33, 73 p.

3.3 I-35N (Phosphate nodule lag): This outcrop features Upper Woodford phosphate nodules at the contact with the overlying Sycamore Limestone on the eastern side of the I35 roadcut (Figure 3.3.1). Although one can park off the shoulder of the highway, for safety considerations it is best to park at the Heart of the Arbuckles (Stop 3.2), and then walk around the corner and then proceed up section. To reach this relatively small outcrop on the hillside beware of the thick patches of poison ivy. This outcrop is only suitable for small groups.

The highlight of this outcrop is a “bed” of phosphate nodules about 4.5ft / 1.5m thick with about 80 nodules per square meter, 2X greater than the Wyche Quarry. The nodules are loosely packed into an argillaceous matrix (Figures 3.3.2 and 3.3.3) and highly concentrated relative to all other outcrops we have observed. Their concentration and the thickness of the phosphate bearing zone contrasts relative to other Upper Woodford sections (Wyche, I35-S, and MCQ) where the Phosphate nodules are both less concentrated and found in a significantly thicker zone suggests they may have been concentrated along a submarine(?) unconformity by marine currents and then infiltrated by clays prior to deposition of the overlying basal Sycamore. This is important to appreciate in understanding the complexity of the Upper Woodford contact.

Boardman (2012) compared the nodules at I35-N and the McAlister Cemetery Quarry (MCQ) and classified them into 5 types on the basis of shape, banding, and degree of preservation of radiolarians within each nodule (Figure 3.3.4). Boardman (2012) documented that at I-35N the nodules are more elongate and have less internal structure than the nodules at MCQ. Note that many of the nodules are elongate rather than spherical, a feature noted by Boardman, who also documented the preferential enrichment of trace metals in the darker bands of the concentric nodules (Figure 3.3.4b and 3.3.5). The origin of this variation is not known, but a first pass hypothesis is that these bands reflect changing redox conditions.

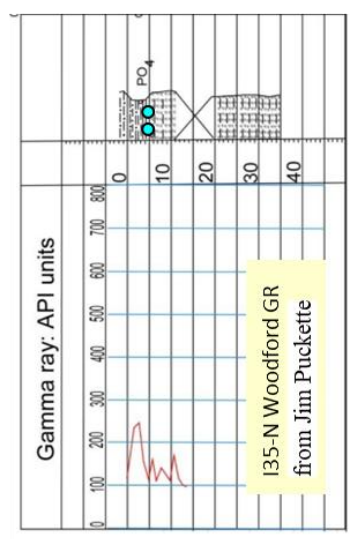
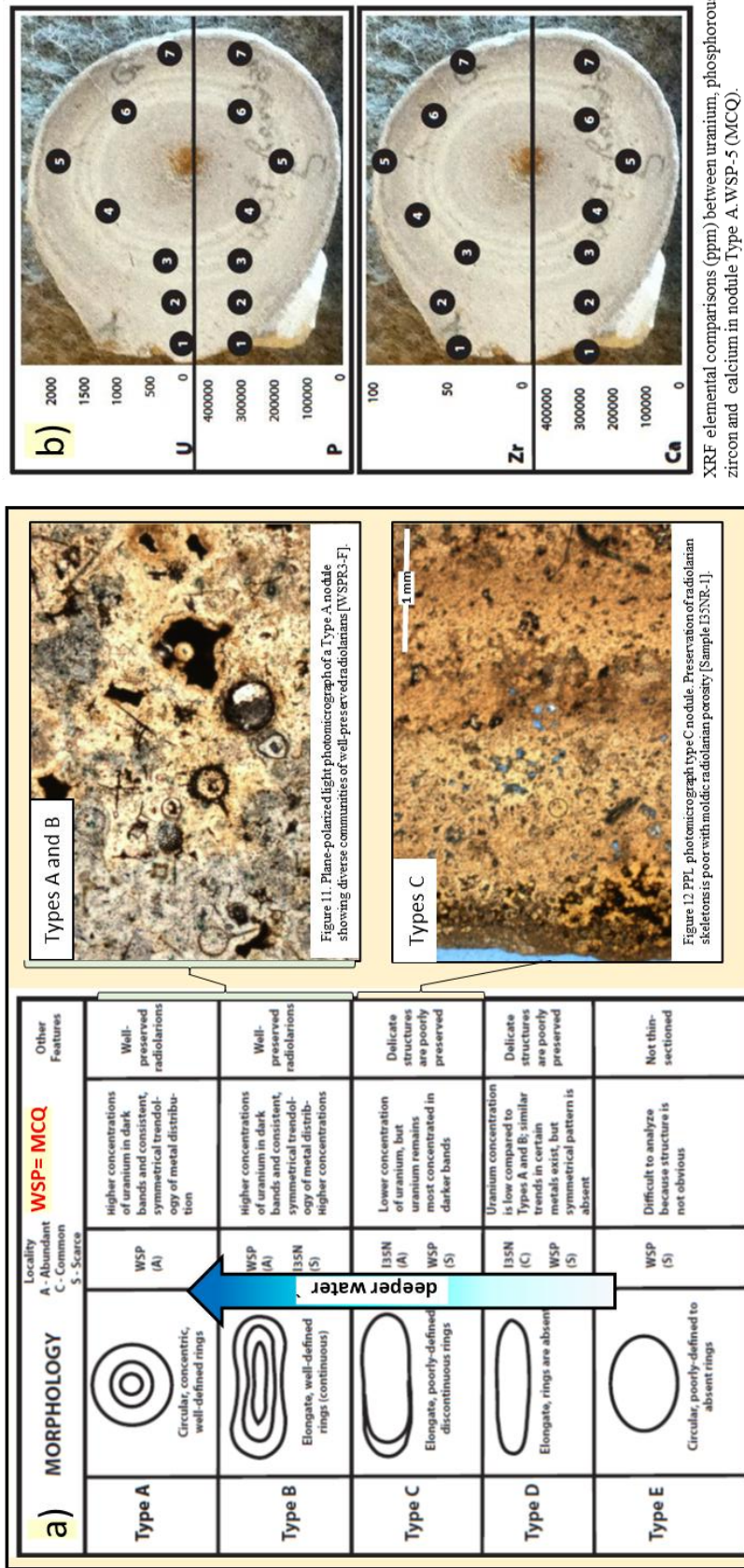


Figure 3.3.2 Photo of Woodford-Sycamore contact with interval of phosphate nodules at the top of the Woodford.



Figure 3.3.3 Close up of phosphate-nodule conglomerate (winnowed?) at the top of the Woodford ~ 85 nodules/m² ~ 2X > Wyche. Note the predominance of elongate nodules over spherical nodules, all packed in a argillaceous matrix

Figure 3.3.4 a) Nodule classification based on morphology and internal structure with examples b) example of XRF analyses (Boardman, 2012).c) Outcrop GR I35N section (Boardman, 2012 / from J. Puckette) d) Type A PO nodule w/ 3 dark rings associated with higher U, V, & Cr.





3.3.5 Photo of a Type-A Phosphate nodule with 3 dark rings generally associated with higher U, V, Cr, and other metals.

REFERENCES

Boardman, D.R., III, 2012, Preliminary analysis of phosphate nodules in the Woodford Shale, Late Devonian-Early Mississippian, southern Oklahoma: Stillwater, Oklahoma State University, unpublished M.S. thesis, 77 p.

3.4: Camp Classen YMCA Spillway 2N-6E SW/NE Sec 2: This stop is to examine the excellent exposures of vertically dipping Lower Woodford along Lick Creek starting at the barely concealed contact with the Hunton Group below the spillway of Lake Classen about 2mi from Stop 3.3 (Figures 3.4.1). Permission to visit this outcrop must be granted by Camp Classen staff and an online waiver completed for each visitor. Motor coach parking is possible. The Hunton contact can be easily and clearly seen on the road entering the YMCA, less than 100 meters away on strike. There is about 198ft/60m of Woodford exposed along creek, but only the upper reaches below the spillway are usually dry and easily accessed. Frequent flows over the spillway, as well as the indurated lithology, keep the outcrop well exposed.

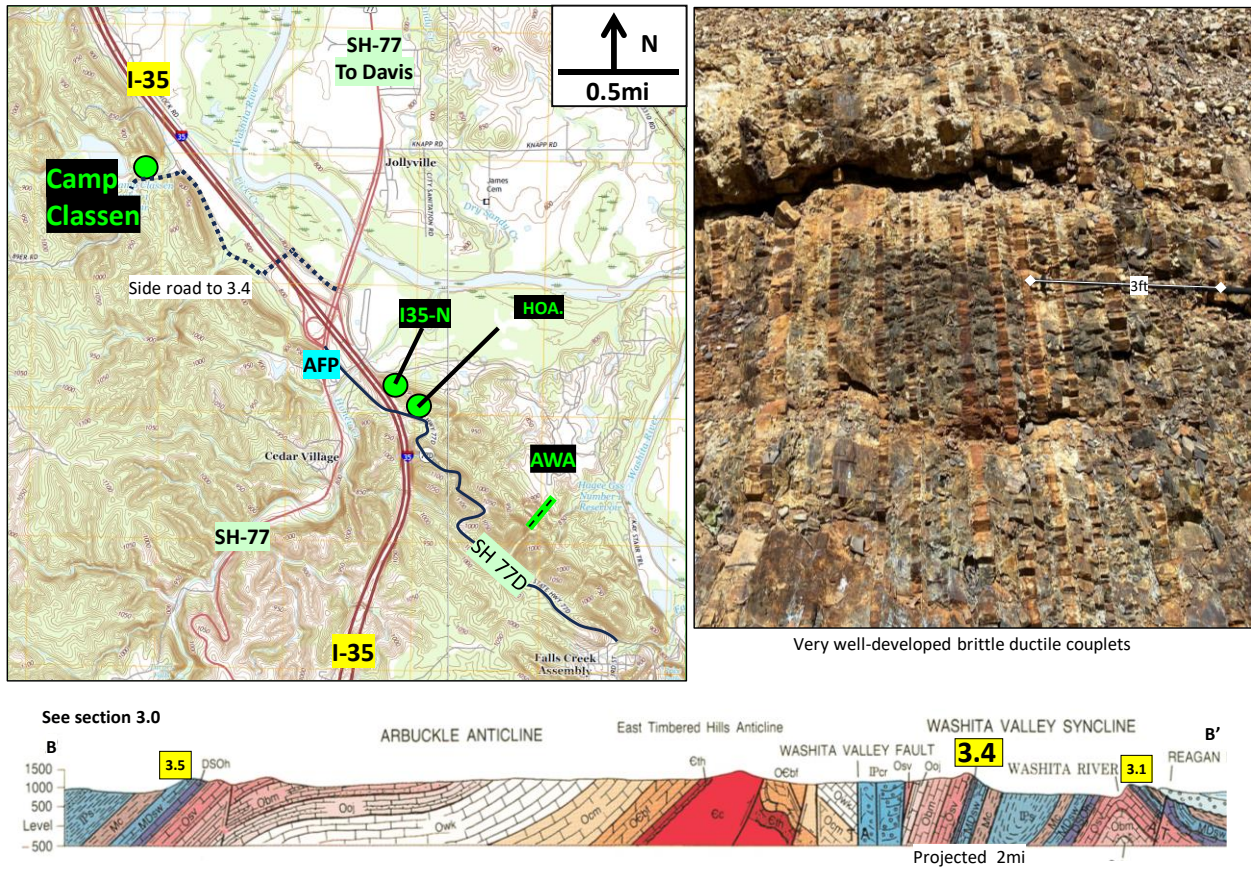
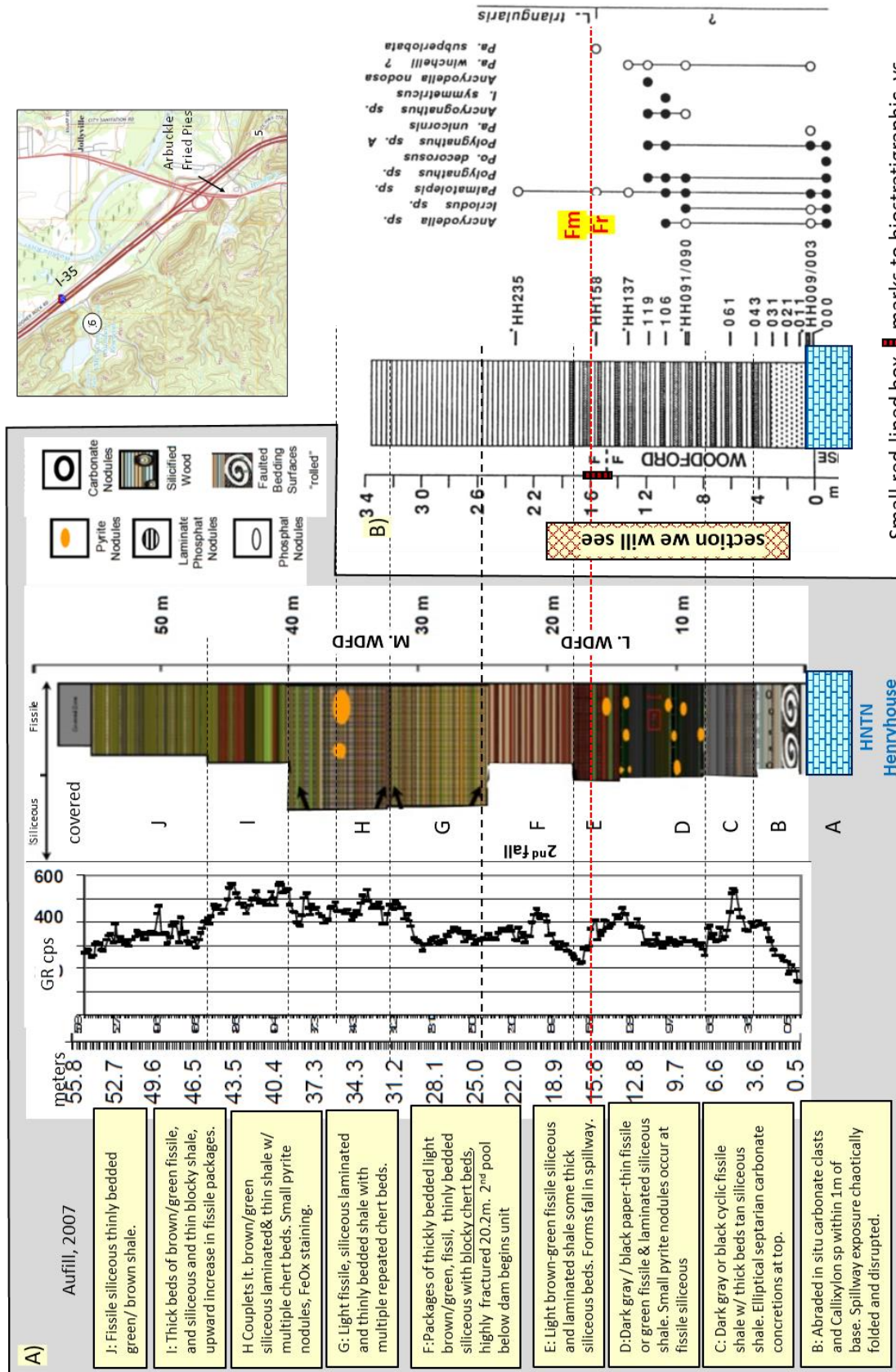


Figure 3.4.1 Location maps with outcrop photo for Camp Classen / YMCA spillway. Other Woodford outcrops in green text in black boxes, AWA- Arbuckle Wilderness Area, HOA-Heart of the Arbuckles. AFP is Arbuckle Fried Pies. Location of section 3.3 is shown on the cross section is projected SW about two miles.



Figure 3.4.2 Photos of basal section at Hunton contact. Single organic-rich fissile black mudrock bed between cherts

Figure 3.4.3.: YMCA (Haas-B) measured Section and lithofacies at spillway (Aufill, 2007). B) Conodont and magnetostratigraphic position of Frasnian/Famennian boundary – Hass and Huddle, 1965; Over, 1990; Crick et al., 2002)



Small red-lined box marks to biostratigraphic vs. magnetostratigraphic position of the F/F boundary, 16.15 vs. 15.7m respectively (Crick et al, 2002)



Figure 3.4.4 Interbedded siliceous cherty mudrock (brittle) and fissile shale of Unit C of Aufill (2007). Dashed box is figure 3.4.5a



Figure 3.5.5 Close up of interbedded cherty mudrock (C) and fissile shale. Sample YM-7, fissile shale with fossil hash on bedding plane.

The YMCA site (Hass-B location) is quite important because the Frasnian-Famennian extinction boundary is well-documented here; it is about 53ft/16.15m above the Hunton-Woodford contact (Figure 3.4.3: Hass and Huddle, 1965; Over, 1990; Crick et al., 2002). Lower Woodford is a remarkably rhythmic succession of black fissile laminated siliceous shale and thin bedded black to grey extremely siliceous mudrock and chert that can be divided into 9 units on the basis of percentage of cherty beds, fissility, and bed thicknesses (Figures 3.4.3, 3.4.4, 3.4.5, 3.4.6). Many of the bedding plane surfaces in the fissile shales have scattered fossil hash on them (Figure 3.4.5c). Whilst there is a modest increase in the net shale and concomitant decrease in bed thickness above the F/F at this location (Figure 3.4.6), one of the more remarkable features of this outcrop is the rather unremarkable lithological expression of the Frasnian/Famennian (F/F) extinction boundary (Figure 3.4.6).

Figure 3.4.6 Geologist standing on the F/F Boundary 16.15m above Hunton. Unremarkable sequence of brown-dark gray fissile siliceous-shale & medium dark cherty beds that make a small rib in spillway.



It is also significant that the Lower Woodford is more siliceous at this location than in the Wyche core below the outcrop or at MCQ where the early transgressive sediments overlying the Hunton are significantly more argillaceous.

Detailed geochemical work, such as XRF or biomarker analyses over this interval remains to be undertaken. Aupil (2007) recorded a hand held gamma ray log over the section allowing it to be tied into the regional stratigraphy. There is an increase in the U/Th ratio (Figure 3.4.7) this could merely represent an decrease in U associated with lower TOC in the less shaly rocks, as hinted at in a very limited set of TOC data.

Figure 3.4.7., YMCA/ Hass-B: Spectral gamma ray, magnetic susceptibility, net shale, and bed thickness data (Aupil, 2007).

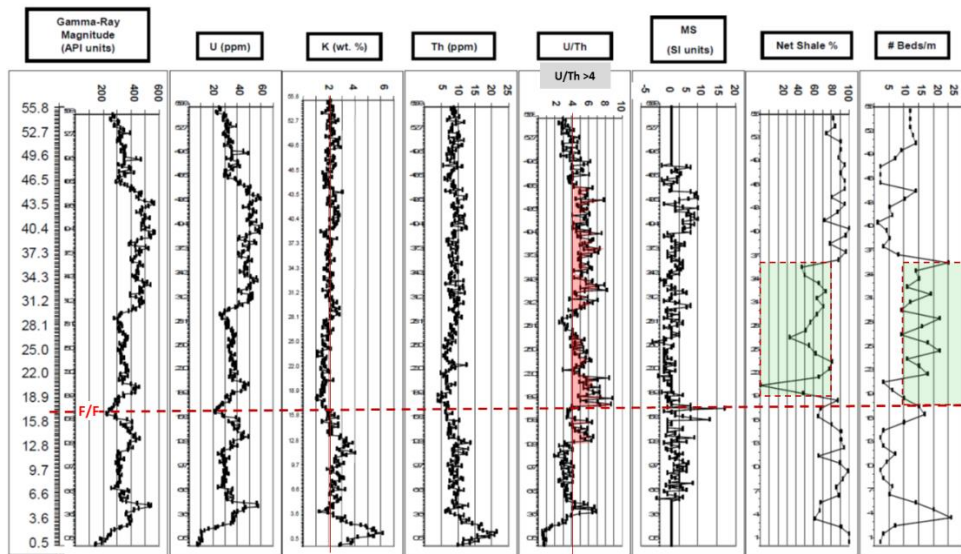


Figure 3.4.7 shows the lithology and gamma correlations between Hass-A (Henryhouse Creek) and Haas-B (YMCA). Note that the F/F boundary is relatively close to the unconformity at the top of the Hunton (see figure 2.1.7). Figure 3.4.9 shows the correlation of the F/F from the YMCA section to the Heart of the Arbuckles (Stop 3.2).

The Devonian/Carboniferous boundary in the Upper Woodford has not been determined at any locations of the north side of the Arbuckles. A conodont biostratigraphic study at Stop 3.3 (I-35N) could yield a favorable result, but the inferred unconformity at the top of the Woodford indicates the D/C boundary could be truncated there similar to the Wyche Quarry (2.1). We have included the biostratigraphic correlations of the F/F boundary to Hass-A (Figure 3.4.8), detailed section at Hass-A (Figure 3.4.9) and correlations to SH-77D (Section 3.3; Figure 3.3.10.).

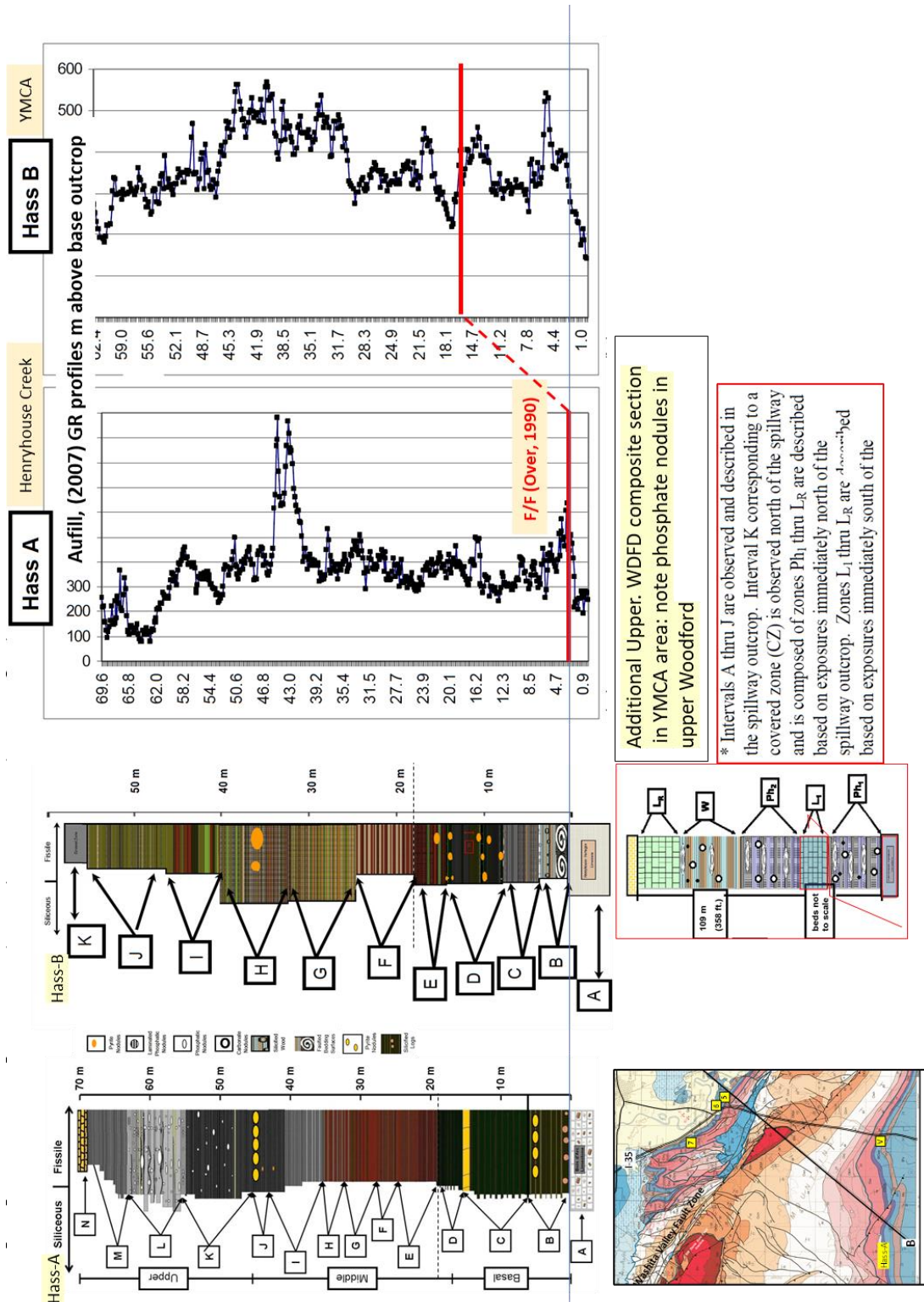


Figure 3.4.8 Correlation from Hass A (Henry House) to YMCA (Hass B) (Auffill, 2007). Note phosphate nodules top of WDFD.

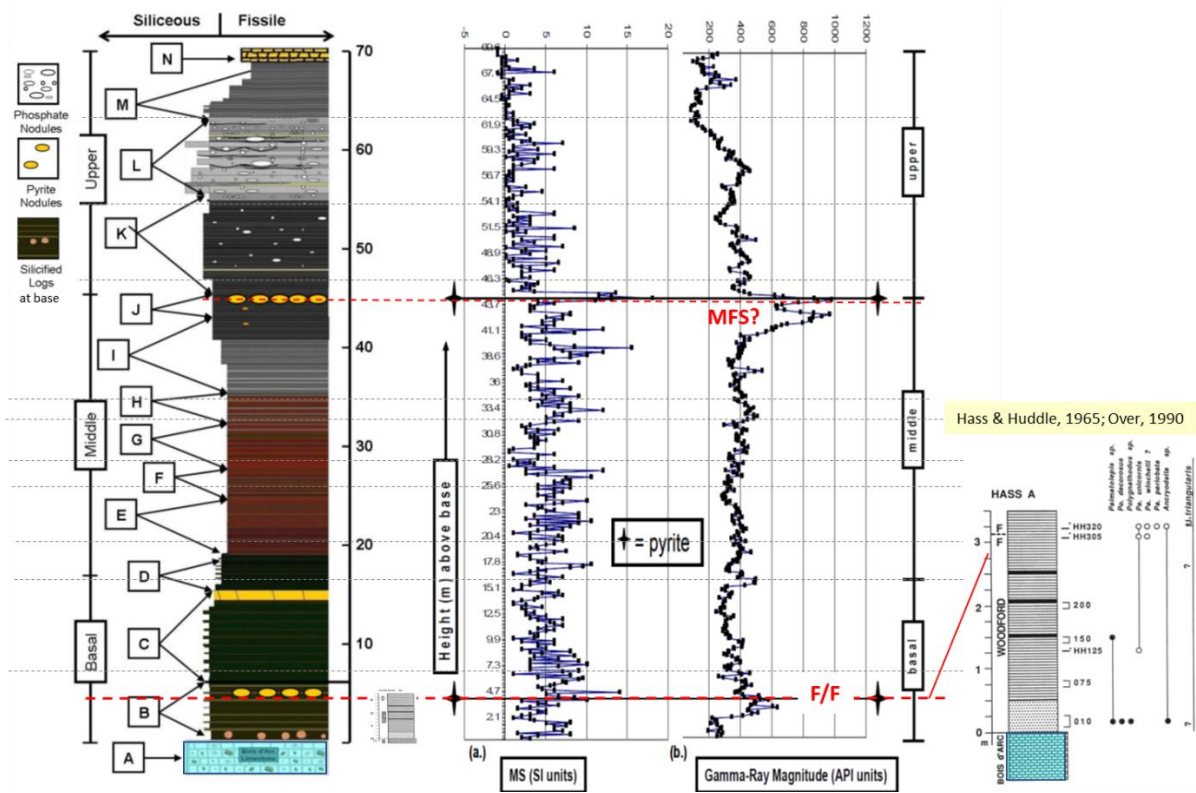
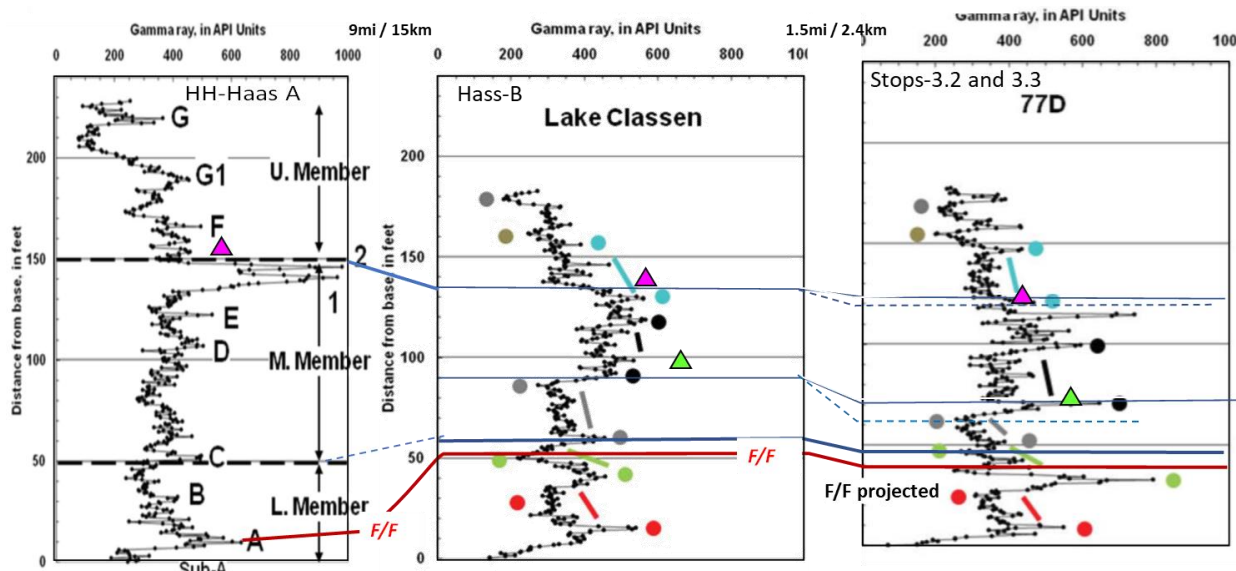


Figure 3.4.9 Hass-A (Henryhouse Creek) lithology log, magnetic susceptibility, and gamma ray profile (Aufill, 2007) with the F/F boundary of Over (1990)

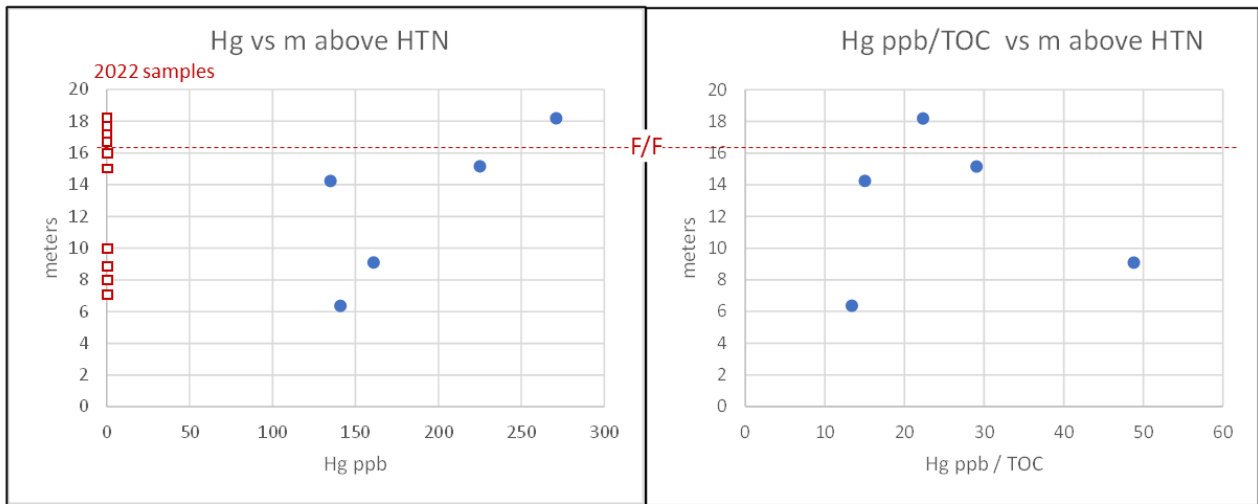


F/F 3.3m / 11.5ft and 16.15m / 53ft above HNTN at Haas A (HH) and Haas B (YMCA) respectively, in LOWER WOODFORD

Figure 3.4.10 Gamma correlation from Hass-A- Hass B (YMCA), and SH77D (Paxton and Cardott, 2008) and tentative correlation of F/F boundary using data of Over (1990).

Racki et al., (2018) document anomalously elevated levels of Hg and Hg/TOC at and just below the F/F boundary at several locations in Germany, Morocco, and Russia, They attribute these anomalies to volcanic activity and suggest this activity contributed to the mass extinction at that boundary. Similar anomalies associated with the D/C boundary are reported by Rakocinski et al., (2020), who also document elevated levels of the highly compound methylmercury. Figure 3.4.11 shows preliminary Hg data from the YMCA spillway. These data indicate some possible anomalous points are present, but the section is clearly under-sampled. Further work is currently underway to fill-in sampling gaps (2020 samples Figure 3.4.11).

Figure 3.4.11 Mercury and TOC data in Lower Woodford across Frasnian-Famennian boundary. No clear anomaly, additional samples are being analyzed.



All samples exceed the 0.5% TOC cutoff for normalization

	2020 samples	FM	ft above HTN	m above HTN	TOC wt%	Hg ppb	Hg ppm		Hg ppb/TOC
YMCA	Y-1	WDFD	21	6.36	10.55	141	0.141		13
YMCA	Y-2	WDFD	30	9.09	3.3	161	0.161		49
YMCA	Y-3	WDFD	47	14.24	9	135	0.135		15
YMCA	Y-4	WDFD	50	15.15	7.75	225	0.225		29
YMCA	Y-5	WDFD	60	18.18	12.15	271	0.271		22

REFERENCES

- Aufill, M., 2007, High resolution magnetic susceptibility of the Oklahoma Woodford Shale and relationship to variations in outcrop spectral-gamma response: Stillwater, OK, Oklahoma State University, unpublished M.S. thesis, 210 p.
- Crick, R.E., Ellwood, B.B., Feist, R., El Hassani, A., Schindler, E., Dreesen, R., Over, D.J., and Girard, C., 2002, Magnetostratigraphy susceptibility of the Frasnian/Famennian boundary: *Palaeogeography, Palaeoclimatology, Palaeoecology*, v. 181, p. 67–90.
- Hass, W.H., and J.W. Huddle, 1965, Late Devonian and early Mississippian age of the Woodford Shale in Oklahoma as determined from conodonts, in *Geological Survey Research 1965: U.S. Geological Survey Professional Paper 525-D*, p. 125-132.
- Over, D. J., 1990, Conodont biostratigraphy of the Woodford Shale (Late Devonian- Early Carboniferous) in the Arbuckle Upper Mountains, South-Central Oklahoma, Texas Tech University PhD Dissertation, 186 p.
- Racki, G., Rakocinski, M., Marynowski, L., Wignall, P.B., 2018, Mercury enrichments and the Frasnian-Famennian biotic crisis: a volcanic trigger proved? *Geology* 46, p. 543–546.
- Rakociński, M., Marynowski, L., Agnieszka, P., & others, 2020, Volcanic related methylmercury poisoning as the possible driver of the end-Devonian Mass Extinction, *Nature Reports* 10-7344, 8p.

3.5: I35-S (The Last Ridge) 2N-6E SW/NE Sec 2

This Woodford outcrop is a roadcut on the west side of I35-S along the last ridge on the southern, back limb, of the Arbuckle Anticline on the north side of the Ardmore basin (Figure 3.5.1). Traffic is heavy and moves very fast at the base of a long downhill section of highway. There is nearly constant din which makes hearing any lecture difficult to hear. Although there is a very wide shoulder, the pull out is still dangerous. The roadcut is somewhat steep with loose scree. For the above factors this outcrop is better suited for smaller groups.

The earliest work was that of Robert Fay who prepared a guidebook for the Ardmore Geological Society when I-35 was first cut through the Arbuckle Mountains in 1970. The original guidebook is out of print but was reissued by the Oklahoma Geological Survey (Fay, 1989). An important feature of that work was the placement of a brass marker 9ft below the top of the Woodford (Figure 3.5.2b) that serves as a key datum for numerous subsequent studies. Cardott and Chaplin (1993) report that the Woodford at this location is marginally mature: %Ro average = 0.5% n=77 with a range of 0.43 to 0.65; Tmax average = 417°C. Becerra (2017) reported an average Ro of 0.6 calculated from Tmax. Conodont biostratigraphy places the Devonian-Carboniferous 9ft below the top of the Woodford (Over, 1992).

The Last Ridge on I35-S also has an excellent section of Sycamore Limestone above the Woodford and in Philips Creek, further up dip, there is a rare, well exposed, section of the Caney Shale with a basal quartz arenite sandstone unit (Figure 3.5.2). The Henry House Creek (Hass-A of Over, 2002) and the Speake Ranch (Galvis, 2013) sections are 5mi and 11mi west, respectively, along strike from the Last Ridge (see Section 3.6). Structurally, it should be noted that the north flank of the Springer oil field can be mapped below the Last Ridge which implies the ridge is on the hanging wall of a back thrust (Figure 3.5.1c and d).

Woodford Geological Features: The Woodford is about 290ft / 88m thick at this location but much of the Lower and Middle Woodford are covered (Figure 3.5.2a). Most of the exposed section is upper Woodford. There is about 10ft of cherty Lower Woodford above the unconformity with the Hunton (Figure 3.5.3). The Upper Woodford is about 90ft thick, becoming more siliceous, thicker bedded, and increasingly phosphatic upwards (Figure 3.5.2b).



Figure 3.5.2: a) Oblique west-looking view of Hunton-Woodford-Sycamore-Caney section on south limb of the Arbuckle Anticline b) Upper Woodford outcrop with footages from MFS of Becerra (2017). Yellow dot is Ardmore Geological Society marker 9ft below top of Woodford.

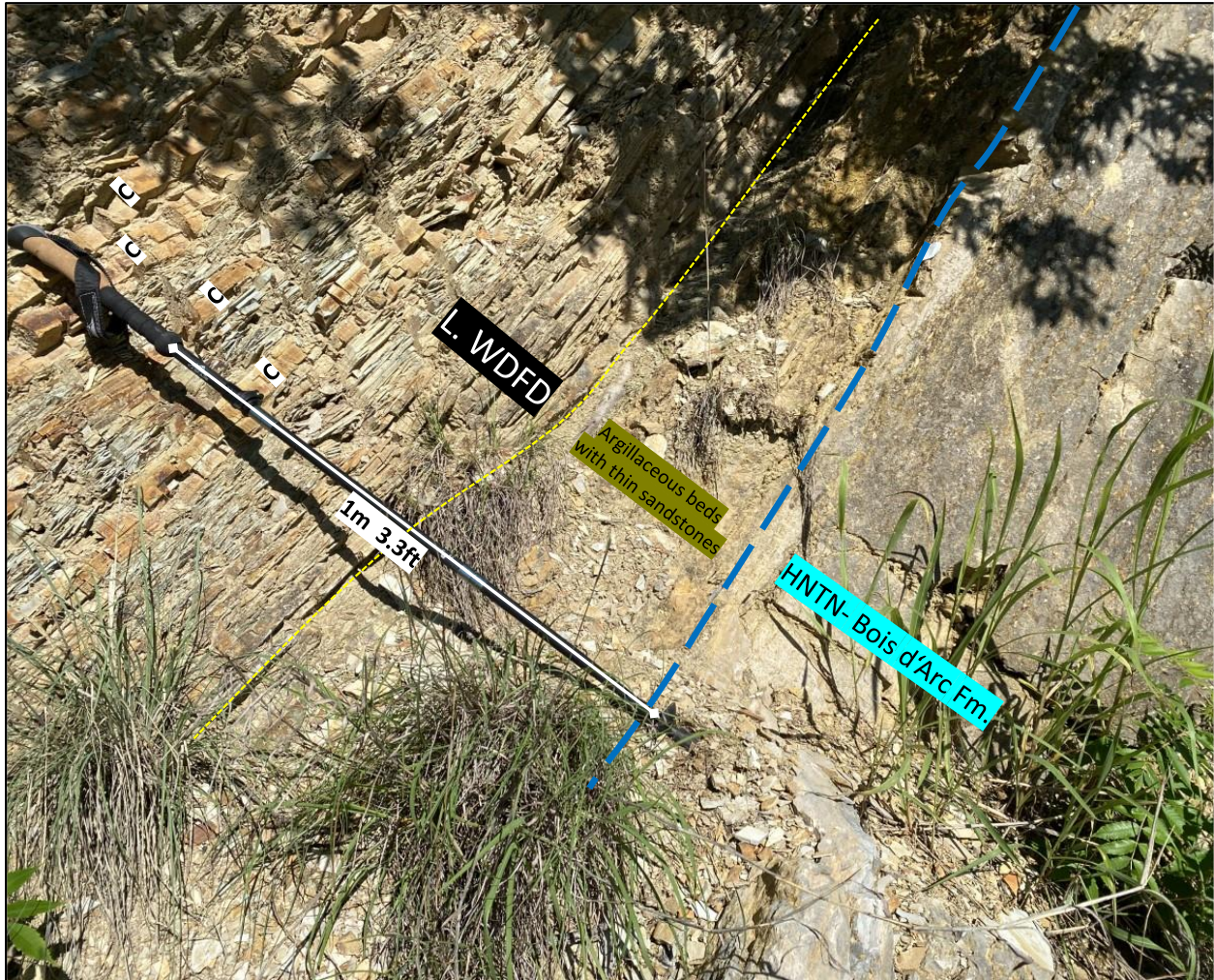


Figure 3.5.3 Photo of the unconformable contact between the Bois d'Arc (Hunton Group) and the overlying Lower Woodford. "C" denotes chert beds. Note similarity to the brittle-ductile couplets in the Lower Woodford at Camp Classen Spillway (Section 3.4).



Figure 3.5.4) Outcrop photo 65-75ft above the base of the Upper Woodford showing the transition to a thicker more siliceous chert beds (C) with a greater abundance of phosphate nodules, P.

The most comprehensive study of the Upper Woodford on the Last Ridge is that of Becerra (2017); 157 samples were collected and studied using petrography supplemented with SEM, X-ray diffraction, X-Ray fluorescence, source rock analyses (TOC and RockEval), micro-rebound tests for rock hardness and uniaxial compressive strength tests for mechanical properties. Becerra divided the Upper Woodford into 5 stratigraphic units (a-e) and 4 main lithofacies on the basis of lithology, gamma ray, bed thickness patterns, and the percentage of brittle to ductile beds (Figure 3.5.5a and 3.5.5b). Consistent with other studies of the Woodford, Becerra also shows that %TOC is preferentially enriched in the ductile, less siliceous beds (Figure 3.5.5c). Biomarker data from Jones (2017) indicates there are several pulse of photic zone euxenia in the lower part of Upper Woodford (Figure 3.5.6). Increasing Zr in the uppermost unit of the Woodford indicates increasing land derived detrital input.

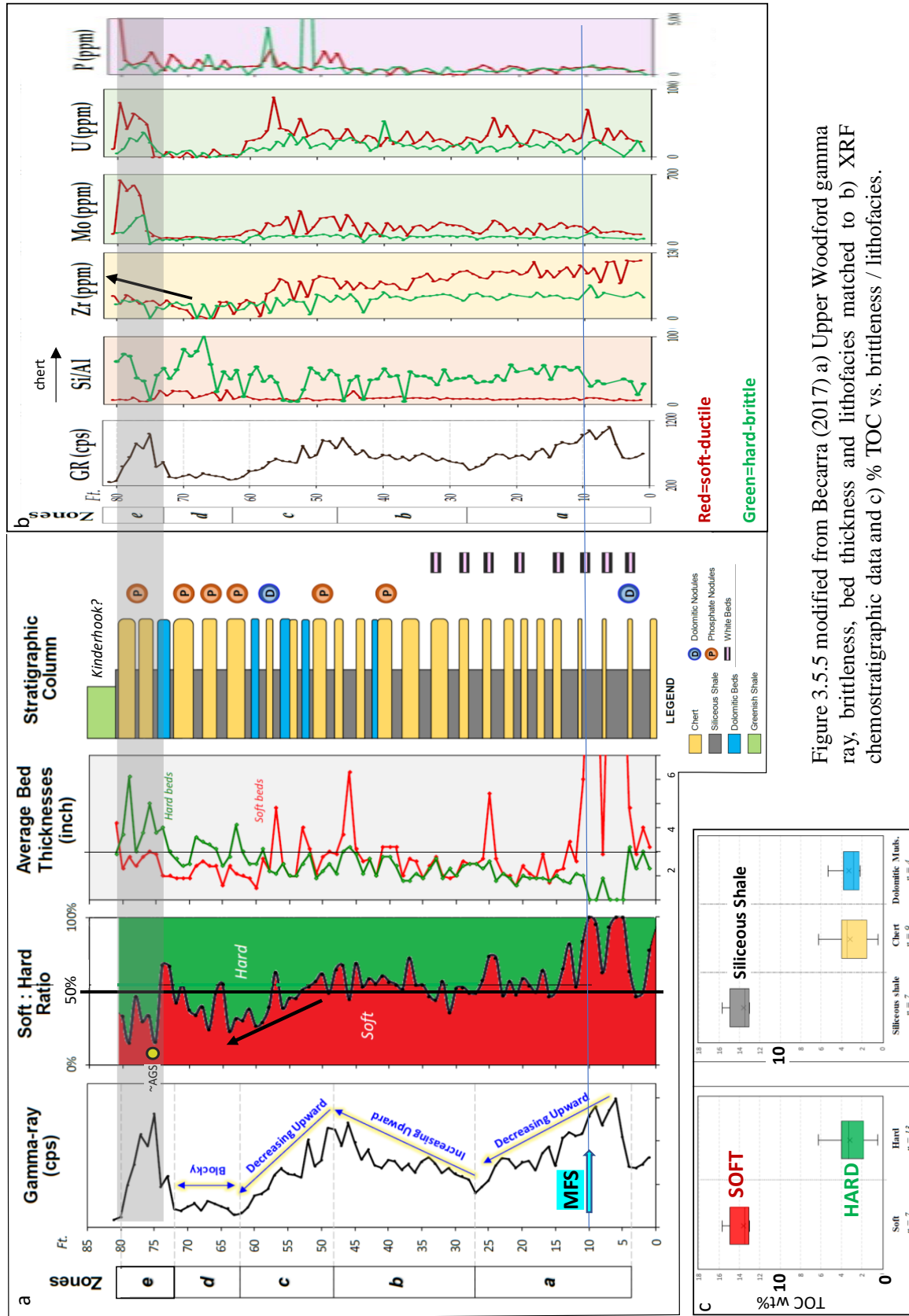


Figure 3.5.5 modified from Becarra (2017) a) Upper Woodford gamma ray, brittleness, bed thickness and lithofacies matched to b) XRF chemostratigraphic data and c) % TOC vs. brittleness / lithofacies.

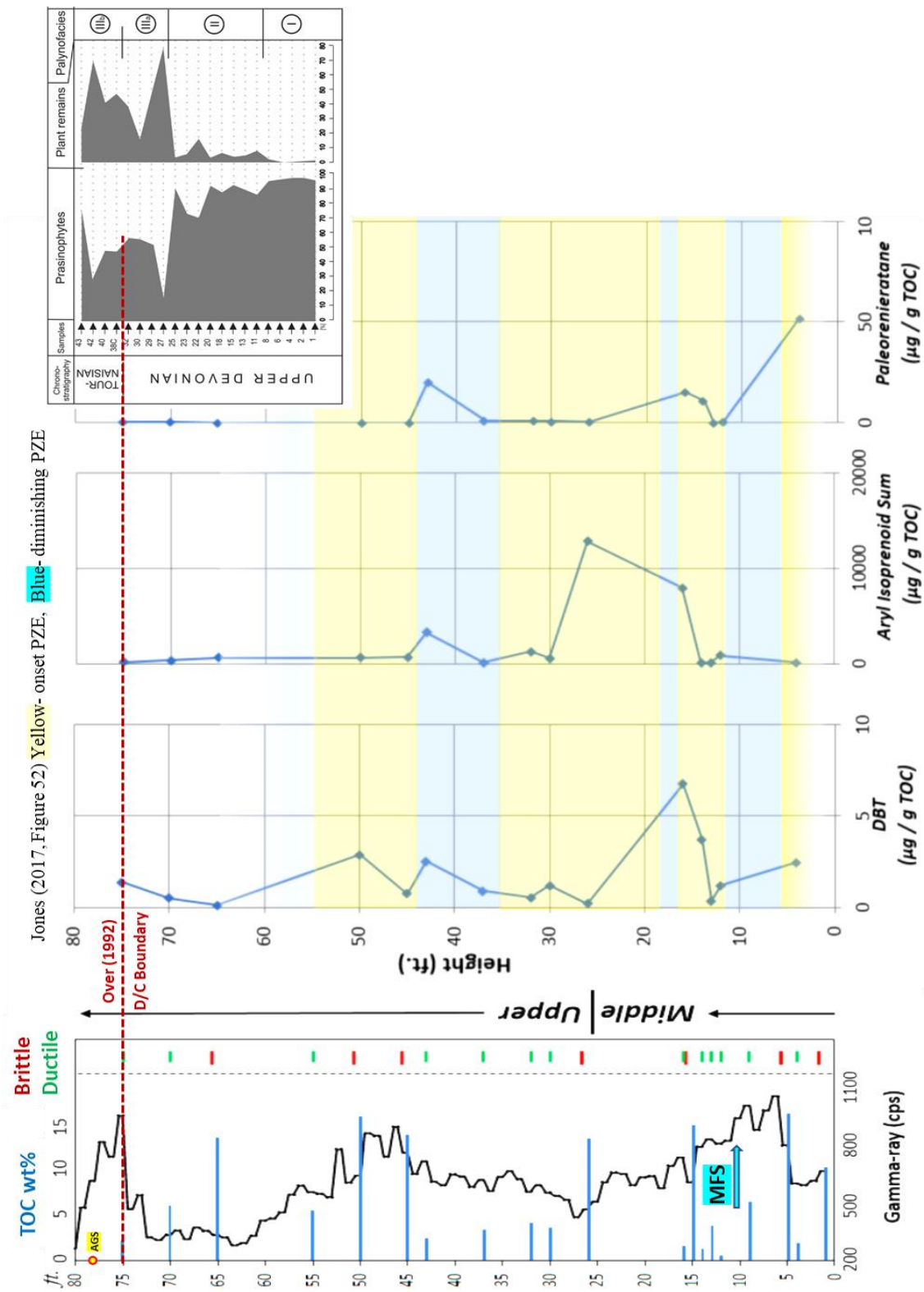


Figure 3.5.6 Biomarker data indicating episodes of photic zone euxenia (PZE) and input of conifer combustion (Jones, 2017). Small graph is land plant data from Kondas et al., 2018

There are several features worth additional discussion.

1. On figure 3.5.5 Unit-e (top of the section) has an elevated GR that corresponds to a higher percentage of “hard” siliceous beds relative to lower section (Unit-a) where the elevated GR is associated with shalier beds). Unit-e has elevated U, Mo, V, and P. These characteristics suggest that the elevated GR in Unit-e may be elevated from incorporation of U phosphates and possibly zircons rather than increased fixation by organic carbon.
2. Palynology data from I35-S could not resolve specific zonal boundaries but confirms the uppermost part of the section is early Mississippian (Tournaisian) in age (Kondas et al., 2018). The increased plant debris in the uppermost section carries a signal of regression and increasing terrestrial input (Figure 3.5.6).
3. The interval of abundant phosphate nodules in the upper section is about 40ft thick. There has been no systematic study and classification of the nodule morphology at this locality, but casual observation indicates that spherical, concentric nodules are the most abundant type (Figure 3.5.7).
4. There is a strong mercury/TOC anomaly at the conodont biostratigraphically constrained D/C boundary (Figure 3.5.8). Similar anomalies have been documented at at top of the Woodford at McAlister Cemetery Quarry (Section 3.6, Cullen 2019). Similar anomalies at other global locations have been interpreted as evidence for volcanism as a contributing factor in the D/C extinctions (Rakocinski et al., 2020).
5. Lastly, in terms of normalized REE concentrations Upper Woodford phosphate nodules from 135-South (Figure 3.5.9) have similar relative distributions in the medium and heavy REE but lower concentrations than nodules from other locations.



Figure 3.5.7 Examples of spherical and elliptical e phosphate nodules with well expressed compactional drape in mudrocks

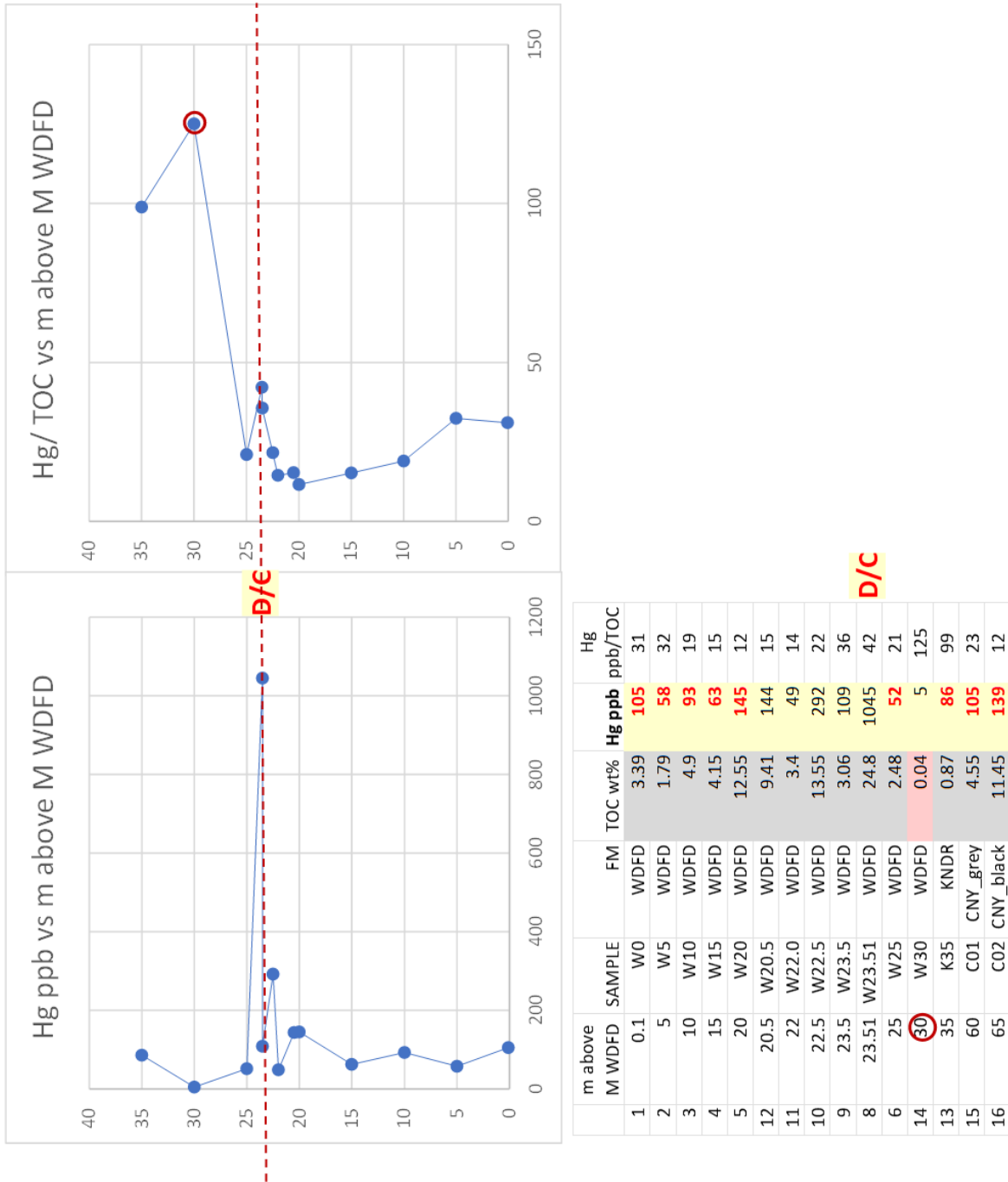


Figure 3.5.8: a) Upper Woodford mercury concentrations* vs. height above top of outcrop in Middle Woodford b) Mercury normalized to % TOC data. Red circle denotes sample too low in TOC to be considered reliable for normalization. c) Table of data

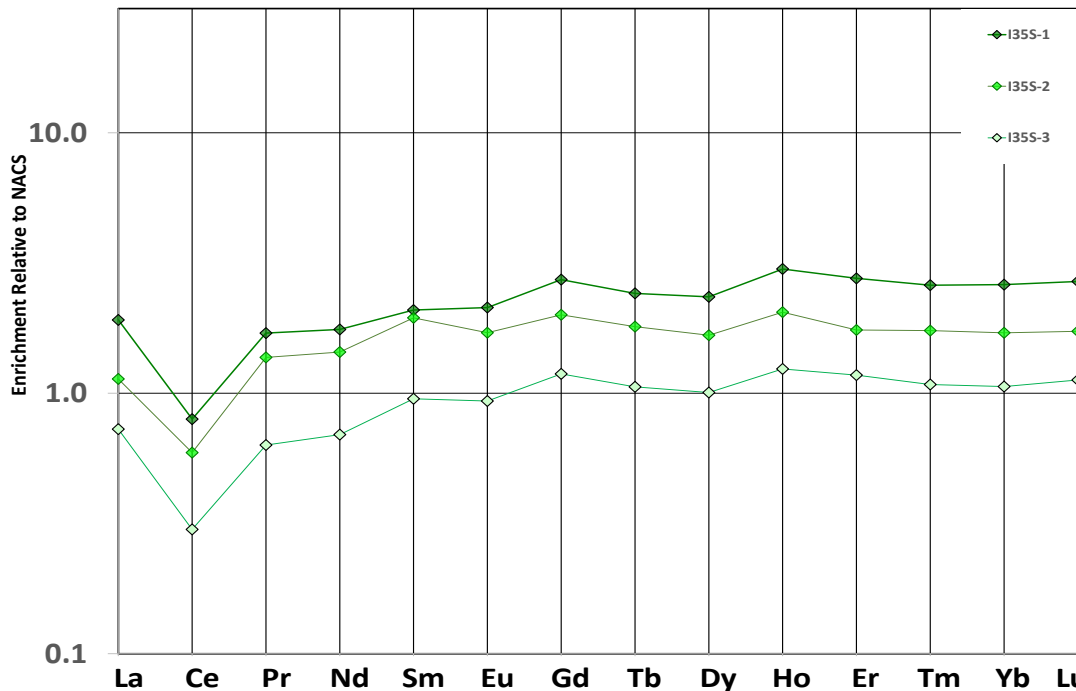
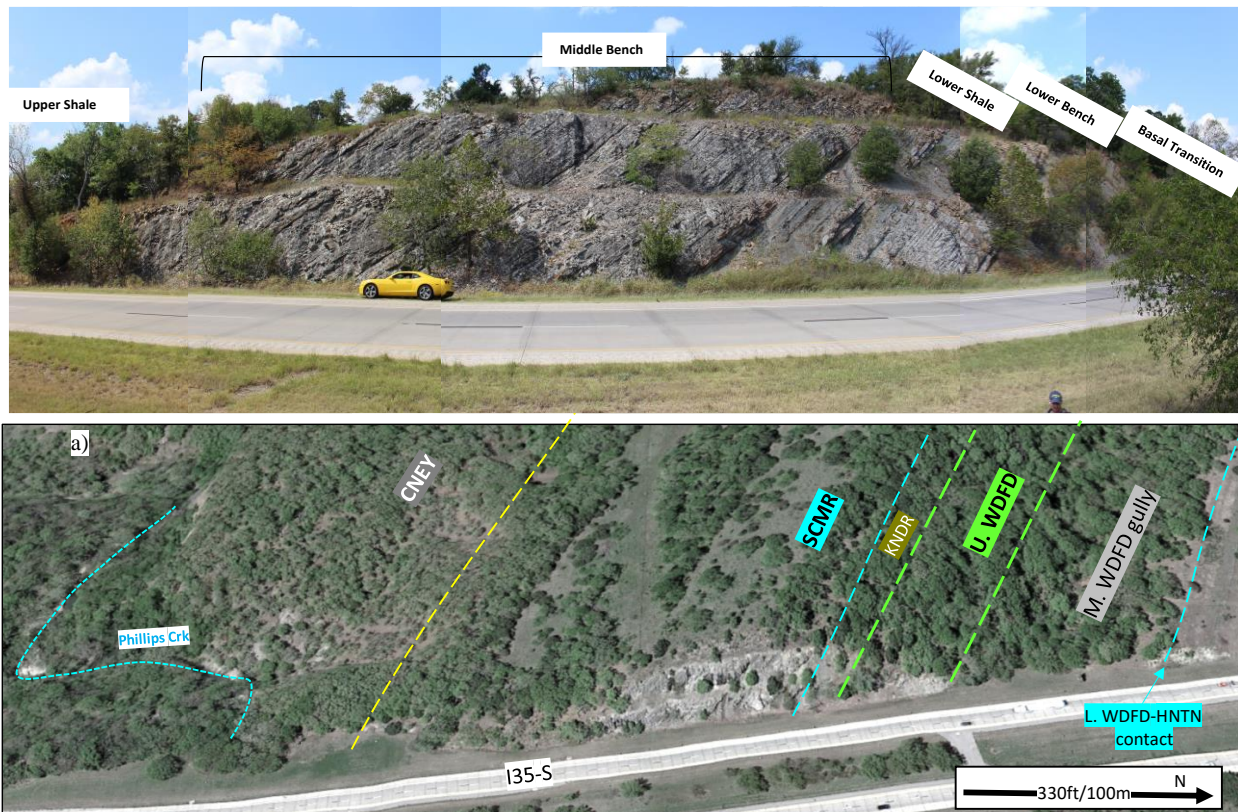


Figure 3.5.9 REE data (ICP-MS) from phosphate nodules in the Upper Woodford at I35-S normalized to North American Composite Shale (McLennan, 1987)

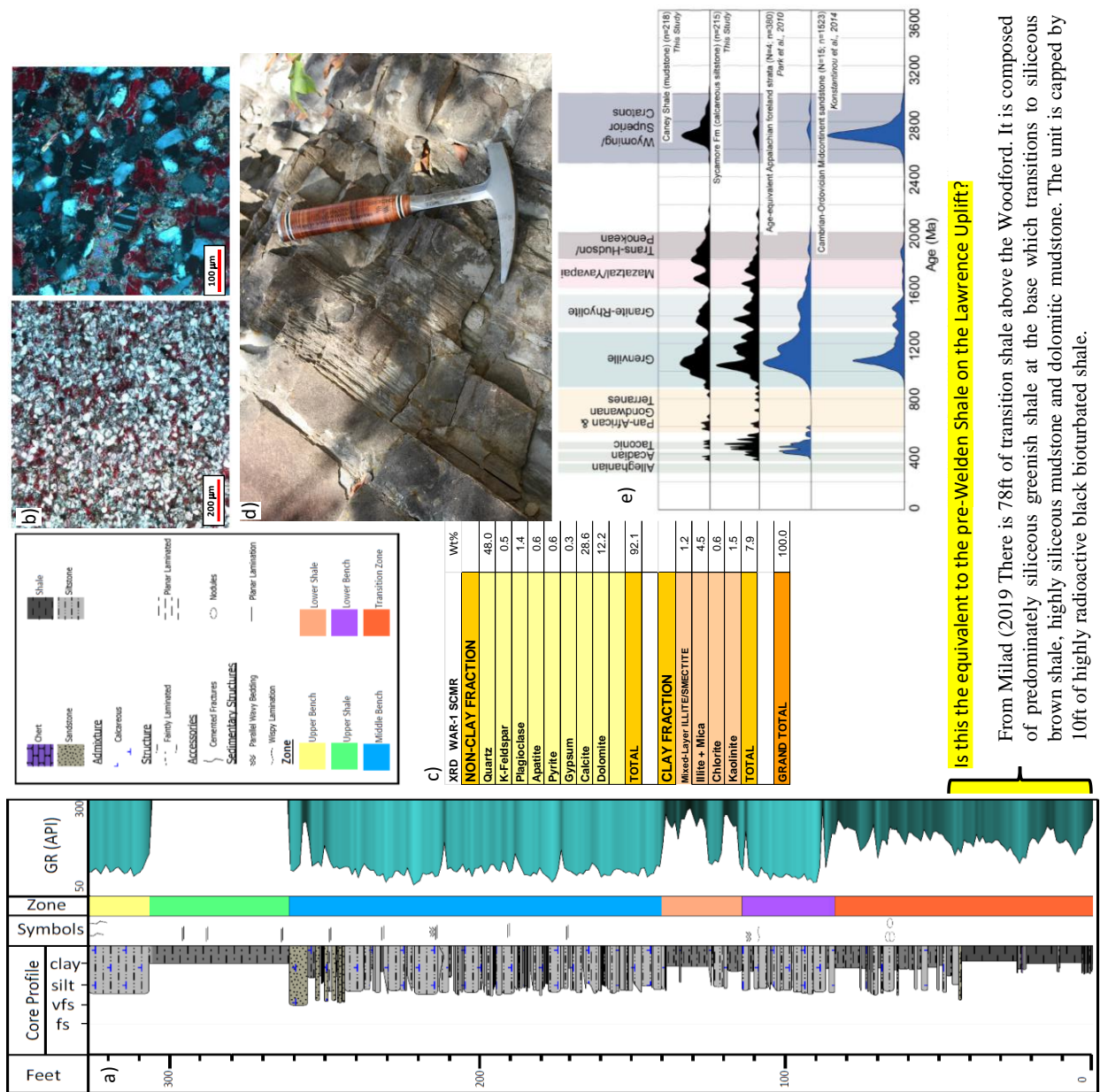
Sycamore at I-35S: Included herein is a synopsis of the well exposed 327ft section of Sycamore Limestone and Caney Shale above the Woodford along I35-S (Figure 3.5.10). This section has been studied by Miller and Cullen (2017) and Milad (2020). Cullen (2019) discussed some of the features a sandstone in the Caney (Delaware?) Shale along Philips Creek. From the top of the Hunton to the Goddard shale one could easily take a half day to cover the full section.

First and foremost the Sycamore Limestone is a formal stratigraphic name, not an apt description of this section. The section is composed of several rhythmically stacked lithofacies of calcareous siltstones, cherty mudstones, and shales (Figure 3.5.11a). These are composed of detrital quartz, carbonate peloids, with differing amounts of calcite cement and clay matrix (Figure 3.5.11 b,d). In our estimation 50% of the calcite is cement in most cases. Sedimentary structures such as partial bouma sequences, scours, clay draps, fining upward sequences strongly indicate these are dominantly mass flow deposits (Figure 3.5.11d). Most beds are continuous and with uniform thickness some beds are lenticular with swaley tops. Detrital zircon data indicate multiple North American source terranes (Figure 3.5.11e).



3.5.10 Mosaic photo and arial view of Sycamore Limestone section at I35-S (west side)

Below the Sycamore there is are 87ft of transition beds in the basal part of the Sycamore. These are lithologically similar to the greenish shales of the pre-Welden Shale on the Lawrence uplift, albeit much thicker. Milad reports that this lower transition shale is 50ft thick at Speake Ranch. The age of this section is not well established. It was not studied by Over. Early conodont studies indicate this interval is Kinderhookian to Osagean in age and that basal Caney is Meramecian in age (Ormiston and Lane 1976). Kleehammer (1991) concluded the Sycamore is largely Meramecian and certainly no older than late Osagean on the basis of *Gnathodus texanus*-*Gnathodus girtyi* conodont assemblages. A younger age is also supported by radiolarian biostratigraphy indicating an age to be no older than Middle Meramecian (Schwartzapfel, 1990). Thus, the basal Sycamore transition beds could be age correlative with the Welden and/or the pre-Welden shale on the Lawrence uplift (see Section 1.3 figure 1.3.6.)



Is this the equivalent to the pre-Weldenshale on the Lawrence Uplift?

From Milad (2019) There is 78ft of transition shale above the Woodford. It is composed of predominately siliceous greenish shale at the base which transitions to siliceous brown shale, highly siliceous mudstone and dolomitic mudstone. The unit is capped by 10ft of highly radioactive black bioturbated shale.

Figure 3.5.11 a) Measured section with hand held gamma ray profile b) thin sections (plain and cross-polars) of Sycamore siltstone c) Representative XRD data for siltstones d) Outcrop photo of fining upward partial Bouma sequence e) Detrital zircon ages from Sycamore siltstone and Caney shale.

REFERENCES

Becerra, D., 2017, Integrated Geological Characterization at the Bed-Scale of the Woodford Shale at the I-35 Outcrop, Southern Oklahoma, University of Oklahoma Master's Thesis, 226 p.

Boardman, D.R., III, 2012, Preliminary analysis of phosphate nodules in the Woodford Shale, Late Devonian-Early Mississippian, southern Oklahoma: Stillwater, Oklahoma State University, unpublished M.S. thesis, 77 p.

Cardott, B.J., and J.R. Chaplin, 1993, Guidebook for selected stops in the western Arbuckle Mountains, southern Oklahoma: Oklahoma Geological Survey, Special Publication 93-3, 55 p.

Fay, R.O., 1989, Geology of the Arbuckle Mountains along Interstate 35, Carter and Murray Counties, Oklahoma: OGS Guidebook 26, 50 p.

Galvis, H., 2017, Detailed lithostratigraphic characterization and sequence stratigraphy of a complete Woodford Shale outcrop section in southern Oklahoma: Norman, University of Oklahoma, unpublished M.S. thesis, 155 p.

Ham, W.E., and others, 1973, Regional geology of the Arbuckle Mountains, Oklahoma: OGS Special Publication 73-3, 61 p. (Guidebook for fieldtrip #5 Geological Society of America Meeting, 1973).

Jones, L.C., 2017, An integrated analysis of sequence stratigraphy, petroleum geochemistry, and Devonian mass extinction events in the Woodford Shale, southern Oklahoma: Norman, University of Oklahoma, unpublished M.S. thesis, 198 p.

Kleehammer, R.S., 1991, Conodont biostratigraphy of Late Mississippian shale sequences, south-central Oklahoma: Norman, University of Oklahoma, unpublished M.S. thesis, 135 p.

Kondas, M., P. Filipiak, M. Paszkowski, A. Piszczowska, R.D. Elmore, I. Jelonek, and M. Kasprzyk, 2018, The organic matter composition of the Devonian/Carboniferous deposits (south flank of Arbuckle Anticline, Oklahoma, USA): *International Journal of Coal Geology*, v. 198, p. 88-99.

McLennan, S.M. (1989) REE in sedimentary rocks: Influence of provenance and sedimentary processes. *Reviews Mineralogy* 21, 170-199.

Milad B, Slatt R, Fuge Z. 2020 Lithology, stratigraphy, chemostratigraphy, and depositional environment of the Mississippian Sycamore rock in the SCOOP and STACK area, Oklahoma, USA: Field, lab, and machine learning studies on outcrops and subsurface wells *Marine and Petroleum Geology*. 115.

Miller, J. and Cullen, A.B., 2017, My Favorite Outcrop: Sycamore Formation I-35 South, Arbuckle Mountains, OK. *Shale Shaker* v. 69-2, p. 87-99

Over, D. J., 1990, Conodont biostratigraphy of the Woodford Shale (Late Devonian- Early Carboniferous) in the Arbuckle Upper Mountains, South-Central Oklahoma, Texas Tech University PhD Dissertation, 186 p.

Over, D. J., 1992, Conodonts and the Devonian-Carboniferous Boundary in the Upper Woodford Shale, Arbuckle Mountains, South-Central Oklahoma, *Journal of paleontology*, Vol. 66, No. 2, p. 293-311.

Ormiston, A.R. and Lane, H.R., 1976, A Unique Radiolarian Fauna from the Sycamore Limestone (Mississippian) and its Biostratigraphic Significance: *Paleontographica*, Abteilung A, 154, 158-170.

Rakociński, M., Marynowski, L., Agnieszka, P., & others, 2020, Volcanic related methylmercury poisoning as a possible driver of the end-Devonian Mass Extinction, *Nature Reports* 10-7344, 8p.

Schwartzapfel, J. A., 1990, Biostratigraphic investigations of Late Paleozoic (Upper Devonian to Mississippian) radiolaria within the Arbuckle Mountains and Ardmore Basin of south-central Oklahoma: PhD dissertation, University of Texas at Dallas, Dallas, TX, 475p.

Taff, J.A., 1902, Description of the Atoka quadrangle [Indian Territory]: U.S. Geological Survey Geologic Atlas Folio 79, scale 1:125,000, 8 p. (named Woodford Chert)

3.6 Additional Woodford Sections in Arbuckle Mountains: There are at least 3 well-exposed sections of Woodford in the Arbuckle Mountains not covered in this guidebook (Figure 3.6.1) but which may be added in subsequent editions.

1. Henry House Creek is the Hass-A site where Over (2002) placed the F/F boundar ~10ft above the Hunton (Figure 3.6.2). This section was part of an excellent Master’s thesis by Auffer (2007).

2. The Speake Ranch section is about 5mi west of Henry House Creek and 10mi west of I35-South. Galvis (2017) completed a thorough characterization of the Woodford at this location (Figure 3.6.2b). This section also has a well-developed transition zone between the Woodford and Sycamore units.

3. The Arbuckle Wilderness Area (AWA) on the north flank of the Arbuckle anticline is less than a mile SE of the I35-South location. The AWA section from the Viola through the Caney (Sayeddolali et al., 2019) is reasonably well exposed. Surprisingly, no specific studies have been published at the AWA.

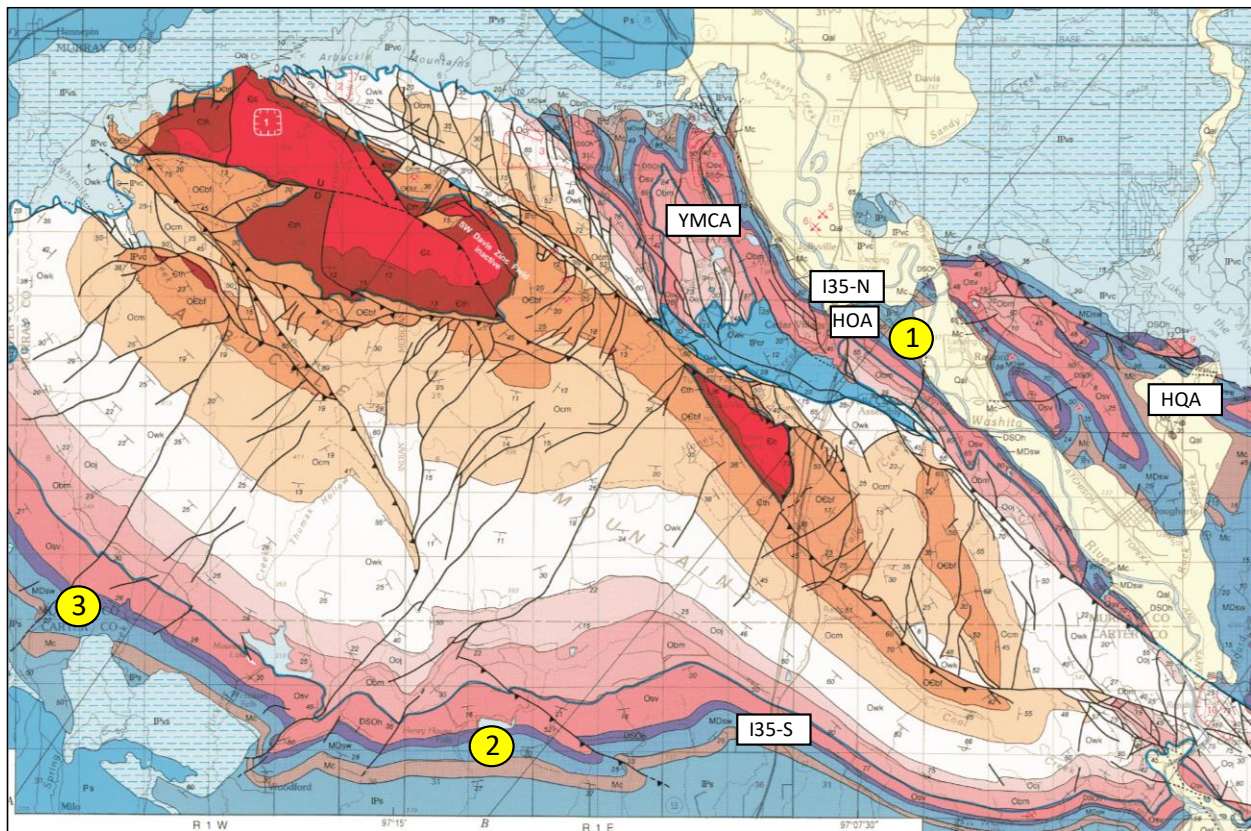


Figure 3.6.1 Location map for other Woodford sections not covered in this guidebook: 1) Arbuckle Wilderness Area, 2) Henry House Creek (Hass-A), 3) Speake Ranch

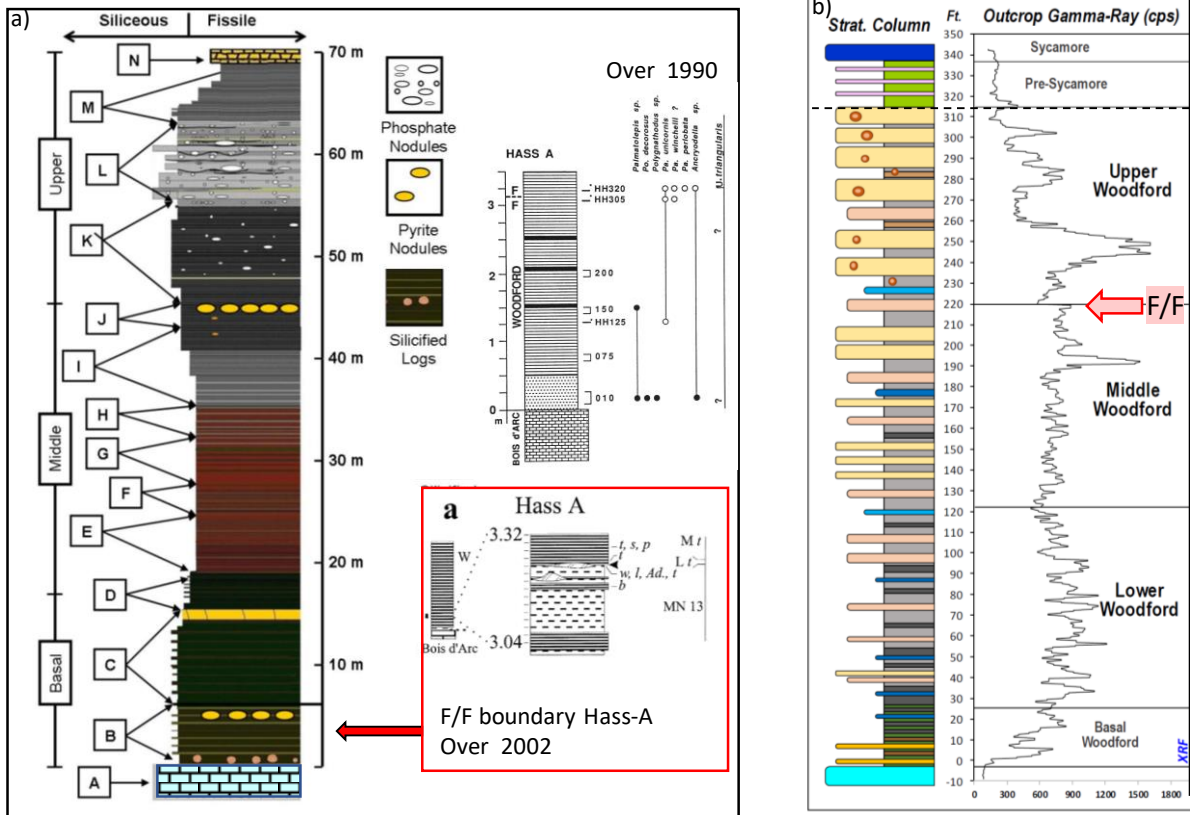


Figure 3.6.2 Stratigraphic sections for a) Henry House Creek (Over, 2002; Aufil 2008) b) Speak Ranch (Galvis 2017). F/F boundary from Molinares (2019). Note the large difference in the thickness of the Frasnian (10ft vs. 220ft) between the 2 locations.

References

Aufill, M., 2007, High resolution magnetic susceptibility of the Oklahoma Woodford Shale and relationship to variations in outcrop spectral-gamma response: Oklahoma State University, unpublished M.S. thesis, 210 p.

Galvis, H., 2017, Detailed lithostratigraphic characterization and sequence stratigraphy of a complete Woodford Shale outcrop section in southern Oklahoma: Norman, University of Oklahoma, unpublished M.S. thesis, 155 p.

Molinares Blanco, C.E., 2019, Paleoenvironments and sediments around the Frasnian/Famennian (F/F) transition in the Woodford Shale, south central Oklahoma—A multiproxy approach: Chapter 3, University of Oklahoma, PhD, p.32-102.

Over, D.J., 2002, The Frasnian/Famennian boundary in central and eastern United States, *Palaeogeography, Palaeoclimatology, Palaeoecology* 181, p.153-169.

Seyedolali, A., Cardott, B.J., Torres, E.J., and others, 2019 Integrated Geological & Geochemical Characterization of the Mississippian Caney Shale, Oklahoma –Subsurface & Outcrops Delineation, presentation Oklahoma Geological Survey Shale Resource Plays Workshop.

4.1: McAlister Cemetery Quarry / Ardmore Basin

The McAlister Cemetery Quarry (MCQ) is 19mi/31km south of stop 3.5, last ridge of I-35S, and is the southernmost exposure of the Woodford in Oklahoma (Figure 4.1.1a). In addition to its strategic location, easy access & parking, and good exposures make the MCQ a subject of numerous studies on subjects ranging from lithofacies, sequence stratigraphy, geomechanics, organic geochemistry, and the genesis of calcite and phosphate concretions (Kirkland et al., 1992; Krystyniak, 2005; Walker, 2006; Paxton and Cardott, 2008; Boardman 2012, Bernal, 2013; Ekwunife, 2017; Klockow, 2017; Martin, 2017; Philp and DeGarmo, 2020). Ekwunife (2017) is the most comprehensive study to date in terms different analytical methods.

At the MCQ a 380ft/115m thick complete Woodford section about is exposed on the northeast limb of a regional Pennsylvanian-age structural feature, the Criner Hills-Overbrook anticline which rises through a breach in the Cretaceous onlap succession (Figure 4.1.1b and 4.1.1c). Most of the quarry is flat with several low-relief berms of more resistant rock in the Middle Woodford. The northeast edge of the quarry is a small hill of uppermost Woodford and Sycamore (Figure 4.1.2). Dips range from 35° to 45°. The Woodford at the MCQ is marginally mature, 0.52% Ro (Paxton and Cardott, 2008). The Woodford at the MCQ is marginally mature, 0.52% Ro (Paxton and Cardott, 2008). On the basis of lithology, bedding thickness / degree of fissility, and gamma ray character Ekwunife (2017) divided the Woodford into Lower, Middle and Upper members and place them in a regional stratigraphic context including defining the maximum flooding surface at the Middle-Upper Woodford contact (Figure 4.1.2b). These also tie into the conodont biostratigraphy by Over (1990; 1992, 2002) which define the D/C boundary and the F/F boundary near the top and base of the Woodford respectively.

The unconformable contact between the Hunton Group limestones and the overlying Lower Woodford is covered but well-constrained (Figure 4.1.3a). The basal Woodford section (~20ft) is a light gray to white, organically lean, clay-rich, unit with a few dark gray fissile shale beds (Figure 4.1.3b) and very rare phosphate nodules (Figure 4.1.3c). From a palaeoceanographic / sequence stratigraphic perspective this unit likely represents the earliest oxygenated shallow water deposits of the initial marine transgression over the unconformity at the top of the Hunton Group.

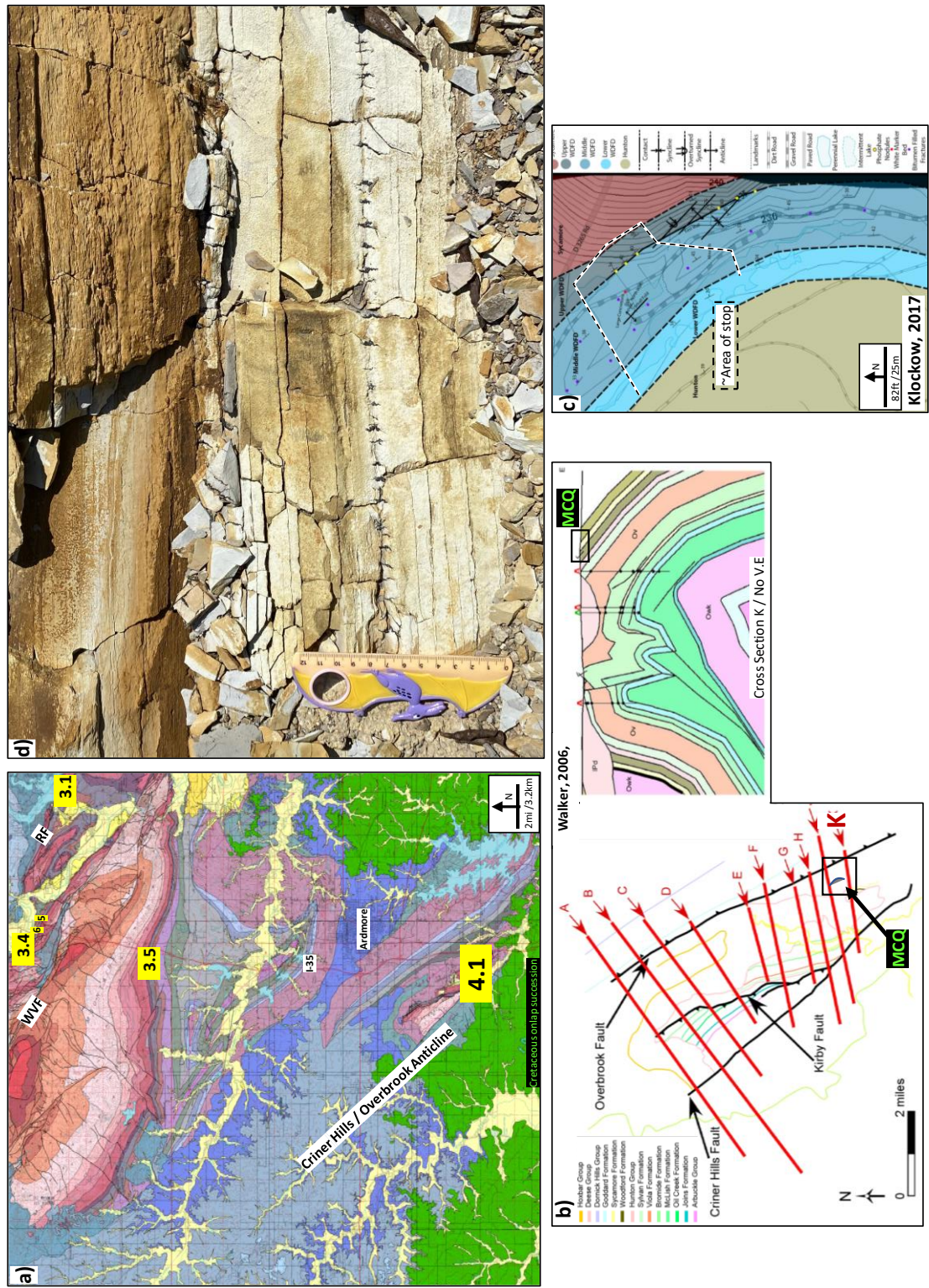


Figure 4.1.1: a) Location map for McAlister Cemetery Quarry (MCQ) Ardmore 2° geological map (Chang and Stanley, 2012) b) Outcrop pattern map and x-section Criner Hills uplift c) MCQ geological map d) Bitumen filling irregular fractures along a bedding plane.

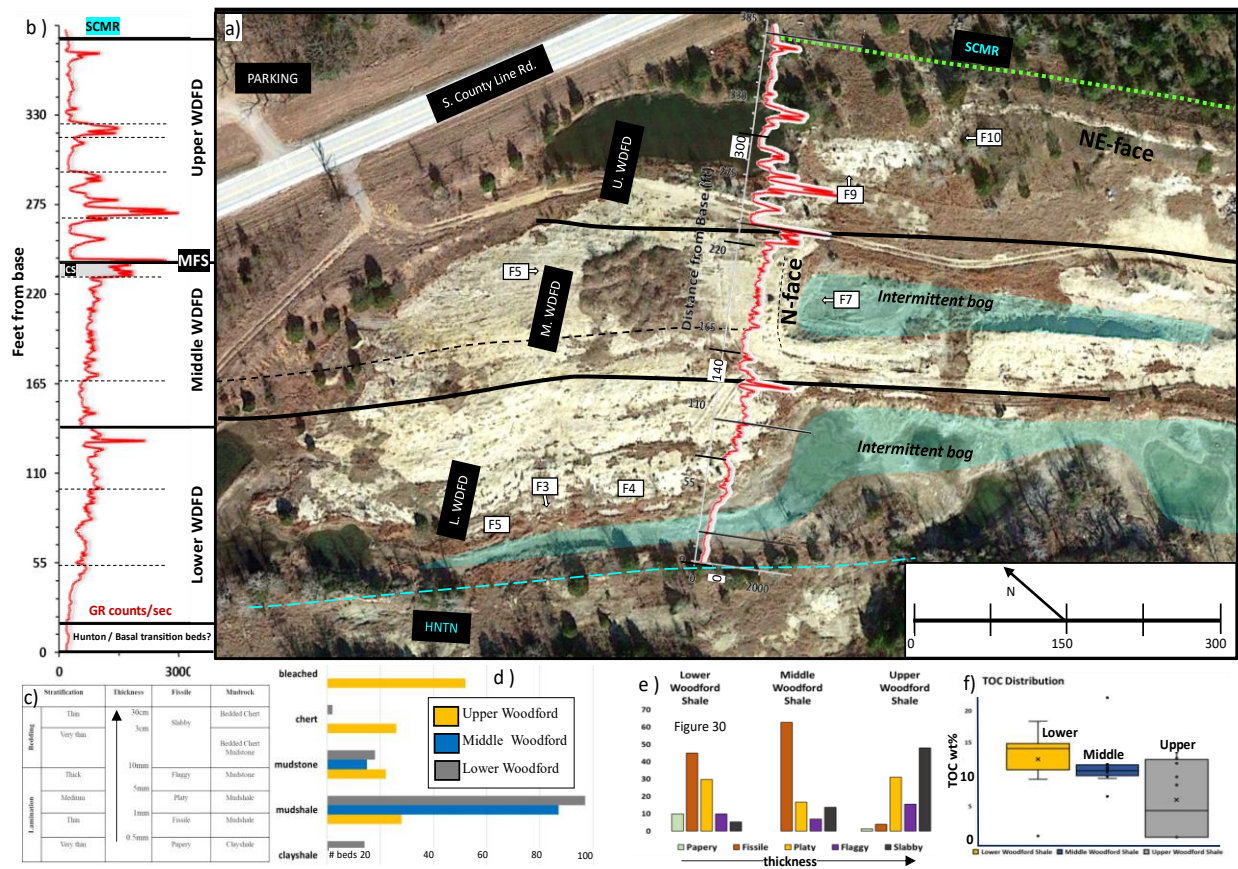


Figure 4.1.2: a) Oblique aerial view of the northern part of the MCQ with stratigraphic contacts & GR gamma ray log, data displayed, are adapted from Ekwunife (2017). White boxes w/ arrows indicate photos in figures. b) Outcrop GR log; CS is condensed section; MFS is the regional maximum flooding surface. c) Table of fissility & parting thickness d) Abundance of the 5 dominant lithofacies in each member (technically “bleached” is not a lithofacies). e) Histogram of bed thickness & classes of the 3 Woodford members f) TOC distribution by Woodford members.

The Lower Woodford is about 140ft/42m thick (Figure 4.1.2a) and is composed of light gray to black laminated to papery argillaceous shale and mudrock. Several mudrock beds in the lower part of the Lower Woodford have a light green surface patina but are dark gray on fresh surfaces (Figure 4.1.5). In contrast to outcrops in the Arbuckle Mountains, there is very little chert in the Lower Woodford in the MCQ. Consequently, in outcrop differences between the Lower and Middle Woodford (Figure 4.1.6) are difficult to detect without analytical data (XRF, TOC, GR, etc) and the boundary between these units is picked primarily of the pattern of the outcrop gamma ray (Figure 4.1.2c).



Figure 4.1.3 a) Hunton-Woodford contact on west side of quarry. b) Photo of hand sample of basal/transitional Woodford c) Photo of rare phosphate nodules in basal/transitional Woodford.



Figure 4.1.4: Typical Lower Woodford thin bedded to papery siliceous silty shale weathered surface is to white and light grey, fresh surface dark brown to dark grey (sample M-10). Notable lack of chert, ruler is 12cm.



Figure 4.1.5: Lower Woodford greenish shales that are dark grey to black on fresh surfaces for sample MY.



Figure 4.1.6: Typical Middle thin bedded to papery siliceous silty shale and mudrock on small upraised rib (mound); presumably more siliceous and resistant to erosion than surrounding section.

The Middle Woodford is approximately 100ft/33m thick and is composed of organic-rich argillaceous and siliceous mudrock and shale with siliceous mudrock being the dominant lithofacies (Figures 4.1.2 a,b,c). The upper Middle Woodford (UM ~160-230ft) shows an increase the gamma ray (Figure 4.1.2b) that may reflect an increase in clay content as well as potential TOC and mineral accumulation at the MFS. That interval also has several sets of beds with strong surface iron oxide staining (Figure 4.1.7 and 4.1.8) indicative of the weathering of pyrite, an interpretation supported by limited XRD data (Figure 4.1.8b) and elevated S and Fe concentrations of XRF data (Figure 4.1.13a). This pyrite is also indicative of a change in paleoceanographic environment supported by the organic geochemistry data (Philp and Degarmo 2020).



Figure 7.1.7 a) Photo of north face (Figure 4.1.2) looking north at upper Middle Woodford. CC is a large carbonate concretion. Yellow lines mark surfaces of more FeOx / jarosite(?) from intervals with more pyrite (see inset figure, Ekwunife, 2017).) b) Horizontally squeezed photo of most of north wall with GR and bed division (Ekwunife, 2017)

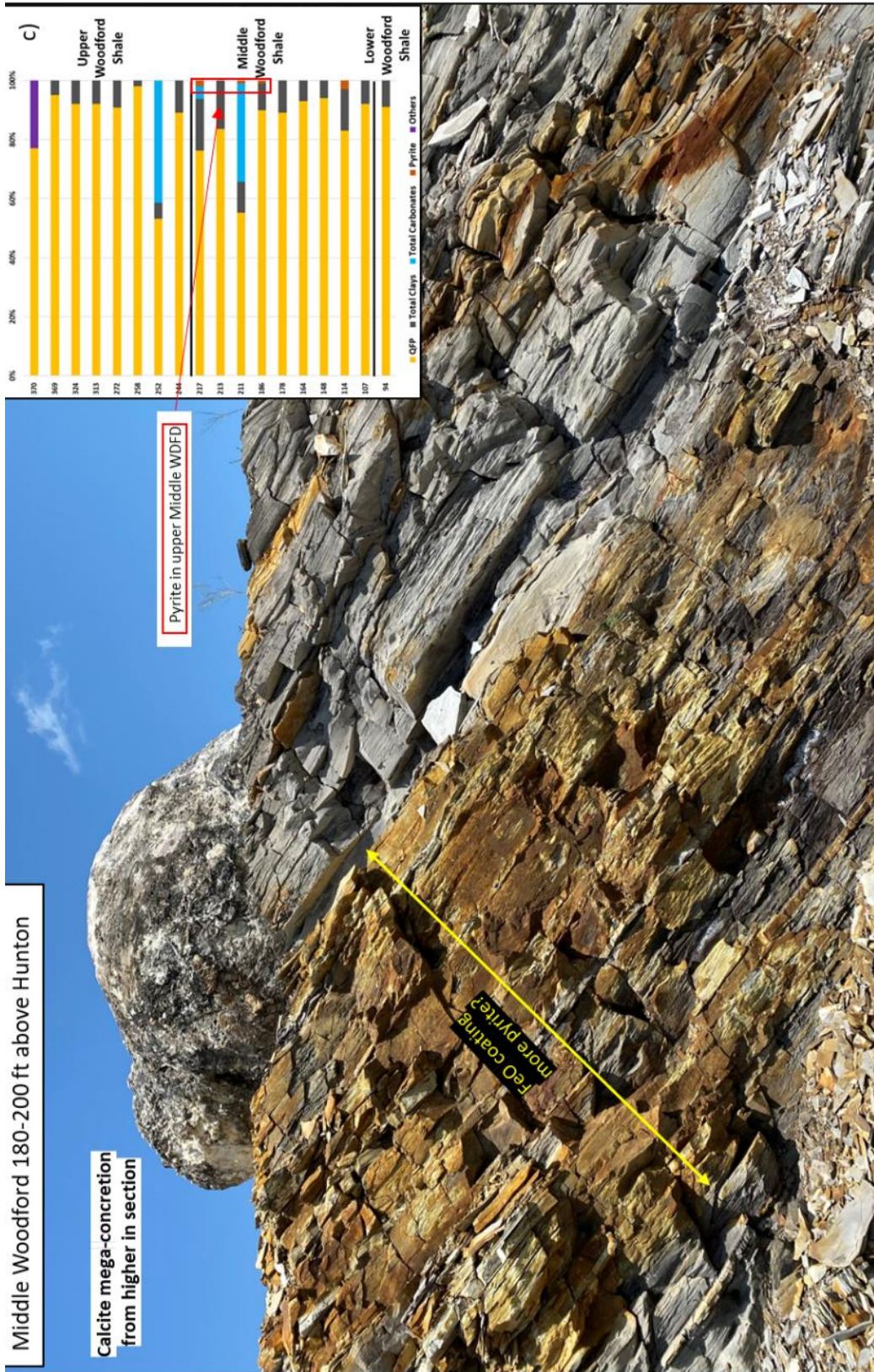


Figure 4.1.8 a) Closer look at pyritic bed on Middle Upper WDFD (north wall) b) XRD data from the Woodford (Ekwunife, 2017).

The Upper Woodford is approximately 125ft/38m thick. As seen at Sections 3.1, 3.3, 3.5, the distinctly more siliceous nature of Upper Woodford is marked by overall lower GR readings (Figure 4.1.9b) and a distinct increase in the Si/Al ratio (Figure 4.1.13a). In the Upper Woodford the beds are thicker with more flaggy mudstone and slabby chert (Figures 4.1.2d and 4.1.2d). At the MCQ the Upper Woodford is associated with appearance of abundant, mostly spherical, phosphate nodules. An upward increase in the abundance and size of the phosphate nodules in the uppermost Upper Woodford at the McAlister Cemetery Quarry is coincident with an increase in the abundance and thickness of chert beds starting about 320ft (Figures 4.1.2e, 4.1.9b, 4.1.10b).

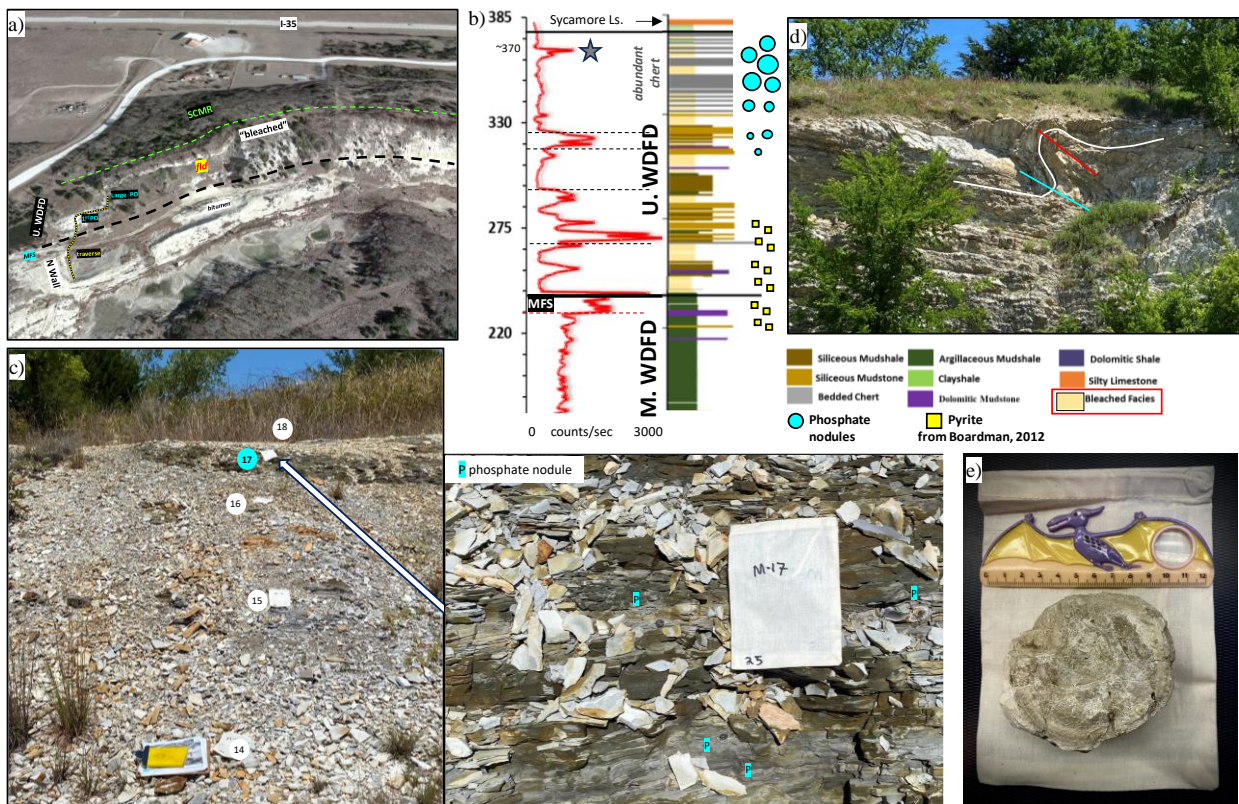


Figure 4.1.9 a) Oblique view of NE quarry wall and bleached Upper Woodford b) GR log and lithofacies of Upper Woodford (Ekwanife, 2017) b) GR log and lithofacies (Ekwanife 2017. Gray star ~370ft denotes grey mudrock in “bleached zone” c) Lower U. WDFD at base of small hill 1st phosphate nodules at M-17 d) Minor folds near top of the Upper Woodford on NE wall. e) Large (7cm diameter) phosphate nodule from “bleached” zone. Note faint concentric banding and the sample bag for comparative scale the nodules near sample M-17.

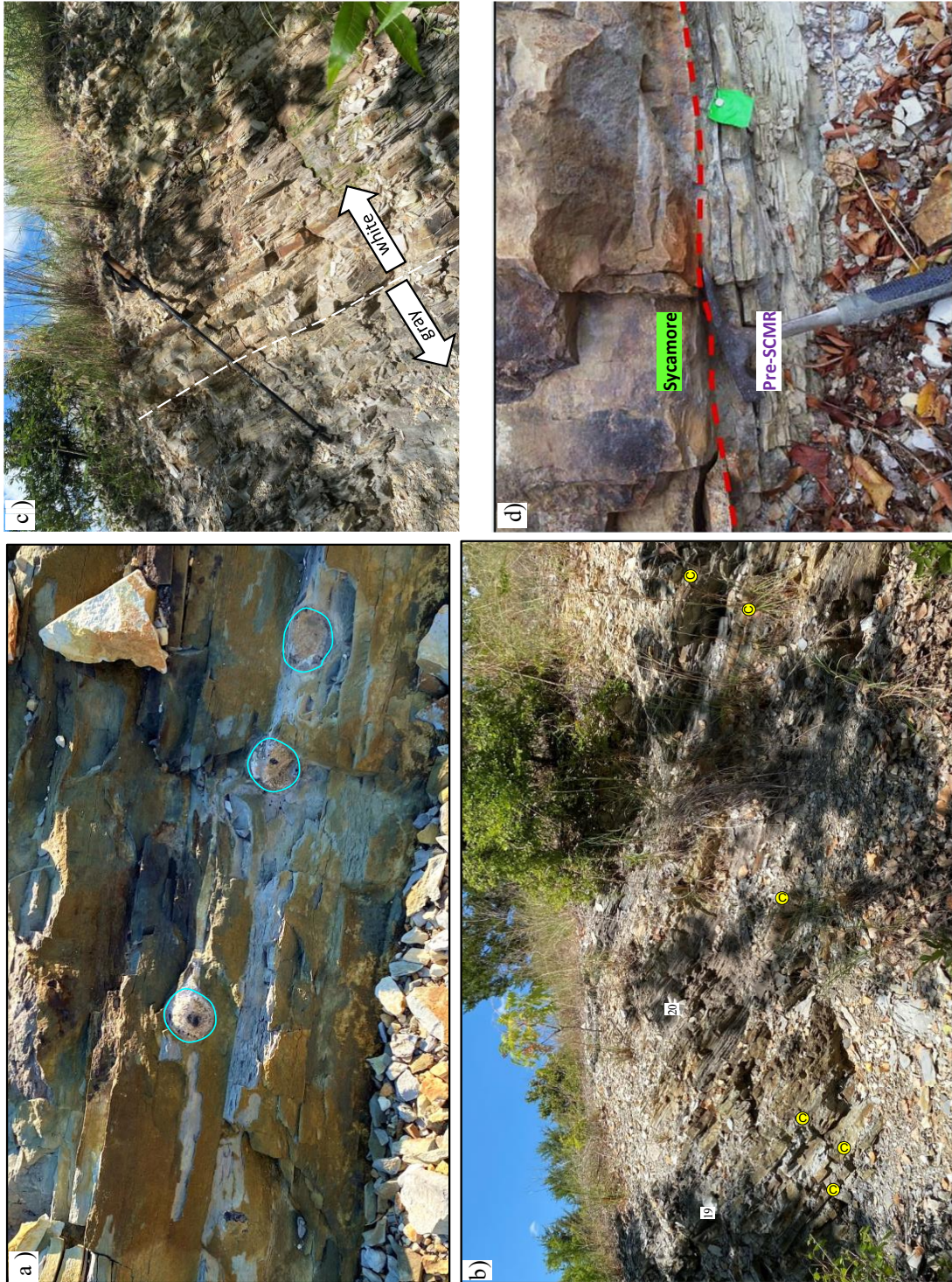


Figure 4.1.10 a) Spherical phosphate nodules in the Upper Woodford. b) Photo of small cliff face of Upper Woodford in the “bleached” facies, which does not appear as vertically extensive as shown on Figure S7-9b; C denotes chert beds. c) Conformable transition from gray to bleached beds d) Sycamore contact with thin pre-Sycamore greenish mudrocks (Fig. 33: Ekwunfie, 2017). Note the lack of bleaching.

A striking and unusual feature of the MCQ is a 55ft white interval at the top of Upper Woodford (Figure 4.1.2a and 4.1.9b). This interval has a 5x increase in Si/Al and much lower TOC, S, Fe, and U lower values than in the Middle and Lower Woodford (Figure 4.1.12a). Kirkland (1992) suggested that this whitening is the result of bleaching and oxidation in the Pleistocene and also stated that bleaching of the Upper Woodford occurs elsewhere. However, no other locations were given, and Kirkland's reference is a personal communication with no additional information. We know of no other locations where this interval is present. There are several features of this white zone that lead us to question the relatively young bleaching interpretation. First, exposures in the wall of small south-facing cut wall shows that the gray to white transition appears to be structurally conformable (Figure 4.1.10c) rather than cross-cutting as would be expected if bleaching post-dated deformation. Second, at the contact with the Upper Woodford a thin light green shale (pre-Welden equivalent?) and the Sycamore Limestone show no evidence of bleaching (Figure 4.1.10d). Third, there are rare thin, grey siliceous mudrocks in the upper part of the interval and several sharp high gamma ray zones (Figure 4.1.9b) indicating deposition under more reducing conditions.

Chemostratigraphic data yield an alternative explanation. Based on XRF elemental chemofacies Ekwunife (2017) concluded that the Upper Woodford experienced mostly open circulation (Figure 4.1.12b), which would account for the lowered preservation of organic carbon in the Upper Woodford. Although the elevated Ni/Co ratios indicate anoxic conditions (Figure 4.1.12c) both of these elements are in extremely low abundance, rendering those ratios suspect. Increasing open circulation is supported by biomarker data in Philp and Degarmo (2020) and Parks and Lui (2023) at Wyche Quarry, particularly of isorenieratane and related biomarkers that indicate photic zone euxinia decreased dramatically in the upper Woodford. As an alternative to Holocene bleaching model, we propose the white zone at the McAlister Cemetery Quarry resulted from a shift in depositional conditions in the Latest Devonian. This could be consistent with models related to a fall in sea level and influx of terrigenous material and more oxygenated water from shallow sources or possibly the encroachment of oxic deep marine bottom water as indicated by the section at Scratch Hill (see section 5.2) where most of the Arkansas Novaculite was deposited in non-reducing conditions. Clearly this interval at the MCQ is worthy of further study including stable isotopes.

In addition to its large phosphate nodules several very large calcite-dominated mega-concretions (up to 5ft/1.5m in diameter; Figure 4.1.8) have been dug out from the Upper Woodford near the

base of the interval with abundant phosphate nodules (Kirkland et al., 1992). These concretions have relict bedding and precipitated around phosphate nodules indicating they are a post-deposition diagenetic event (Figure 4.1.11a and 4.1.11b). Internally, well-preserved radiolarian tests indicate the nodules grew before significant compaction. The well-defined increasingly light $\delta^{13}\text{C}$ values from core to rim may reflect an increase in carbon related to sulphate reduction (Kirkland et al., 1992). These carbonate concretions typically have hematitic calcite rinds with very light $\delta^{13}\text{C}$ values. Trace element concentrations (V, Ni, Mo) increase in the sparry rinds, indicating an increase in metal availability during rind growth. These rinds have been interpreted as recording a Cretaceous event (Figure 4.1.11d; Martin, 2017). One of the enigmatic features of the calcite concretions is the presence of several normal marine infaunal fossils which are not present in the Woodford mudrocks (Figure 4.1.11e). Whether these were washed in or lived in-situ these fossils point to a brief interval of a shallow water open marine conditions.

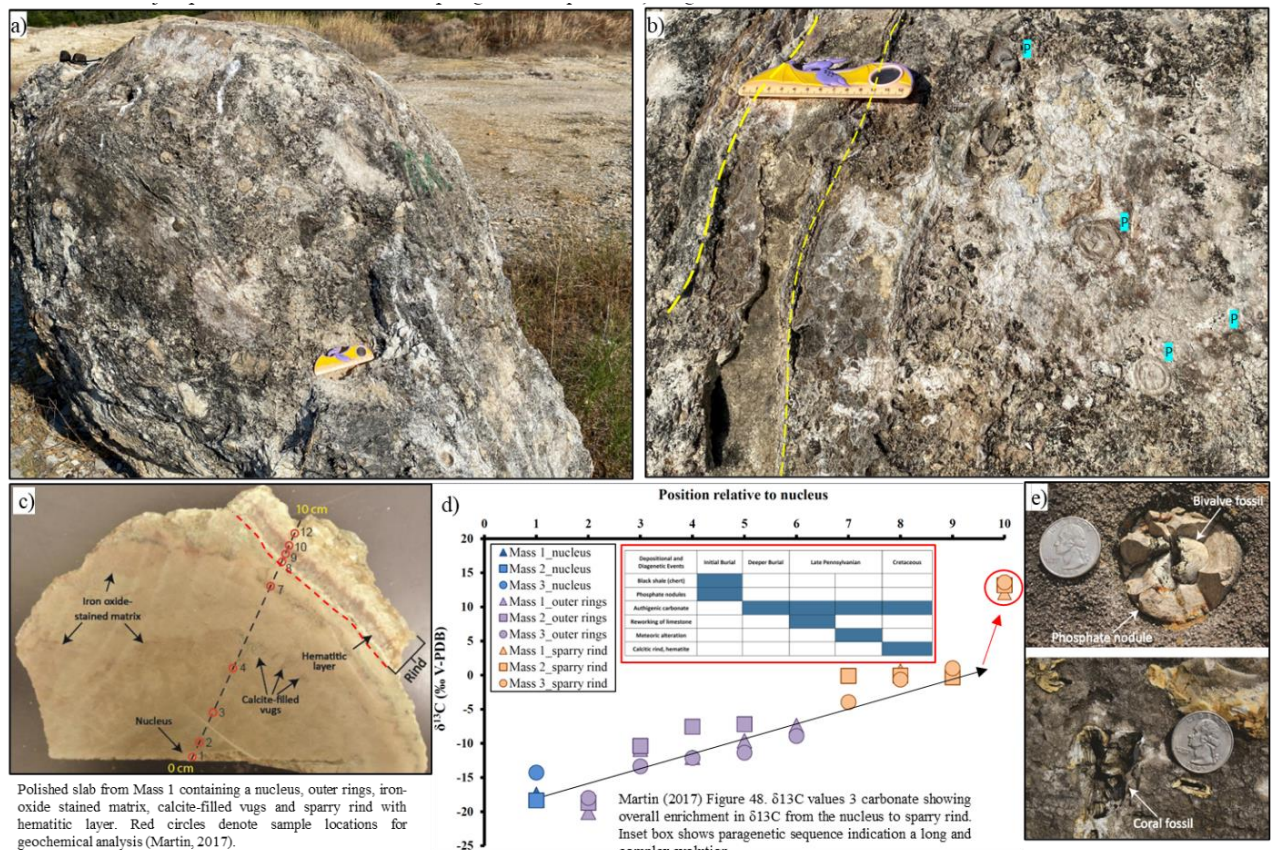


Figure 4.1.11: a) Large calcite-rich concretion b) Close up of a) showing embedded phosphate nodules (P) and relict bedding- yellow dashed lines c) Example of banding in Ca-nodule with outer rind d) Carbon isotope variations for 3 carbonate masses shower lighter values from core to rim with sudden jump at rim. Inset box indicates paragenetic sequence. e) Enigmatic infaunal fossils- bivalves and coral.

The MCQ outcrops also feature bitumen filled fractures and small tar balls (Figure 4.1.13a and 4.1.13b). The tar balls occur on bedding planes and likely represent biodegraded hydrocarbons from a submarine seep (Kirkland et al., 1992).. One of the most photographed features at the MCQ are the visually striking bitumen-filled fracture sets exposed on bed tops (Figure 4.1.13). These fractures have an extremely limited extent. Considering the difficulty for oil to migrate into the Woodford, the limited extent of bitumen filling coupled with the low level of thermal maturity at the MCQ and extremely small S1 yields in Rock Eval (Figure 4.1.12d) suggest that the bitumen is in-situ early generated oil rather than migration from deeper in the basin.

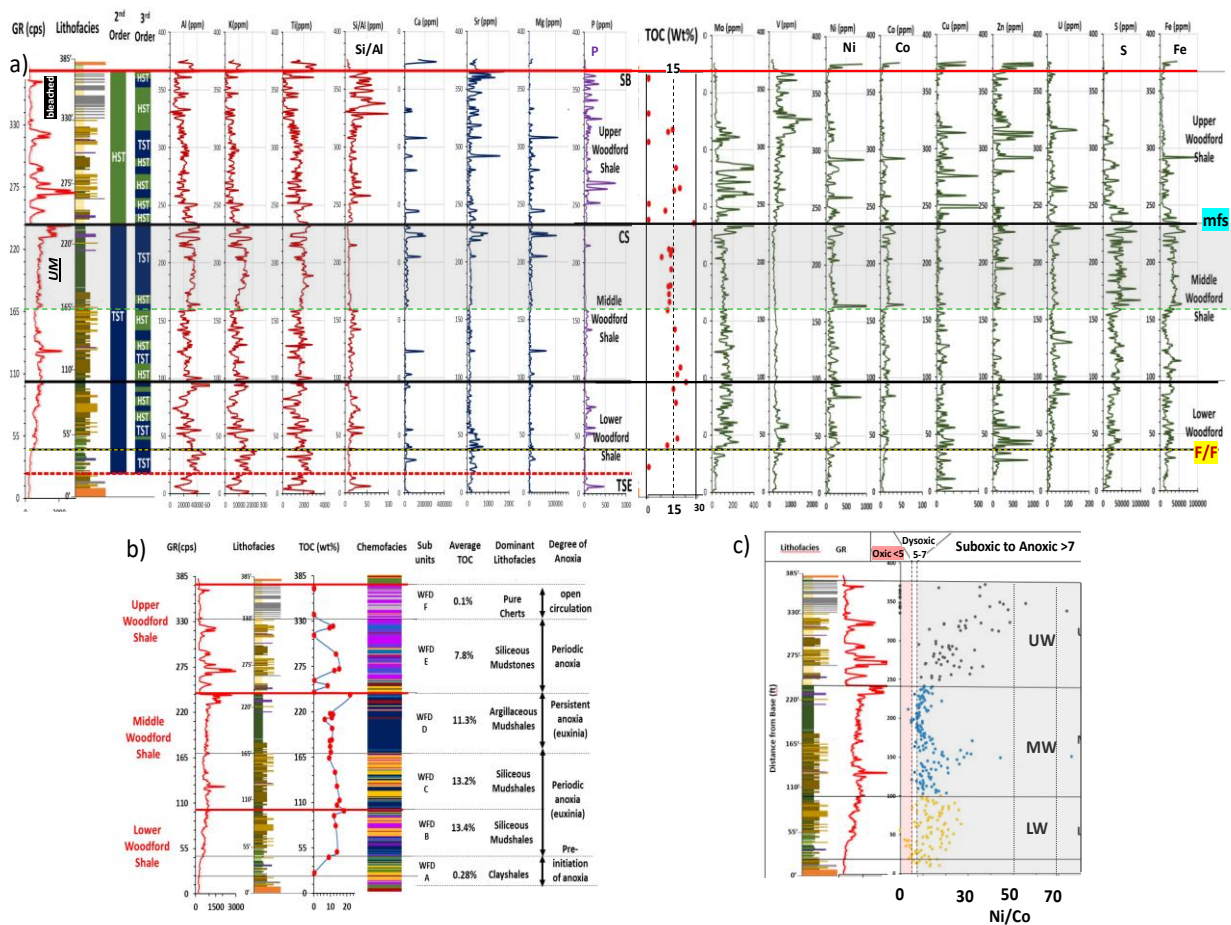


Figure 4.1.12 a) XRF data with red-ox sensitive elements in green to right (combined figures from Ekwunife, 2017). b) Chemofacies from XRF data (figure 51 Ekwunife, 2017) c) Ni/Co data is used as a proxy for degree of anoxia (Bernal, 2013). Although the high Ni/Co ratios in the bleached zone appears inconsistent with oxic bottom facies waters discussed above, this zone has extremely low Ni and Co concentrations that render the ratio suspect.

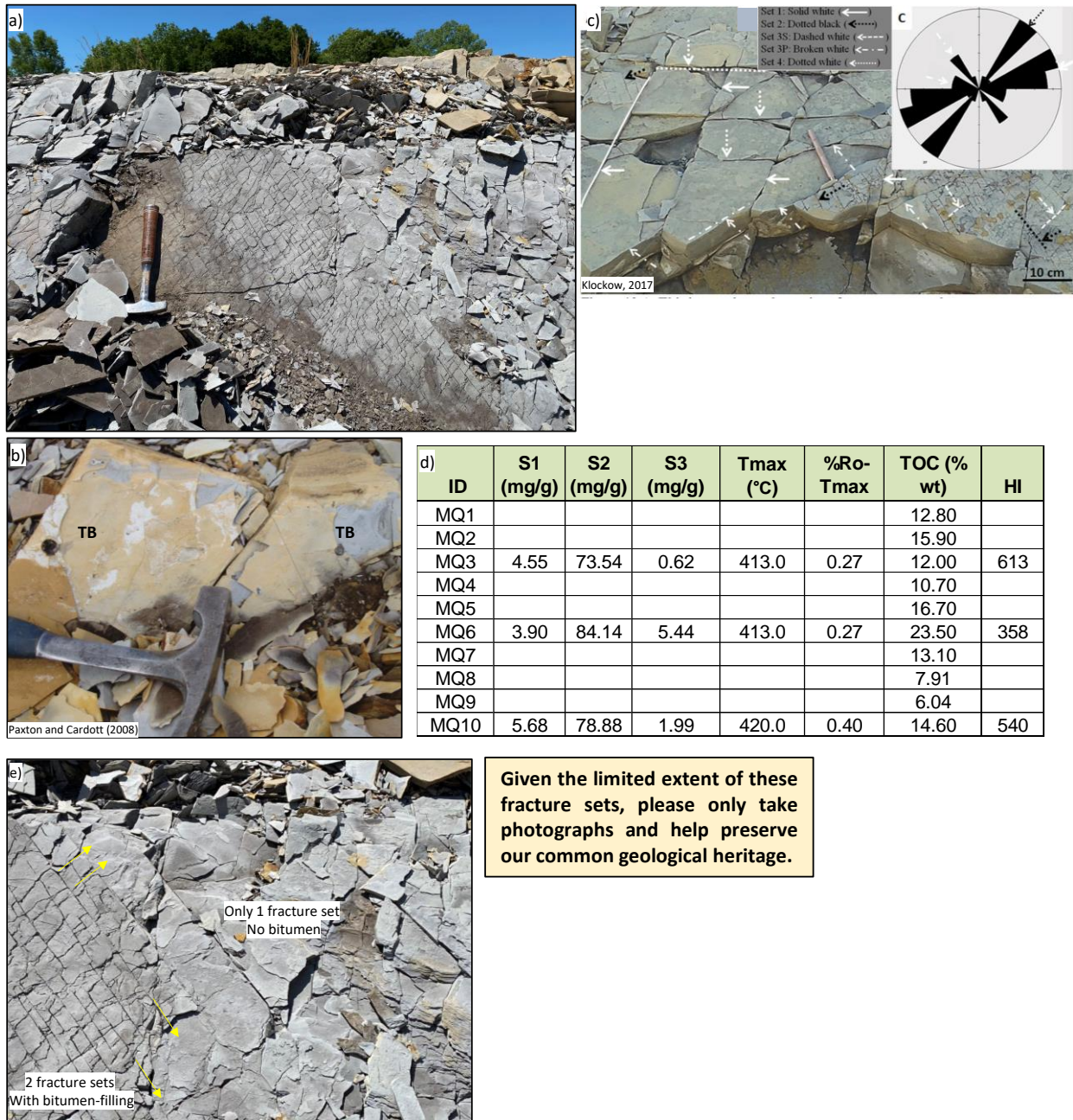


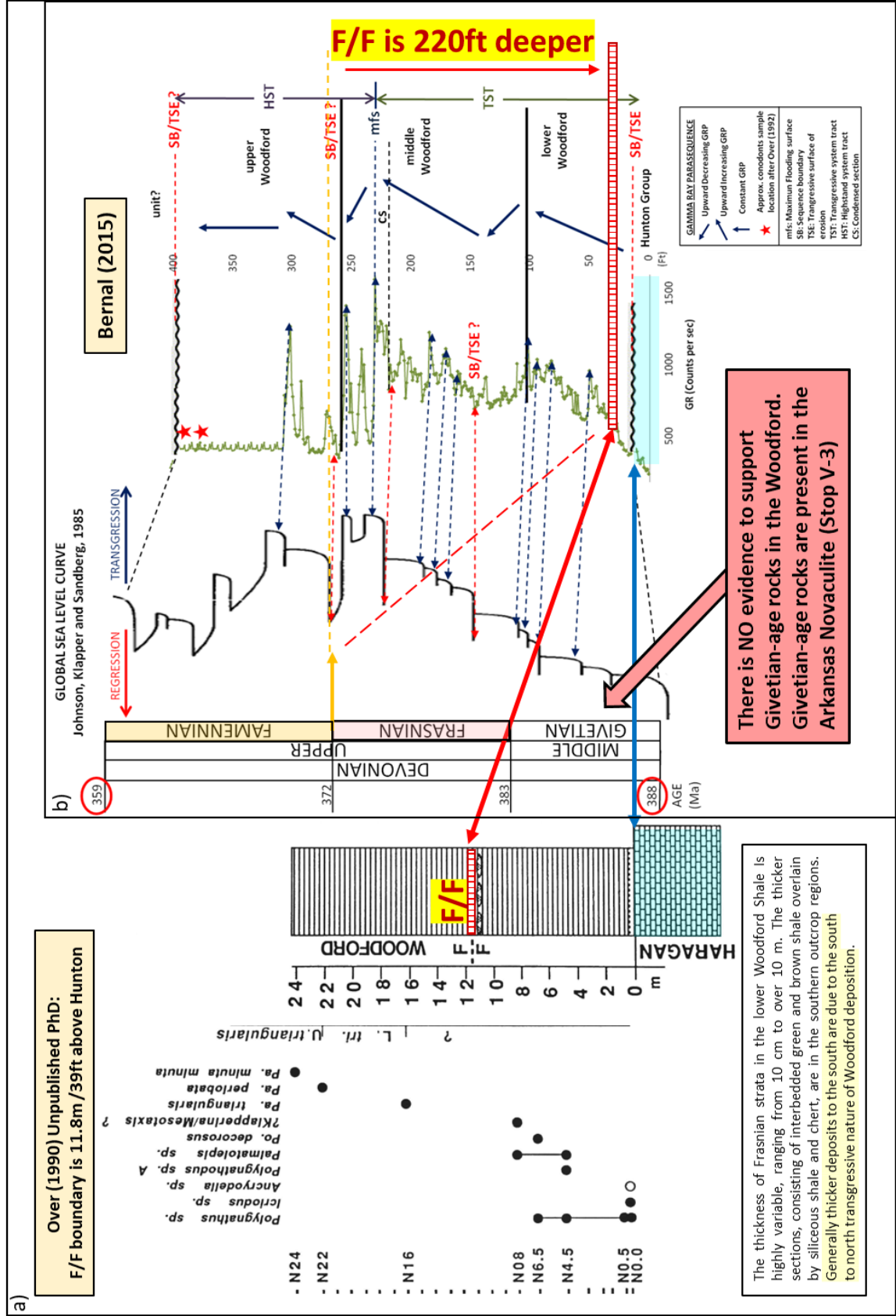
Figure 4.1.13 a) Bitumen-impregnated fractures on a single bedding plane b) Tar balls on bedding plane c) Fracture set strike directions. d) RockEval and TOC data from MCQ, e) Closer view of limited extent of bitumen-filled fractures.

Biostratigraphically the MCQ is an important location. Conodonts from the MCQ outcrops, studied by Over (1990, 1992, 2002). In his published study on the Devonian-Carboniferous boundary Over (1992) reported poor recovery from Upper Woodford shales but did find Devonian

conodonts from one of the calcite concretions. Recall that these concretions were not in place, but the quarrymen noted they came from near the base of the phosphate zone. Thus, the D/C boundary at the MCQ could be present in the upper 50ft of the Woodford in a similar position to Section 3.5, I-35S Last Ridge.

As noted regarding the Wyche Quarry, the unpublished part of Over's dissertation (1990) addressing the Frasnian-Famennian boundary is often overlooked. At the MCQ Over (1990, 2002) conodont biostratigraphy places the F/F boundary ~39ft/11.8m above the Hunton contact (Figure 4.1.14a) which is 220ft/67m beneath the boundary as interpreted by Bernal (2013) and Molinares (2019) who, ignoring the work of Over, used Transgressive-Regressive cycles and multi-proxy methods. It follows then that Philp and DeGarmo's interpretation of biomarkers indicative paleo-wild fires associated with the F/F boundary event is not correct (Figure 4.1.15). The increase in the combustion proxy used by Philp and DeGarmo (2020), however, is consistent increased terrestrial input during a fall in base level during the Famennian Wildfire Event (van der Meer et al., 2022; Lu et al., 2021).

Figure 4.1.14 a) Placement of the Frasnian/Famennian extinction boundary using Over's conodont data (1990). Figure shows Bernal-Serna (2015) placement of the F/F boundary near the MFS at ~260ft above the is incorrect; the boundary is ~11.8m / 39ft above the Hunton.



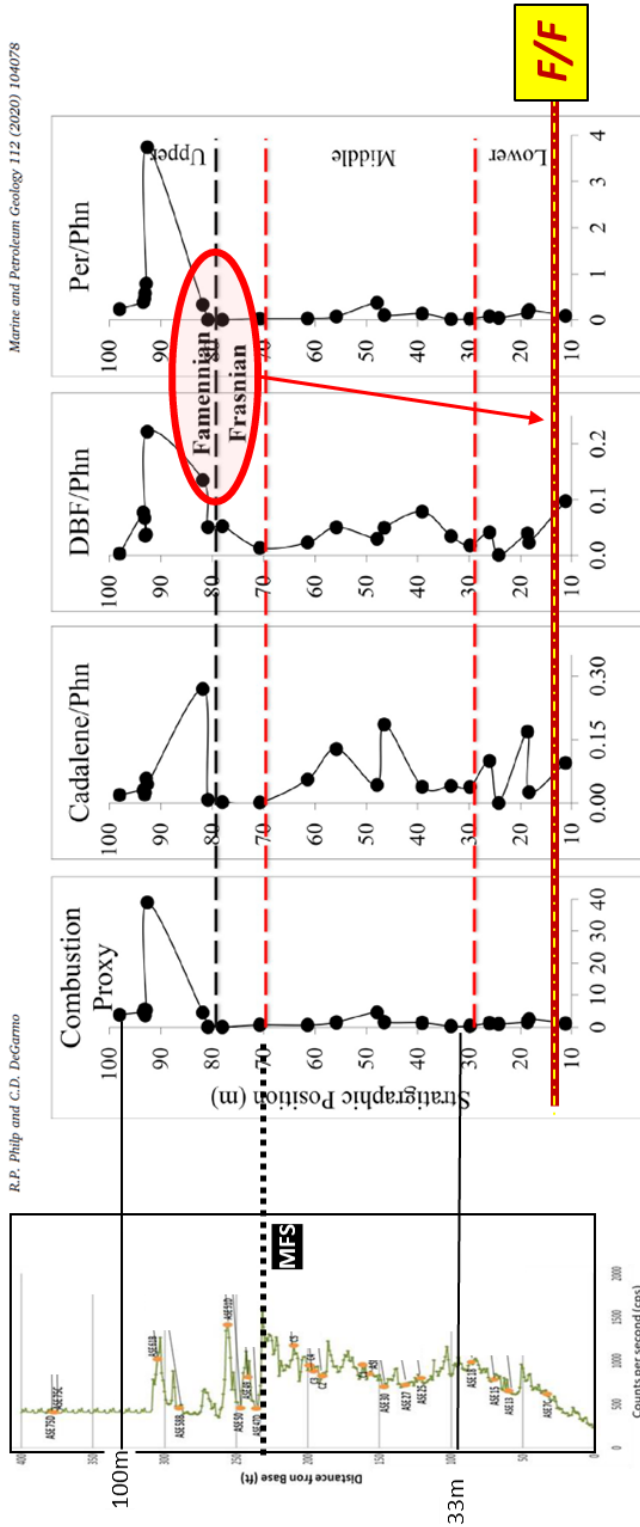
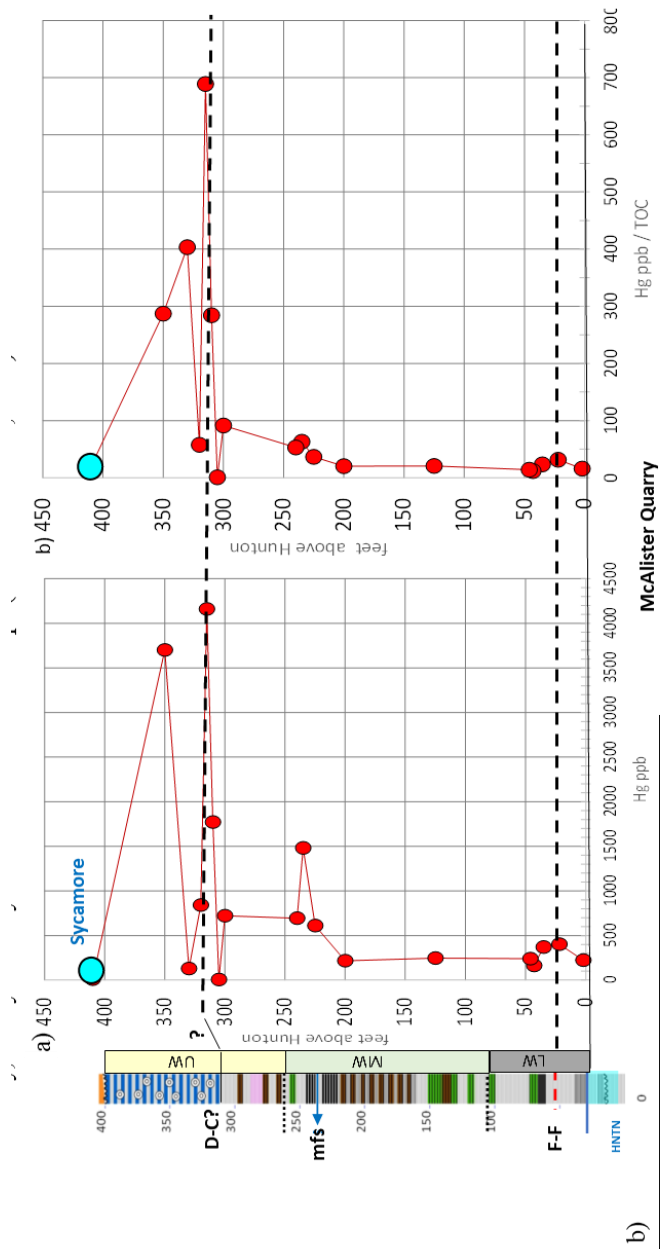


Fig. 16. Variations in ratios that reflect a combustion proxy (benzo(e)pyrene + benzo(ghi)perylene/phenanthrene); a vascular land plant indicator (cadalene/phenanthrene); a soil erosion proxy (dibenzofuran/phenanthrene) and perylene/phenanthrene.

Figure 4.1.15 Philp and DeGarmo (2020) showing influx of paleo-wildfire detritus as inferred from biomarker data. The F/F boundary should be placed much lower (Over, 1990, 2002).

Lastly, we consider the case for using mercury as an indication of volcanism as a major driver of the F/F and D/C extinctions, as suggested by Racki et al., (2018) and Rakocinski et al., (2020), respectively. At the MCQ the Frasnian-Famennian boundary is well constrained. The Devonian-Carboniferous boundary is inferred to be in the uppermost Woodford at the MCQ. This permitted sampling for Hg anomalies to test the volcanic trigger hypothesis for the Late Devonian Mass Extinction events to be focused on those boundaries (Figure 4.1.16a and 4.1.16b; Cullen, 2020). There are small Hg and Hg/TOC anomalies around the F-F boundary at the MCQ, as seen at the Camp Classen section (3.4), but the anomalies are rather low to assign much confidence that they are related to volcanism. Samples from the base of a cherty phosphatic lithofacies in the Upper Woodford near the Devonian-Carboniferous boundary show world class enrichments in Hg and Hg/TOC (Figure 4.1.16c). Although these enrichments that are supportive of the volcanic triggering hypothesis recent studies involving Hg isotopes (Zhang et al., 2021) suggest that further work is needed to test the volcanic triggering hypothesis vs. terrestrial input. An important issue to consider is whether terrestrially-derived Hg could overwhelm the input from volcanic aerosols.



#	SAMPLE	FM	FT above HNTN	TOC wt%	Hg ppb	Hg ppb / TOC	Hg EF	Hg/TOC EF
13	MCO-11	WDFD	2	13.9	223	16	0.57	0.52
4	MQ-1	WDFD	22	12.8	402	31	1.02	1.01
5	MQ-2	WDFD	35	15.9	369	23	0.94	0.75
14	MCO-12	WDFD	43	14.05	162	12	0.41	0.37
15	MCO-13	WDFD	46	17.05	240	14	0.61	0.45
6	MQ-3	WDFD	125	12	245	20	0.62	0.66
7	MQ-4	WDFD	200	10.7	216	20	0.55	0.65
8	MQ-5	WDFD	225	16.7	609	36	1.55	1.18
1	MQ-6	WDFD	235	23.5	1480	63	3.76	2.03
9	MQ-7	WDFD	240	13.1	693	53	1.76	1.71
10	MQ-8	WDFD	300	7.91	721	91	1.83	2.94
11	MQ-9	WDFD	305	6.04	4.16	1	0.01	0.02
16	MCO-14	WDFD	310	6.23	1770	284	4.49	9.16
2	MQ-9	WDFD	315	6.04	4160	689	10.56	22.22
3	MQ-10	WDFD	320	14.6	839	57	2.13	1.85
17	MCO-15	WDFD	330	0.32	129	403	0.33	13.00
18	MCO-16	WDFD	350	12.9	3700	287	9.39	9.25
19	MCO-17	SCMR	410	0.5	10	20		

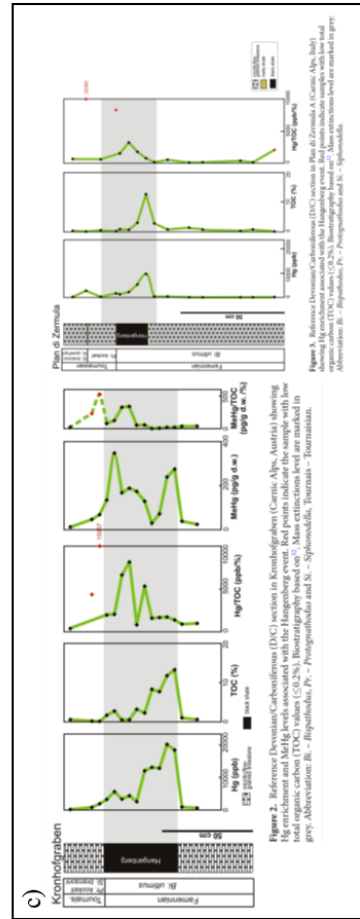


Figure 4.1.16 a) Mercury and TOC data from McAlister Cemetery Quarry (Cullen, 2020) b) Hg, methylmercury and TOC data from Europe (Rakocinski et al., 2020)

REFERENCES

- Bernal, A.S., 2013, Geological characterization of the Woodford Shale, McAlister Cemetery Quarry, Criner Hills, Ardmore Basin, Oklahoma: Norman, University of Oklahoma, unpublished M.S. thesis, 141 p.
- Boardman, D.R., III, 2012, Preliminary analysis of phosphate nodules in the Woodford Shale, Late Devonian-Early Mississippian, southern Oklahoma: Stillwater, Oklahoma State University, unpublished M.S. thesis, 77 p.
- Chang, J.M., and Stanley, T.M., 2011, STATEMAP: Mapping the Ardmore 1 Degree Sheet and the Oklahoma Part of the Gainsville 1 Degree Sheet, Oklahoma: Oklahoma Geology Notes, v. 71, no. 4, pp. 4-6.
- Cullen, A., 2020, Woodford Shale mercury anomalies from the McAlister Cemetery Quarry, Oklahoma: A North American test of the volcanic-trigger hypothesis for Late Devonian mass extinctions: Oklahoma City Geological Society, Shale Shaker, v. 71-5, p. 188-203.
- Ekwunife, I. C., 2017, Assessing mudrock Characteristics, high-resolution chemostratigraphy, and sequence stratigraphy of the Woodford Shale in the McAlister Cemetery Quarry, Ardmore Basin, Oklahoma, University of Oklahoma MSc thesis, 168 p.
- Johnson, J.G., Klapper, G., and Sandberg, C.A., 1985, Geological Society of America Bulletin Devonian eustatic fluctuations in Euramerica: Geological Society Of America Bulletin
- Kirkland, D.W., R.E. Denison, D.M. Summers, and J.R. Gormly, 1992, Geology and organic geochemistry of the Woodford Shale in the Criner Hills and western Arbuckle Mountains, in: Johnson, K.S., and Cardott, B.J., 1992, eds., Source rocks in the southern Midcontinent symposium: Oklahoma Geological Survey, Circular 93, p. 38-69.
- Klockow, C.M., 2017, Structural survey of the Woodford Shale at McAlister Cemetery, Quarry Carter County, Oklahoma: unpublished M.S. thesis, University of Oklahoma, 45 p.
- Krystyniak, A.M., 2005, Outcrop-based gamma-ray characterization of the Woodford Shale of south-central Oklahoma, unpublished M.S. thesis, Oklahoma State University, 145 p.
- Lu, M., Ikejiri, T., and Lu, Y., 2012, A synthesis of the Devonian wildfire record: Implications for paleogeography, fossil flora, and paleoclimate, *Palaeogeography, Palaeoclimatology, Palaeoecology* 571, p.1-16.

Martin, D.P., 2017, Geological Characterization of Large Carbonate Masses in the Woodford Shale, Criner Hills, Oklahoma, M.S. thesis, Oklahoma State University, 100p.

Molinares Blanco, C.E., 2013, Stratigraphy and palynomorphs composition of the Woodford Shale in the Wyche Farm Shale Pit, Pontotoc County, Oklahoma: Norman, University of Oklahoma, unpublished M.S. thesis, 90 p.

Over, D. J., 1990, Conodont biostratigraphy of the Woodford Shale (Late Devonian- Early Carboniferous) in the Arbuckle Upper Mountains, South-Central Oklahoma, Texas Tech University PhD Dissertation, 186 p.

Over, D. J., 1992, Conodonts and the Devonian-Carboniferous Boundary in the Upper Woodford Shale, Arbuckle Mountains, South-Central Oklahoma, *Journal of paleontology*, Vol. 66, No. 2, p. 293-311.

Over, D.J., 2002. The Frasnian-Famennian Boundary in the Appalachian Basin, Michigan Basin, Illinois Basin, and southern continental margin, central and eastern United States. *Palaeogeogr. Palaeoclimatol. Palaeoecol.* 181, 153–170.

Parks, D. and Lu, X, 2012, Distributions of vanadyl and nickel porphyrins in the Woodford Shale and selective chelation of metal species by different tetrapyrrole configurations, *Organic Geochemistry* 186, p. 1-8.

Paxton, S.T., and B.J. Cardott, 2008, Oklahoma Gas Shales Field Trip, Oklahoma Geological Survey Open File Report 2-2008, 110 p.

Philp, R.P. and DeGarmo, C.D., 2020, Geochemical characterization of the Devonian-Mississippian Woodford Shale from the McAlister Cemetery Quarry, Criner Hills Uplift, Ardmore Basin, Oklahoma, *Marine and Petroleum Geology* 112, p.1-21.

Rakociński, M., Marynowski, L., Agnieszka, P., & others, 2020, Volcanic related methylmercury poisoning as a possible driver of the end-Devonian Mass Extinction, *Nature Reports* 10-7344, 8p.

van der Meer, d., Scotese, C.R., Mills, B, and others, 2022, Long-term Phanerozoic global mean sea level: Insights from strontium isotope variations and estimates of continental glaciation, *Gondwana Research* 11, p. 103–121.

Walker, W.M., 2006, Structural analysis Criner Hill, South-Central Oklahoma, MSc Thesis, Baylor University, 73p.

Zhang, J., Deng, C., Liu, W., and others 2021, Anomalies Link to Extensive Volcanism Across the Late Devonian Frasnian–Famennian Boundary in South China, *Frontiers Earth Science*, p.1-9.

4.2 Marietta Basin: Jetta Core Grayson County Texas

The Marietta basin is essentially a southeast plunging synclinorium on a regionally uplifted block bounded by the Criner Hills-Wichita fault(s) to the NE and the Muenster thrust to the SW (Figure 4.2.1a and b). The basin extends across the Oklahoma-Texas state line and is largely concealed by flat-lying Cretaceous-age marine sediments. In Love County Oklahoma, adjacent to the Texas State line, the 45° to 50° API gravity window is between 14,000ft and 16,500ft, much deeper than the in main part of the Woodford play to the north where that API window is between 12,000ft and 13,000ft (Cullen, 2018). We attribute deepening of the maturity window to a lower geothermal gradient possibly due to the observation that the much of Marietta basin appears to be floored by Grenville metasediments rather than igneous rocks (Figure 4.2.1).

The Woodford does not crop out in or around the Marietta basin. However, Jetta Operating Company (Ft. Worth TX) cored 127ft of Woodford in Grayson Co, TX; hereafter referred to as the Jetta core. Jetta Operating Company has completed several Woodford wells which, to our knowledge, is the southernmost Woodford production. Brito (2019) made extensive use of the core taken by Jetta Operating Company. We have included a brief discussion of the Jetta core as it represents key data to extend the regional picture further south into deeper paleo-water depths. Although the upper 50ft of Woodford was not cored, the well and core permit making several key observations.

1. The lithologies and vertical succession represent the same 5-6 basic lithofacies and mineralogy present up dip (Figure 4.2.2a, 2b), implying a continuum of controlling depositional process.
2. Chemostratigraphic data show an upward increasing Si/Al similar to the up dip outcrops (Figure 4.2.3
3. Core data show the Upper Woodford is chert-rich and has relatively abundant round phosphate nodules similar to up dip outcrops (Figure 4.2.3) that are distinctly black (4.3.4).
4. In the Upper Woodford decreasing %TOC correlates with lower gamma ray readings. The gamma ray readings continue to decrease (<100API) above the cored interval; presumably TOC decreases as well.

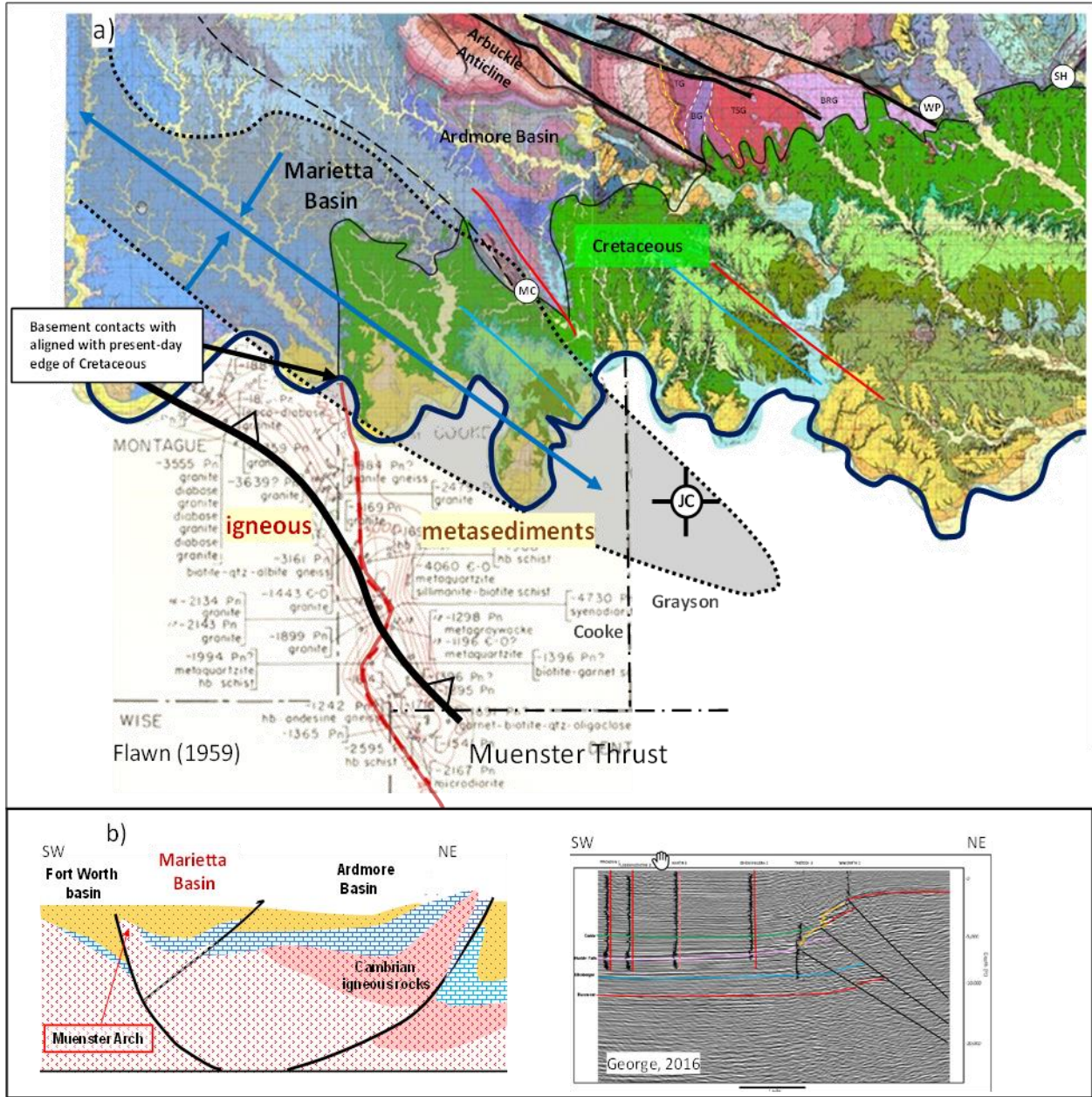


Figure 4.2.1 a) Location map for Jetta Core with key geological features of the Marietta basin. b) Regional cross section and seismic line across Muenster thrust (George, 2016).

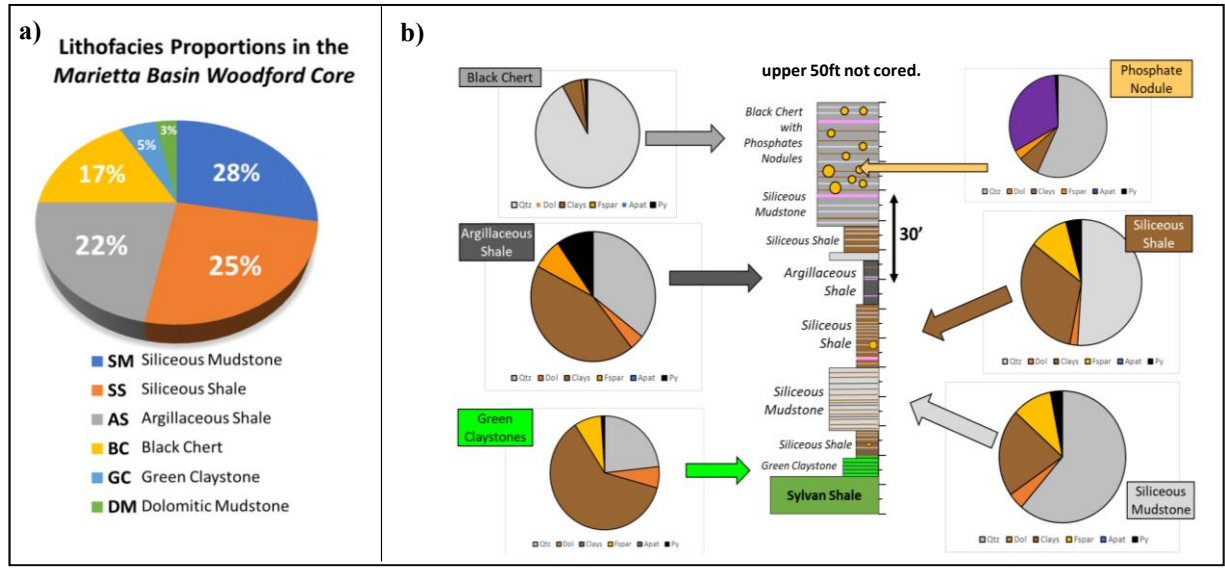


Figure 4.2.2 a) Plot of % of Jetta core lithofacies b) XRD mineralogy of lithofacies (Brito 2019)

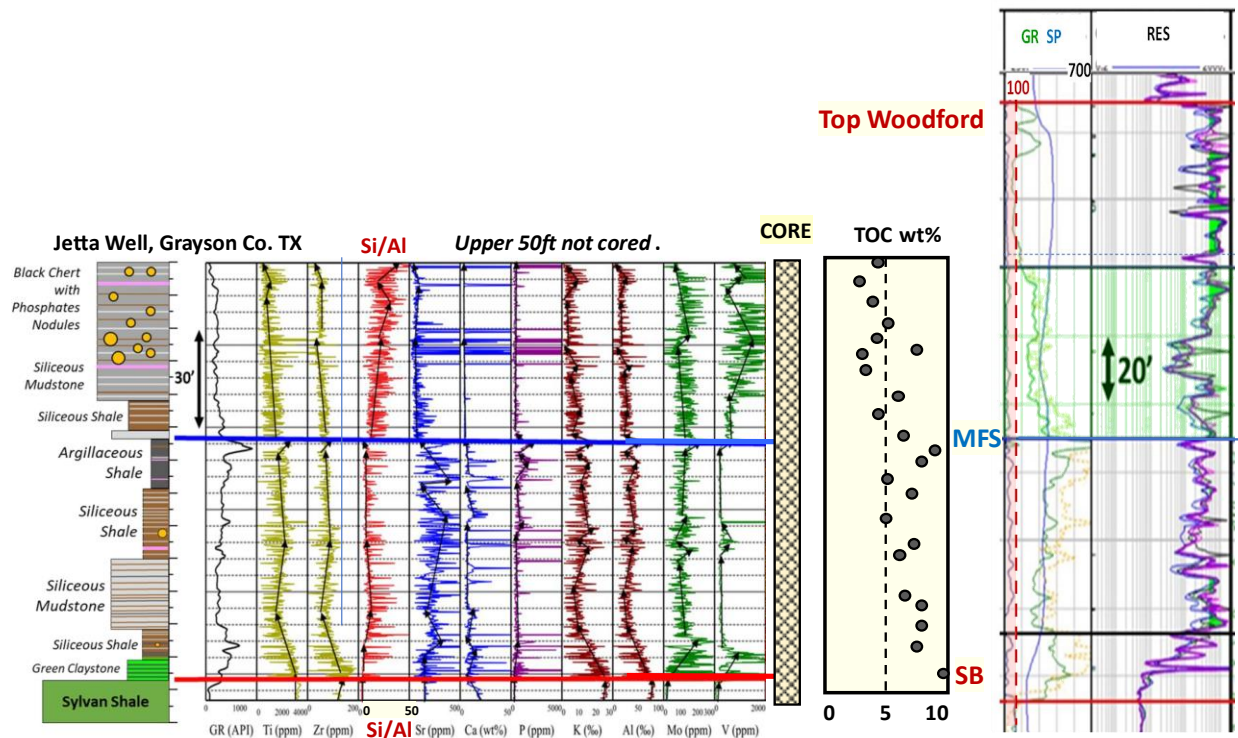


Figure 4.2.3 Jetta core lithofacies, elemental XRF data, TOC measurement and wireline log (Brito, 2019.)

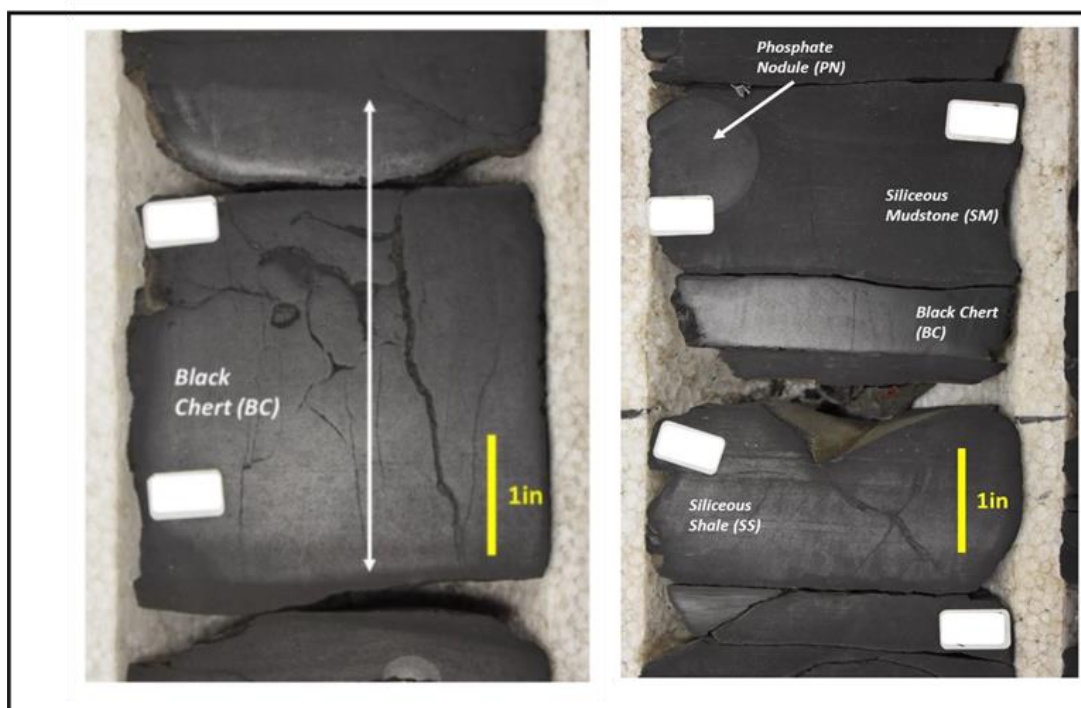


Figure 4.2.4 Photographs of dark phosphate nodules associated with black chert in the Upper Woodford (Brito, 2019).

Thus, the upper part of the Jetta core has similar features as the top of the Woodford section at the MCQ. Whether whitening is present in the uncored section is not known, but the data do support the notion of greater open marine circulation and more oxic conditions.

REFERENCES

Brito, R., 2019, The Woodford Shale in the Marietta Basin, University of Oklahoma PhD (unpublished), 208 p.

Cullen, A., 2018, My favorite outcrop (really): Blue River Gneiss at Hughes Crossing, Johnston County, OK: Oklahoma City Geological Society, Shale Shaker, v. 69-1, p. 36-46.

Flawn, P. T., 1956, Basement Rocks of Texas and Southeast New Mexico. University of Texas Publication 65, 276p.

George, 2016, The Muenster Uplift of North Texas: The eastern most expression of the Pennsylvanian Ancestral Rockies, University of Texas at Dallas, unpublished MSc thesis, 42p.

5.1 Wapanucka Shale Pit: The Wapanucka shale pit (SW/SW Sec. 26 T2S R8E) is about 20mi SE of the Wyche Quarry (figure 5.1.1a). The pit is cut by Rock Hill Road about two miles south of the intersection of OK48 and SH7 in the town of Wapanucka (Figure 5.1.1b, 1c). Although Rock Hill Road is relatively narrow dirt road, infrequent traffic makes it suitable for large groups. The shale pit is inactive and judging from the overgrowth it appears to have been dormant for quite a while (Figure 5.1.1d). Here only the Upper Woodford is exposed, including a substantial portion in the Carboniferous not present further West, the Lower and Middle Woodford are covered. The better exposures are on the north side of Rock Hill Road.

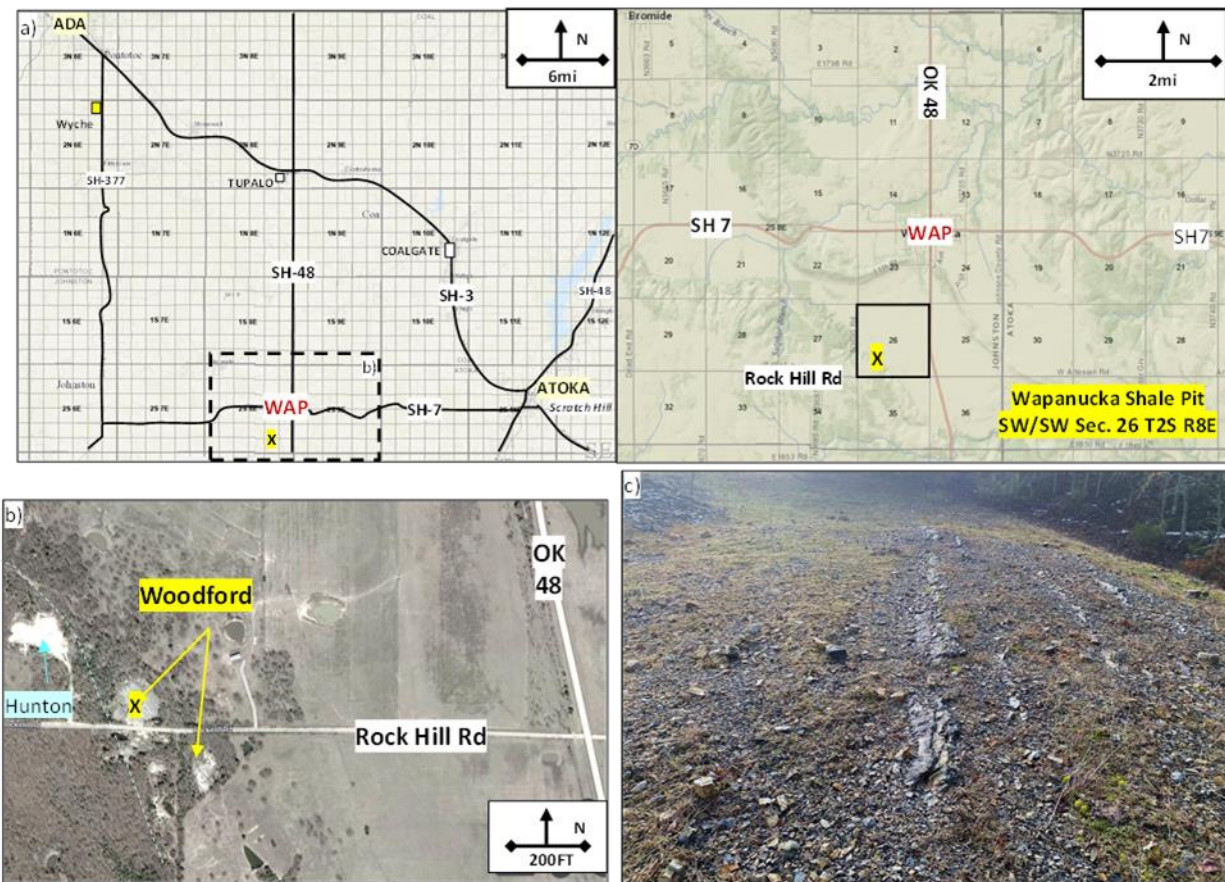


Figure 5.1.1 a) Regional and local location maps, WAP-Wapanucka, X marks shale pit. b) Google Earth image locating shale pit in relation to Rock Hill Road c) Photo of siliceous mudstones in Upper (Mississippian) Woodford, N26°W dipping 20°E. Photo is southeast looking, note partial grassy cover.

The Wapanucka shale pit has an interesting structural setting. The pit lies near the SW edge of the Arkoma Basin on the downthrown side of the Sulphur fault (Figure 5.1.2). The Sulphur fault, or more accurately the Sulphur fault zone, strikes WNW and can be traced at the surface more than

50mi. Near the shale pit there are two faults. The first juxtaposes the Blue River Gneiss (Figure 5.1.3a) against steeply dipping ($\sim 75^\circ$) Cambrian carbonates (Figure 5.1.3b). Along second, more northerly fault, steeply dipping Cambrian carbonates abut modestly dipping ($\sim 20^\circ$) Woodford Shale. The Peters-1 well less than a half mile SW of the shale pit, spudded on the Mesoproterozoic Blue River Gneiss, drilled 775ft of basement before crossing the fault into Paleozoic carbonates. Data from the Peters-1 well show it is a reverse fault dipping 45° S (Figure 5.1.2 inset to right). Two major unconformities can be examined in this area: U-1) The Cambrian age Timbered Hills Group rests nonconformably on Blue River Gneiss, no rhyolites are present at the base of the Timbered Hills Group, and U-2) The relatively flat-lying Cretaceous-age Antlers Sandstone rests on both the Blue River Gneiss and the Antlers Sandstone.

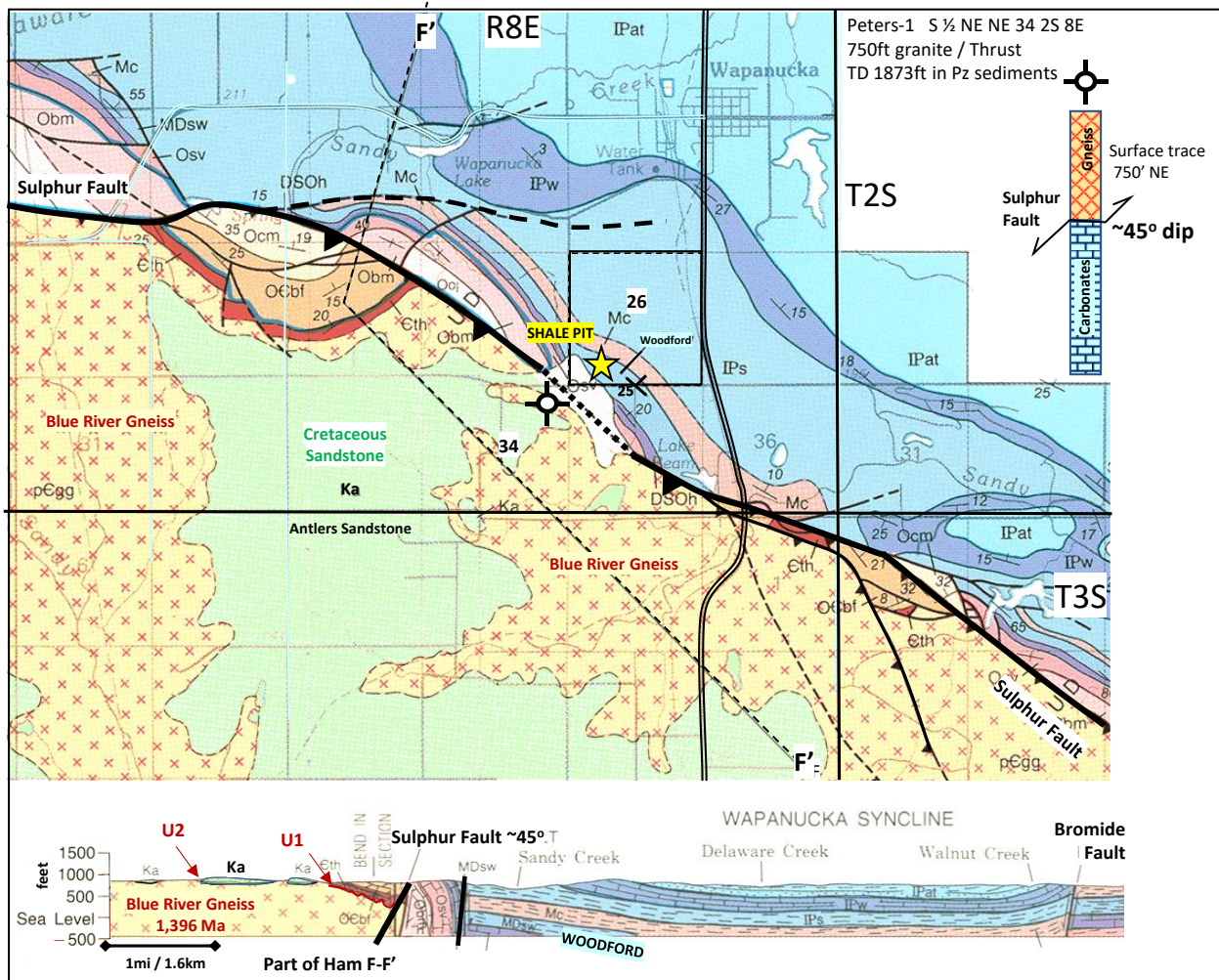


Figure 5.1.2 Geological map and cross section of Wapanucka area (Ham, 1956). Data from Peters-1 well is from Ham et al., 1964).



Figure 5.1.3 a) Photos of Mesoproterozoic Blue River Gneiss, b) Photo of steeply north-dipping Lower Arbuckle Group carbonates.

Over the prior several decades several studies of the Woodford have included the Wapanucka shale pit location. Siy (1988) published a stratigraphic section of the shale pit that placed the Devonian-Carboniferous boundary (DCB) about 8m above the base of the section in a greenish-gray shale at the top of an interval rich in phosphate nodules. On the basis of conodont biostratigraphy, Over (1990 and 1992) confirmed the DCB in the Wapanucka shale pit is about 23ft/7m from the base of his measured section at the occurrence of *Siphondella suculata* (Figure 5.1.4a and Table 5.1.1) It is interesting that Siy's study pre-dates the biostratigraphic work Over (1990, 1992) and that the Wapanucka site was not included in Hass and Huddle (1965). We speculate that Siy positioned that boundary based on regional correlation with the nodule-rich siliceous Upper Woodford section dated on the Lawrence Uplift, the Arbuckle Mountains, and the Criner Hills (Hass and Huddle, 1965). Unlike those locations, however, the Wapanucka shale pit has a relatively thick section (~90ft) Early Mississippian, Kinderhookian-age, Upper Woodford.

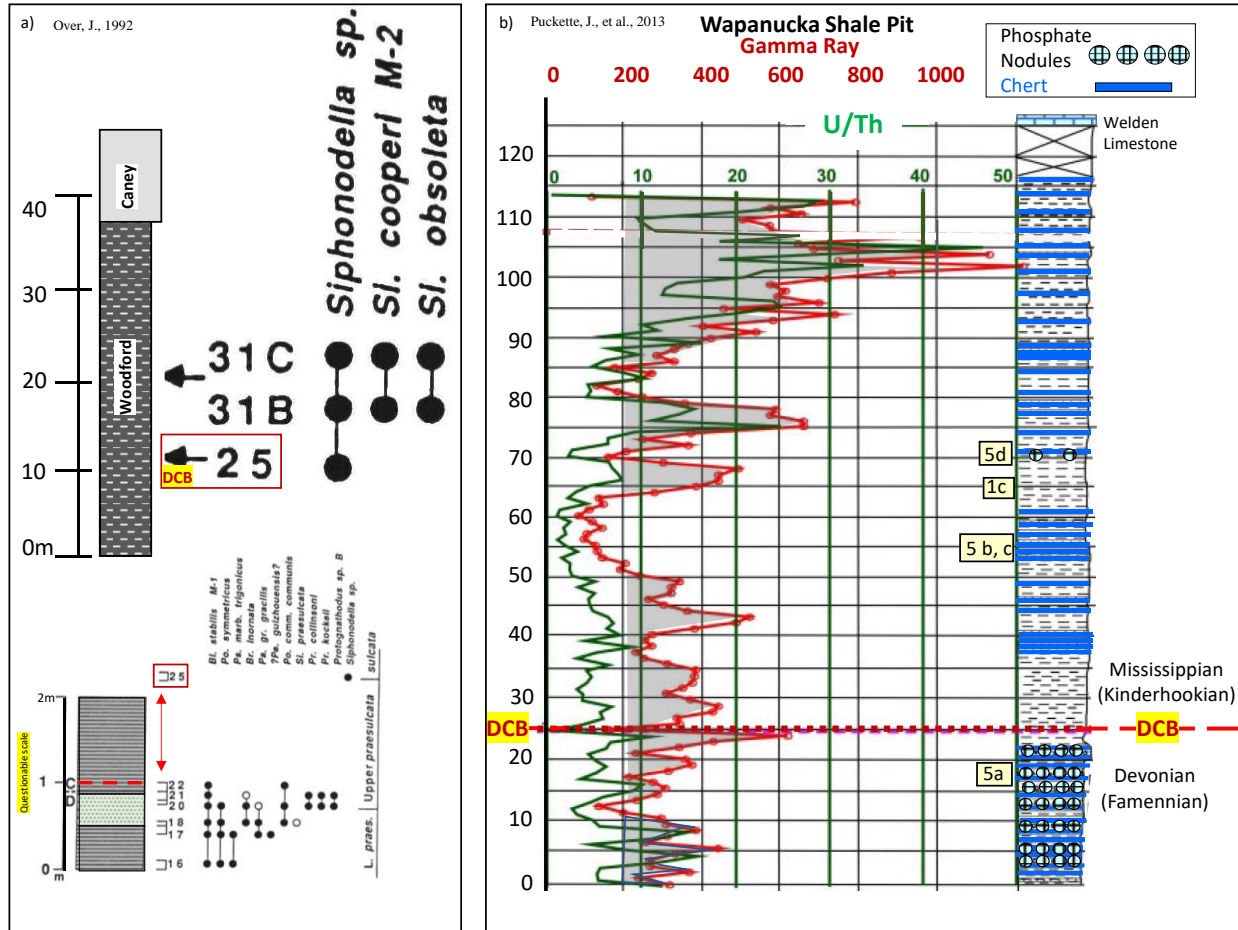


Figure 5.1.4 a) Lithologic column and conodont interval from Wapanucka shale pit (Over, 1992), b) Measured section and spectral gamma ray log (Puckette et al., 2013). Inset yellow boxes

Puckette et al., (2013) provided a detailed measured section tied to an outcrop spectral gamma ray log (Figure 5.1.4b). Below the DCB, the lower 25ft of section consists of chert interbedded with siliceous mudrocks that bear abundant phosphate nodules (figure 5.1.5a). The nodules tend to be spherical to elliptical and some are concentrically banded (Figure 5.5a inset). The overlying Mississippian section has only a single, thin, phosphate nodule-bearing bed (Figure 5.1.5d). The Wapanucka shale pit was one of several sites Ellis (2013) used to conduct cyclostratigraphic study of the DCB, but those data did not yield sufficiently robust result to refine correlations and ages on a regional scale.

Although the overlying section has fewer chert beds, there are several thick intervals of well-developed brittle ductile couplets (well exposed in the pit face; Figures 5.1.5b, 5c) that could be suitable for horizontal well landing zones. Unfortunately, it is not clear based on the U/Th that

these beds contain sufficient TOC and a similar pore system to other Woodford wells given the low U/Th ratio from the gamma ray as U is generally the TOC proxy (Figure 5.1.4). We also note that single sample from the Wapanucka shale pit had 13.7% TOC (Siy, 1988) and a visual Ro of 0.56% (Cardott and Comer, 2021).

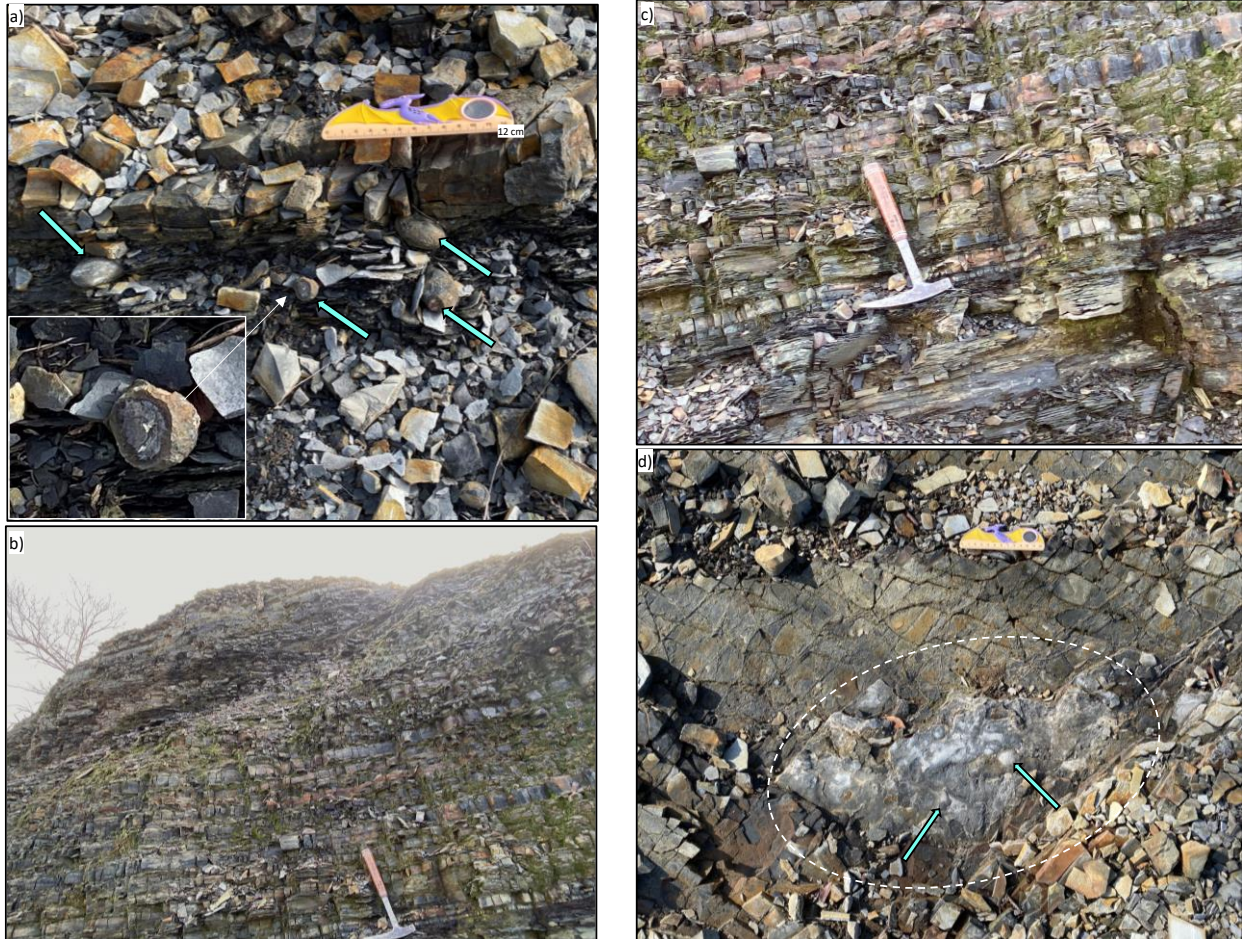


Figure 5.1.5 a) Photograph of lower section of siliceous shales with abundant phosphate nodules interbedded with chert, b and c) Photos an interval of brittle-ductile couplets in the upper (Kinderhookian) section exposed in the pit face, d) Thin nodule-bearing bed in upper section. The nodules are relatively small. Note the secondary calcite of the bedding plane surface.

Puckette et al., (2103) correlated the Mississippian interval at the Wapanucka shale pit to a nearby industry well (Figure 5.1.6). This thick Mississippian interval has an overall lower gamma ray and lies above the traditional Upper Woodford of the Arbuckle Mountains and Ardmore basin. The very high gamma ray associated with the Woodford maximum flooding surface and the top Hunton can be projected into the Wyche-1, albeit with some uncertainty. The lower gamma ray of Mississippian interval at the shale pit resembles the interval in the Wyche-1 core that Turner et al.,

REFERENCES

- Ellis, R., 2013, Analysis of the cyclostratigraphy at the Devonian-Carboniferous boundary in south-central Oklahoma, Louisiana State University, unpublished M.S. 52p.
- Ham, W., McKinley, M., and others, 1964, Geologic Map and Sections, Arbuckle Mountains, Oklahoma, (revised by Johnson, 1990), Oklahoma Geological Survey, Circular 90.
- Ham, W. E., Denison, R. E., and Merritt, C. A., 1964, Basement rocks and structural evolution of southwestern Oklahoma: Oklahoma Geological Survey Bulletin 95, 302 p.
- Over, D. J., 1990, Conodont biostratigraphy of the Woodford Shale (Late Devonian- Early Carboniferous) in the Arbuckle Upper Mountains, South-Central Oklahoma, Texas Tech University PhD Dissertation, 186 p.
- Over, D. J., 1992, Conodonts and the Devonian-Carboniferous Boundary in the Upper Woodford Shale, Arbuckle Mountains, South-Central Oklahoma, *Journal of paleontology*, Vol. 66, No. 2, p. 293-311.
- Puckette, J., D.R. Boardman, and W.L. Watney, 2013, Woodford Shale: Correlating rock properties in outcrop and core with wireline log characteristics: AAPG Search and Discovery Article #50885, 46 p.
- Siy, S.E., 1988, Geochemical and petrographic study of phosphate nodules of the Woodford Shale (Upper Devonian-Lower Mississippian) of southern Oklahoma: Texas Tech University, unpublished M.S. thesis, 172 p.
- Turner, B., C. Molinares-Blanco, and R. Slatt, 2015, Chemostratigraphic, palynostratigraphic, and sequence stratigraphic analysis of the Woodford Shale, Wyche Farm Quarry, Pontotoc County, Oklahoma: *Interpretation*, v. 3, p.1–9.

5.2 Scratch Hill: Ouachita Thrust Belt

Scratch Hill, just outside Atoka, OK about 18mi east of the Wapanucka Woodford section, lies at the south end of Black Knob Ridge where the Choctaw fault becomes covered by the present-day erosional edge of the Cretaceous onlap sequence (Figure 5.2.1a and b). This location is a quarry with good access and parking. The Arkansas Novaculite and older units of the deepwater “Ouachita Facies” have been brought to the present surface by the Choctaw thrust, the leading edge of the Ouachita-Marathon fold/thrust belt (Figure 5.2.1c). The outcrops along Black Knob Ridge have thrust a minimum of 92mi/150km from their original depositional position relative to the “Arbuckle Facies” (Arbenz, 2008), as shown by the Sohio 1-22 in McCurtain County which drilled through upper plate Ouachita facies rocks into subthrust “Arbuckle facies” rocks. This shortening must be accounted for when considering paleoceanography models for Devonian-Mississippian upwelling and oceanic stratification models. The equivalent formation in Texas is the Caballos Novaculite in the Marathon thrust belt.

Scratch Hill is just east of Atoka, OK, and is cut by Court Road (figure 5.2.2a, b). There are small quarries in both the Big Fork and Arkansas Novaculite (Figure 5.2.2c). Well and seismic data in the area demonstrate that the “Ouachita facies” rocks have been thrust over the block faulted Arbuckle-Woodford section which represent footwall targets for petroleum exploration (Figure 5.2.3). From a petroleum geology perspective, it should be noted that these cherts produce as fracture reservoirs in crests of toe thrust anticlines the Isom Springs and several fields in west Texas (Godo et al., 2011).

Regional mapping along Black Knob Ridge shown in the OGS state quadrangle geological map (Chang and Stanley, 2003) reports that the Arkansas Novaculite is composed of 4 units: 1) The lowest member composed of thin bedded, light gray to apple-green novaculite, interbedded with hard green shale makes up about half of the formation, 2) light gray to black novaculite with thin beds and partings of black shale, 3) Red and green, micaceous shale intercalated with thin beds of novaculite and black, blocky shale, 4) the upper member consists of thin to medium green, brown, and gray novaculite.

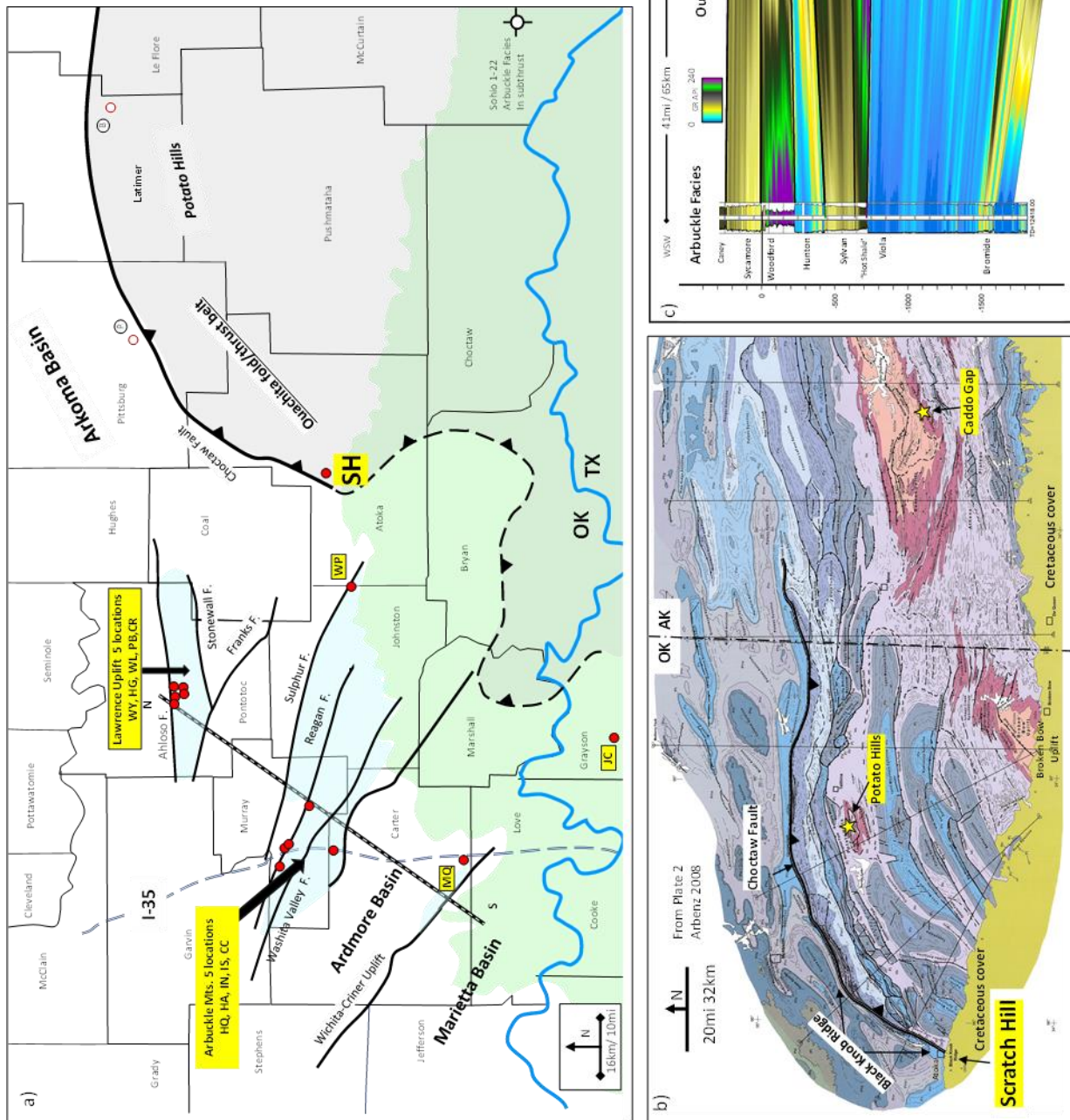


Figure 5.2.1 a, b) Location map with key geological features for Scratch Hill and the Ouachita fold and thrust belt. c) Interpolated gamma ray stratigraphic section show correlation between the Arbuckle and Ouachita facies rocks.

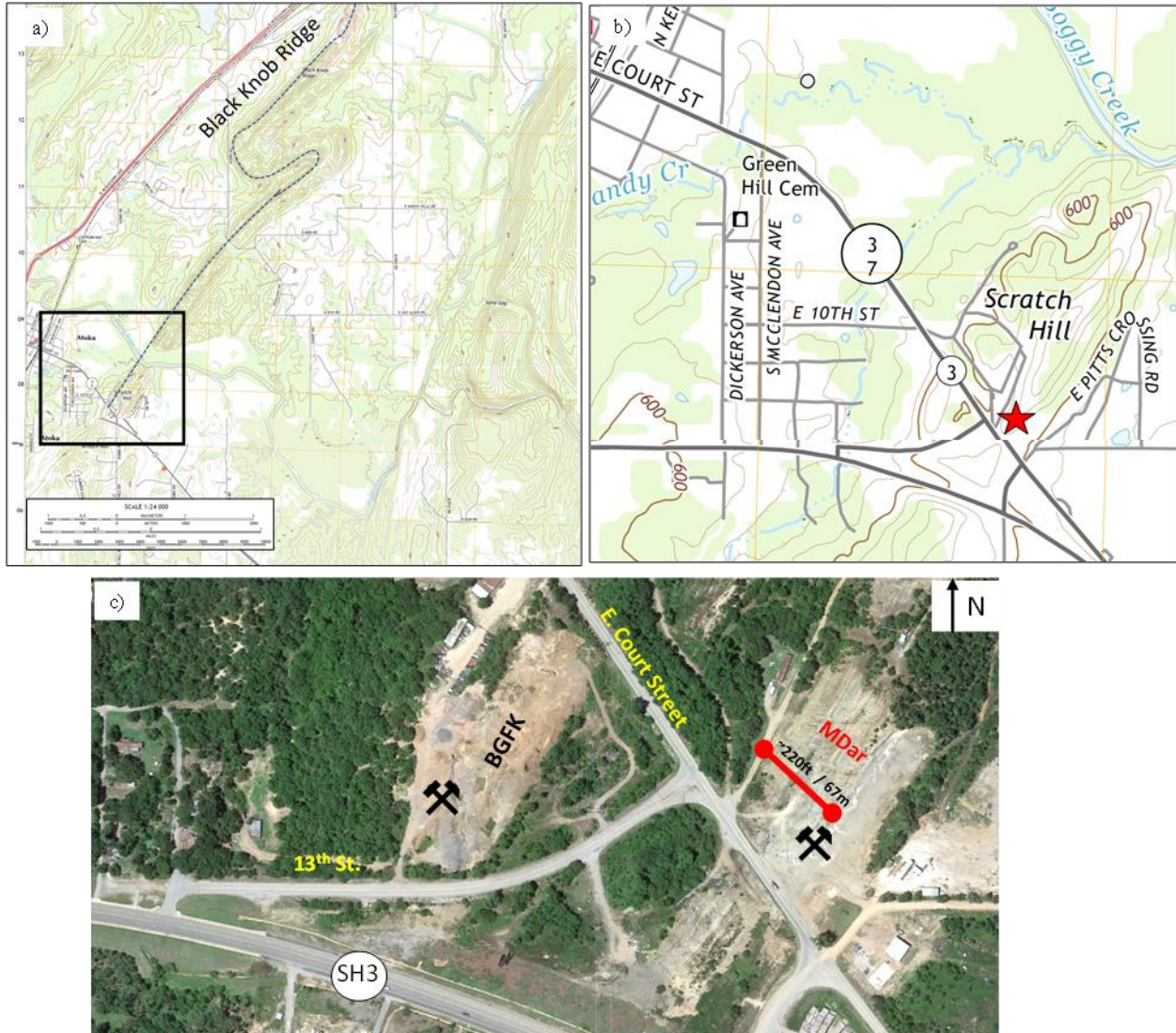


Figure 5.2.2 a, b) Black Knob Ridge and Scratch Hill location maps c) Google Earth image of Scratch Hill.

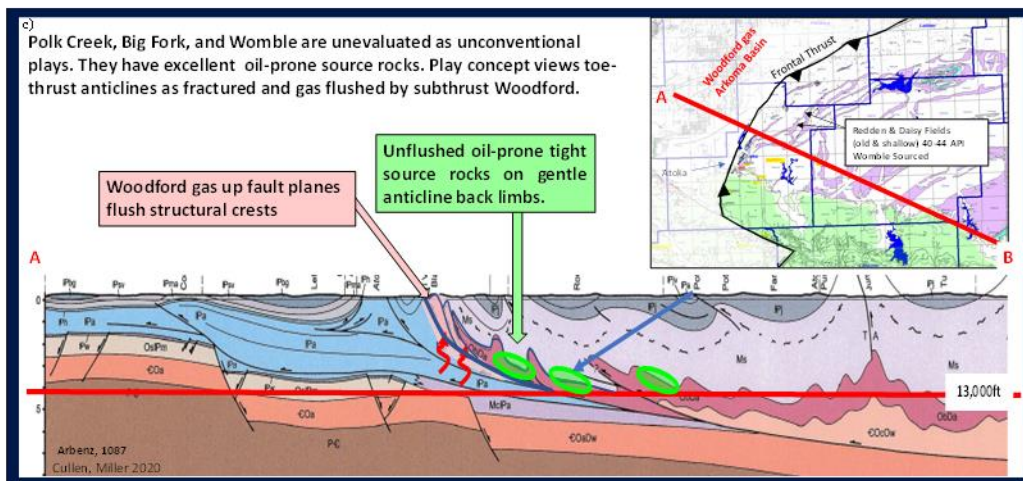
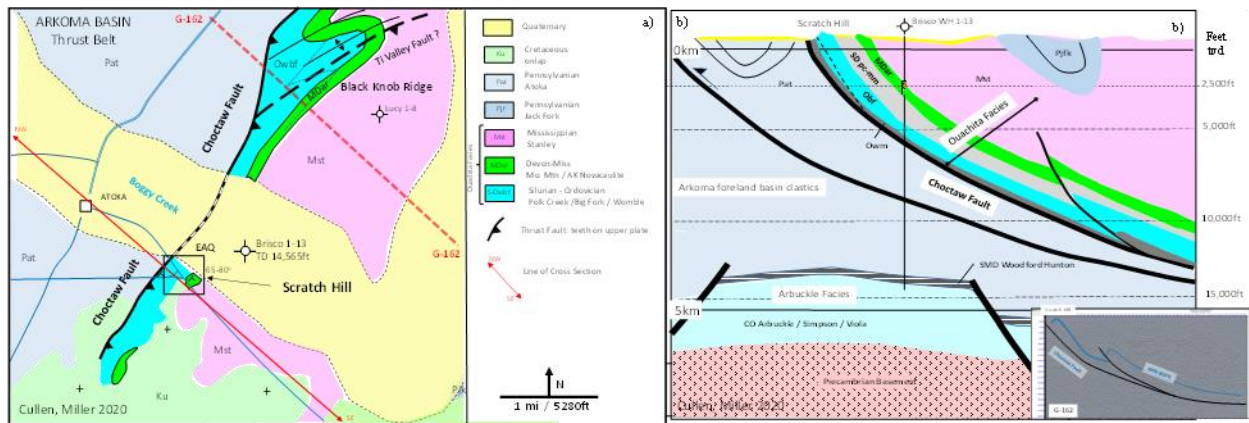


Figure 5.2.3 a, b) Local geological map and cross section for Scratch Hill c) Regional cross section illustrating upper plate unconventional play concepts.

Measured sections at Scratch Hill (Figure 5.2.4) indicate only the lower three units from Chang and Stanley appear to be present (Barrick and Haywa-Branch, 1994; Cullen and Miller, 2020). The description found in Cullen and Miller, 2020 for these units and sub-units are as follows: Unit 1a (0-59ft) is primarily couplets of thin to medium bedded grey chert with about 15% laminated mudrock (Figure 5.2.5a,b) Figure 7b). Unit 1b (59-122ft) is thin to medium bedded light grey chert with about 30% mudrock including distinctly green mudrocks (Figure 5.2.5c). Unit 2 (122-210ft) is primarily couplets of thin to medium bedded grey chert with about 15% laminated mudrock similar to the Lower Arkansas Novaculite. Near the top to Unit-2 there are two intervals with notable beds of black chert and siliceous mudrock Figure 5.2.5d). Unit 3 is dominated by red and green siliceous mudstone and rare thin chert beds (5.2.6). The more argillaceous nature of unit 3 can be seen on XRD data (Figure 5.2.7a). Source rock / Rock Eval data Figure 5.2.7b, c) show

there are thin intervals of good source rock and that the section is in the early oil window (%Ro calculated 0.53-0.65).

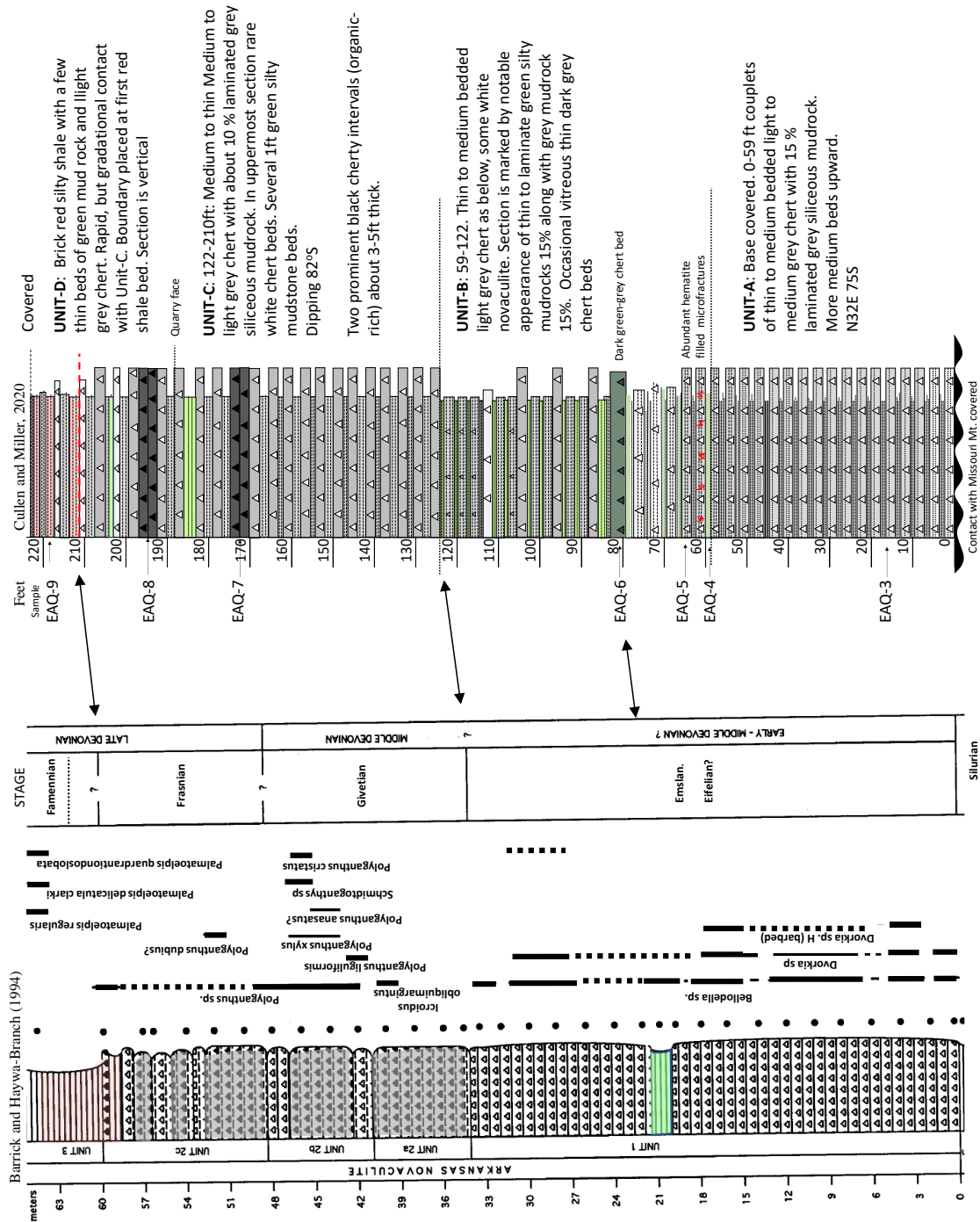


Figure 5.2.4 Correlation of sections measured by Barrick and Haywa (1994) and Cullen and Miller (2020)

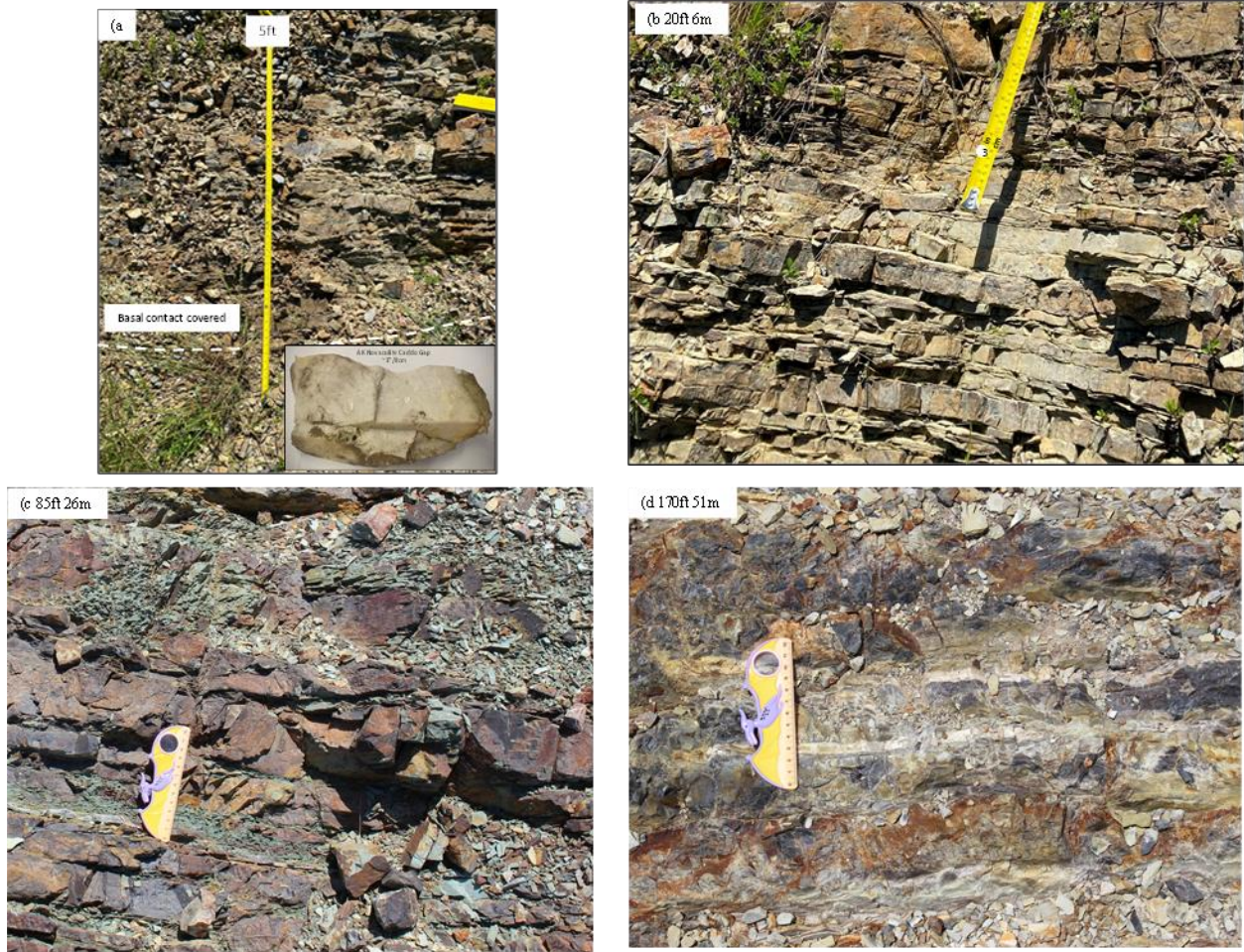


Figure 5.2.5a, b, c, d) Photographic of basic lithofacies at specific footages on measured section of Cullen and Miller (2020).

Barrick and Haywa-Branch (1994) provide important conodont biostratigraphic data that show the Scratch Hill section ranges from Early to Late Devonian in age and that the Frasnian-Famennian boundary below the base of the red and green siliceous shales of Unit 3. Thus, the upper section at Scratch Hill corresponds to the Lower Woodford in the Arbuckle Mountains Figure 5.2.8.



Figure 5.2.6. Photo of Unit-3 red and green mudstones

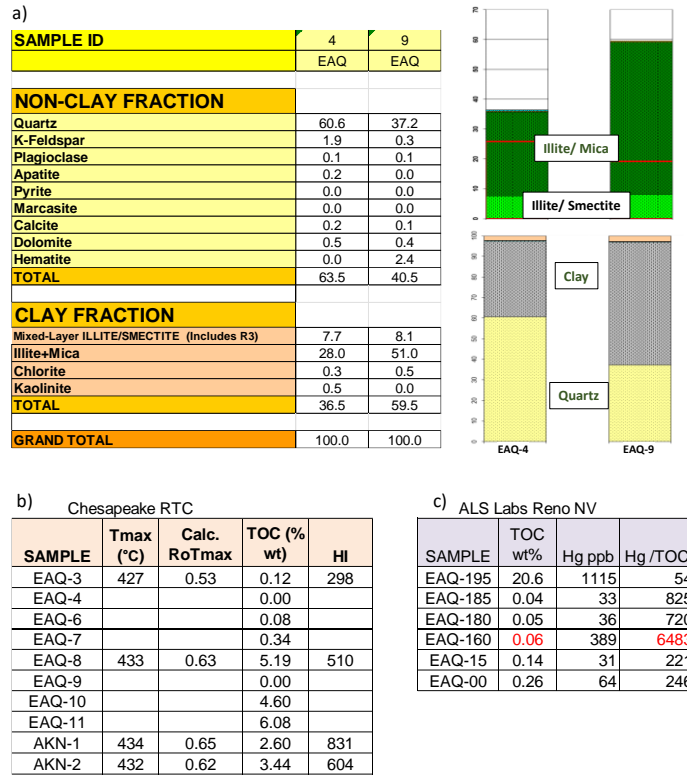


Figure 5.2.7 a) XRD from 2 Scratch Hill samples b) Rock-Eval data c) Mercury-TOC data

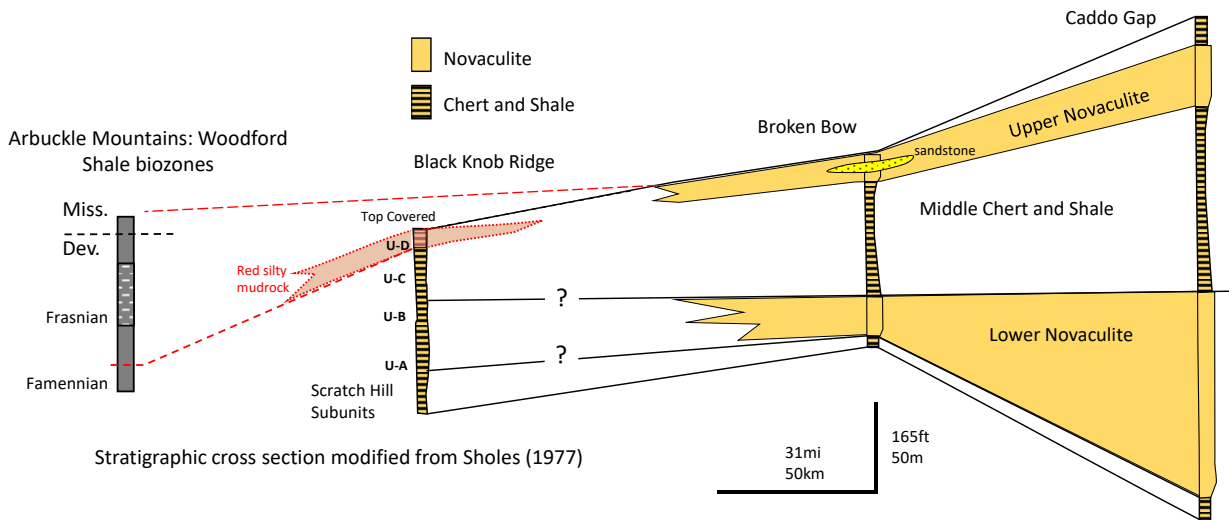


Figure 5.2.8 Regional correlation diagram for Arkansas Novaculite and Woodford Shale.

There are several features of the Scratch Hill section worth highlighting. First, there very little true novaculite (see inset 5.2.5a) but rather chert in the section. Second, as at other novaculite section such as Caddo Gap, AK, bed coloration the Scratch section appears to record more oxic bottom water conditions than in the Woodford. The fact that the AKN section records predominately oxic deposition, as opposed to the anoxic to dysoxic conditions in the Woodford, poses the question as to the nature of the Late Devonian to Early Mississippian oceans in the Midcontinent region.

Three, the exception to this is two organic-rich black shale and chert intervals in the upper part of Unit 2, Late Frasnian(?). These intervals are in the correct stratigraphic position of correlate to the Kellwasser intervals in Europe and Morocco; events that may record volcanogenic mercury poisoning (Racki et al., 2018). Although high Hg concentrations occur at Scratch Hill the TOC-normalized data are ambiguous in this regard. However, we regard the section as under sampled.

Fourth, there are several discrete thin beds rich in nodules, that may represent silicified phosphate nodules (Figure 5.2.9). These beds occur only in the black shale-chert interval, which may have implications about the redox conditions necessary for nodule nucleation and growth.

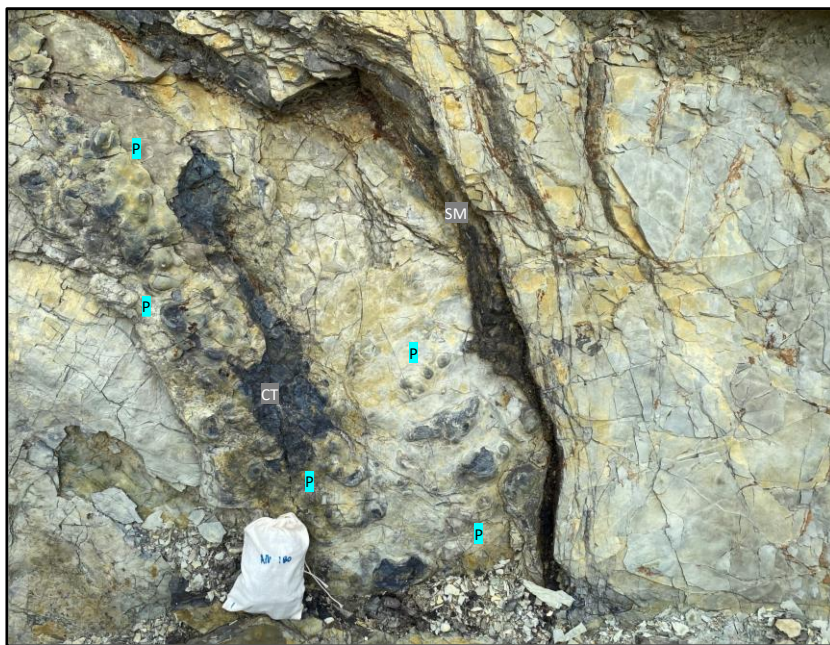


Figure 5.2.9 Probable silicified phosphate nodule in black siliceous mud rock.

Clearly Scratch Hill is an important section deserving further work including but not limited to detailed gamma ray logging supplemented with hand-held XRF, thin section petrography, and better geochemical characterization. Understanding this section may be key to understanding the depositional conditions and model of the Woodford Shale.

REFERENCES

- Arbenz, J.K., 2008, Structural framework of the Ouachita Mountains, in N.H. Suneson, ed., Stratigraphic and structural evolution of the Ouachita Mountains and Arkoma Basin, southeastern Oklahoma and west-central Arkansas: application to petroleum exploration: Oklahoma Geological Survey, Circular 112A, p. 1-40.
- Barrick, J.E., and J.N. Haywa-Branch, 1994, Conodont biostratigraphy of the Missouri Mountain Shale (Silurian-Early Devonian?) and the Arkansas Novaculite (Devonian), Black Knob Ridge, Atoka County, Oklahoma, in N.H. Suneson and L.A. Hemish, eds., Geology and resources of the eastern Ouachita Mountains frontal belt and southeastern Arkoma Basin, Oklahoma: Oklahoma Geological Survey, Guidebook 29, p. 161-177.
- Chang, J., and Stanley, T. 2013, Oklahoma Geologic Quadrangle OGQ-88 Geologic Map of the Tishomingo-Sherman 30 X 60 Quadrangle
- Cullen, A.B., and Miller, G., Scratch Hill, Atoka, Oklahoma: Proposed Type Section for the lower (Early to Middle Devonian) Arkansas Novaculite in Oklahoma, : Oklahoma City Geological Society, Shale Shaker, v. 71-4, p. 160-171.
- Good, T., Li. P., and Ratchford, M., 2011, Exploration for the Arkansas Novaculite Reservoir, in the Southern Ouachita Mountains, Arkansas, AAPG Search and Discovery, #10337, 25p.
- Miser, H.D., and A.H. Purdue, 1929, Geology of the DeQueen and Caddo Gap quadrangles, Arkansas: U.S. Geological Survey Bulletin 808, 195p.
- Purdue, A.H., 1909, Slates of Arkansas: Arkansas Geological Survey Report, 95p.
- Lowe, D.R., 1977, The Arkansas Novaculite: Some aspects of its physical sedimentation. in C.G. Stone, B.R. Haley, D.F. Holbrook, N.F. Williams, W.V. Bush, and J.D. McFarland III, eds., Symposium on the geology of the Ouachita Mountains, v. 1: Arkansas Geological Commission, Miscellaneous Publication MP-13, p. 132-138.
- Racki, G., Rakocinski, M., Marynowski, L., Wignall, P.B., 2018, Mercury enrichments and the Frasnian-Famennian biotic crisis: a volcanic trigger proved? *Geology* 46, 543–546.
- Sholes, M.A., 1977, Arkansas Novaculite stratigraphy, in C.G. Stone, B.R. Haley, D.F. Holbrook, N.F. Williams, W.V. Bush, and J.D. McFarland III, eds., Symposium on the geology of the Ouachita Mountains, v. 1: Arkansas Geological Commission, Miscellaneous Publication MP-13, p. 139-145.

5.3 Additional Woodford sections in Arkoma Basin: There are at several sections of Woodford in the Arkoma basin in this guidebook (Figure 5.3.1).

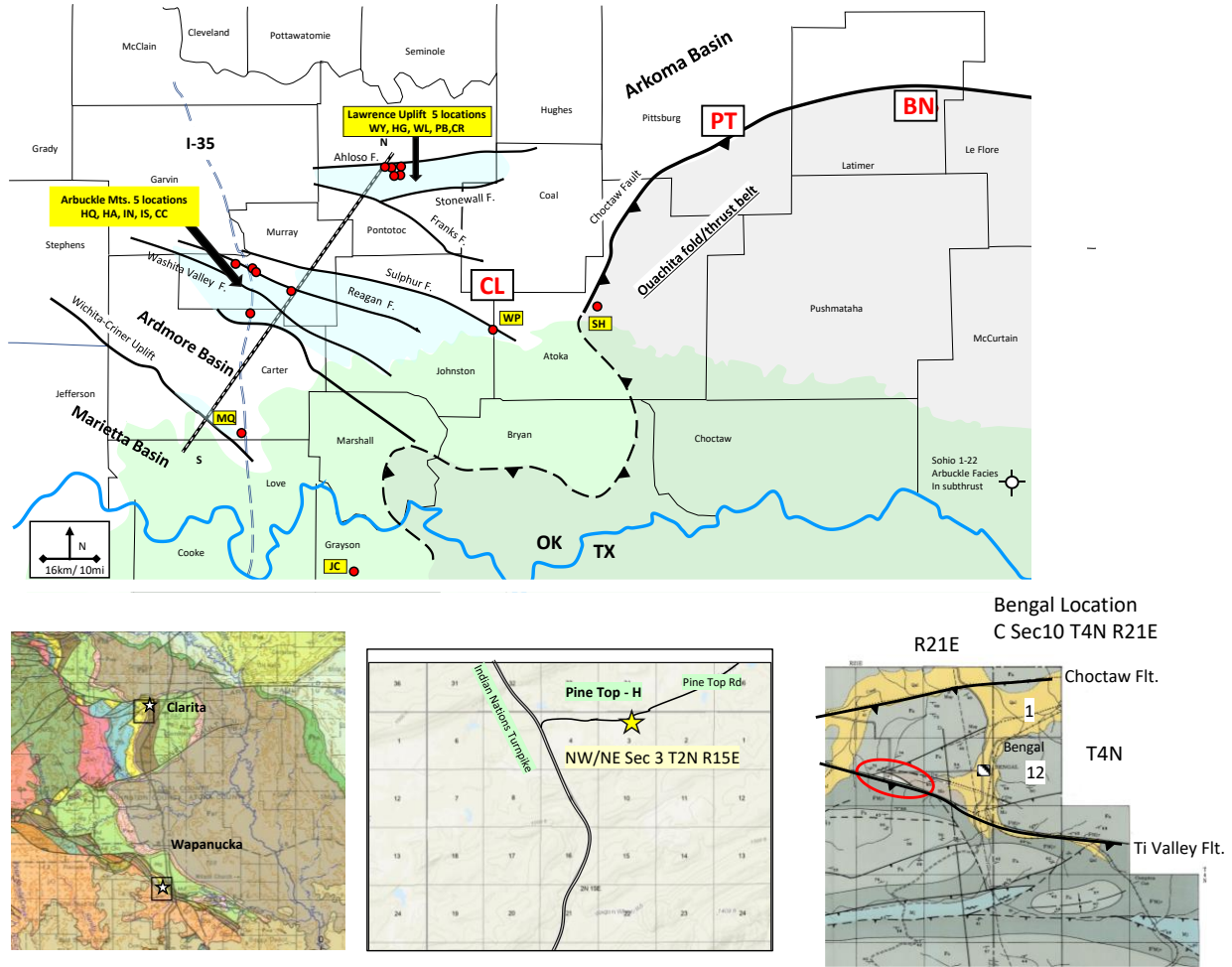


Figure 5.3.1 3 Woodford sections in the Arkoma basin not covered in this guidebook, a) Clarita shale pits (see Section 6.5), b) Pine Top (Hass-H from Hass and Huddle, 1965), c) Bengal section (Hass and Huddle, 1965).

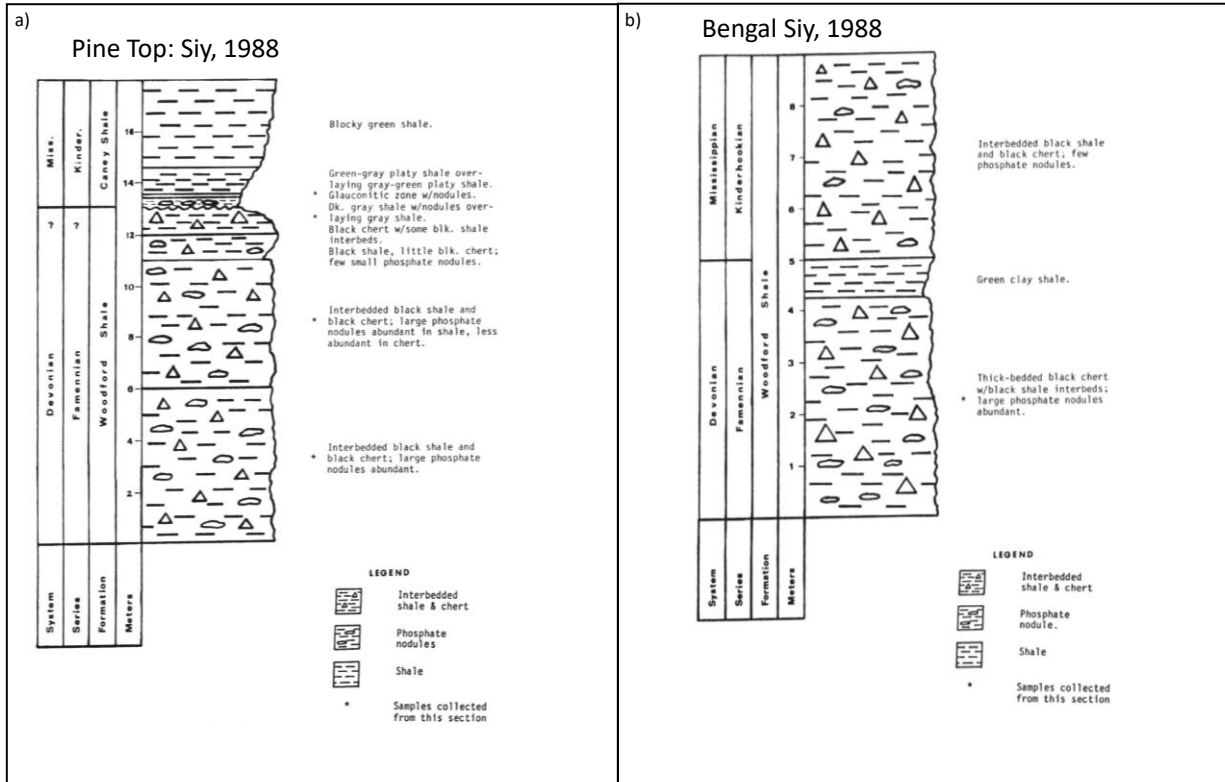


Figure 5.3.2 a) Pine Top measured section, b) Bengal measured section (Siy, 1988).

References

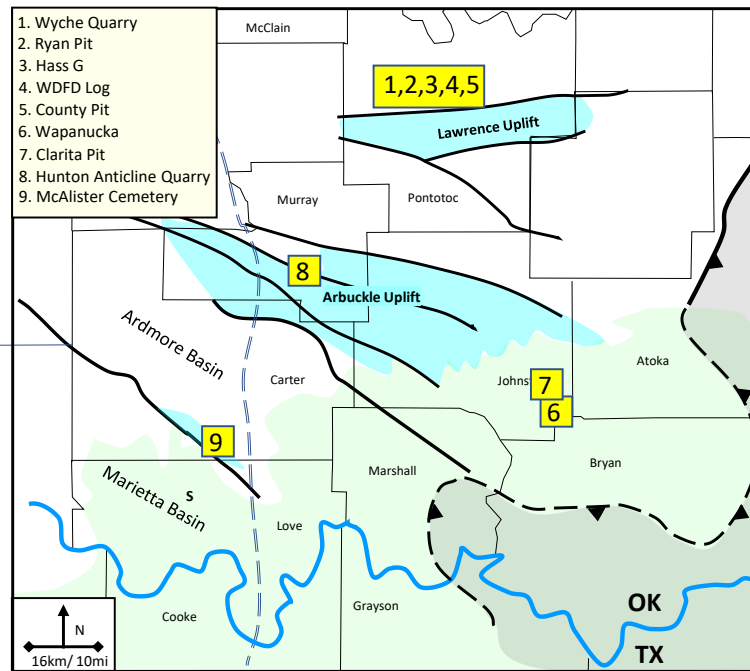
Ataman, O., 2008, Natural fracture systems in the Woodford Shale, Arbuckle Mountains, Oklahoma: Stillwater, Oklahoma State University, unpublished M.S. thesis, 139 p.

Hass, W.H., and J.W. Huddle, 1965, Late Devonian and early Mississippian age of the Woodford Shale in Oklahoma as determined from conodonts, in Geological Survey Research 1965: U.S. Geological Survey Professional Paper 525-D, p. 125-132.

Siy, S.E., 1988, Geochemical and petrographic study of phosphate nodules of the Woodford Shale (Upper Devonian-Lower Mississippian) of southern Oklahoma: Texas Tech University, unpublished M.S. thesis, 172 p.

6.1 Regional Fracturing: Lithologically the Woodford ranges from siliceous argillaceous mudrock to chert. Its overall high silica content is ultimately due to the abundance of radiolarian tests. Although there are ductile thin bedded units, especially in the Middle Woodford, overall the formation is mechanically a brittle and yields by fracturing as opposed to pressure solution and/or calcite twinning which can occur in carbonates.

Fracture geometry can reflect the regional stress field as well as local conditions related to folding and faulting. Regional fracture studies are best conducted where bed tops are best conducted where bed tops are widely and well exposed to permit making sufficient and proper measurement to characterize the outcrop as a whole. Over the study area there are at least 9 Woodford outcrops suitable for regional analysis (Figure 6.5.1).



Several of these outcrops in the Arbuckle Mountains have been studied by Ataman (2008) and Ghosh (2019). We have also included our less rigorous observations at several locations on the Lawrence uplift. These data show that there are two dominant regional fracture orientations, N30E and E-W. The sixty degree angle between these trends strongly suggests these fractures represent conjugate shear fractures (assuming Mohr-Coulombic criteria). This indicates a mean maximum horizontal stress orientation of N60E. This direction is oblique to regional macro structural trends but is consistent with an overall compressive to transpressive tectonic regime (Perry, 1989).

Considering that most Woodford horizontal wells are drilled north-south, hydraulic fracturing on those wells would appear to be more likely to potentially re-open the E-W fractures, degrading stimulated rock volume. We suggest that understanding subsurface fracture density is a key component to planning completions.

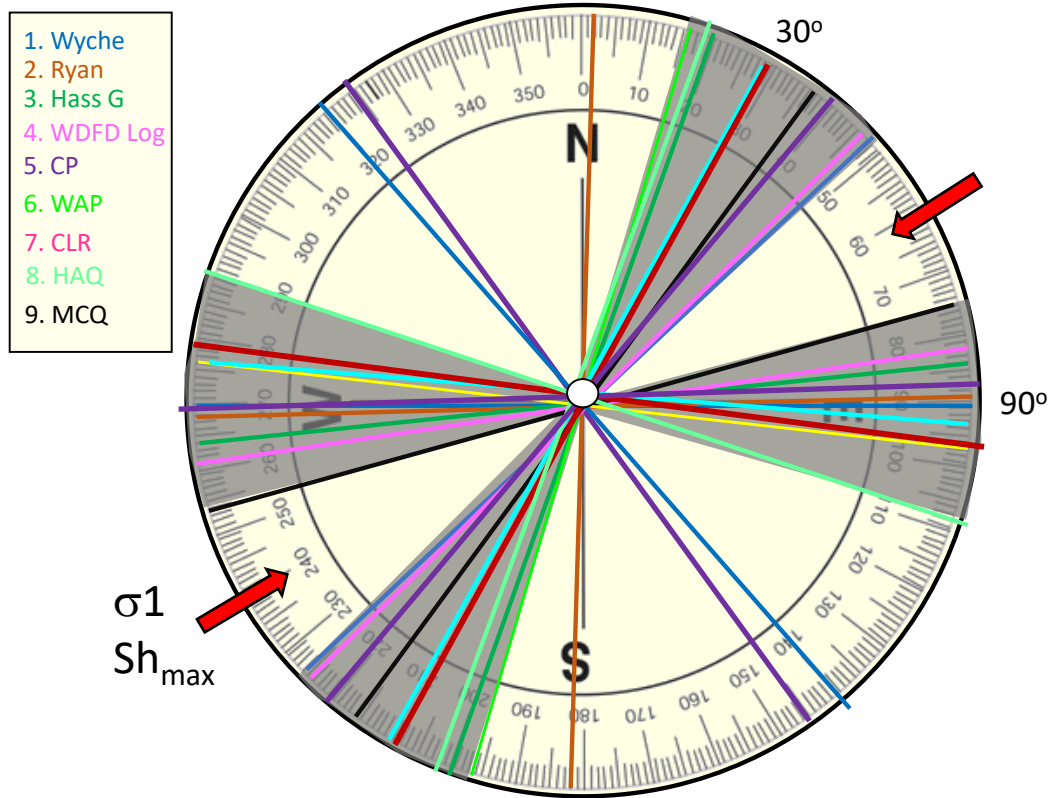


Figure 6.5.2 Mean strike directions of major Woodford fracture sets at nine locations in southern Oklahoma.

References

Ataman, O., 2008, Natural fracture systems in the Woodford Shale, Arbuckle Mountains, Oklahoma: Stillwater, Oklahoma State University, unpublished M.S. thesis, 139 p.

Ghosh, S.G., 2017, Integrated studies on Woodford Shale natural fracture attributes, origin, and their relation to hydraulic fracturing: Norman, University of Oklahoma, unpublished PhD dissertation, 264 p.

Perry, W. J. 1989. Tectonic Evolution of the Anadarko Basin Region, Oklahoma. US Geological Survey Bulletin 1866-A, A1–19.

6.2 Rare earth elements enrichment in Woodford phosphate nodules

The persistent occurrence of abundant phosphate nodules in the Upper Woodford Shale at or near the Devonian-Carboniferous boundary is one of the striking features presented in this atlas (Figure 6.2.1a). Apatite, the dominant constituent of the nodules, accepts tri-valent REE ions into the mineral lattice and thus can concentrate REEs. Thus, phosphate nodules in the Upper Woodford represent a potential source for REEs that are critical for the manufacturing of generators, electrical vehicles, and photo-voltaic cells.

Outcrop and core data presented in this atlas show that phosphate nodules in the Upper Woodford extend over an area of at least 4,000mi² (Figure 6.1.1b). If subsurface data in central Oklahoma is included (Kvale and Bynum, 2014) this area expands to 14,000mi² which is still a conservative estimate because it does not include the subthrust extension under the Ouachita fold and thrust belt (Figure 6.2.1). The primary Woodford phosphate intervals range from 3-15m in thickness, occur at or near timelines related to intense faunal change, and have a variety of morphologies from spherical to elliptical to discontinuous lenses (Figure 6.2.2). Discussion of the phosphate nodules and associated REEs revolves around several factors and related questions: 1) Was deposition environmental facies or an event? 2) What is the relationship between nodule morphology and formation? 3) Did deep oceanic or terrestrial processes drive nodule development?

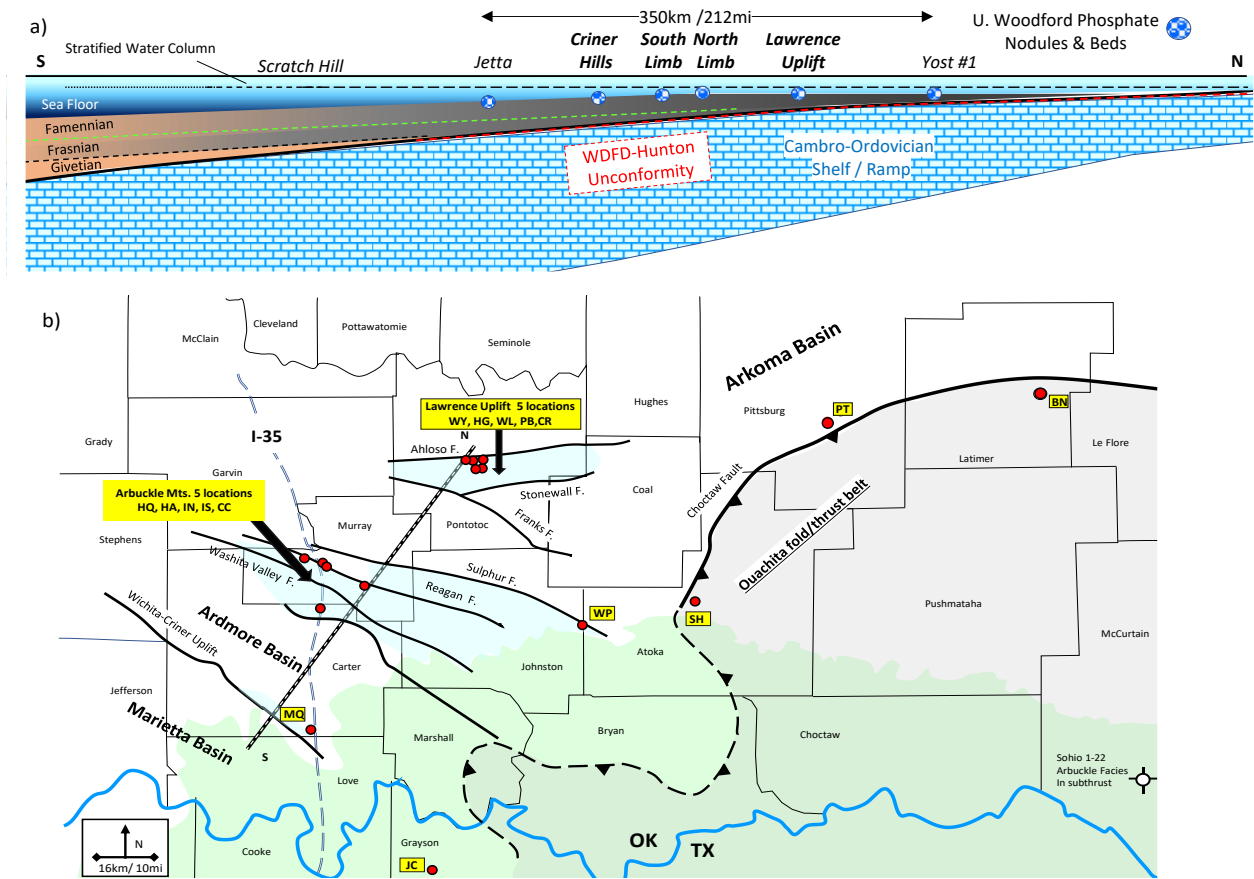


Figure 6.2.1 a) Regional stratigraphic section highlighting persistent interval of phosphate nodules near the top of the Woodford (Devonian-Carboniferous boundary, b) Map show locations for different PN studies.



Figure 6.2.2 Example of phosphate nodule morphologies and internal structure from several localities discussed in this guidebook.

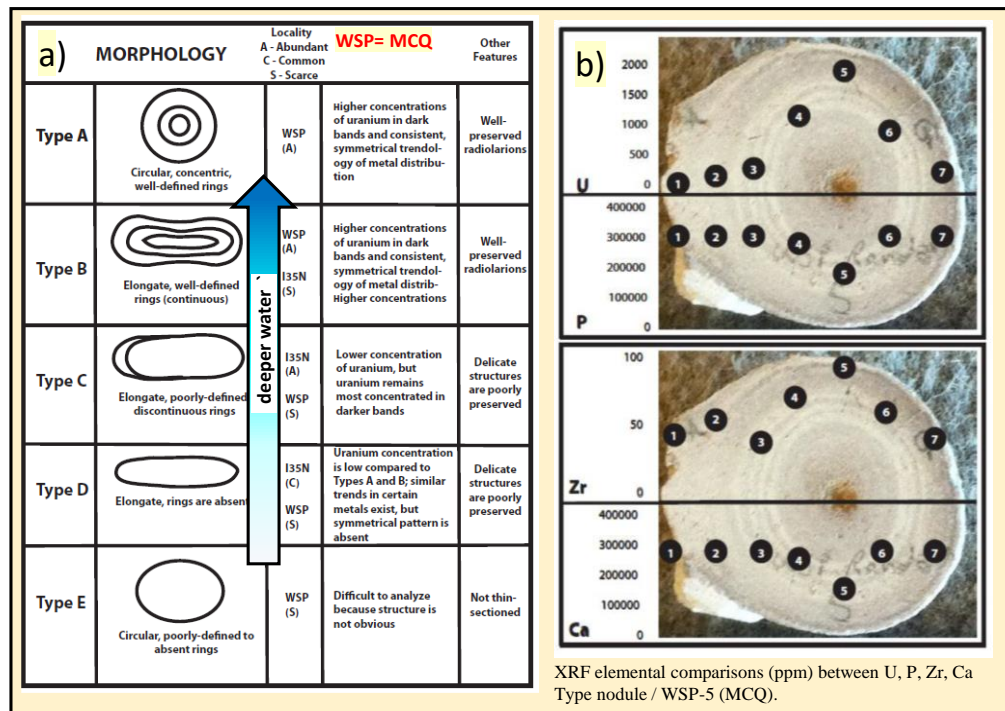
Phosphate nodules (PNs) of the Woodford have been the subject of three principal prior studies (Siy; 1988; Kirkland et al., 1992; Boardman; 2014). Siy (1988) collected PNs and laminae from 6 localities, including the Pine Top and Bengal sites. Siy noted that the nodules have spherical to elliptical to bedded morphologies and that many have internal concentric light and dark rings. Most PNs have diameters between 2-3cm but range from 0.5 to 9cm. The nodules are primarily massive cryptocrystalline fluorapatite and some have patches of acicular to prismatic crystals. Inclusions of palynomorphs, radiolarians, and sponge spicules are common. Secondary pore filling cements include amorphous silica, calcite, and pyrite. Compactional drape around the nodules shows phosphogenesis preceded shale compaction. Kirkland et al., (1992) studied the geology and organic geochemistry of the Woodford in the McAlister Cemetery Quarry (MCQ). Kirkland noted most PNs have a core nucleus of a fossil fragments and that the nodules tended to be spherical with little difference in mineralogy between the distinct light and dark concentric rings, which were interpreted to result from changes in ocean geochemistry and/or microbiology during growth.

Boardman's (2012) detailed petrographic and geochemical study of the PNs from the I35-N and the MCQ locations defined 5 types of nodules based on morphology, internal organization, and degree of radiolarian preservation (Figure 6.2.3a):

- A) Circular: well-defined, concentric rings, well-preserved radiolarians.
- B) Elongate: well-defined, continuous rings, well-preserved radiolarians.
- C) Elongate: poorly-defined and discontinuous rings, poorly preserved radiolarians.
- D) Elongate: no apparent internal ring structure.
- E) Circular: no apparent internal structure.

Boardman (2012) documented that types A and B are dominant at the MCQ, whereas types C, D, and E are more prevalent at I-35N. High definition XRF elemental analyses (3mm diameter spots) along transects across 22 bisected PNs established that the darker rings are enriched in Mo, V, and U (Figure 6.2.3b). Boardman interpreted the well-organized, spherical nodules with well-preserved radiolarians at MCQ to reflect stable conditions in deeper water compared to elliptical nodules at I-35N and proposed that nodule morphologies were controlled by differences in water depth. Elemental data were interpreted as recording oscillating sea water chemistry, but it is not established whether elemental variations resulted from changes in redox conditions or temporal differences in the concentration of metals delivered to the basin.

Figure 6.1.3 a) Nodule morphology classes
b) Elemental data across nodule bands (Boardman, 2012)



REEs and Trace Elements in Woodford Phosphates: We collected 19 nodules from from the Upper Woodford at 6 different locations, 1) MCQ, 2) I-35S, 3) I-35N, 4) Wyche Quarry (WQ), County Pit, and Hass-G. These locations represent sites progressively closer Latest Devonian shorelines (see Figure 6.2.1a). Each sample (~51gm) consisted of several nodules taken from the same bed set. At WQ we collected additional through a stratigraphic succession from rounded to elliptical nodules to lenticular thin phosphorite beds (Figure 6.2.2 center top photo) . Encasing mudrock was chiseled away from the phosphates which were then lightly scrubbed in purified water. The samples were sent to ALS Geochemistry where they were crushed, pulverized, subjected to the lab's standard 4 acid digestion protocol, and analyzed by ICP-MS for 60 elements including the 14 REEs.

The plot of REEs in the PNs, normalized to North American Composite Shale (McLennan, 1986) shows a 10-fold difference across our locations (Figure 4a). All samples show a negative cerium anomaly. Having an average of 1150ppm total REEs the WQ samples are the most highly enriched samples. Particularly striking is the preferential enrichment in range of light to middle REEs in the WQ samples. Most other samples have a fairly flat pattern across that range. MCQ-4 is not enriched at all and has a flat pattern. The normalized REE distributions for the Woodford PNs for each site plot as relatively distinct groups with minimal overlap. With the exception to the I-35S location more landward nodules are more enriched. We note that the WQ samples also have anomalously high concentrations of Rb, Se, and Tl, trace elements associated with continental provenance, relative to the other locations (Figure 4b). A few samples from different localities overlap.

The biostratigraphically constrained zone of REE enriched PNs at the Devonian-Carboniferous boundary extends the length of the study area. At I35-N we interpret the unusually thin nodule-rich interval (2m) as a concentrated lag deposit at the top Woodford unconformity (Figure 6.2.2c upper right photo). The I35-S location is along strike from fracture filled with hydrothermal mineralization in a Woodford core in the Ardmore basin (Roberts, 2017). Siy (1988) noted that some altered, silicified, nodules carried lower REE concentrations. As a group, our distributions are similar to unpublished data from the Woodford and time correlative sections in Chattanooga Shale (Figure 6.2.4) and are within the Devonian secular variations in phosphate REE concentrations (Emsbo et al., 2015).

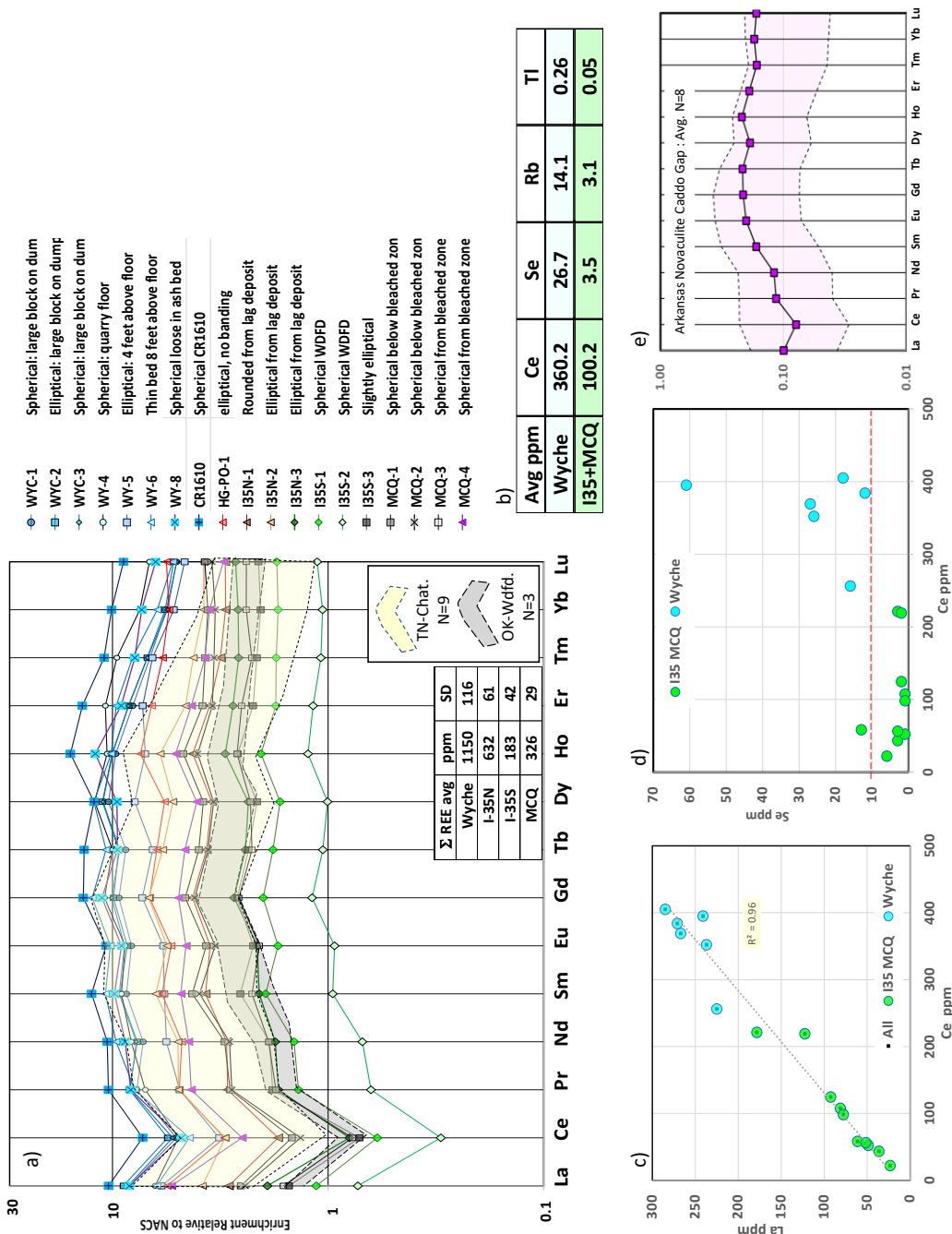


Figure 6.2.4a) Normalized REE plot of nodules from this study (North American Composite Shale, (McLennan, 1989). Shaded polygons are normalized REE plots from the Devonian-Carboniferous sections of Woodford and Chattanooga Shale, courtesy of Pat McLaughlin. Inset shows mean and standard deviation (SD) of total REE concentrations by site. 4b) Average concentrations of selected trace metals from Wyche and the combined values from the 3 other locations. 4c) Cross plot of La vs. Ce from nodules of this study, 4d) Cross plot of Se vs. Ce from nodules in this study 4e) NACS-normalized REE plots from the Arkansas Novaculite at Caddo Gap, AK (Caines, 2019).

Our data shows that sites with the highest REE enrichments (particularly on the Lawrence Uplift, Figure 6.2.4a inset) are those closest to the paleo-shoreline. The samples in stratigraphic succession at WQ show no systematic relationship between REE enrichment and phosphorite morphology. This overall up-dip REE enrichment is consistent with that fact that REEs in shales are ultimately derived from continental provinces (McLennan, 1986). Additionally, several trace elements associated with continental provenance, Se, Rb, and Tl, are also enriched in the WQ samples (Figure 6.2.4c). These relationships indicate that the REE and some trace element concentrations in the U. Woodford phosphates were influenced more by relative proximity to exposed areas in the hinterland than by water depth. Poly-aromatic hydrocarbon biomarkers in the Upper Woodford at the McAlister Cemetery Quarry (Section 4.1) indicate contribution of organic matter from forest fires in the hinterland (Philp and DeGarmo, 2020). Widespread Famennian wildfires and the demise of Late Devonian forests could have provided a massive influx of phosphorus to the Laurentian epeiric seas, possibly driving deposition of phosphatic intervals in the Woodford, New Albany, and Chattanooga shales (Section 1.2, figure 1.2.2).

Bentor (1980) noted that Ce anomalies can serve as a measure of the relative influx river water vs, deep ocean water. Ce is unique among the REE in having two valence states +3 and +4. Ce⁺³ like the other REE can substitute in trivalent sites apatite. Ce⁺⁴ readily combines with Mn and is readily removed from oxygenated bottom waters characteristic of oceanic upwelling zones. Although Siy's (1988) did not analyze a full REE suite, she established that La and Ce were positively correlated and interpreted the enrichment of La over Ce as evidence for precipitation from deep marine, reduced, bottom waters. Like Siy (1988), we note a strong positive correlation between Ce and La ($R^2=0.96$) with WQ samples being more enriched in both elements than all other samples. Because La is not sensitive to redox conditions, the fact that La and Ce are so strongly correlated implies that their relative concentrations were not a function of changing redox conditions but from mixing bottom water with river input. This is consistent with biomarker geochemistry indicating that the Woodford was deposited in a poorly-mixed, highly stratified water column (Connock et al., 2018). In light of the more oxic sediments at the Scratch Hill (Arkansas Novaculite; Section 5.2), it is interesting that localities in the Arkansas lack significant negative cerium anomalies (Figure 4e, Caines, 2019), a problematic observation for model that invoke the encroachment of anoxic deep water on to the shelf as a mechanism to drive mass extinctions (Section 6.3).

References

Boardman, D.R., III, 2012, Preliminary analysis of phosphate nodules in the Woodford, Late Devonian-Early Mississippian, southern Oklahoma: Stillwater, Oklahoma State University, unpublished M.S. thesis, 77 p.

Brito, R., 2019, The Woodford in the Marietta Basin, University of Oklahoma unpublished PhD, 208 p.

Caines, 2019, Geochemical Analysis of Mississippian Cherts and Devonian-Mississippian Novaculites, Southern Midcontinent Region, MSc thesis, University of Arkansas, 84p., <https://scholarworks.uark.edu/etd/3248>

Connock, G., Nguyen, T.X., Philp, R.P., 2018, The development and extent of photic-zone euxinia concomitant with Woodford deposition, AAPG Bulletin 102-6, p. 959–986.

Emsbo, P., McLaughlin, P.I., Breit, G.N., and others, 2015, Rare earth elements in sedimentary phosphate deposits: Solution to the global REE crisis?, *Gondwana Research*, 27, p. 776–785

Kirkland, D.W., R.E. Denison, D.M. Summers, and J.R. Gormly, 1992, Geology and organic geochemistry of the Woodford in the Criner Hills and western Arbuckle Mountains, in: Johnson, K.S., and Cardott, B.J., 1992, eds., *Source rocks in the southern Midcontinent symposium: Oklahoma Geological Survey, Circular 93*, p. 38-69.

Kvale, E.P., and J. Bynum, 2014, Regional upwelling during Late Devonian Woodford deposition in Oklahoma and its influence on hydrocarbon production and well completion, AAPG Search and Discovery Article #80410, 34 p.

McLennan, S.M. (1989) REE in sedimentary rocks: Influence of provenance and sedimentary processes. *Reviews Mineralogy* 21, 170-199.

Siy, S.E., 1988, Geochemical and petrographic study of phosphate nodules of the Woodford (Upper Devonian-Lower Mississippian) of southern Oklahoma: Texas Tech University, unpublished M.S. thesis, 172 p.

6.3 Mass Extinctions, Volcanism, and Mercury Anomalies: Deposition of the Woodford spans multiple, closely-timed Late Devonian mass extinction events that when considered together constitute one of the 5 major global mass extinctions events. (Figure 6.3.1). The other 4 global mass extinctions tended to occur as single events. The clustering of multiple extinction events in Late Devonian raises the question of the interaction of multiple driving mechanisms.

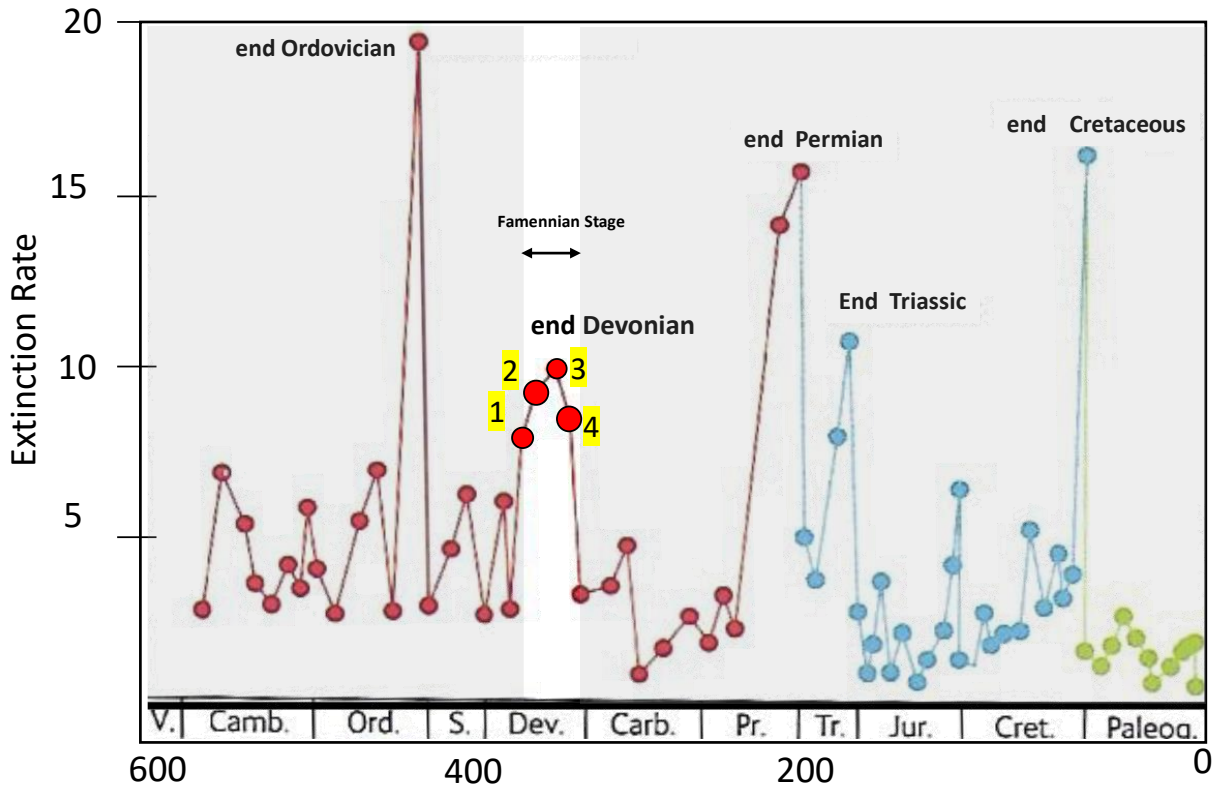


Figure 6.3.1 Phanerozoic Global extinction record using Family level marine family extinction rates families/myr (McLeod, 2013). Devonian extinctions highlighted: 1, 2 Lower and Upper Kellwasser (Frasnian/Famennian), 3-Dasberg event (middle Famennian, 4- Hangenberg D/C Devonian/Carboniferous boundary).

The end Frasnian Stage occurred at the sea level highstand at the climax of the transgression phase of the Kaskaskia Super Sequence. The Frasnian-Famennian (F/F) Stage boundary extinctions are often referred to as the Kellwasser event named after two organic-rich black shales in the Harz Mountains, Germany that have strong positive $\delta^{13}\text{C}_{\text{organic}}$ anomaly (Buggisch, 1991). The F-F boundary is dated at 371.93–371.78 Ma (Percival et al., 2018). The F-F extinctions

disproportionately degraded marine life on the tropical shelves; strongly reducing armored fish (placoderms), goniatite groups, many conodont species, groups of trilobites & brachiopods, colonial corals, and stromatoporoid siliceous sponges. At this time reef ecosystems were eliminated. Interestingly, there was little impact on terrestrial plant diversity.

The Dasberg event is a lesser extinction event that impacted conodonts. Black shales associated with the Dasberg event have a slight positive $\delta^{13}\text{C}_{\text{organic}}$ anomaly and are associated with a modest, but rapid, marine flooding event (Figure 6.3.2). The $\delta^{13}\text{C}$ anomaly in the Wyche core may record the Dasberg event rather than the F/F boundary (see Section 2.1).

The end Famennian Stage extinctions, also known as the Hangenberg Event, define the Devonian-Carboniferous (D-C) boundary. Like the F/F extinction, the Hangenberg event strongly affected shallow marine life, but also had an impact on terrestrial plant diversity. The Kellwasser and Dasberg events are associated with rising sea levels, whereas Hangenberg event occurred during a sea level fall.

The Devonian Period is one of the most dynamic intervals time in the evolution of Earth's biosphere and atmosphere (Figure 6.3.2). The most important event was the widespread colonization a diverse assemblage of vascular plants, such as lycophytes and ferns that formed the planet's first forests leading to higher levels of photosynthesis with a resultant massive drawdown in CO_2 (Pawlick et al., 2020). Atmospheric oxygen levels were low, ~15%, but increased to ~20% by the at the end of the Period. The development of thick soils and increased chemical weathering (see Figure 1.2.3) provided more nutrients into rivers, such as phosphorus, and may have helped trigger eutrophication and subsequent anoxia on the shelf (Algeo and Scheckler, 1998). Short terms sea level fluctuated rapidly which represents an important control of the shifting of facies in the epeiric seas of Laurentia. Very rapid extinction rates, high extinction percentages, and global geochemical & lithofacies correlations demand an explanation with respect to causal mechanisms that carry implications of an external triggering mechanisms.

Proposed causal extinction mechanisms fall into two categories. Terrestrial causes, including massive Large Igneous Province (LIP) volcanism, changes in ocean circulation patterns, and glacio-eustatic sea level changes, ultimately fall under the broad umbrella of tectonics. Potential extra-terrestrial causes include boloid bombardment (e.g., Alamo, Siljjan, impacts; Sandburg et

al., 2002) and X-ray bursts from super novae (Fields et al., 2020). Attribution to the Siljan and Alamo impacts appears unlikely as they predate the Late Devonian extinction events. Globally the upper Devonian section at the F/F and D/C boundaries with elevated mercury concentrations (Figure 6.3.3) have been interpreted to record volcanic-triggering of mass extinctions via delivery of Hg-rich aerosols to shallow seas (Racki, 2020; Rakociński, et al., 2020).

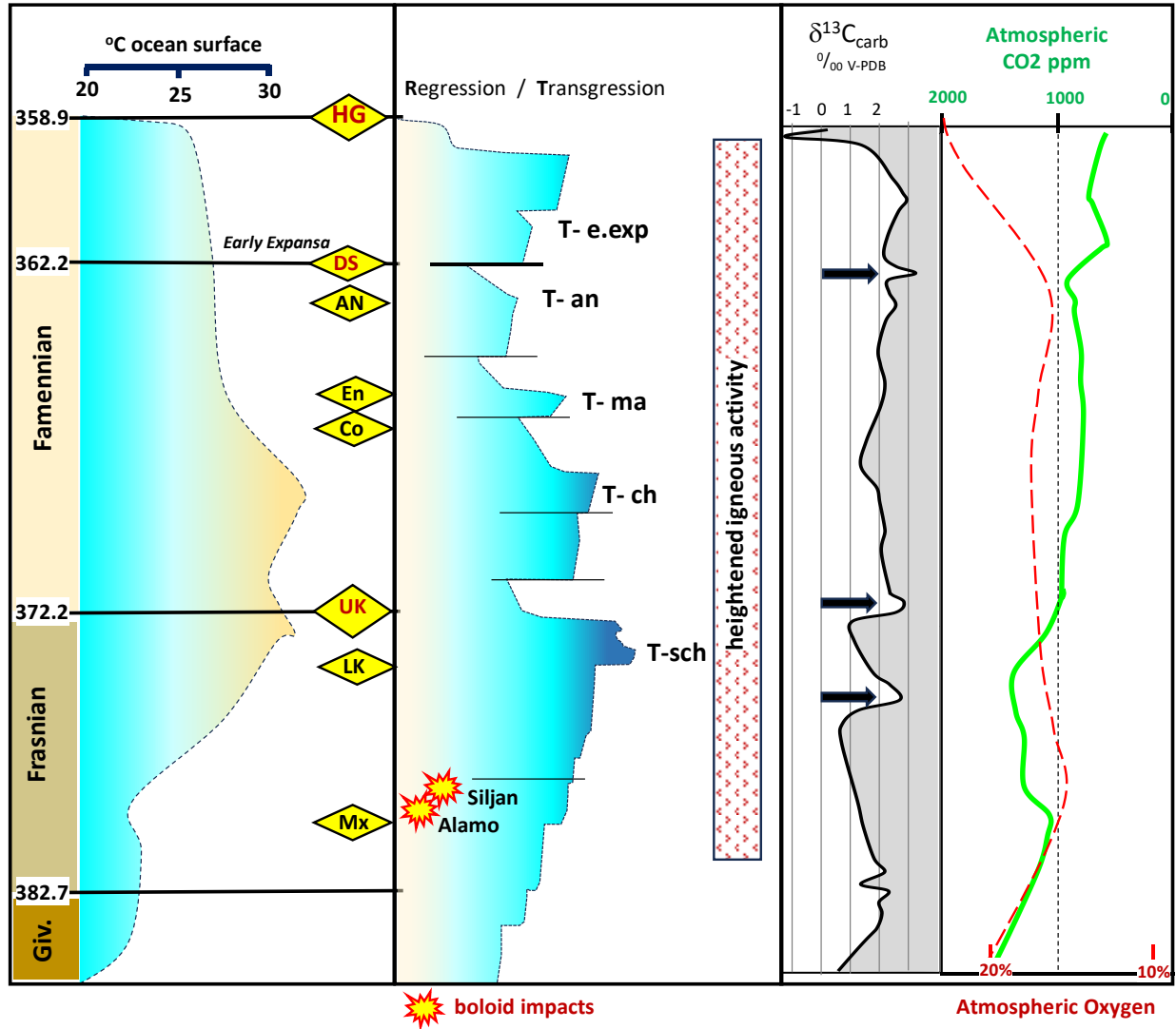


Figure 6.3.2 Late Devonian event stratigraphy with transgressive-regressive cycles (from Racki, 2020) and geochemical data- CO₂ data (Foster et al., 2017), oxygen data (Krause et al, 2018). HG- Hangenberg, DS- Dasburg, AN- Annulata, En- Enkeberg, Co- Condroz, U-LK Upper and Lower Kellwasser, Mx- Middlesex. Transgression conodont markers, exp- exposita, an- annulate, ma- marginifera, ch- chieloceras, sh- semichatovae.

There are three main mechanisms that can supply Hg to marine sediment (Grasby et al., 2019) 1) dispersed atmospheric deposition from volcanic aerosols, 2) focused terrestrial influx from river systems that may locally overwhelm any signature of atmospheric-sourced Hg in nearshore areas, 3) Hg released from submarine volcanics. For the Late Devonian, distinguishing terrestrially derived Hg from wildfires and erosion from Hg in volcanic aerosols is particularly problematic. Use of mercury stable isotopes is a promising discriminator of volcanic vs. sedimentary sources, but further calibration is required to account of mass-dependent and mass-independent isotopic fractionation in its bio-geochemical chemical cycle (Grasby et al., 2019).

Terrestrial vs. volcanic inputs are not mutually exclusive and aerosols fall out on land as well as the oceans. Thus, one of the major difficulties when interpreting Hg data is considering the potential of large volumes of terrestrial input (Chattanooga Shale / Zheng et al., 2023) to overwhelm volcanic aerosols in the marine environment (Horn River Group / Kabenov et al., 2023). To this end the use of the biomarker coronene, a 6-ring polycyclic aromatic hydrocarbon that is only known in association with large igneous province emissions and extraterrestrial impacts, represents a promising tool to resolve the relative inputs of terrestrial vs. volcanogenic mercury (Kaiho et al., 2021).

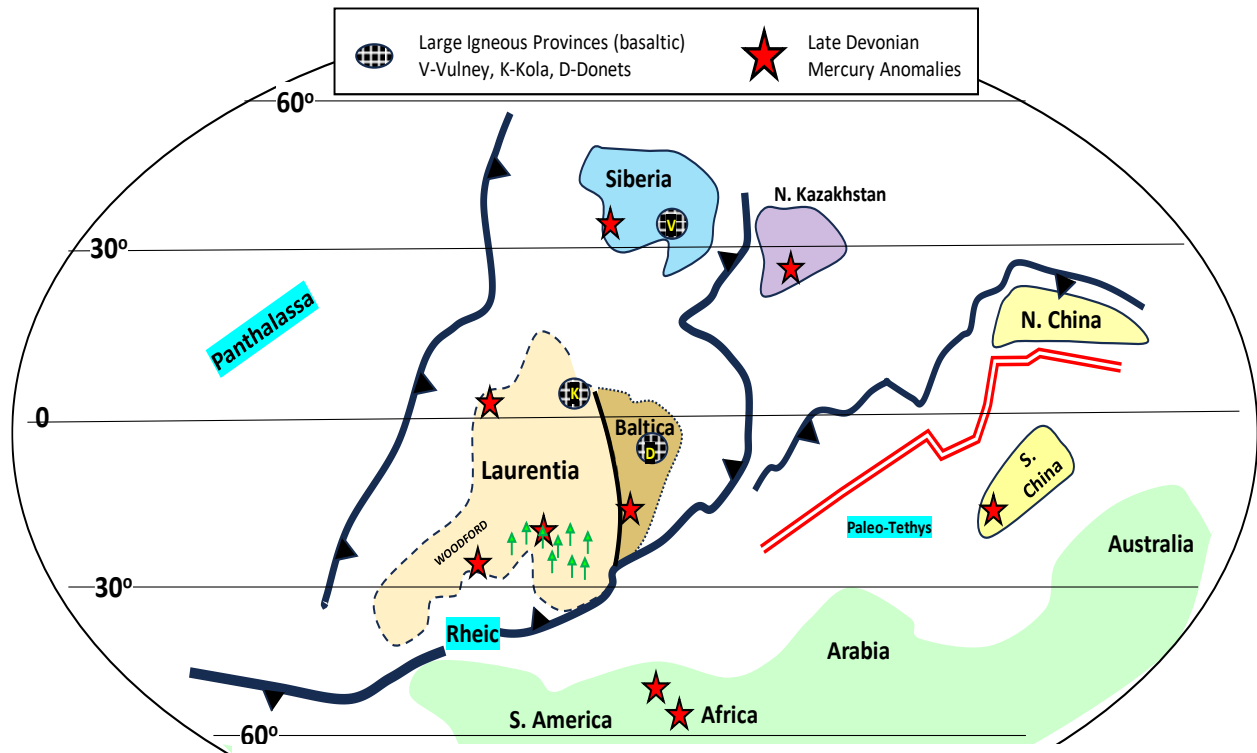


Figure 6.3.3 Simplified Late Devonian tectonic reconstruction, oceanic ridges in double red lines, subduction zones heavy black lines with teeth on upper plate (Golonka, 2020) LIP and Devonian mercury anomalies (Racki, 2020; Rackocinski, et al., 2020; Zhang et al., 2021, Zheng et al., 2023, Kabanov et al., 2023)

We have included herein Woodford Hg and Hg/TOC data at Haas-G, YMCA Spillway, I35-S, and McAlister Cemetery Quarry (4 sites in the Arbuckle region) and a single site, Scratch Hill, in the Arkansas Novaculite. The data from the Arbuckle region show the D/C boundary has a strong anomaly, whereas the F/F is much subdued (Figure 6.3.3). These data show proof of concept, but a tighter sampling grid and additional geochemical analysis (biomarker and trace metals) are required before stronger statements can be made as how the Woodford intervals relate to the global picture of volcanically-triggered Devonian mass extinctions.

Further studies should include the Arkansas Novaculite, which would complete a shelf to deep basin transect. If the fully array of analytical tools can be applied such work could not only help resolve the issue of terrestrial vs. volcanic-sourced Hg, but would improve our basic understanding of Devonian to Early Mississippian ocean redox geochemistry.

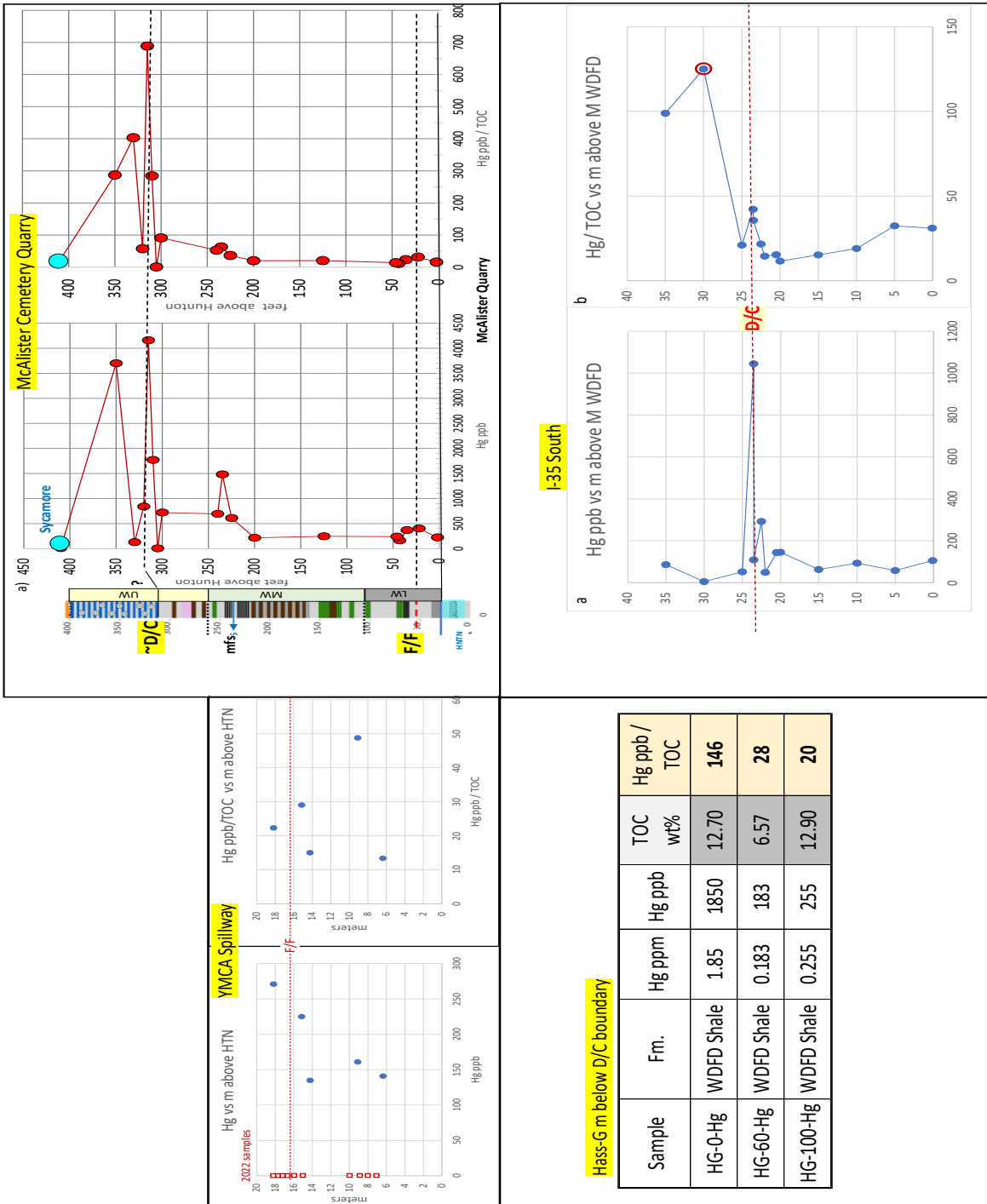


Figure 6.3.3 Woodford mercury data across the F/F and D/C boundaries in the Arbuckle region.

References

Algeo, T.J. and Scheckler, S.E., 1998, Terrestrial-marine teleconnections in the Devonian: links between the evolution of land plants, weathering processes, and marine anoxic events, *Philosophical Transactions of the Royal Society B: Biological Sciences*. 353 (1365): 113–130.

Buggisch, W., 1991, The global Frasnian-Famennian Kellwasser event, *Geologische Rundschau* 80-1, p. 49–72.

Cullen, A.B., 2019, Woodford Shale Mercury Anomalies from the McAlister Cemetery Quarry, Oklahoma: A North American Test of the Volcanic-Trigger Hypothesis for Late Devonian Mass Extinctions, *Oklahoma City Geological Society Shale Shaker*, v.71-5, p.188-202.

Fields, B.D., Melott, A.L., Elise, J., Ertela, A.F., and others, 2020, Supernova triggers for end-Devonian extinctions, *Paper National Academy of Sciences* 35-117, 3p.

Foster, G. L., Royer, D. L., & Lunt, D. J. (2017). Future climate forcing potentially without precedent in the last 420 million years. *Nature Communications*, 8, p.1-8.

Golonka, J., 2020. Late Devonian paleogeography in the framework of global plate tectonics. *Global Planetary Change* 186, p.1–19.

Grasby, S.E., Them, T.R., II, Chen, Z., Yin, R., and Ardakani, O.H., 2019, Mercury as a proxy for volcanic emissions in the geologic record: *Earth-Science Reviews*, v. 196, p.1-18.

Kabanov, Gouwy, S., van der Boon, A., Grasby, S., 2023, Nature of Devonian anoxic events based on multiproxy records from Panthalassa, NW Canada, *Global Planetary Change*, 227, p.1-19.

Kaiho, M., Miura, M., Tezuka, M., Hayashi, N., and others, 2021, Coronene, mercury, and biomarker data support a link between extinction magnitude and volcanic intensity in the Late Devonian, *Global and Planetary Change*, 99 p.1-17.

Krause, A.J., Mills, B.J.W., Zhang, S., Planavsky, N.J., and others, 2018. Stepwise oxygenation of the Paleozoic atmosphere. *Nature Communications* 9, p. 4081–4109.

MacLeod, N., 2013, *The Great Extinctions: What Causes Them and How They Shape Life*, Firefly Books, United Kingdom.

Pawlik, L., Bum, B., Samonil, S., Kvacek J., and others, 2020, Impact of trees and forests on the Devonian landscape and weathering processes with implications to the global Earth's system properties – A critical review, *Earth Science Reviews*, 205, p. 1-17.

Percival, L.M.E., Davies, F., Schaltegger, U., and others, 2018, Precisely dating the Frasnian–Famennian boundary: implications for the cause of the Late Devonian mass extinction, *Nature Scientific Reports*, 8:9578, 10p.

Racki, G., 2020, Volcanism as a prime cause of mass extinctions: Retrospectives and perspectives, *Geological Society of America, Special Paper 544*, 35p.

Rakociński, M., Marynowski, L., Agnieszka, P., and others, 2020, Volcanic related methylmercury poisoning as the possible driver of the end-Devonian Mass Extinction, *Nature Reports* 10-7344, 8p.

Sandberg, C.A.; Morrow, J.R.; Ziegler, W., 2002, Late Devonian sea-level changes, catastrophic events, and mass extinctions, in Koeberl, C.; MacLeod, K.G. (eds.). *Catastrophic Events and Mass Extinctions: Impacts and Beyond*, Geological Society of America Special Paper 356, p. 473-487.

Zheng J, Deng C, Liu W, Tang Z, and others, 2021, Mercury Anomalies Link to Extensive Volcanism Across the Late Devonian Frasnian–Famennian Boundary in South China. *Front. Earth Sci.* 9:691827.

Zheng, W., Geoffrey J. Gilleaudeau, G.J., Algeo, T.J., and others, 2023, Mercury isotope evidence for recurrent photic-zone euxinia triggered by enhanced terrestrial nutrient inputs during the Late Devonian mass extinction. *EPSL* 613, p.1-11.

6.4 Paleogeography/ Ocean Circulation/ Depositional Environment

The organic-rich Woodford Shale was deposited during a 15-20my interval during a dynamic period for sea-level, climate, and tectonics. Demaison and Moore (1980) in their classic paper “Anoxic Environments and Oil Source Bed Genesis”, outlined several sets of paleogeographic and paleo-oceanographic circumstances in which oil-prone source rocks beds can form: 1) silled basins 2) upwelling environments, 3) the open ocean. Global climatic events during Woodford time, including the Hangenberg, Dasberg, Annulata, and Upper and Lower Kellwasser oceanic anoxic events, occurred in different paleogeographic and sequence stratigraphic settings and may have been global in nature but inconsistent in cause and effect (Kaiser et al. 2016, Sahoo et al. 2023, Carmichael et al. 2019). It is unlikely that any single model can encompass the entire depositional framework of the Woodford Shale.

Many excellent, data-rich, studies of the Woodford evoke a simplistic cause for organic carbon sequestration, source rock deposition, but rarely do these papers address multiple hypotheses head on, differentiate different depositional environments for different parts of the Woodford, or address the sheer extent and frequency of black shale deposition in the Woodford and Laurussia interior seas as detailed in figure 6.3.1. Many of these studies fail to take a regional perspective, instead focusing on a specific outcrop or modern sub-basin without considering the whole system; notably the downdip oxygenated deposits of the Scratch Hill outcrop (5.2) as well as the upper reaches of the system at the Wyche pit (Stop 2.1).

We also wish to add several cautionary notes regarding the use of analogs to explain deposition of the Woodford. First, although anoxic/euxenic conditions occur in different settings their use as analogs for the Woodford will always suffer from the fact that there are no modern epeiric seas. For example, Turner and Slatt (2015) use the Framvaren Fjord (Norway) and the Cariaco Basin (offshore Venezuela) as modern analogs for the Lower and Middle-Upper Woodford, respectively, without addressing how one can transition between these vastly different settings. Likewise, one must consider relative differences in paleogeography for upwelling models. Reconstructions for the Rheic Ocean at 360Ma and 345Ma show east-west striking coast lines and a south-dipping subduction zone (Figure 6.3.1a). From this geometry not only is it problematic to source polar bottom waters for upwelling (Figure 6.3.4), upwelling should occur from the deepest waters, presumably from the trench along Gondwanaland, not along the Laurentian margin. For the 360-

Connock 2018, Cardott and Comer 2021, and others point to a silled basin and give evidence such as gypsum crystals indicating hypersaline conditions, evidence of a stratified water column, and the development of photic zone euxenia in addition to high TOC to justify a restricted basin many of which are summarized in figure 6.3.2. Other papers such as Brito (2019) focus on small sub-basins despite the regional extent of the Woodford Shale. While pointing out that many features recognized in Oklahoma paleogeography unrelated to Pennsylvanian thrusting were present in the Devonian (Cardott and Comer 2021; and Kvale and Bynum 2014) these papers, amongst others, do not locate a specific basin wide sill often pointing vaguely towards an offshore island arc and encroaching Gondwana shown in paleogeographic maps (Figure 6.3.1, Blakey 2016). Often the strike sections shown to illustrate the highs and lows of the Anadarko basin, Nemaha uplift and Arkoma basin, fail to caption the down dip open connection to the Rheic Ocean or lateral limits to the bathymetric highs.

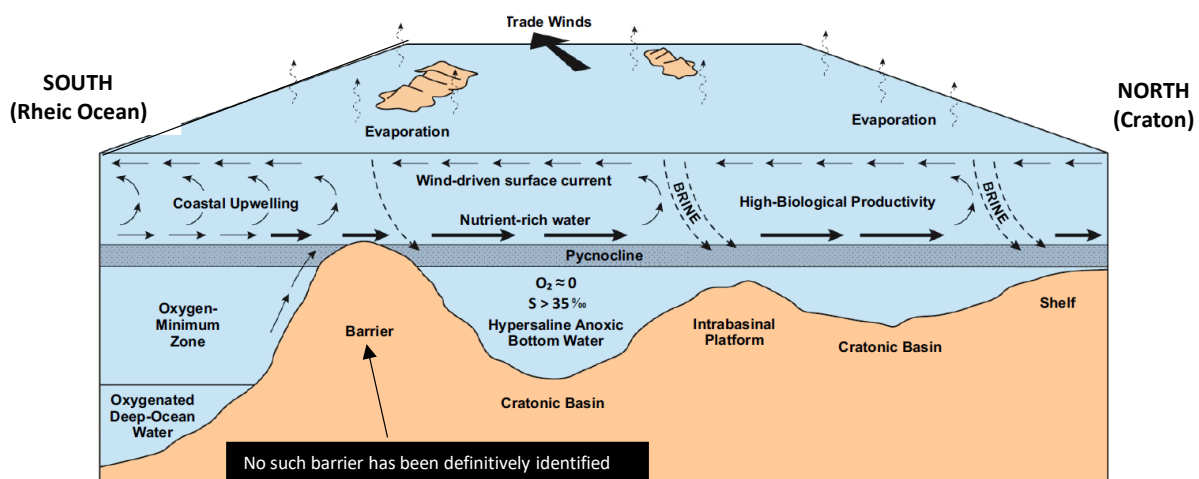


Figure 6.3.2 Block diagram with extreme vertical exaggeration emphasizing paleogeographic restriction (Cardott and Comer, 2022). The cratonic basins indicated (Anadarko and Arkoma) would have been open to the south into the Rheic Ocean.

Upwelling is commonly cited as the chief culprit in eutrophication and preservation of TOC in the Woodford Shale (Boardman, 2012, Cardott and Comer, 2021, Kvale and Bynum, 2014). Upwelling occurs when winds and currents pull cold, oxygenated, nutrient-rich water from the oceans into shallow environments on the shelf. This results in excessive biological productivity in surface waters driving reducing conditions in bottom waters, the development of radiolarian rich sediment leading to the formation of chert, and the deposition of phosphate nodules at the

up-dip extents of the upwelling zone as detailed in figure 6.3.3 (Wignall 1994). Currently, this commonly occurs at low latitudes along the western margins of continents, conditions that fit the Woodford Shale (Kvale and Bynum, 2014; Boardman 2012; Siy 1988). Unfortunately, modern analogues for this theory, offshore of West Africa and Peru (Demaison and Moore 1980; Kvale and Bynum 2014), exhibit very different geometries than the Woodford. These modern systems have significantly narrower shelves that strike north-south over vast distances (Ulrike et al. 2016) as opposed to wide east-west oriented epeiric seas of the late Devonian Figure 6.3.3. The advancement of nutrient rich water across such a broad expanse of not only the Woodford but the contemporaneous Chattanooga, Floyd Shales, New Albany Shale, Antrim, Huron, Rhinestreet, and Lower Bakken Shale is problematic as these nutrients are consumed driving large expanses of organic shale deposition in several contiguous basins with different tectonic settings. These problems are further exacerbated by the different sea level conditions of the various oceanic anoxic events where sea levels are overall transgressing at the Lower Woodford F/F boundary (Kellwasser events (Carmicheal et al. 2019)) and falling during the Hangenberg events at the D/C boundary (Hangenberg events (Kaiser et al. 2016)) of the Upper Woodford. Also given the prevalence of phosphate and chert these models appear to apply more to the Upper Woodford than the Lower Woodford.

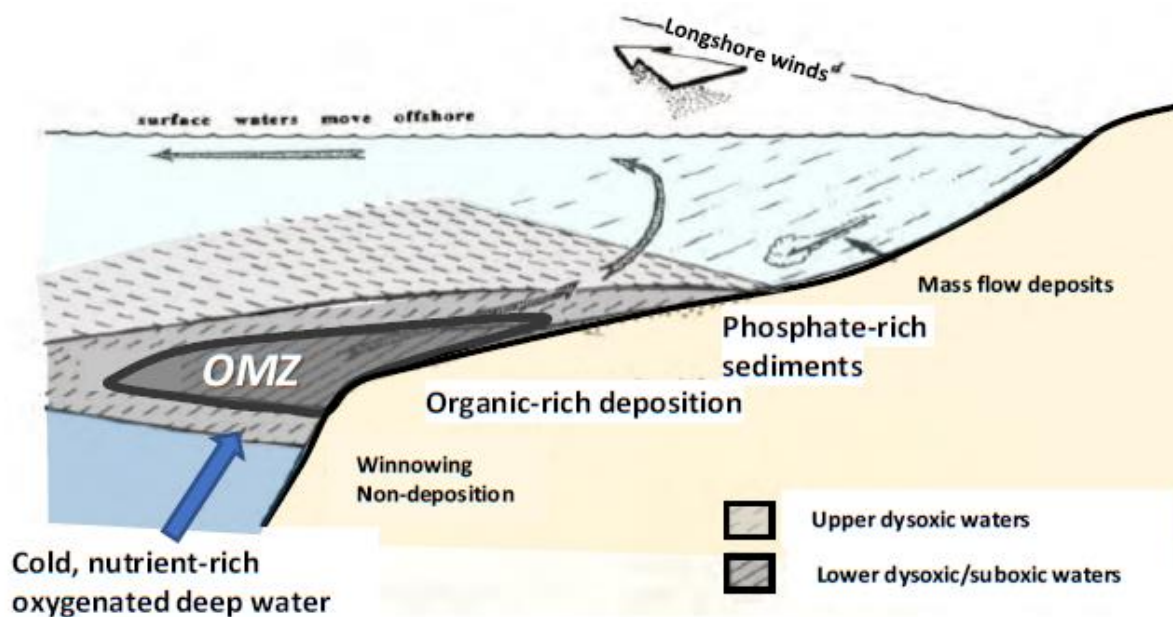


Figure 6.3.3 Block diagram from Wignall (1994) Illustrating zones of oxygenation as well as phosphate deposition and continental input. This model is strongly weighted towards the modern day Peruvian upwelling zone.

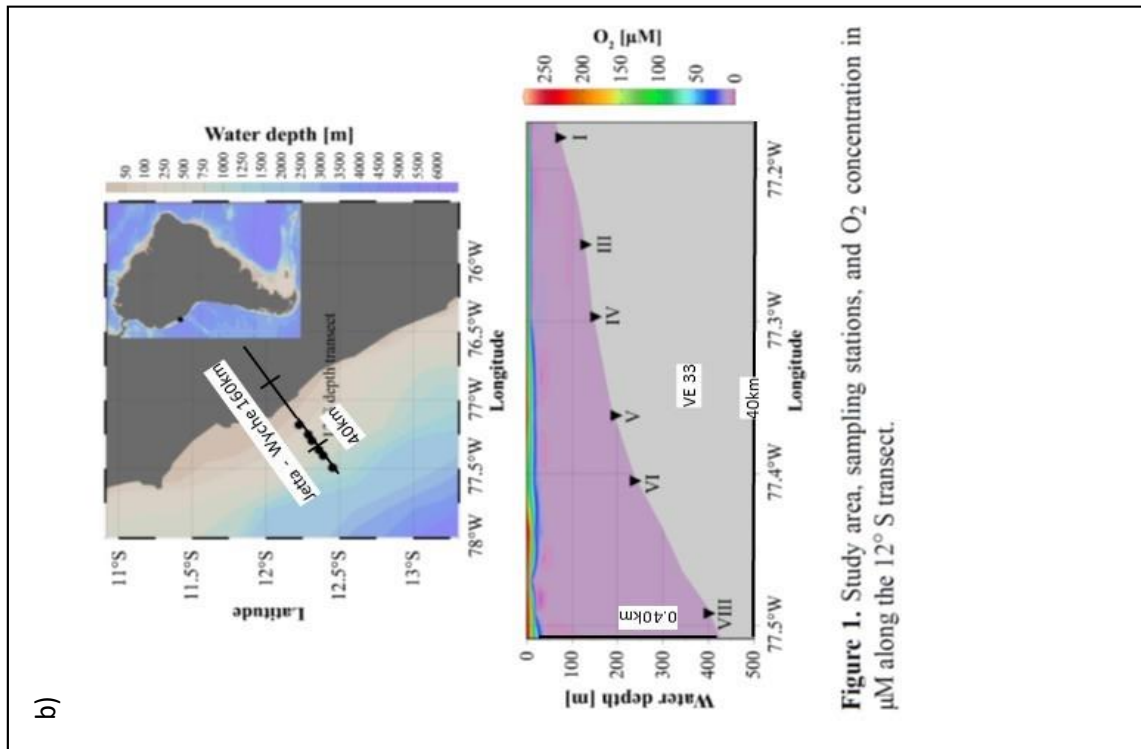
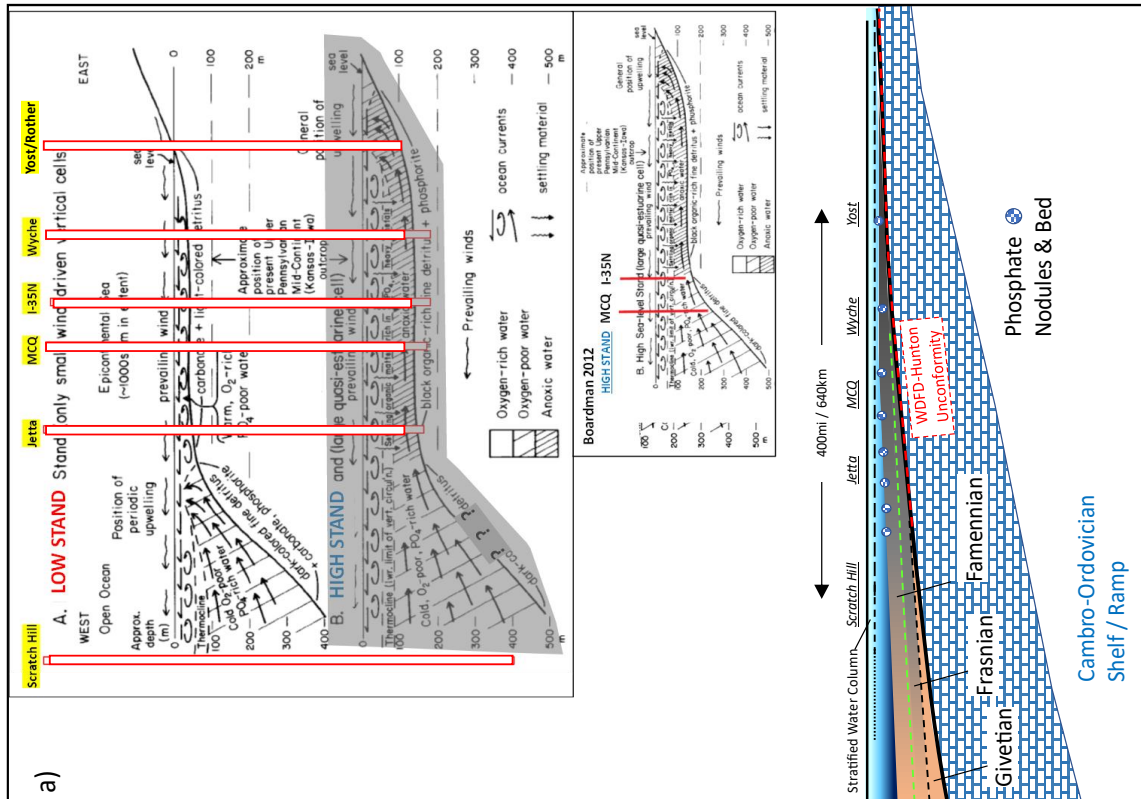


Figure 1. Study area, sampling stations, and O₂ concentration in μM along the 12° S transect.

Figure 6.3.4 a) Boardman's (2012) application of Heckel (1977) upwelling model b) Scale of Peruvian Oxygen Minimum Zone (Ulrike et al., 2016) compared to minimum distribution Woodford phosphates nodules

The valid alternative to eutrophication from upwelling is eutrophication from terrestrial sources. The implication here is that land derived organics and/or iron-bearing dust fed algae blooms resulting in the deposition of Type I and II kerogen. This alternate model ties to changes in weathering and nutrient delivery associated with the development of land plants (Algeo et al. 1995; see Section 1.2). Siy (1988) considered this in her analysis of the origins of phosphate nodules in the Woodford before ultimately concluding that upwelling was more likely, however she did not conclusively rule out a terrestrial phosphate source. However numerous authors have found convincing evidence of terrestrial-sourced eutrophication.

1. Philp and Degarmo (2020) and Connock et al (2018) found evidence of forest fires in the organic material from McAllister Cemetery (stop 4.1) and Wyche Quarry (stop 2.1).
2. Data presented in this volume and by Cullen (2020) have also found mercury anomalies (section 6.4) equivalent in time and quantity to anomalies which Racki et al 2018 and Rakocinski et al 2020 have attributed to volcanic triggers.
3. REE and other trace element data presented in this volume (section 6.2) is likely derived from continental sources (McLennan, 1986) and the negative cerium anomalies in the REE data suggest they were not from upwelling.
4. Sahoo et al (2023) attribute trace element accumulations, often linked to reducing conditions, to continental input in the Lower Bakken Shale. Many of their interpretation could apply to the work of Turner et al 2015, Ekwunife 2017, and others.
5. Cecil (2004) suggests that eolian dust could have seeded and supplied silica for both deep and shallow water chert in the Devonian and Mississippian of Arkansas, Texas, and Oklahoma.

The sheer size, variable conditions of deposition in the Woodford, and oceanic anoxic events requires a deeper multifaceted approach to considering the depositional environment rather than finding a single solution. This will mean looking beyond the petroleum system, considering other attached basis and a 3D orientation along with connecting other data such as $\delta^{13}C$ curves, REE data, phosphate nodule data, and Hg data. While we have explored some of these we believe that we have only begun to stack the building blocks of excellent previous research.

As a working hypothesis based on limited data we suggest that that the Lower Woodford Kellwasser events reflect restriction over pre-existing Hunton topography, whereas the Middle Woodford and Lower Upper Woodford are dominated by eutrophication due to upwelling, the upper most Devonian Woodford is dominated by land derived eutrophication, and the Carboniferous Woodford is more of a classic grey shale.

REFERENCES

Algeo, T.J., Berner, R.A., Maynard, J.B., and Scheckler, S.E. (1995). Late Devonian Oceanic Anoxic Events and Biotic Crisis: “Rooted” in the Evolution of Vascular Land Plants?. *GSA Today* 5, p63-66

Boardman, D.R., III, 2012, Preliminary analysis of phosphate nodules in the Woodford Shale, Late Devonian-Early Mississippian, southern Oklahoma: Stillwater, Oklahoma State University, unpublished M.S. thesis, 77 p.

Brito, R., 2019, The Woodford Shale in the Marietta Basin, University of Oklahoma PhD (unpublished), 208 p.

Cardott, B.J., and Comer, J.B., 2020, Woodford Shale (Upper Devonian to Mississippian) from Hydrocarbon Source Rock to Reservoir, *Oklahoma Geological Survey Bulletin* 152, 100 p.

Carmicheal, S.K., Waters J.A., Konigshof, P., Suttner, T.J., Kido, E., 2019 Paleogeography and paleoenvironments of the Late Devonian Kellwasser event: A review of its sedimentological and geochemical expression. *Global and Planetary Change* 183 p1-17

Cecil, C.B. (2004) Eolian Dust and the Origin of Sedimentary Chert. *USGIS Open-File Report* 2004-1098

Connock, G., Nguyen, T.X., Philp, R.P., 2018, The development and extent of photic-zone euxinia concomitant with Woodford Shale deposition, *AAPG Bulletin* 102-6, p. 959–986

Cullen, A., 2020, Woodford Shale mercury anomalies from the McAlister Cemetery Quarry, Oklahoma: A North American test of the volcanic-trigger hypothesis for Late Devonian mass extinctions: *Oklahoma City Geological Society, Shale Shaker*, v. 71-5, p. 188-203.

Demaison, G. J., Moore, G.T. (1980) Anoxic Environments and Oil Source Bed Genesis *AAPG Bulletin* (1980) 64 (8): 1179–1209.

Ekwunife, I. C., 2017, Assessing mudrock Characteristics, high-resolution chemostratigraphy, and sequence stratigraphy of the Woodford Shale in the McAlister Cemetery Quarry, Ardmore Basin, Oklahoma, University of Oklahoma MSc thesis, 168 p.

Heckel, Phillip. "Origin of Phosphatic Black Shale Facies in Pennsylvanian Cyclothem of Mid-Continent North America," *The American Association of Petroleum Geologists Bulletin*. Vol. 61. No. 7 (July 1977). P. 1045-1068. 7 Figs.

Kaiser, S.I., Aretz, M., Becker, R.T., 2016. The global Hangenberg Crisis (Devonian–Carboniferous transition): review of a first-order mass extinction. *Geol Soc. Lond., Spec. Publ.* 423, 387–437.

Kvale, E.P., and J. Bynum, 2014, Regional upwelling during Late Devonian Woodford deposition in Oklahoma and its influence on hydrocarbon production and well completion, AAPG Search and Discovery Article #80410, 34 p.

McGlannan, A., Bonar, A., Pfeifer, L., 2022, An Eolian Dust Origin for Clastic Fines of Devonian–Carboniferous Sedimentary Research.

Philp, R.P. and DeGarmo, C.D., 2020, Geochemical characterization of the Devonian–Mississippian Woodford Shale from the McAlister Cemetery Quarry, Criner Hills Uplift, Ardmore Basin, Oklahoma, *Marine and Petroleum Geology* 112, p.1-21.

Racki, G., Rakocinski, M., Marynowski, L., Wignall, P.B., 2018, Mercury enrichments and the Frasnian-Famennian biotic crisis: a volcanic trigger proved? *Geology* 46, p. 543–546.

Rakociński, M., Marynowski, L., Agnieszka, P., & others, 2020, Volcanic related methylmercury poisoning as the possible driver of the end-Devonian Mass Extinction, *Nature Reports* 10-7344, 8p.

Sahoo, S.K, Gilleaudeau, G.J., Wilson, K., Hart, B., Barnes, B.D., Faison, T., Bowman A.R., Larsen, T.E. Kaufman, A.J. 2023. Basin Scale Reconstruction of Euxinia and late Devonian Mass Extinctions. *Nature* 10-1038. P.1-6

Siy, S.E., 1988, Geochemical and petrographic study of phosphate nodules of the Woodford Shale (Upper Devonian-Lower Mississippian) of southern Oklahoma: Texas Tech University, unpublished M.S. thesis, 172 p.

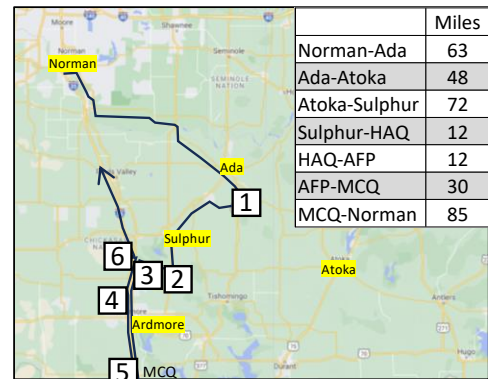
Turner, B., Molinares, C., Slatt, R.M., 2015, Chemostratigraphic, palynostratigraphic, and sequence stratigraphic analysis of the Woodford Shale, Wyche Farm Quarry, Pontotoc County, Oklahoma, Interpretation, v. 3, p.1–9

Ulrike L., et al., 2016, Benthic phosphorus cycling in the Peruvian oxygen minimum zone
Biogeosciences 16, p. 1367-1386

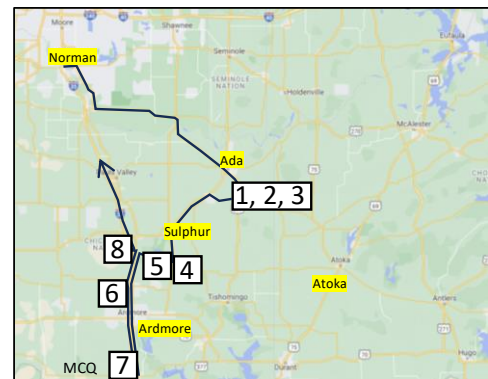
Wignall, P.B., 1994, Black Shales, Clarendon Press – Oxford Monograph, 127p.

7.0 Three Notional Field Trips: This atlas guidebook represent a menu of outcrops that could be served up for different field trips depending on the purpose, length of the trip, and number of participants. Below are 3 notional trips- including one for a motor coach with 30+ participants. Regarding logistics: 1) We recommend having pre-packed lunches. 2) Arbuckle Fried Pies (AFP) is an excellent stop for bathrooms & short lectures and outdoor benches for lunch. 3) For overnight stays, Sulphur is preferred for the shorter route (SH177) the Hunton Quarry Anticline. 4) We have put the Camp Classen / YMCA stop last, after the McAlister Cemetery Quarry, to ensure sufficient time at MCQ and to break up the ride back to Norman/OKC with a bio-break and a snack at AFP.

1 day	LARGE GROUP (~30) Motor Coach	
1	Wyche Quarry: Upper WDFD	U. Woodford/ PO nodules
2	Hunton Quarry Anticline HAQ	Full section
3	Heart of the Arbuckles	L. WDFD fractures
4	I-35S (?)	WDFD-HNTN, U WDFD D/C
5	McAlister Cemetery Quarry	Full section
6	Camp Classen	L. WDFD strat, F/F boundary



1 Day	SMALL GROUP (~20) Vans / SUVs	
1	Wyche Quarry: Upper WDFD	U. Woodford/ PO nodules
2	Hass G	WDFD-Welden, D/C
3	Woodford Log	Fractures, petrified log
4	Hunton Quarry Anticline HAQ	Full section
5	Heart of the Arbuckles	L. WDFD fractures
6	I-35S (?)	WDFD-HNTN, U WDFD D/C
7	McAlister Cemetery Quarry	Everything
8	Camp Classen	L. WDFD strat, F/F boundary



2 Days	SMALL GROUP (~20) Vans / SUVs	
1	Wyche Quarry: Upper WDFD	U. Woodford/ PO nodules
2	Hass G	WDFD-Welden, D/C
3	Woodford Log	Fractures, petrified log
4	Scratch Hill (Atoka)	Arkansas Novaculite
5	Wapanucka	Upper Woodford (Miss)
6	Hunton Quarry Anticline HAQ	Full section
7	Heart of the Arbuckles	L. WDFD fractures
8	I-35N	U. WDFD nodule lag
9	I-35S	WDFD & Sycamore
10	McAlister Cemetery Quarry	Full section
11	Camp Classen	L. WDFD strat, F/F boundary

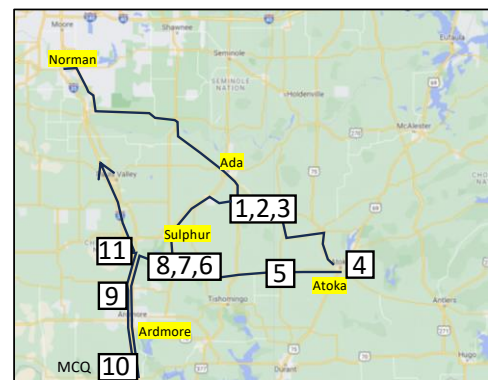


Figure 7.1 Three examples of the many different possible field trips that may "...to lead you to an overwhelming question. Oh, do not ask, "What is it?" Let us go and make our visit." *The Love Song of J. Alfred Prufrock* / T.S. Elliot